Characterisation of the Domain in Sla1p Required for Regulation of the Yeast Actin Cytoskeleton

ProQuest LLC.
789 East Eisenhower Parkway
P.O. Box 1346
Ann Arbor, MI 48106 – 1346

Characterisation of the Domain in Sla1p Required for Regulation of the Yeast Actin Cytoskeleton

A thesis submitted to the
Faculty of Biomedical and Life Sciences
for the degree of
DOCTOR OF PHILOSOPHY

By

Hilary Dewar

Division of Biochemistry and Molecular Biology
Institute of Biomedical and Life Sciences
University of Glasgow

July 2002

Acknowledgements

First of all I'd like to thank my supervisor Kathryn Ayscough for her encouragement over the past 4 and a half years, and especially for taking time to edit my thesis. I also want to give special thanks to the following people who have helped with experiments and have kept me entertained in and out of the lab: Derek Warren, Campbell Gourlay, Tommy Jess, Paul Andrews, Mark Peggie, Ian Broadbent, Sarah Mackelvie and Cath Waters. Also thanks to everyone else I haven't mentioned by name from the labs of Steve Winder, Mike Stark (past and present), Doug Stirling, Anne Donaldson, Gwyn Gould, and many other people in the Wellcome Trust Building, Dundee University and the Division of Biochemistry and Molecular Biology, Glasgow University. I'd also like to thank my current boss, Tomoyuki Tanaka for his support while I finished off the thesis. Finally I'd like to thank my Mum and Dad for their never-ending support and encouragement. Thanks.

Contents

List of Figures

List of Tables

Abstract

Sla1p is a protein required for cortical actin cytoskeleton structure and organisation in the budding yeast *Saccharomyces cerevisiae*. *Sla1* null cells display aberrant cortical actin patches which are fewer in number but significantly enlarged. Movement of these patches is also significantly reduced in *sla1* null cells. Expression of mutant forms of Sla1p in which distinct domains within its primary sequence are deleted has shown that phenotypes associated with the full deletion are functionally separable. In particular, the C-terminal repeat region is required if cells are to grow in the absence of cortical patch protein Abp1p and a region encompassing the third of its three SH3 domains is important for the highly polarised and punctate appearance of cortical actin patches in wildtype cells. To investigate the role of Sla1p in actin dynamics further an *sla1* mutant lacking the third SH3 domain has been integrated into the yeast genome (*sla1-Δ118-511*) and expressed as the sole form of Sla1p in cells. Rhodamine-phalloidin staining of this mutant showed aberrant cortical actin patches similar to the *sla1* null phenotype. Both myc and GFP tagged mutant proteins localise to the cell cortex but do not show any co-localisation with the aberrant actin patches, implicating this domain in actin cytoskeleton interaction but showing it to be unnecessary for cortical localisation. A role for Sla1p in enhancing actin turnover is also suggested by the observation that yeast expressing the mutant Sla1p exhibit a significantly reduced sensitivity to Latrunculin compared to wild-type cells (indicating increased F-actin stability). A two-hybrid screen using the *sla1-118-511* domain as bait identified two actin- associated proteins as binding partners: Sla2p and

Ysc84p. Sla2p was identified in the same synthetic-lethal screen as Sla1p and is required for a normal actin cytoskeleton and endocytosis. Ysc84p is a novel protein that requires Abp1p (but not Sla1p) for localisation to cortical actin patches. Ysc84p is not essential for viability, actin organisation or uptake of vital dyes. However, cells that lack Ysc84p and a novel protein encoded by the ORF *YCL034W* were inviable at 37 °C. *YCL034W* encodes a protein that has previously been identified in a two-hybrid screen as interacting with the *S.cerevisiae* Arp2/3 complex activator and WASp homologue Las17p. Thus the sla1p-118-511 domain, was found to play an essential role in regulating cortical patch structure and organisation as it couples actin cytoskeleton associated proteins and endocytic complex associated proteins.

Chapter 1

Introduction

1.1. Introduction

The control of F-actin assembly and turnover is important for many cellular processes such as motility, morphological changes, cell polarity and intracellular movement of organelles. Although the term cyto-skeleton implies a rigid, unchanging structure, the actin cytoskeleton is actually highly dynamic and assembles and disassembles into bundles and networks in response to intrinsic and extrinsic factors. The ability of G-actin to polymerise into F-actin and of F-actin to depolymerise into G-actin is an important property of actin.

Although the budding yeast *Saccharomyces cerevisiae* is non-motile, its actin cytoskeleton is dynamic (Ayscough *et al* 1997) and filamentous actin (F-actin) is found in two structures, actin cables and actin patches as observed by fluoresence microscopy. These structures also consist of many other interacting proteins that contribute to the morphology and function of the actin cables and cortical patches. Some proteins play a structural role, some bind to actin monomers or polymers to affect their function, while others are members of functional subassemblies.

This chapter will examine the actin cytoskeleton of the budding yeast *Saccharomyces cerevisiae* in greater depth. The structure, organisation and regulation of the actin cytoskeleton including some of the many actin-binding and associated proteins will be discussed alongside the role the actin cytoskeleton plays in this single-celled eukaryotic organism.

1.2. Yeast as a model organism

The budding yeast *S. cerevisiae* has become a widely used, eukaryotic model organism for the study of many cellular processes due to its ease of genetic manipulation by classical and molecular genetics and well established biochemical techniques. It is a unicellular organism that grows well in culture and is stable as either a diploid or haploid cell type. The approximately 6000 genes of the yeast genome (Goffeau *et al* 1996) have been sequenced and annotated (http://genome-www.stanford.edu/Saccharomyces/). The study of the actin cytoskeleton and cell polarity is aided by collections of actin mutants generated by *in vitro* mutagenesis (see section 1.5.1) or identified in genetic screens that allow structure-function relationships to be analysed (Wertman *et al* 1992, Ayscough and Drubin 1996, Whitacre *et al* 2001). The high level of conservation between yeast actin and actin of higher organisms indicates that findings from studies of the *S. cerevisiae* actin cytoskeleton will apply to other eukaryotes. Tools for studying the yeast actin cytoskeleton and genes and proteins associated with it are discussed in section 1.5.

1.3. The Eukaryotic Cytoskeleton

The cytoskeleton is a common feature of all eukaryotic cells and is composed of a network of protein polymer filaments: microfilaments; microtubules, and intermediate filaments (for reviews see Botstein *et al* 1997, Winsor and Schiebel 1997). These cytoskeletal fibres are well-ordered polymers built from small protein subunits held together by noncovalent bonds. The actin cytoskeleton is made up of

flexible polymers of globular actin (5-7nm in diameter) and a large number of actin-binding and associated proteins. Microtubules are composed of tubulin, a heterodimer of α- and β-tubulin which form hollow tubes 25nm in diameter. Actin filaments are thinner and more flexible, and usually much shorter, than microtubules. Polymers of any of a number of related fibrous coiled-coil proteins, such as vimentin or lamin, called intermediate filaments (10nm in diameter) constitute the third type of cytoskeletal filament found in eukaryotic cells (reviewed by Herrmann and Aebi, 2000) though there are no intermediate filaments in *S. cerevisiae*.

The microtubule cytoskeleton, including microtubule-associated proteins, functions in animal cells and many fungi to mediate long range transport of organelles to the cell periphery, whereas the actin cytoskeleton acts in anchorage and short-range transport. However, the microtubule cytoskeleton in the budding yeast *Saccharomyces cerevisiae*, is not thought to be primarily involved in intracellular transport. Cytoplasmic microtubules function in nuclear positioning and migration of the nucleus into the bud, and chromosome segregation is performed by nuclear microtubules (for review see Segal and Bloom, 2001). Budding yeast, probably due to its relatively small size (4-7μm) utilises the actin cytoskeleton to polarise growth to a single point of growth by the transport of cellular components to and from the cell cortex.

In contrast to other eukaryotes, interactions between the microtubule and actin cytoskeletons in budding yeast are limited. An example of a protein that may bind both actin and microtubules is coronin. Coronin is a highly conserved actin-binding

protein found in *S. cerevisiae* that binds microtubules *in vitro,* and Δ*crn1* yeast display microtubule defects (Goode *et al* 1999). One example of interaction occurs during early bud growth as the mitotic spindle orients through microtubule-actin interactions (Palmer *et al* 1992, Theesfield *et al* 1999).

1.4. Actin

Actin is a highly conserved and ubiquitous eukaryotic protein which plays a fundamental role in many diverse and dynamic cellular processes. Actin is a globular protein (G-actin) that polymerises into filaments (F-actin) for its biological function.

Actin is encoded by a large, highly conserved gene family. In vertebrates there are six, multiple tissue-specific isoforms encoded by a family of actin genes. There are three classes of actin, classified according to their isoelectric point, called α-, β-, and γ-actins. Four α-actin isoforms are found in various types of muscle, whereas β- and γ-actins are expressed in non-muscle cells. Some plants have as many as 100 actin isoforms (Meagher and Williamson 1994).

Recently, a protein called MreB has been identified in rod-shaped bacteria that assembles into filaments with a helical repeat similar to that of eukaryotic F-actin. Crystallisation of the protein allowed the visualisation of actin-like strands at atomic resolution. Such studies revealed that MreB has similar secondary and tertiary structure to actin. The MreB protein has actin-like properties and forms large fibrous

spirals under the cell membrane of rod-shaped cells, where they are involved in cell morphology (van den Ent *et al* 2001).

Although there are subtle differences in the properties of different forms of actin, the amino acid sequences have been highly conserved in evolution, for example there are no amino acid substitutions between chicken skeletal muscle and human skeletal muscle actin (Orlova *et al*, 2001). *In vitro* tests performed on the various isoforms showed that they could assemble into filaments that are essentially identical (Alberts *et al* 1996). The different functions that the actin isoforms are able to perform, even within the one cell type, depends largely on the interactions actin can make with actin binding proteins, thus allowing different actin structures to co-exist.

1.4.1. G-actin Structure

Each G-actin molecule is a single polypeptide approximately 375 amino acids long which binds a divalent ion complexed with either ATP or ADP (figure 1.1). High-resolution crystal structures of G-actin bound to actin-binding proteins DNaseI, gelsolin and profilin have been used to help determine the three-dimensional structure of actin (Kabsch *et al* 1990, McLaughlin *et al* 1993, Schutt *et al* 1993). These X-ray crystallographic analyses revealed that G-actin is separated by a central cleft, into two approximately equal-sized domains each composed of two subdomains. The subdomains are numbered I – IV. Mg^{2+} and ATP bind at the bottom of the cleft, and the nucleotide contacts both domains. The N- and C-termini lie in subdomain I. There is some flexibility in the actin monomer as the base of the cleft acts as a hinge that

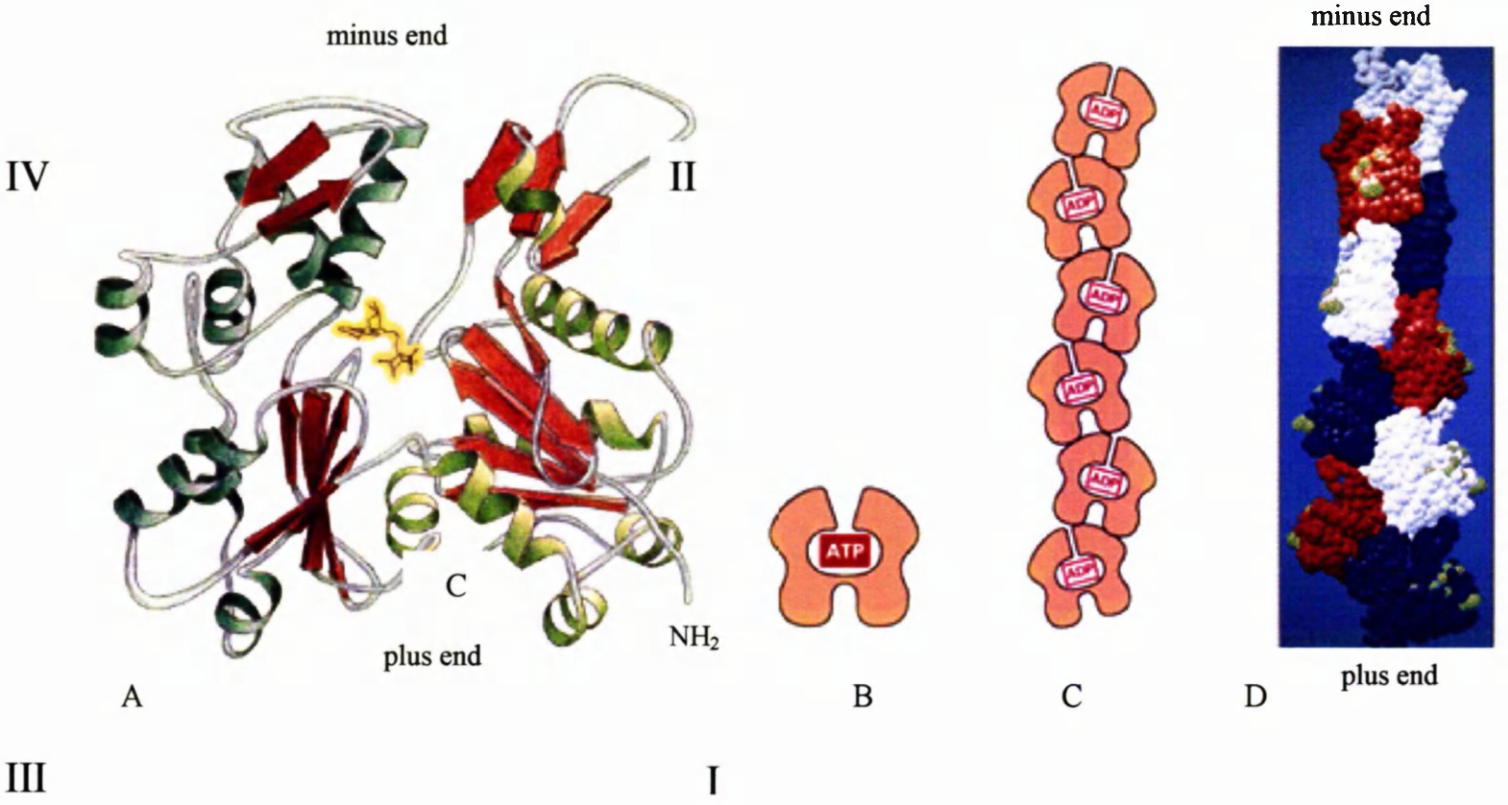

Figure 1.1. Structure of globular and filamentous actin. (A) Ribbon diagram of the actin monomer showing subdomains marked I to IV and amino and carboxy terminii marked N and C respectively. The yellow stick model shows the adenine nucleotide. (B) Cartoon of an actin monomer with ATP bound which assembles into (C) filamentous actin with the accompanying hydrolysis of ATP into ADP. (D) Filamentous actin is composed of uniformly oriented globular actin monomers. Adapted from Alberts *et al* 1996.

allows the large domains to flex relative to each other. The conformation of G-actin is affected when ATP or ADP binds.

1.4.2. F-Actin Has Structural and Functional Polarity

The first atomic model of F-actin (Holmes *et al* 1990) was constructed from the atomic structure of the actin monomer fitted to the observed X-ray fibre diffraction data from oriented gels of F-actin. Electron micrographs show negatively stained actin filaments appearing as long, flexible, and twisted strands of beaded subunits.

The polarity of actin filaments has been demonstrated by electron microscopy in so-called "decoration" experiments (Moore *et al* 1970). In this type of experiment, the globular head domain of myosin (which binds specifically to actin filaments) is mixed with actin filaments. Myosin attaches to the sides of a filament with a slight tilt, and appears arrowhead-shaped. Under electron microscopy, when all subunits are bound by myosin, the actin filament appears coated ("decorated") with arrowheads that all point toward one end of the filament.

As all the actin subunits in F-actin have the same polarity, the actin filament has two structurally different ends (figure 1.1d). Since the ATP-binding cleft is oriented in the same direction in all actin subunits in the filament, the ATP-binding cleft of the actin subunit is exposed to the surrounding solution at one end of the filament. This end is designated the minus end or pointed end. At the opposite end, the plus end or barbed end, the cleft contacts the neighbouring actin subunit. The descriptions 'barbed end'

and 'pointed end' for the ends of the actin filament arose from the myosin decoration experiments.

1.5. Tools for studying the yeast actin cytoskeleton

Actin is encoded by the single, essential gene *ACT1* in *S. cerevisiae* (Shortle *et al* 1982). Yeast actin is 88 % identical at the amino-acid level with rabbit muscle actin (Gallwitz and Sures 1980, Ng and Abelson 1980) and is biochemically similar to it (Nefsky and Bretscher 1992, Kron *et al* 1992, Cook *et al* 1992), so studies of yeast actin are potentially relevant to all eukaryotic organisms.

A wide range of genetic, cell biological and biochemical techniques exist to study the actin cytoskeleton of *S. cerevisiae* (reviewed in Ayscough and Drubin 1996). The following sections will discuss some of the techniques available relevant to this study.

1.5.1. Genetic techniques to find and analyse cytoskeletal genes and proteins

The advantage of using genetic methods in yeast is that it is easy to isolate, identify and manipulate mutations. *S. cerevisiae* has a single essential gene encoding actin, which can be replaced with mutant alleles by homologous recombination (Shortle *et al* 1982). The mutant actin allele can therefore be assessed as the sole source of actin in the cell. A set of *ACT1* mutants were systematically constructed by clustered charged-to-alanine scanning mutagenesis, a procedure designed to alter residues on the surface of the molecule in order to maximise the probability of disrupting specific

interactions with actin-associating proteins (Wertmann *et al* 1992). The functions and interactions of actin that have been determined using the alleles generated by the alanine scan have been particularly useful and have identified the binding sites on actin for both actin-binding proteins and actin-associating drugs (Drubin *et al* 1993, Holtzman *et al* 1994, Honts *et al* 1994, Amberg *et al* 1995, Karpova *et al* 1995, Smith *et al* 1995, Ayscough *et al* 1997).

Other cytoskeletal genes can be manipulated in this way. Yeast mutants are then assessed for viability (which determines if the gene is essential) or if the mutation is conditional.

S. cerevisiae contains many genes that encode proteins associated with the actin cytoskeleton and these act together to perform a common function. Mutation or deletion of any of them can produce a common mutant phenotype (Novick and Botstein 1985). Actin cytoskeleton mutants exhibit temperature-conditional phenotypes e.g. heat sensitivity so cannot grow well at higher temperatures. Other phenotypes commonly exhibited include randomised bud site selection in diploid cells, hypersensitivity to osmotic pressure in the medium, slow growth, impaired endocytic function and most obviously, a disrupted actin cytoskeleton when visualised by microscopy (see chapter 3).

Domain deletions are particularly interesting as a single protein can be multi-functional and have separable functional protein domains that perform different functions. Deletion of one domain will result in a partially functional protein, allowing the role of the deleted domain to be inferred. Functional redundancy in the

yeast actin cytoskeleton exists where these multifunctional proteins contain domains associated with similar functions in other proteins (section 1.15.3).

Synthetic-lethality occurs when deletions or mutations in single genes produce viable cells but in combination are lethal. This phenomenon is very common among genes that affect parallel processes in the cell (section 1.15.1).

1.5.2. The use of actin binding drugs to study the actin cytoskeleton

1.5.2.1. Phalloidin

Phallotoxins are a group of bicyclic heptapeptides from poisonous mushrooms (Wieland and Faulstich 1978). Phalloidin is the major representative of this group and binds to actin filaments much more tightly than to actin monomers (Estes *et al* 1981). The binding site for phalloidin on actin was determined using an actin mutant and by modelling to be at residues 177 and 179 (Drubin *et al* 1993, Lorenz *et al* 1993). These residues lie proximal to the interface between two or three actin monomers in the filament and so the stabilisation of actin filaments by phalloidin binding *in vitro,* appears to occur by binding the monomers at this interface. Fluorescent derivatives of phalloidin have been extremely useful for localising actin filaments in living and fixed cells and visualising actin filaments *in vitro* (Wulf *et al* 1979, Yanagida *et al* 1984).

1.5.2.2. Latrunculin-A

Latrunculin-A (LAT-A) is a drug, extracted from the Red Sea sponge *Latrunculia magnificans,* that disrupts filamentous actin structures. LAT-A acts by sequestering actin monomers (forming a 1:1 complex), which are then prevented from repolymerising into actin filaments. This effect is rapid, reversible and specific (Ayscough *et al* 1997). It binds monomeric actin close to the nucleotide-binding site and this subsequently restricts the rotation of subdomains II and IV which is necessary for polymerisation (Morton *et al* 2000).

Studies using LAT-A on the yeast actin cytoskeleton have demonstrated that yeast actin filaments are highly dynamic, undergoing rapid cycles of assembly and disassembly *in vivo* (Ayscough et a 1997). Treatment of yeast cells with LAT-A causes the complete disruption of the actin cytoskeleton within 2 – 5 minutes (section 2.8.10). By adding LAT-A, the actin monomers are sequestered and so prevented from adding to the filamentous actin. This consequently prevents the assembly step into new filaments.

Several yeast strains with mutant actin-associated proteins display different sensitivities to LAT-A (Ayscough *et al* 1997). Mutations in proteins that normally act to stabilise the actin cytoskeleton, such as fimbrin, have an increased sensitivity to LAT-A as there is a larger pool of free actin monomers in these yeast. In contrast, mutations in proteins which normally act to destabilise filamentous actin structures cause cells to have a decreased sensitivity to LAT-A, as these mutant yeast are expected to have increased levels of F-actin, which is also less dynamic. Differences

in sensitivity to LAT-A could therefore indicate whether a given protein acts in a stabilising or destabilising capacity *in vivo* (see section 3.8).

1.5.3. Techniques to isolate interacting proteins

Protein-protein interactions can be studied by a variety of methods including biochemical methods, affinity co-purification and co-immunoprecipitation. Affinity chromatography using polymerised actin has identified several proteins that interact with F-actin, such as Abp1p (Drubin *et al* 1988) and tropomyosin (Liu and Bretscher 1989). Immunoprecipitation relies on either isolating purified protein on inert substrate directly using specific antibodies or a tagged-protein by antibodies directed against the tag (e.g. myc or HA (haemagluttinin)), then adding cell extract to allow cellular proteins to bind. Alternatively, ground cell extract can be applied directly. Interacting proteins can then be identified by screening a western blot with a panel of antibodies or by MALDI-TOF MS.

The two-hybrid system is a genetic approach to isolating interacting proteins (Fields and Song 1989, Chien *et al* 1991). This technique utilises the fact that many eukaryotic transcriptional activators, including those in yeast, consist of two discrete modular domains, a DNA-binding domain and an activation domain. The protein of interest is cloned in such a way that it is expressed as a fusion to a DNA binding domain. A second protein (or library of proteins) is cloned so that it is expressed as a fusion to the activation domain. Interaction between two proteins brings the DNA binding peptide together with the activation domain, and initiates transcription of the

reporter genes, usually a nutritional gene required for growth. Variations of the two-hybrid system can use different DNA binding domains, activation domains and reporters. Interacting proteins can then be identified quickly due to the availability of the genomic yeast sequence (http://genome-www.stanford.edu/Saccharomyces/). The two-hybrid system can also be used to narrow down the sites of interaction by mutagenesis of the proteins of interest (Amberg *et al* 1995).

1.6. F-Actin structures in *S. cerevisiae*

Polymerised actin structures can be visualised in yeast by fluorescent-labelling using immunofluorescent microscopy with anti-yeast actin antibodies, or with rhodamine-phalloidin, a fluorochrome-labelled phallotoxin that specifically binds filamentous actin structures (Wulf *et al* 1979, Adams and Pringle 1991). Both methods reveal two morphologically different filamentous actin structures, actin cables and cortical actin patches. Actin cables are long bundles of actin filaments, as their name suggests, which are aligned along the periphery of the cell. Cortical actin patches appear as discrete patches also at the periphery, or cortex of the cell (Adams and Pringle 1984, 1991, Amberg 1998).

Both structures are composed of F-actin and a large variety of different actin-binding and associated proteins that regulate actin dynamics and organisation (table 1.1). Assembly of both types of structures is regulated spatially and temporally during bud emergence, mating and pseudohyphal growth.

1.6.1. Cortical actin patches

Cortical actin patches are highly motile structures with velocities of up to 0.5 μm/second (Doyle and Botstein 1996, Waddle *et al* 1996) that concentrate at sites of polarised growth during the yeast cell cycle where they appear to be involved in secretion and endocytosis (Geli and Reizman 1998, Wendland *et al* 1998). Actin patches contain many actin-binding and regulatory proteins as listed in table 1.1., including capping proteins (Cap1p and Cap2p)(section 1.8.3), fimbrin (Sac6p)(section 1.8.6), cofilin (Cof1p), coronin (Crn1p), protein kinases (Ark1p and Prk1p)(section 1.15.5), myosin I proteins (Myo3p and Myo5p)(section 1.8.8), a myosin I-binding protein (Vrp1p), actin nucleation proteins (Arp2/3 complex)(section 1.10), and actin nucleation regulators (Las17p/Bee1p) (section 1.14.2) and Abp1p (section 1.14.1) (for review see Pruyne and Bretscher 2000b).

Cortical actin patches move across the plasma membrane (Waddle *et al* 1996). However, the mechanisms underlying the rapid changes in cortical actin distribution that occur during cell polarisation have not yet been elucidated. Actin patch motility does not require the myosin motor proteins (Waddle *et al* 1996) but does require the Arp2/3 complex (Winter *et al* 1997) suggesting that actin polymerisation may be important. Latrunculin-A studies have shown that F-actin turnover in cortical patches is highly dynamic and F-actin turns over within 10 seconds (Karpova *et al* 1998). However actin patch dynamics are not altered in a mutant yeast strain with stabilised actin filaments which indicates that movement may not be driven by actin polymerisation (Belmont and Drubin, 1998). Recent observation, by Smith and

Table 1.1 Actin cytoskeletal and polarity determinants

Protein name	**Homologies and motifs**
Cortical patch components	
Abp1p (sections 1.9.1.3 and 1.14.1)	Cofilin related, SH3 domains
Act1p (section 1.6)	Actin
Aip1p	Actin-interacting protein 1
Arp2p, Arp3p, Arc15p, Arc18p, Arc19p, Arc35p, Arc40p (section 1.10)	Arp2p-Arp3p complex
Cap1p, Cap2p (1.8.3)	Actin capping proteins αβ
Cof1p (1.8.2)	Cofilin
Crn1p	Coronin
End3p	Eps 15 homology
Ent1p, Ent2p, Ent3p, Ent4p	Epsins
Hog1p	p38 (MAPK)
Las17p/Bee1p (section 1.10 and 1.14.2)	WASP (Wiskott-Aldrich syndrome protein)
Myo3p, Myo5p (section 1.8.8)	Myosin I, SH3 domain
Pan1p/Dim2p (section 1.15.5)	Eps 15 homology, binding repeats
Prk1p, Ark1p (section 1.15.5)	Cyclin-G-associated kinase
Rvs161p/End6p, Rvs167p	Amphiphysins,
Sac6p (section 1.8.6)	Fimbrin
Sla1p (section 1.15)	3 SH3 domains
Sla2p/End4p (section 1.14.3)	Talin-related, Hip1
Srv2p	Adenylyl-cyclase-associated protein
Twf1p (section 1.8.2)	Cofilin-like repeats
Vrp1p/End5p	WIP (Wasp Interacting Protein), proline rich
Yap1801p, Yap1802p	AP180 (clathrin assembly protein 180)
Yfr024c-a, Ysc84p (chapter 4 and 5)	Ysc84 homology domain, SH3 domain
Actin Cable components	
Act1p	Actin
Bni1p, Bnr1p	Formin, 3 FH domains, GBD, DAD
Sac6p	Fimbrin
Tpm1, Tpm2p (section 1.8.5)	Tropomyosin
Myo2p (section 1.8.8)	Myosin V
Other cytoskeletal and polarity determinants	
Axl2p	
Bem1p	2 SH3 domains
Bni1p/Bnr1p	Formin
Bni4p	
Bud2p	RasGAP
Bud3p	

Table 1.1. Actin cytoskeletal and polarity determinants (continued)

Protein name	Homologies and motifs
Other cytoskeletal and polarity determinants	
Bud4p	
Bud6p/Aip3p	
Cdc24p	RhoGEF, PH (plekstrin homology) domain
Cdc3p, Cdc10p, Cdc11p, Cdc12p, Shs1p/Sep7p	Septins
Cdc42p	Cdc42p RhoGTPase
Chs2p, Chs3p, Chs4p	Chitin synthase subunits
Cmd1p	Calmodulin
Cla4p, Ste20p, Skm1p	p21-activated kinase, CRIB (Cdc42p/Rac-interacting binding) domain, PH domain
Gks1p, Gsc2p	1,3-β-glucan synthases
Gic1p, Gic2p	CRIB domain
Hsl1p, Gin4p, Kcc1p	Nim1-related kinases
Hof1p/Cyk2p	PSTPIP
Iqg1p/Cyk1p	IQ-GAP
Kar9p	
Mlc1p	Myosin light chain
Myo1p	Myosin II
Myo2p, Myo4p (1.8.8)	Myosin V
Pea2p	
Pfy1p	Profilin
Rho1p	RhoA
Rho3p	Rho GTPase
Rom2p	RhoGEF, PH domain
Sec1p	Sec1/UNC18/Rop
Sec3p, Sec5p, Sec6p, Sec8p, Sec10p, Sec15p, Exo10p, Exo84p	Exocyst
Sec4p	Rab8
She3p	
Slt2p/Mpk1p	MAPK
Smy1p	kinesin-related
Spa2p, Sph1p	Spa2p-box
Yck2p	Casein kinase I
Wsc1p	Transmembrane

Adapted from Pruyne and Bretscher (2000b).
Proteins highlighted in bold are discussed further elsewhere

colleagues 2001, of the life cycle of Abp1p-GFP-labelled actin patches in living *S. cerevisiae* cells indicated that cortical actin patches do not move to sites of polarised growth but are instead assembled there. Movement away from sites of active cell surface growth in contrast results in the disassembly of actin patches. The lifetime of these patches was measured to be 10.9±4.2 seconds. Proteins involved in Arp2/3 actin polymerisation, the type I myosins and Vrp1p appear to be required for late stages of this actin patch assembly process at polarisation sites.

1.6.2. Actin cables

Actin cables are bundles of actin filaments that align along the mother-bud axis during cell polarisation and are involved in processes such as organelle inheritance and vesicle targeting (Drubin *et al* 1993, Simon *et al* 1997). Actin cables consist of F-actin and contain fimbrin (Sac6p)(section 1.9.6), tropomyosin (Tpm1p and Tpm2p) section 1.8.5)(and the myosin V proteins (Myo2p and Myo4p)(section 1.8.8)(table 1.1). Actin cables are essential as cells lacking cables due to loss of the function of both tropomyosin isoforms or Act1p undergo lethal arrest as large unbudded cells (Drees *et al* 1995).

Recent studies have demonstrated that the formation of polarised actin cables depends on a family of proteins called formins (Evangelista *et al* 2002, Sagot *et al* 2002). The formins in budding yeast are encoded by *BNI1* and *BNR1* and are conserved Rho-GTPase effectors that communicate Rho-GTPase signals to the cytoskeleton (Evangelista *et al* 1997, Kohno *et al* 1996). Profilin binds to formin

homology motifs in Bni1p and Bnr1p and is required for cable assembly. However, unlike cortical actin patches, the Arp2/3 complex is not required for cable assembly (Evangelista *et al* 2002).

1.7. Actin polymerisation and depolymerisation

The assembly (polymerisation) and disassembly (depolymerisation) of actin filaments occurs by the addition and removal of actin subunits from the filament ends. A solution of G-actin can be induced to polymerise into actin filaments *in vitro* by the addition of ions, Mg^{2+}, K^{+} or Ca^{2+}(Greer and Schekman, 1982a, 1982b). Equally, the reverse reaction, depolymerisation, will occur if the ionic strength of the solution is lowered .

1.7.1. Actin polymerization *in vitro* proceeds in three phases.

There are three phases for *de novo* G-actin polymerisation *in vitro* (figure 1.2.a), nucleation, elongation and steady state. The initial phase of polymerisation, known as nucleation, requires the formation of a 'nucleus' of three actin monomers. The formation of actin dimers, and then trimers is the rate limiting step (or lag phase) of polymerisation. Once a stable trimer of actin is formed, polymerisation proceeds. Addition of actin monomers occurs at different rates at each end of the actin filament. The plus, or barbed end of the filament, elongates five to ten times faster than does the opposite end, the minus or pointed end. This difference is due to the kinetic rate constants for polymerisation and depolymerisation being greater at the barbed end.

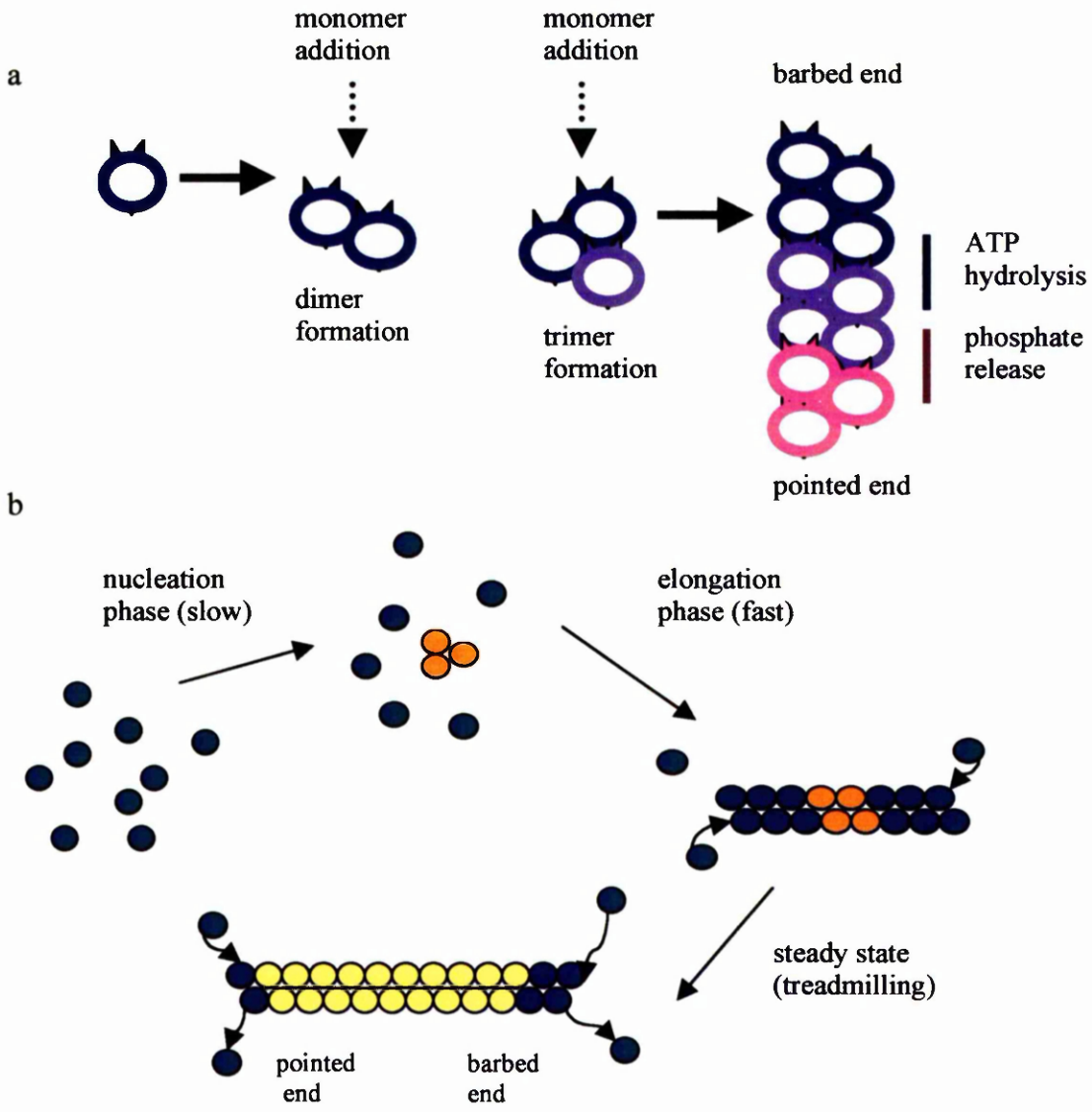

Figure 1.2. The polymerisation of actin monomers into actin filaments. (a) During the initial nucleation phase, ATP-G-actin monomers (blue) slowly form stable trimeric complexes which are then more rapidly elongated in the second phase of polymerisation Shortly after their incorporation into a filament, subunits slowly hydrolyse ATP to ADP and unreleased-phosphate(Pi) (purple).The 'oldest' or pointed end contains ADP-bound monomers from which the Pi has been released (pink). The actin filament displays polarity as G-actin adds primarily to the barbed end and loss occurs mainly at the pointed end. Adapted from May 2001. (b) There are three phases for *de novo* G-actin polymerisation *in vitro*; nucleation, elongation and steady state.

The critical concentration (C_c) values at the two ends are described as C_c (pointed end) > C_c (barbed end). The C_c for actin polymerisation is the free actin monomer concentration at which the proportion of actin in polymer stops increasing. The process where the actin polymer maintains constant length despite a net flux through the polymer is called treadmilling (figure 1.2.b). Steady state is achieved and the polymer maintains a constant length because the rate at which actin molecules are coming off the pointed end is identical to the rate at which they are adding to the barbed end.

1.8. The dynamic assembly and disassembly of actin filaments is controlled by actin binding proteins

Signalling pathways such as those that regulate actin assembly are governed largely by dynamic interactions between proteins. Proteins that bind the filament ends and/or the sides of actin filaments have specific effects on actin polymerisation/ depolymerisation events (figure 1.3) (for reviews see Cooper and Schafer, 2000, Ayscough 1998).

Actin dynamics can be regulated by severing/depolymerisation of filaments (Arber *et al* 1998, Yang *et al* 1998) capping and uncapping filament ends (Hartwig *et al.* 1995), and by *de novo* nucleation (Zigmond, 1998). Actin filaments can also be stabilised by actin binding proteins for example by bundling filaments together or by crosslinking. Proteins that bind to monomeric actin also play a significant role by regulating the amount of free actin available to bind to free filament ends. In a cell, in contrast to *in*

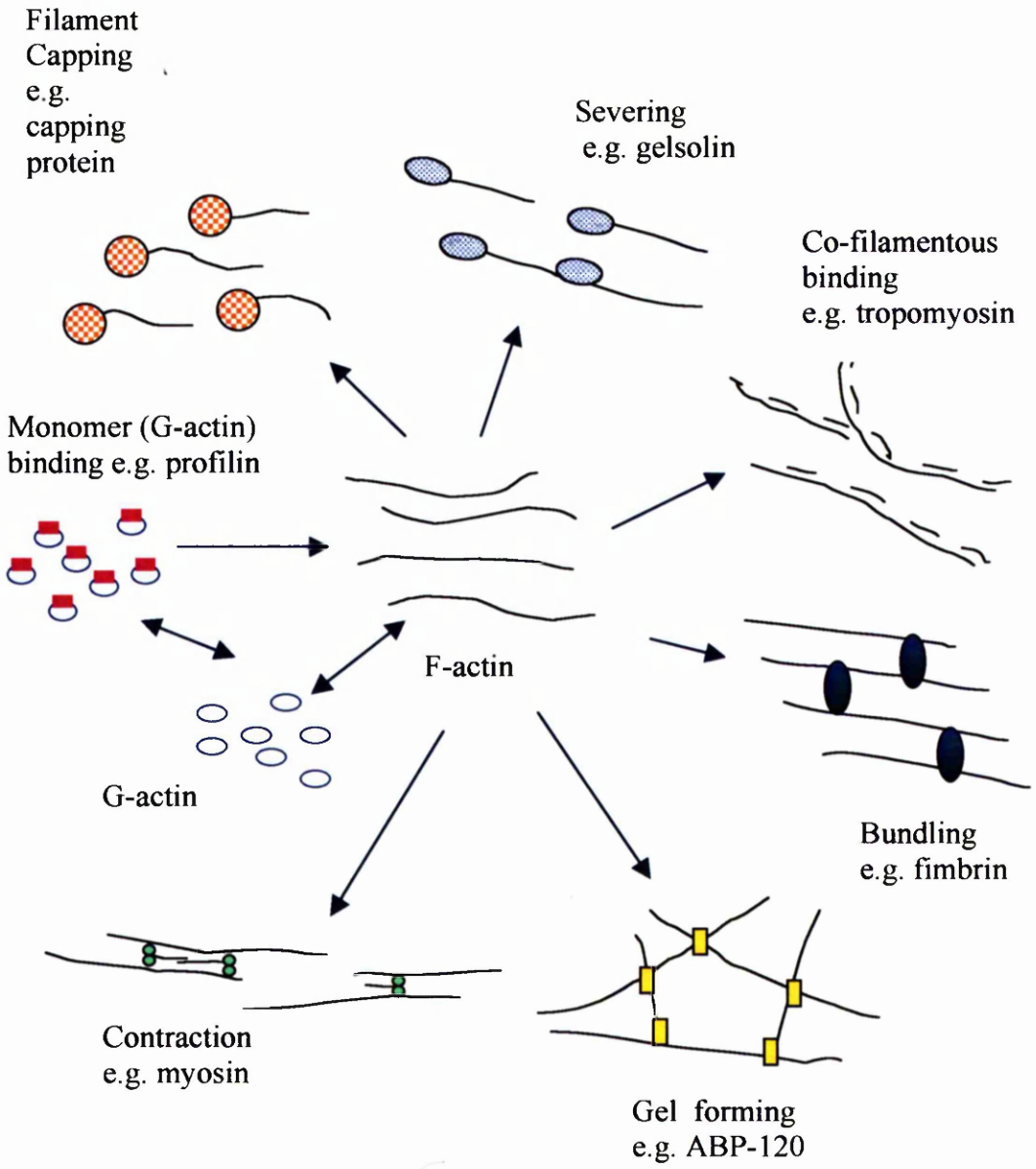

Figure 1.3. The function of actin-binding proteins regulates actin filament structure. Specific functions of actin-binding proteins as determined by *in vitro* research are shown with a diagram of how each protein may interact with F-actin. Adapted from Ayscough 1998.

vitro studies which use a limited number of purified proteins, accessory proteins greatly amplify the different kinetics and affinities of the two filament ends (Carlier and Pantaloni 1997).

1.8.1. Actin monomer binding by profilin

Profilin is a low molecular weight protein (12-15 kDa) found in a wide range of organisms (reviewed in Ayscough 1998). It was originally thought to simply bind and sequester G-actin thus reducing the availability of monomeric actin to growing actin filaments (Carlsson *et al* 1977). The function of profilin appears to be more complex. It also influences the dynamics of actin filaments *in vitro* by enhancing nucleotide exchange on actin (Mockrin and Korn, 1980, Goldshmidt-Clermont *et al* 1991) and promoting barbed-end assembly (Pantaloni and Carlier, 1993, Kang *et al.* 1999). Profilin has numerous binding partners: the Arp2/3 complex (section 1.7) was discovered by affinity-chromatography as a result of this interaction (Machesky *et al* 1994). Experiments using cell extracts from higher organisms have shown that Cdc42-induced actin polymerisation is enhanced by profilin in an Arp2/3 complex dependent manner (Ma *et al* 1998, Mullins and Pollard 1999, Yang *et al* 2000, Wolven *et al* 2000). *In vivo* studies in several organisms have suggested a role for profilin in promoting actin filament formation (Verheyen and Cooley, 1994, Theriot and Mitchison, 1993).

S.cerevisiae profilin is encoded by a single gene *PFY1*. Yeast that lack profilin grow extremely slowly, become large and rounded, lack detectable actin cables and no longer polarise their patches to the bud (Haarer *et al* 1990). Profilin and cofilin

(section 1.8.2) act synergistically *in vivo* to control actin dynamics by regenerating ATP actin from ADP actin-cofilin generated during filament disassembly (Wolven *et al* 2000). Profilin interacts directly with proteins containing formin homology domains, Bni1p and Bnr1p which are downstream targets of the Rho family small G-protein Cdc42p (Kohno *et al* 1996, Evangelista *et al* 1997, Imamura *et al* 1997).

1.8.2. Regulation of actin assembly by promoting depolymerisation

The dynamic nature of the actin cytoskeleton demands that disassembly of actin filament is as crucial as assembly for actin remodelling. Actin filament disassembly is mediated by members of the ADF (actin depolymerising factor)/cofilin family found ubiquitously in eukaryotes (reviewed in Theriot 1997, Maciver 1998a, Bamburg *et al* 1999, Southwick 2000). Members of the ADF/cofilin family bind to actin monomers *in vitro* and stimulate depolymerisation. ADF/cofilin may act in two ways: by severing which results in more filament ends that disassemble (Maciver *et al* 1998b); and by increasing the off-rate of actin subunits from filament ends (figure 1.4) (Carlier *et al*, 1997b, Maciver *et al* 1998b).

Yeast cofilin is encoded by the essential gene *COF1* and is 40 % identical to mammalian ADF/cofilin and localises to cortical actin patches (Moon *et al* 1993, Iida *et al* 1993). *In vivo*, LAT-A studies using partial loss-of-function mutants have shown cofilin to promote rapid actin filament turnover via stimulating disassembly of F-actin (Lappalainen and Drubin 1997, Lappalainen *et al* 1997). A protein regulator of ADF/cofilin, Aip1p (actin-interacting protein) from yeast can bind to both actin and

cofilin. Aip1p restricts the localisation of cofilin to cortical actin patches and acts as an enhancer of cofilin's actin depolymerisation activity (Rodal *et al* 1999).

An actin monomer binding protein that contains two cofilin-like regions called twinfilin has also been identified in *S. cerevisiae* which is involved in the regulation of the cortical actin cytoskeleton (Goode *et al* 1998). Despite its similarity to cofilin, twinfilin has no significant effect of dissociation of actin monomers from filament ends and instead acts to sequester monomers. This activity, combined with cofilin function may be used to maintain a pool of actin monomers available for assembly (Palmgren *et al* 2002).

1.8.3. Regulation of actin polymerisation by capping proteins

Actin binding proteins that bind (or cap) filament ends prevent the addition and removal of actin monomers (figure 1.3). Actin filament barbed ends are found localised to sites undergoing dynamic actin assembly such as at the leading edge of motile cells or at the motile pathogenic bacteria *Listeria monocytogenes* to produce actin 'comet' tails. Outwith these areas, capping protein binds to the barbed end of the majority of actin filaments in the cell consequently preventing filament growth. Actin polymerisation is effectively 'funnelled' to a specific area within the cell, generating the force required for directed movement of some cell types (figure 1.4) (Gouin *et al* 1998, Hug *et al* 1995). Capping protein acts in a regulatory capacity. Actin filament growth in a cell extract system, induced by the small GTPase Cdc42p, was shown to be inhibited by capping protein binding to filament barbed ends (Huang *et al* 1999). *In vitro* studies have shown that capping protein is removed from

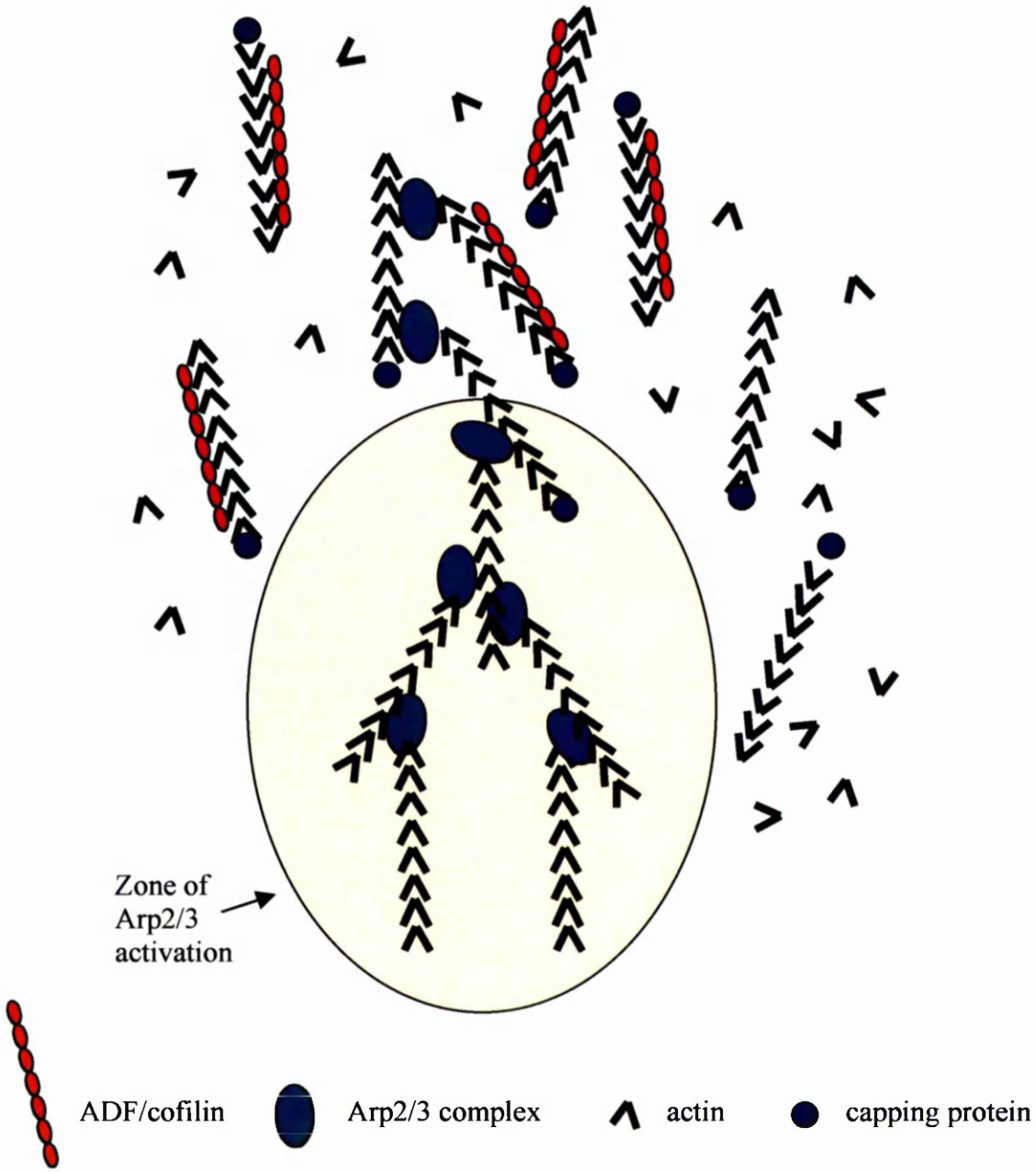

Figure 1.4 – Stimulation of actin polymerisation model. Actin polymerisation is activated within a zone of signals that activate the Arp2/3 complex. Filaments nucleated by the Arp2/3 complex in the active zone have free barbed ends and capped pointed ends. Capping protein is inhibited in the active zone. ADF/cofilin binds preferentially to older actin filaments that contain ADP which then increases the dissociation rate of actin subunits from pointed ends. ADF/cofilin binding may also increase the dissociation of the Arp2/3 complex due to altered filament structure. Actin monomers lost from the pointed end are available to add to new barbed ends. Actin polymerisation is 'funneled' to the active zone because free barbed ends are created there and because older barbed ends are capped by capping proteins. Adapted from Cooper and Schafer 2000.

the actin filament barbed end by phosphoinositides demonstrating another means of regulation (Schafer *et al* 1996).

CAP1 and *CAP2* encode the two capping proteins in *S.cerevisiae*. Cells deleted of *CAP1* or *CAP2* are viable, but lethal in combination with *sac6* null mutation (Adams *et al* 1993). *CAP2* mutant cells exhibit a loss of capping activity, abnormal cortical actin distribution, absence of actin cables and morphological defects (Amatruda and Cooper 1992, Amatruda *et al* 1992, Karpova *et al* 1995).

1.8.4. Gelsolin

Gelsolin is activated by μM Ca^{2+} to bind and sever actin filaments. Gelsolin caps the actin filament barbed end *in vitro* after severing preventing assembly and disassembly at this end (Yin *et al* 1981). The severing activity of gelsolin creates free barbed ends and so induces actin polymerisation (Cooper and Schafer, 2000). Actin polymerisation can also be induced *in vitro* by the dissociation of gelsolin from the barbed ends by the activation of the small GTP-binding protein Rac or phosphotidylinositol 4,5-bisphosphate (reviewed in Weeds and Maciver 1993, Arcaro 1998). In cells, gelsolin transiently associates with actin, indicating that its primary function is severing rather than barbed end capping (Howard *et al* 1990, Qiao *et al* 1999). There is no gelsolin homologue in *S.cerevisiae*. The only severing activity is that of cofilin (section 1.8.2).

1.8.5. Tropomyosin

Tropomyosins are found ubiquitously and bind along actin filaments and serve to stabilise filaments. In muscle cells tropomyosin regulates the interaction between myosin and actin. Tropomyosin is encoded in *S.cerevisiae* by *TPM1* and *TPM2* which have partially overlapping functions and deletion of both genes is lethal (Drees *et al* 1995). Tropomyosin appears to play a role in the stabilisation of actin filaments as deletion of *TPM1* (but not *TPM2*) causes loss of cytoplasmic actin cables and aberrant cell morphologies (Liu and Bretscher 1989).

1.8.6. Bundling of actin filaments by fimbrin

Actin bundles have profound effects on cellular shape, division, adhesion, motility, and signalling. Fimbrin belongs to a large family of actin-bundling proteins and is involved in the formation of tightly ordered cross-linked bundles by binding to two actin filaments simultaneously (figure 1.3).

S.cerevisiae contains a sole actin-bundling protein, a fimbrin homologue, encoded by *SAC6* (Adams *et al* 1989). Sac6p is the only protein found associated with both actin cables and the cortical actin patches. Deletion of the *SAC6* gene produces temperature sensitive cells that have aberrant actin structures and cell morphology (Adams *et al* 1991). These mutant yeast cells are also fragile (Adams *et al* 1991) and have defective endocytosis (Kubler and Reizman, 1993) which indicate a role for Sac6p in strengthening actively growing regions by forming stable actin networks. Sensitivity

of the null mutant to LAT-A (section 1.5.2.2) also suggests that Sac6p stabilises the actin cytoskeleton (Ayscough *et al* 1997).

1.8.7. Cross-linking by ABP-120 and α-actinin

Proteins that have the ability to self-associate and to bind actin at an exposed site on the filament should crosslink filaments. *S.cerevisiae* does not contain cross-linking protein homologues. However, actin crosslinking activity in more complex eukaryotes creates diverse actin filament assemblies.

Dictyostelium has several proteins with cross-linking activities. *In vivo* studies have shown that double mutants in the gelation factor, actin-binding protein 120 (ABP-120) and α-actinin have enlarged, more rounded cells which are osmotically sensitive and show a reduced rate of phagocytosis. Development is blocked before the fruiting body stage and motility is reduced.

α-actinin was first isolated from rabbit skeletal muscle (Ebashi and Ebashi 1965) and has subsequently been found in both muscle and non-muscle cells from a variety of organisms (Critchley and Flood 1999). α-actinin forms a homodimer of antiparallel polypeptides. α-actinin mutants produce mild phenotypes suggesting redundancy with other proteins.

1.8.8. Myosin

Myosins are a large family of proteins characterised by actin-based motor activity. The best characterised is that found in muscle myofibrils where F-actin is assembled

into thin filaments which interact with the myosin II heads of the thick filaments to produce contraction.

There are five genes in *S. cerevisiae* that code for myosins, *MYO1-MYO5*. In budding yeast, unconventional myosins of the class V type (Myo2p and Myo4p) are non-processive barbed end directed motor proteins that use actin cables as tracks for polarised movement of organelles and vesicles (section 1.13.2) (Johnston *et al* 1991, Govindan *et al* 1995, Hill *et al* 1996).

The yeast type I myosins (Myo3p and Myo5p)(figure 1.7b) associate with cortical patches and are required for the uptake step of endocytosis and the polarisation of the actin cytoskeleton (Goodson and Spudich 1995, Geli and Reizman 1998, Goodson *et al* 1996). Myo3p and Myo5p are proposed to play a role with verprolin in regulating actin polymerisation *in vitro* and *in vivo* (Evangelista *et al* 2000, Lechler *et al* 2000, Geli *et al* 2000).

The MYO1 gene codes for a heavy chain myosin which is similar to conventional class II myosins found in both muscle and non-muscle cells. Myo1p is necessary for deposition of chitin and cell wall components necessary for cell separation, and for the maintenance of cell-type specific budding patterns (Rodriguez and Paterson 1990).

1.9. The Arp2/3 complex regulates actin polymerisation in eukaryotes

The Arp2/3 complex is a multi-functional 220 kDa protein complex that directly promotes the rapid generation of new actin filaments (figure 1.5) (for review see May 2001). It was originally identified in a search for binding partners of profilin (Machesky *et al* 1994) and has since been found to be one of the most important players in remodelling the actin cytoskeleton. The complex is composed of seven subunits, including two actin-related proteins, Arp2 and Arp3, and five further subunits that have different molecular weights in different species (Machesky and Gould 1999). The complex appears to be conserved in all eukaryotes and has been purified from *Acanthamoeba castellanii* (Machesky *et al* 1994), *S. cerevisiae* (Winter *et al* 1997), *Xenopus laevis* (Ma *et al* 1998), and humans (Welch *et al* 1997).

In contrast to the capping proteins described above (section 1.6.1.) which bind to the barbed end of filaments, the Arp2/3 complex caps the pointed end of actin filaments (Mullins *et al* 1998). Filaments then elongate at the fast-growing barbed end. The Arp2/3 complex plays an important role in the nucleation of actin filaments. The complex is proposed to act as a 'pseudo barbed end' as the similarity of the Arp2 and Arp3 subunits to actin allow it to mimic an actin dimer (Kelleher *et al* 1995). Addition of one actin monomer to the Arp2/Arp3 heterodimer would form an actin trimer, thereby bypassing the kinetically unfavourable dimerisation step in actin polymerisation.

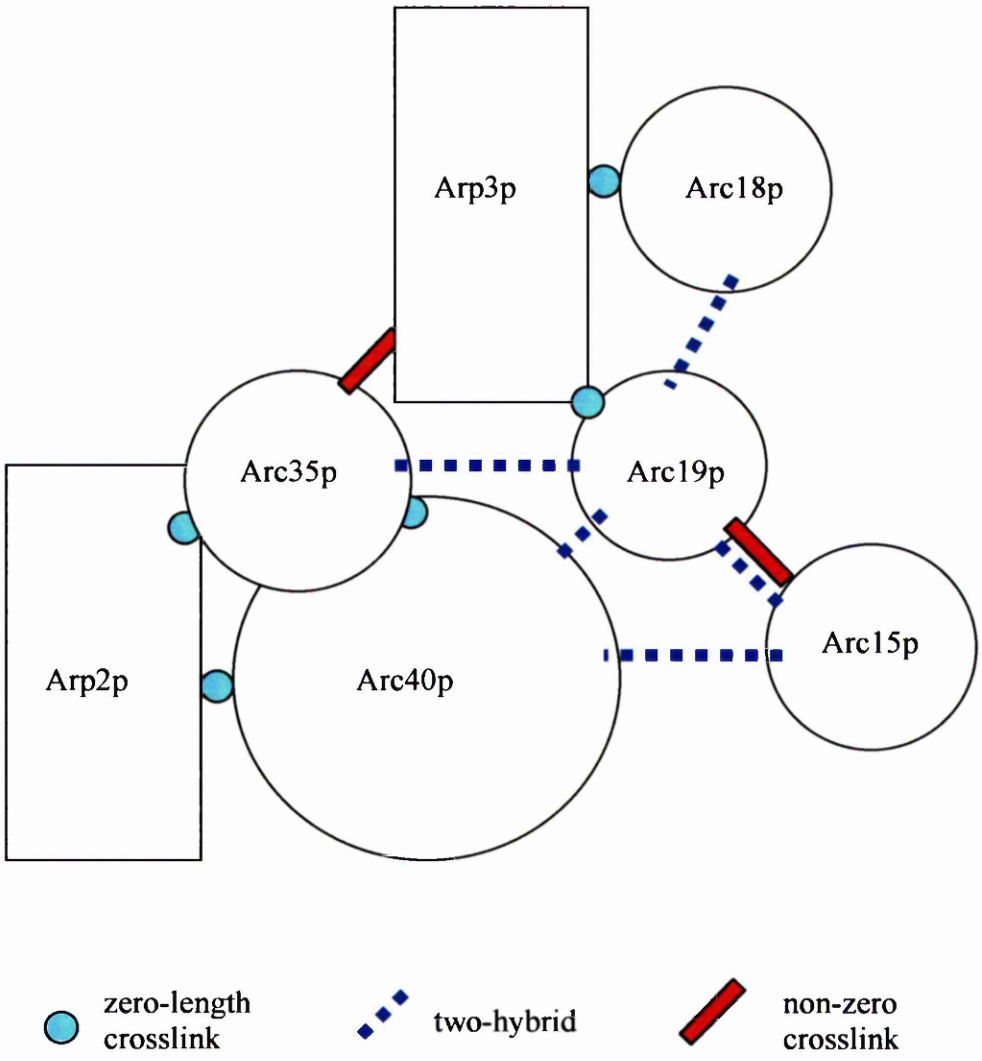

Figure 1.5. Structure of the Arp2/3 complex. This model combines the results of chemical cross-linking and two-hybrid results. The molecular weights of the five Arp2/3 complex components relate to the complex found in *S.cerevisiae*. This model shows the Arp2/3 complex in the inactive form (in the absence of activators) where Arp2 and Arp3 are distant from each other and so are not capable of actin nucleation. Adapted from May 2001.

The Arp2/3 complex also binds to the sides of pre-existing filaments and simultaneously nucleates new filaments allowing branches and networks of cross-linked filaments to be assembled (figure 1.6.) (Bailley *et al* 2001, Mullins *et al* 1998, Machesky and Gould, 1999, Pantaloni *et al*, 2000). This model is called dendritic nucleation (Mullins *et al* 1998, Pollard *et al* 2000). The crystal structure of bovine Arp2/3 complex has recently been solved by Robinson and collegues (2001), who predict that WASp/Scar proteins activate Arp2/3 complex by bringing Arp2 into proximity with Arp3 for nucleation of a branch on the side of a pre-existing actin filament. Actin filaments are cross-linked at 70 °C to the mother filament producing an orthogonal 'Y-branched' network of F-actin (Mullins *et al* 1998b). Dynamic actin-rich structures such as lamellipodia at the leading edge of motile cells are enriched for the Arp2/3 complex and this pattern of cross-linking can be observed at the leading edge of motile cells (Svitkina and Borisy, 1999). Polymerisation of actin at the leading edge is thought to generate the force to move the membrane forward (Small *et al* 1999).

Several pathogenic bacteria have evolved strategies to utilise the host cells Arp2/3 complex to their own advantage. Motile intracellular pathogens such as *Listeria monocytogenes* and *Shigella flexneri* recruit the Arp2/3 complex which then stimulates focal actin polymerisation and propels the bacterium through the cell by a 'comet-like' tail of filamentous actin (Cossart and Bierne 2001, Welch *et al* 1997). The discovery of a role for the Arp2/3 complex in promoting actin nucleation came from the reconstitution of *Listeria's* movement in cell-free extracts (Theriot *et al* 1994, Welch *et al* 1997).

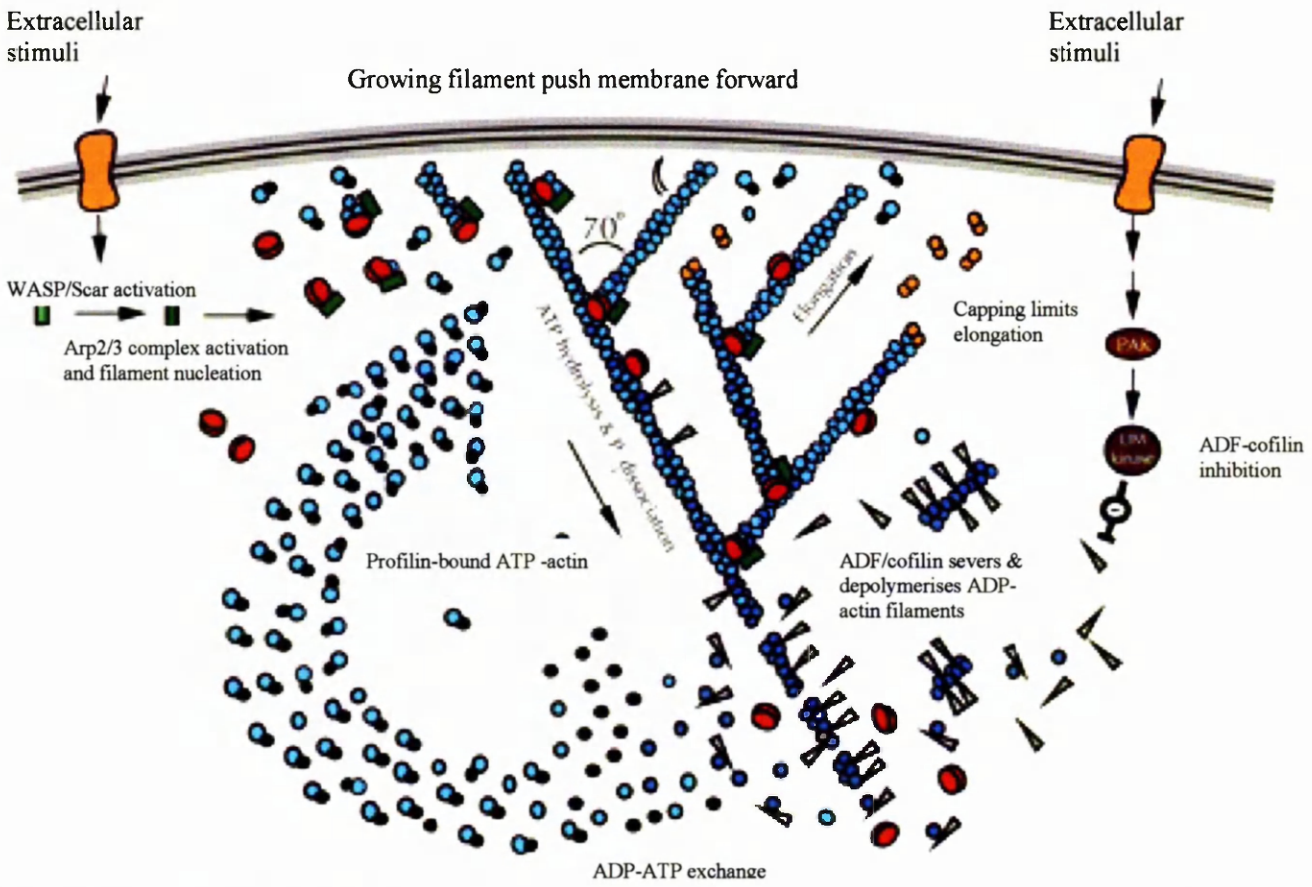

Figure 1.6 Dendritic nucleation model. A pool of ATP-actin are competent for assembly upon activation of WASp family proteins which leads to the activation of the Arp2/3 complex. New barbed ends are created at a constant rate. The rapid growth of filaments pushes the membrane forward. Capping protein binds to barbed ends and stops growth of filaments. ATP hydrolysis triggers ADF/cofilin severing and depolymerisation of older actin filaments. This is inhibited by LIM-kinase. Profilin recycles ADP-actin back into the ATP-actin monomer pool. Assembly and disassembly are balanced in a continuously moving cell. Taken from Pollard *et al* 2000.

In yeast, the genes encoding the subunits of the Arp2/3 complex are required for the assembly, polarisation and motility of cortical actin patches (Moreau *et al* 1996, Winter *et al* 1997). However, this movement appears not to depend on actin polymerisation (Belmont and Drubin 1998, Lappalainen and Drubin 1997). The Arp2/3 complex is also required for endocytosis in yeast (Moreau *et al* 1997).

1.9.1. The activity of the Arp2/3 complex is enhanced by activators

In cells, the Arp2/3 complex is inactive until cellular signals result in its activation (Higgs and Pollard, 1999). On its own, the Arp2/3 complex has weak nucleating activity that can be stimulated by other proteins that play a role in cytoskeletal organisation (figure 1.7) (Mullins *et al* 1998). Arp2/3 complex activators have been identifed in pathogenic bacteria, and eukaryotes from yeast to mammals. Although found in diverse organisms, each activator interacts with Arp2/3 complex through the same conserved motif, called the acidic domain (rich in aspartate and glutamate)(May 2001).

1.9.1.1. ActA

The first activator of the Arp2/3 complex to be identified was the *Listeria* protein ActA (figure 1.7b) and was shown to stimulate the nucleating activity of the Arp2/3 complex recruited by the bacterium (Welch *et al* 1998). The minimal requirements for this process have been identified as actin, the Arp2/3 complex, capping protein, and ADF (Loisel *et al* 1999).

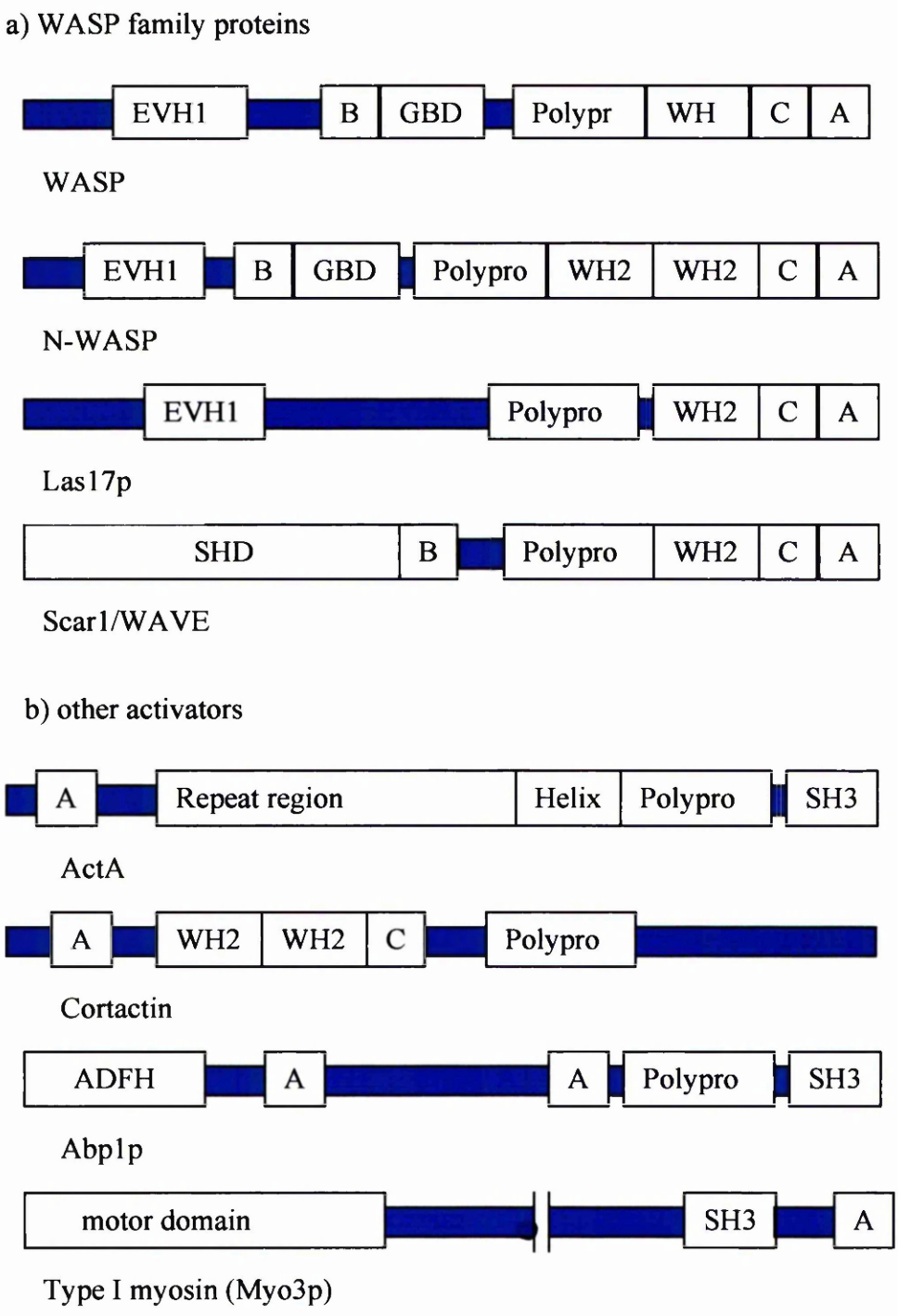

Figure 1.7. Proteins which bind and activate the Arp2/3 complex. (a) WASP family proteins and (b) other activating proteins. Domains are abbreviated as follows; EVH1, EVL/VASP homology 1; B, Basic; GBD, GTPase binding domain also known as CRIB; Polypro, proline-rich sequence; WH2, WASP homology 2; C, central, or cofilin homology; A, acidic; SHD, Scar homology domain; ADFH, actin depolymerising factor homology. The regions involved in activating actin polymerisation are the WH2, C- and A-domains. Adapted from May 2001.

1.9.1.2. The WASP-family proteins

A well-studied group of endogenous activators are the WASP (Wiskott-Aldrich Syndrome protein) family proteins (figure 1.7a)(Machesky and Insall 1998, Machesky *et al* 1999, Yarar *et al* 1999, Winter *et al* 1999, Mullins 2000). This group includes: WASp, N-WASp and WAVE in mammals (Miki *et al* 1996, Miki *et al* 1998); Scar (WAVE homologue) in *Dictyostelium discoideum* (Bear *et al* 1998), and Las17p/Bee1p in *S.cerevisiae* (Li 1997, Winter *et al* 1999). WASP family proteins all contain actin-binding motifs, termed WH2 (WASP homology 2) or V (verprolin homology) domains that bind G-actin (Vaduva *et al* 1997). Recruitment of G-actin is necessary to efficiently activate the Arp2/3 complex (Miki and Takenawa 1998, Yamaguchi *et al* 2000).

Regulation of WASP-family members by Cdc42p and Rac links signalling pathways with the Arp2/3 complex and actin cytoskeleton. In mammalian cells, the Rho family GTPases, Rho, Rac and Cdc42p are critical in cortical actin polymerisation and organisation. Activation of Rac leads to the formation of lamellipodia and membrane ruffles (Ridley *et al* 1992). Rho activation primarily regulates the formation of stress fibres (Hall 1998). Cdc42p stimulates filopodia formation (Miki *et al* 1998b).

Two members of the Rho family of small GTPases, Cdc42 and Rac, have been well established as mediators of extracellular signalling events that impact cortical actin organisation. Changes in the actin cytoskeleton induced by Rac and Cdc42p require the participation of WASP family members, ultimately resulting in activation of the Arp2/3 complex, for example filopodia are induced when activated Cdc42p binds to

N-WASP (Miki *et al* 1998b). Cdc42p interacts with WASP through the conserved WASP GBD (GTPase binding domain), also called a CRIB (Cdc42/Rac interaction/binding) domain (Abdul-Manan *et al* 1999). Scar1/WAVE appears to transduce signals from Rac to promote the formation of branched actin networks (Miki *et al* 2000).

1.9.1.3. Cortactin and Abp1p

Recently, two new activators of the Arp2/3 complex have been described, cortactin and Abp1p (figure 1.7b)(reviewed by Olazabal and Machesky, 2001). They appear to play a different role to the WASP-family proteins and both act by enhancing the ability of the Arp2/3 complex to assemble branched actin filament networks probably by acting in a stabilising capacity (Weaver *et al* 2001, May 2001).

The Src-kinase substrate cortactin localises at sites of dynamic assembly in membrane ruffles and lamellipodia where it binds F-actin and the Arp2/3 complex (Weed *et al* 2000, Kaksonen *et al* 2000, reviewed in Weed and Parsons 2001). The localisation of cortactin is controlled by activation of Rac, so coupling tryosine kinase-based signalling events to cytoskeletal reorganisation (Weed *et al*, 2000). Cortactin does not contain a WH2 (G-actin binding) domain which are found in the WASP-family proteins. However, binding to F-actin occurs via tandem repeats to activate the Arp2/3 complex (Weaver *et al* 2001, Urono *et al* 2001).

Abp1p (actin-binding protein 1) is an activator of the Arp2/3 complex found in *S.cerevisiae* (see section 1.14.1). Activation of the Arp2/3 complex requires the

binding of the ADF-H (actin depolymerising factor homology) domain of Abp1p to F-actin (Goode *et al*, 2001). The mouse homologue of Abp1p, mAbp1 has been identified as an actin binding cytoskeletal protein that is specifically recruited to dynamic actin structures enriched for the Arp2/3 complex (Kessels *et al* 2000).

1.10. The Arp2/3 complex in *S. cerevisiae*

The Arp2/3 complex in *S. cerevisiae* is found associated with cortical actin patches. Arp2-specific antibodies did not reveal localisation with actin cables (Moreau *et al* 1996, Winter *et al* 1997). Assembly of cortical actin patches is dependent on the Arp2/3 complex as mutations in subunits of the Arp2/3 complex cause aberrant actin patch formation and motility (Moreau *et al* 1996, Winter *et al* 1997, Winter *et al* 1999b). Endocytosis is also inhibited by mutations in the Arp2/3 subunits (Moreau *et al* 1997). The movement of a yeast organelle, the mitochondrion, has also been linked to actin polymerisation by the Arp2/3 complex (Boldogh *et al* 2001).

S. cerevisiae has a WASP homologue called Las17p/Bee1p (see section 1.14.2) which has been shown to be associated with the actin cytoskeleton and to activate the Arp2/3 complex (Li 1997, Winter *et al* 1999). Las17p/Bee1p localises to cortical actin patches which become aberrant if *LAS17* is disrupted (Li 1997, Madania *et al*, 1999). Las17p/Bee1p is required for *in vitro* actin assembly in permeabilised yeast cells (Li 1997, Lechler and Li 1997). Recent studies have shown that type I myosins (Myo3p and Myo5p) also participate in activating Arp2/3 complex-dependent actin

assembly of cortical actin patches in yeast (Evangelista *et al* 2000, Lechler *et al* 2000). The interaction between Las17p and type I myosins is likely to occur through interaction of the SH3 domain of the myosins and the proline-rich repeats of Las17p (Lechler *et al* 2000). Las17p/Bee1p also interacts with Vrp1p *in vivo*. Vrp1p is a homologue of mammalian WASP-interacting protein (WIP) (Lechler and Li 1997) and human WIP has been shown to substitute for Vrp1p in yeast cells deleted for *VRP1* (Vaduva *et al* 1999).

From a regulatory point of view, the most significant difference between WASP and Las17p/Bee1p is the lack of a recognisable Cdc42-binding motif in the yeast sequence. Cdc42p activation at the presumptive bud site is a key trigger for cell polarisation as F-actin accumulates at this site (reviewed in Gulli and Peter, 2001). Lechler and collegues 2001 have described a model of a bifurcated signalling pathway downstream of Cdc42p that recruits and activates a Las17p-type I myosin-Vrp1p multivalent Arp2/3- activating complex via the concerted actions of two Cdc42p effectors, formin-like proteins and PAKs (figure 1.8). Localisation of the complex to the polarisation site is F-actin independent. Recruitment then leads to the localised assembly of actin filaments.

1.11. Eukaryotic cell polarity

Polarised cell growth is a fundamental process, essential for the development of eukaryotes. Eukaryotic cells respond to intracellular and extracellular cues to direct asymmetric cell growth and division. Cortical spatial cues received at the cell surface

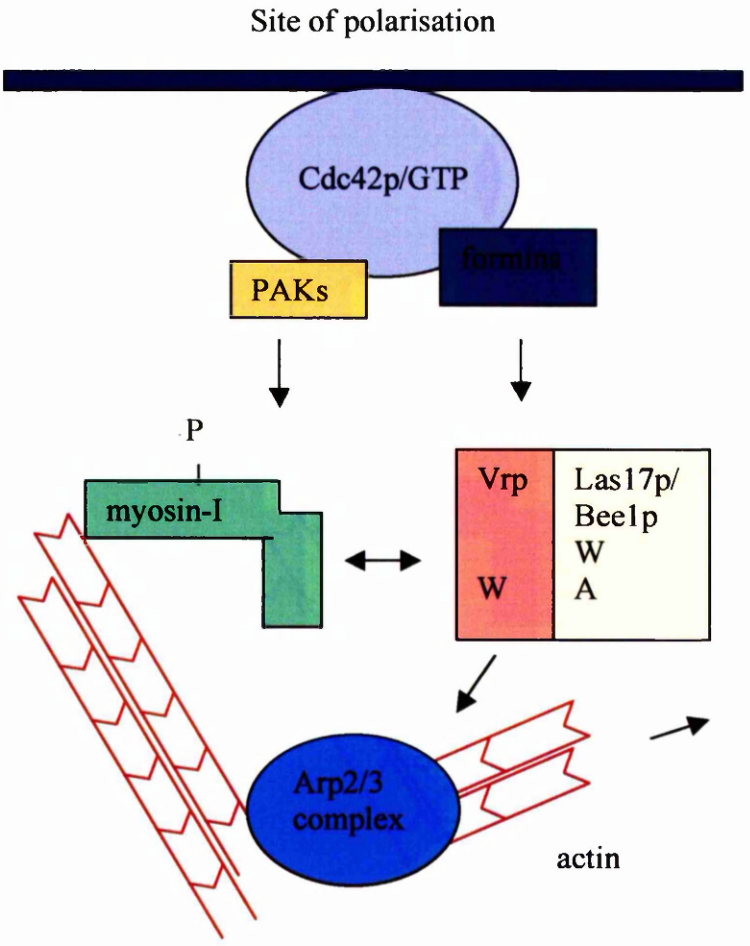

Figure 1.8. The Arp2/3 complex is activated at the site of polarisation by a myosin/Vrp1p/Las17p complex. A bifurcated pathway downstream of Cdc42p is required for polarised actin polymerisation as Cdc42p at the site of polarisation recruits both formins and the PAKs. Adapted from Lechler *et al* 2001.

initiate a cascade of molecular events which induce the localised assembly of specialised cytoskeletal and signalling networks, resulting in the establishment of cell polarity. Cell polarity development is a highly complex process that requires the spatial and temporal organisation of many proteins (Drees *et al* 2001).

Epithelial cells and budding yeast are two phylogenetically distant eukaryotic cell types which have been used to study the phenomenon of cell polarity (for review see Drubin and Nelson 1996). The spatial cue required for polarity development in epithelial cells is cell-cell or cell-ECM adhesion, specifically interaction between integrin and cadherin receptors and extracellular cell surface(s). Partial reorganisation of the epithelial cell results as cytoskeletal and signalling networks form at the site of cell contact. Microtubules reorganise under the apical membrane and parallel to the lateral membrane while actin filaments are found at the tight junction and apical membrane. Components of the secretory apparatus, including the Golgi complex and apical and basal endosomes become restricted to different regions of the cytoplasm. Distinct apical and basal-lateral membrane domains are thus established.

1.11.1. Cell polarity in *S.cerevisiae*

Cell polarity manifests itself somewhat differently in yeast and epithelial cells (Drubin and Nelson 1996). However, despite the large phylogenetic distance between these cell types, there is similarity between response mechanisms to establish and maintain structural and molecular asymmetry at the cell surface in response to

intrinsic and extrinsic cues. Findings from studies into cell polarity in *S. cerevisiae*, a single-celled eukaryotic organism, should therefore be relevant to higher organisms.

S. cerevisiae displays three related cell polarity pathways: one is an asymmetric cell division called budding; the second is the formation of a mating projection, and the third is the formation of pseudohyphae (for reviews see Pruyne and Bretscher 2000a and 2000b, Madden and Snyder 1998). Polarised cell growth is a complex operation that involves the temporal and spatial co-ordination of many different proteins and interactions. The major events which must occur are: (1) the incipient bud (or shmoo, or hypha) site must be selected and established; (2) the cytoskeleton reorganises; (3) vectorial transport of secretory vesicles and organelles; (4) local membrane growth and new cell wall synthesis at regions of the cell surface which are undergoing active growth and remodelling (for review see Orlean, 1997); and, (5) regulation of signal transduction cascades to communicate with other parts of the cell.

1.11.2. Polarised intracellular transport occurs along actin cables

Polarised growth at the yeast cell surface depends upon delivery of secretory vesicles along actin cables. Budding yeast use myosin-dependent transport along actin cables to translocate mRNA molecules, secretory vesicles and cellular organelles such as the vacuole into the newly formed daughter cell (figure 1.9). There are two yeast class V myosins Myo2p and Myo4p (their associated light chains are Cmd1p and Mlc1p). Recent studies have suggested that Myo2p and Myo4p have properties of a non-processive motor and that directed movement of an organelle by Myo2p requires at least five molecules of Myo2p per organelle (Reck-Peterson *et al* 2001). Mutations in

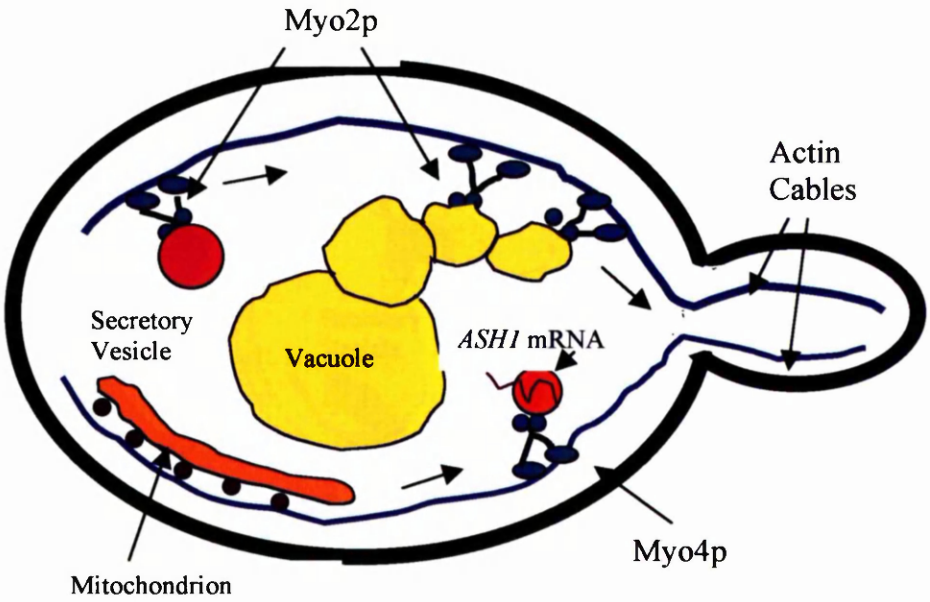

Figure 1.9. Polarised intracellular transport in *S.cerevisiae* during early bud growth. Cellular components are polarised through interactions with actin cables and the cell cortex. Secretory vesicles, and vacuoles are transported along actin cables by Myo2p while Myo4p transports mRNA encoding the transcriptional repressor Ash1p. The movement of mitochondria depends on actin cables by an unknown mechanism. Adapted from Pruyne and Bretscher 2000b.

the genes encoding Myo2p (*MYO2*), actin cable binding proteins tropomyosin 1 (*TPM1*) and tropomyosin 2 (*TPM2*), and *sec* mutants produce phenotypes implicating these proteins in intracellular transport (Govindan *et al* 1995, Liu and Bretscher 1992).

Secretory vesicles and vacuoles are delivered to the sites of cell growth in the bud, by the motor protein Myo2p (Pruyne *et al* 1998, Karpova *et al* 2000). Myo4 transports mRNA encoding the transcriptional repressor Ash1p into the bud. Mitochondria move into the bud in an actin dependant manner (Simon *et al* 1997, Boldogh *et al* 2001).

1.12. Organisation of the Actin Cytoskeleton during the Cell Cycle in *Saccharomyces cerevisiae*

Initial studies which determined the distribution of actin during the cell cycle gave the first indication that there was a link between the actin cytoskeleton and cell polarity as actin appeared organised at the sites of active cell surface growth (Adams and Pringle 1984; Kilmartin and Adams 1984). The role of the actin cytoskeleton in cell polarisation has also been inferred from the phenotypes resulting from mutations in the *ACT1* gene and mutations in genes that code for the proteins associated directly (and sometimes indirectly) with actin (Botstein *et al* 1997).

The distribution of the actin cable and cortical actin patches changes throughout the yeast cell cycle as depicted in figure 1.10. At the beginning of the yeast cell cycle, in

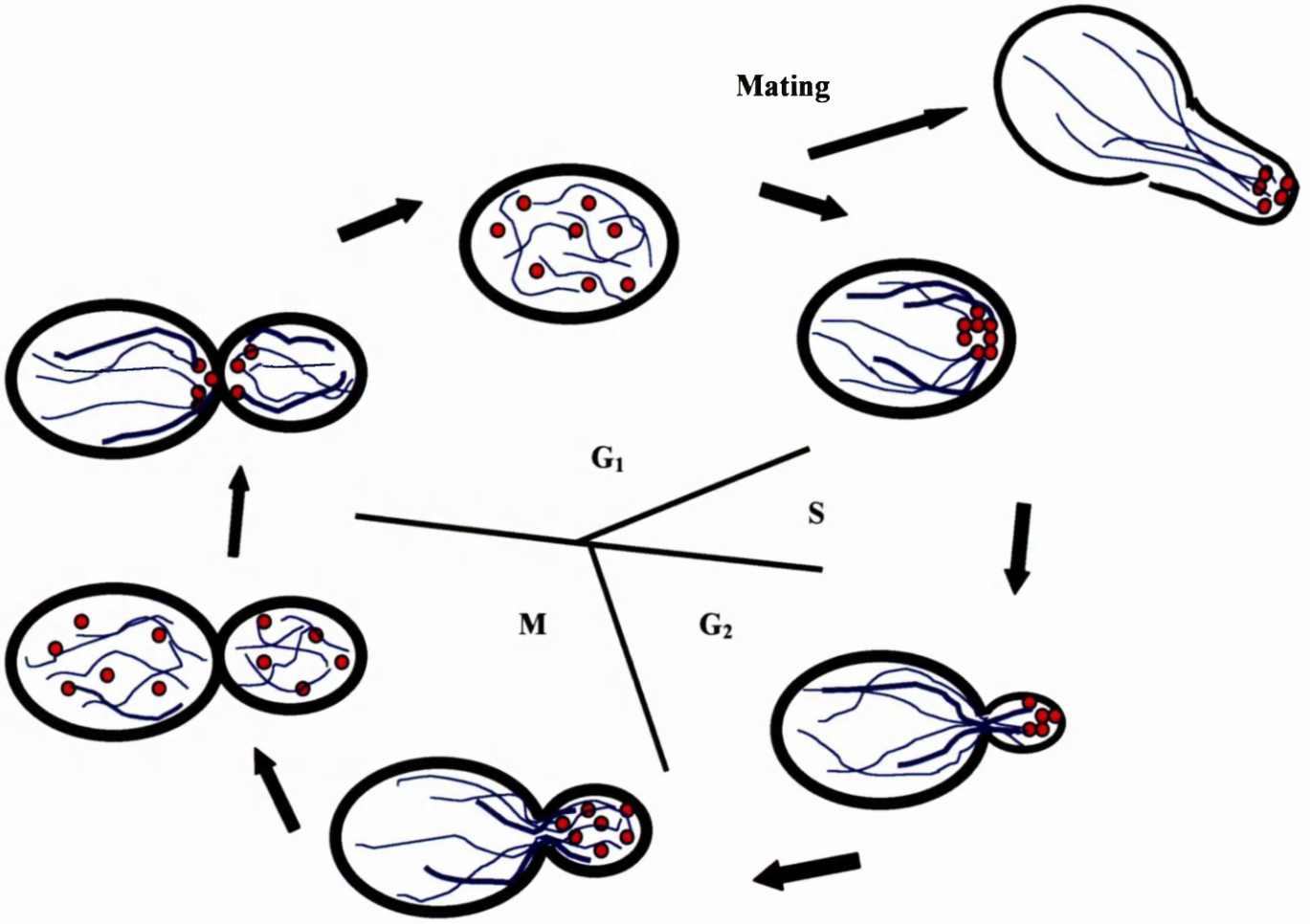

Figure 1.10 Organisation of the actin cytoskeleton during vegetative growth and shmoo formation in budding yeast. Actin cables (blue) and cortical actin patches (red) show a distinctive polarised distribution throughout the cell cycle and during shmoo formation for mating. Cortical actin patches cluster at sites of active growth while the actin cables become arrayed parallel to the mother-bud axis to guide secretory vesicles and organelles to the sites of active growth.

early G_1 both the actin cables and cortical actin patches are evenly distributed and randomly oriented in the cytoplasm of the cell. However, as the yeast cell initiates a new cell cycle, a characteristic cell-cycle dependent asymmetrical distribution of both actin cables and cortical patches develops. This asymmetry is necessary for the role of actin in establishing polarised growth and in directing secretion to the growing bud.

In late G_1 phase, cortical actin patches cluster at the previously marked nascent bud site and cables orient towards this site and become arrayed parallel to the mother-bud axis. In the early budded phase, the cortical actin patches are found principally in the developing bud at the tip, and the bud grows apically (from the distal end). Although actin patches accumulate in the bud, they are not restricted to this site and can move freely through the bud neck (Waddle *et al* 1996).

As the bud matures, actin cables and cortical patches become randomly distributed throughout the bud and the bud expands isotropically. The actin cables within the mother cell still extend to the bud neck as growth remains directed to the growing bud. Later in the cell cycle, once the bud reaches a critical size, the actin cables and patches lose their asymmetric distribution and redistribute randomly in the mother and bud cells. After cytokinesis the cortical actin patches concentrate in a ring at the bud neck as the cell directs growth of cell walls between the two new cells.

The actin cytoskeleton also polarises growth during mating to produce a mating projection. Haploid yeast cells respond to mating pheromones secreted by haploid cells of the opposite mating type. Cells that are undergoing a mating response

become arrested in G_1 and form a mating projection towards potential mating partners. So, as occurs during budding, once a site is selected through pheromone signalling, polarised growth is directed toward that site via the reorganisation of the actin cytoskeleton (Kron and Gow 1995).

Mutant yeast that display cell polarisation defects exhibit various gross morphological defects. Cells that have undergone excessive isotropic growth display spherical buds, whereas cells that have undergone excessive apical growth produce highly elongated buds (Cvrcková *et al* 1995). Studies in which filamentous actin has been disrupted by treatment with the actin-monomer sequestering drug Latrunculin-A have shown that bud enlargement cannot proceed and mother cells grow into large, round unbudded cells (Ayscough *et al* 1997). Similarly, yeast which have defects in components of the mating response polarisation pathway display aberrant mating projection morphology (Madden and Snyder 1998, Chenevert *et al* 1992, Gehrung and Snyder 1990).

1.13. Endocytosis

Endocytosis is the process by which eukaryotic cells including *S. cerevisiae* internalise portions of the plasma membrane and extracellular fluid and particles by invagination of the plasma membrane (for reviews see Wendland *et al* 1998, Munn 2000, Munn 2001, Shaw *et al* 2001). Fluid-phase endocytosis is a constitutive process and occurs without a binding step so uptake of molecules or particles is non-saturable and at rates dependent on their extracellular concentration. Receptor-

mediated endocytosis involves the internalisation of ligand-bound receptor and is a saturable process.

Endocytosis has been well characterised at the morphological level in mammalian cells, where both fluid-phase endocytic markers, such as horse-radish peroxidase, and membrane bound endocytic markers, such as gold-labelled transferrin receptors, can be internalised and visualised by electron-microscopy. The best-characterised endocytic mechanism to date is clathrin-dependent endocytosis in which markers are initially seen in invaginations of the plasma membrane, known as coated pits (Schmid 1997, reviewed by Kirchhausen 2000) (see figure 1.11). It has been shown that receptors are concentrated into these pits via an interaction between their cytosolic tails and clathrin adaptor proteins (AP), which in turn associate with clathrin triskelions to form AP-complexes (Pearse and Robinson 1990).

In higher eukaryotic cells the link between endocytosis and the actin cytoskeleton is contentious, as results are dependent on the cell type and the assay used (Geli and Riezman 1998, Fujimoto *et al* 2000). However, a link is strongly suggested since and increasing number of proteins associated with the endocytic machinery also interact with the actin cytoskeleton (figure 1.11)(reviewed in Qualmann *et al* 2000, Lanzetti *et al* 2001). The actin cytoskeleton could play a structural role by providing a framework for the spatial organisation of the endocytic machinery and also function indirectly by providing the tracks for the movement of myosin motor proteins involved in force generation and vesicle movement (Lamaze *et al* 1997, Buss *et al* 2001).

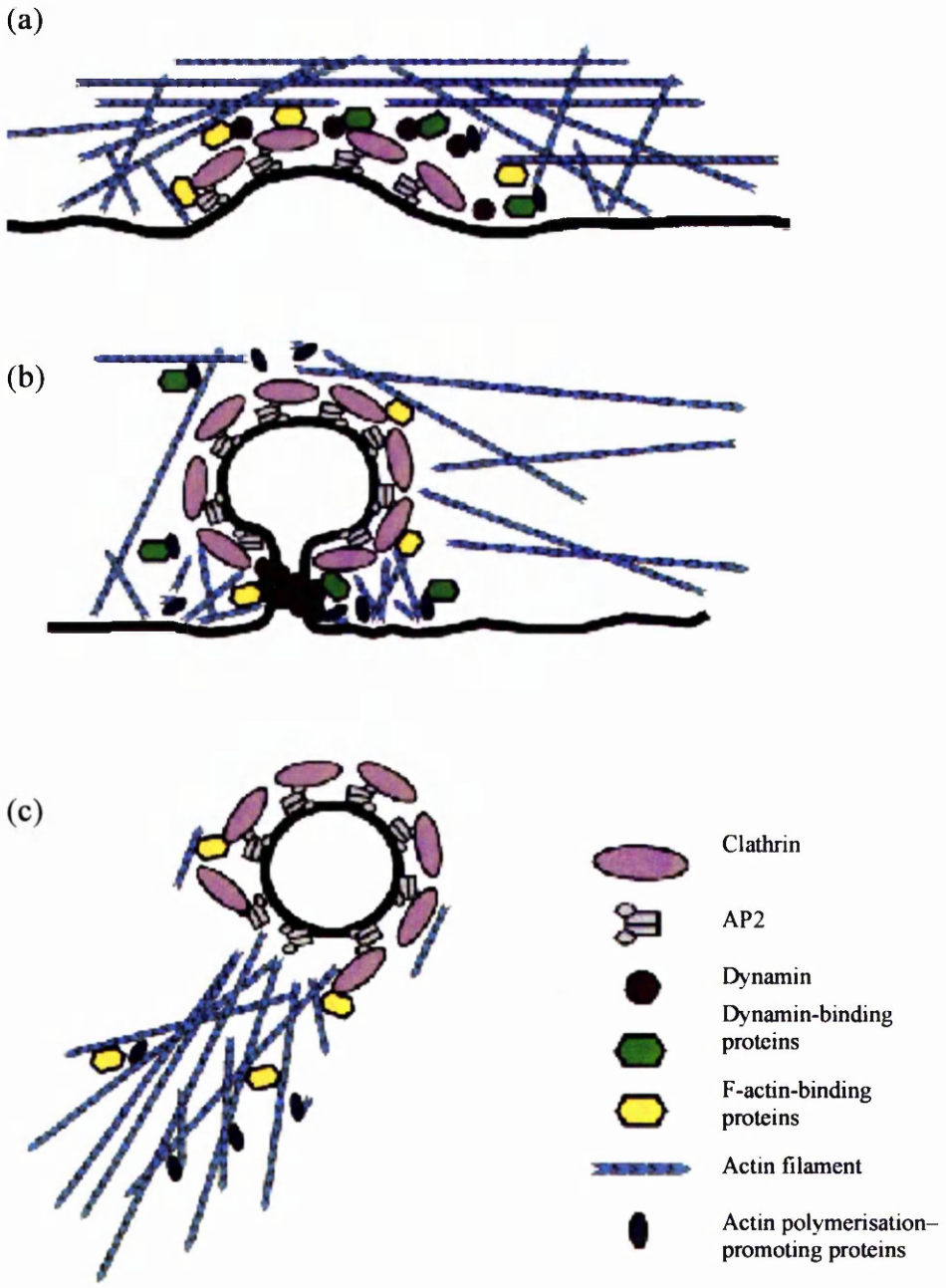

Figure 1.11 Mechanism of clathrin-dependent endocytosis in eukaryotic cells. (a) Endocytosis begins by deformation and invagination of the plasma membrane, a process that may be supported by the cytoskeleton. (b) The cortical actin barrier underlying the growing endocytic vesicle may need to be disassembled and the force provided by actin polymerisation may drive membrane fission as the vesicle develops. (c) Actin polymerisation may promote the movement of the newly formed endocytic vesicle into the cytoplasm. Adapted from Qualmann *et al* 2000.

Dynamin is a GTPase that is involved in the fission of endocytic vesicles and has been linked to the actin cytoskeleton (Damke *et al* 1994, Cao *et al* 1998). Dynamin-interacting proteins bind to the proline-rich C-terminus domain of dynamin most often via their SH3 domains. Amphiphysins I and II are dynamin-interacting proteins with SH3 domains (reviewed by Wigge and McMahon 1998). Amphiphysin also interacts with AP2 and clathrin. *S.cerevisiae* amphiphysin homologues, Rvs161p and Rvs167p show synthetic lethality with a subset of actin *act1* alleles (Breton and Aigle 1998) and Rvs167 and actin interact by two-hybrid assay (Amberg *et al* 1995). Rvs167 also co-localises with cortical actin patches (Balguerie *et al* 1999). The syndapins are a second family of proteins which have been found to exhibit functional links to the actin cytoskeleton and that interact with N-WASP (section 1.9.1.2)(Qualmann *et al* 1999, Qualmann and Kelly 2000). Syndapins could thus couple actin polymerisation to dynamin's function in the fission reaction to allow the newly formed vesicle from the membrane or to move it into the cytosol.

1.13.1. Cortical actin patches and endocytosis in *S. cerevisiae* are linked.

In *S. cerevisiae,* endocytic material is transported through different membrane bound compartments before it reaches the vacuole The best characterised receptor-mediated endocytosis event in *S. cerevisiae* is uptake of Ste2p, the α-factor receptor. Binding of α-factor, a mating pheromone, to its receptor activates an intracellular signal transduction pathway that leads to the physiological changes required for cells of opposite mating types to mate (Herskowitz 1989). Reizman and colleagues used

radio-labelled α-factor to follow the uptake of the receptor-ligand complex from the cell surface to the vacuole via at least two internal membrane-bound compartments, termed early and late endosomes. The receptor-ligand complex was then delivered to the vacuole and degraded by resident proteases (Singer and Reizman 1990, Singer-Kruger *et al* 1993).

In yeast the link between the actin cytoskeleton and endocytosis has been well established. The initial stages of endocytosis in yeast involve the cortical actin patches. Many cortical patch components have been implicated in this process by the correlation between mutations that affect the cortical actin cytoskeleton and mutations that affect internalisation (see table 1.2) (Bénédetti *et al* 1994, Wesp *et al* 1997, Naqvi *et al* 1998, Wendland *et al* 1998).

Evidence that the link between endocytosis and actin is direct comes from studies of temperature-conditional mutations affecting actin. Mutants which are temperature sensitive for actin function such as *act1-1* endocytose normally at permissive temperature but when shifted to 37 °C immediately lose the ability to endocytose (Kubler and Reizman, 1993). Similarly, disruption of the actin cytoskeleton by addition of the monomer sequestering drug Latrunculin-A also causes an immediate abrogation of fluid-phase endocytosis (Ayscough *et al* 1997). A dynamic actin cytoskeleton was also found to be essential for endocytosis in studies using jasplakinolide, a drug which stabilises F-actin (Ayscough 2000). Recently a mutant of the yeast Eps15-like endocytic protein Pan1p was described that has a severe endocytic defect but not the concommitant defective actin cytoskeleton (Duncan *et al*

Gene	Homologies	Motifs/domains	Deletion phenotype
ABP1	mABP	ADF	Viable
ACT1	Actin, Arp2		Lethal
ARK1	Prk1p	Serine/threonine kinase Proline-rich	Viable*
ARP2	mArp2		Lethal
ARP3	mArp3		Lethal
CMD1	Calmodulin	4 EF hands	Lethal
COF1	Cofilin/ADF		Lethal
END3		EH domain	Viable
LAS17/BEE1	Human WASP	WH1, WH2	Viable
MYO5	Type I myosin	SH3	Viable
PAN1	Eps15	2 EH domains	Lethal
PRK1	Ark1p	Serine/threonine kinase Proline-rich	Viable*
RSP5/NPI1	E3 ubiquitin	C2, WW, hect domain	Lethal
RVS161	Amphiphysin	Coiled-coil	Viable
RVS167	Amphiphysin	SH3, Coiled-coil	Viable
SAC6	Fimbrin	CH domains	Viable
SJL1	Synaptojanin	Sac1 homology, 5P'ase	Viable
SLA1		3 SH3 domains	Viable
SLA2/END4	Talin	Coiled-coils	Viable
SRV2		Proline-rich	Viable
VRP1/END5	Verprolin	Proline-rich	Viable

Table 1.2. Yeast proteins implicated in the early stages of endocytosis. Homologies to mammalian or yeast proteins are shown, also motifs or domain encoded by each gene. Phenotypes of yeast cells deleted for each gene is shown as viable or lethal to cell (* double deletion Δ*ark1*Δ*prk1* is lethal).

C2, conserved lipid/Ca^{2+}-binding domains; EF hands, a calcium binding motif; EH, Eps15 homology domain; hect, homologous to E6-AP carboxyl terminus domain; SH3 , Src-homology domain 3 motif; WH, WASP (Wiskott-Aldrich syndrome protein) homology domain; WW protein interaction module containing two conserved tryptophan residues.

Adapted from Wendland *et al* 1998.

2001). Eps15p is a mammalian protein involved in endocytosis that associates with clathrin-coated pits via an interaction with the AP-2 complex (Wendland *et al* 1996, van Delft *et al* 1997). Again, further evidence that endocytic defects are not a secondary effect of a disrupted actin cytoskeleton. A link between actin nucleation and polymerization and endocytosis in yeast emerged from these studies on Pan1p (Duncan *et al* 2001) and Abp1p (Goode *et al* 2001) (see section 1.9.1.3 and 1.14.1). These studies suggest that Pan1p and Abp1p may link activated actin polymerisation to an endocytic function.

1.14. Cortical Patch Proteins

This section looks in more detail at four proteins of the cortical actin cytoskeleton, Abp1p, Las17p, Sla2p and Sla1p of specific relevance to this project. Sla1p is the principal subject of this thesis and section 1.15 looks at the background leading up to my work.

1.14.1. Abp1p

Abp1p is an actin binding protein that plays a role in the organisation of the *S. cerevisiae* actin cytoskeleton. Abp1p is homologous to drebrins and forms a family of proteins conserved from yeast to humans (Lappalainen *et al* 1998). Abp1p was the first actin-associated protein identified in yeast where it is found concentrated in the actin patches (Drubin *et al* 1988). Similarly, the mammalian homologue of Abp1p,

Abp1 is specifically recruited to dynamic actin structures as it translocates to the leading edge of the cell (Kessels *et al* 2000).

Deletion of the *ABP1* gene in yeast does not cause any obvious mutant phenotype (Lila and Drubin 1997) but its overexpression disturbs the actin cytoskeleton and leads to an aberrant budding pattern and cortical actin assembly (Drubin *et al* 1988). However, Abp1p is essential when the genes encoding for either Sla1p, Sla2p or Prk1p is deleted (Holtzman *et al* 1993, Cope *et al* 1999).

Abp1p binds actin filaments via its ADF-H (ADF/cofilin homology) domain and interacts with other proteins, Rvs167/amphiphysin and Srv2p/CAP through its carboxyl-terminal SH3 domain and proline-rich region (figure 1.7)(Lila and Drubin 1997). Abp1p also associates with the cortical patch serine/threonine kinases Ark1p and Prk1p through its SH3 domain, and this is essential for the localisation of the kinases to actin cortical patches (Cope *et al* 1999, Fazi *et al* 2001).

One role for Abp1p in yeast is to enhance the ability of the Arp2/3 complex to assemble branched actin filaments (section 1.10 and 1.10.1.3)(Goode *et al* 2001, reviewed by Olazabal and Machesky, 2001). Abp1p also functions in endocytosis. Evidence comes from studies that show it has a redundant function with Sla2p in endocytic function and it interacts with other proteins that function in endocytosis such as Rvs167p and Prk1p (Munn *et al* 1995, Lila and Drubin 1997, Zeng and Cai, 1999). Phage display using the Abp1p SH3 domain discovered Inp52p/Sjl2p as a binding partner. Inp52p/Sjl2p is similar to synatojanin, a mammalian protein suggested to have a role in the regulation of membrane trafficking actin cytoskeleton

organisation (Guo *et al* 1999). Taken together, the role of Abp1p appears to act as F-actin associated link between proteins implicated in endocytosis and protein complexes involved in actin polymerisation. Mammalian Abp1 is also proposed to play an analogous function linking the actin cytoskeleton to endocytosis via the GTPase dynamin (Kessels *et al* 2001).

1.14.2. Las17p

Las17p is the *S.cerevisiae* WASp homologue and activates the yeast Arp2/3 complex (see section 1.10)(Winter *et al* 1999, Madania *et al* 1999). *LAS17* overexpression can suppress certain temperature-sensitive *arp2* mutations (Madania *et al* 1997). Las17p is a component of cortical actin patches. Cells deleted for *LAS17* are defective in budding and cytokinesis and is essential for the assembly of cortical actin patches *in vivo* and *in vitro* as determined by a permeabilised cell assay (Li 1997).

Las17p has a domain structure as described in section 1.9.1.2 and figure 1.7a. The carboxy-terminal domain of Las17p has been shown to stimulate the nucleation activity of purified Arp2/3 complex *in vitro* (Winter *et al* 1999). Unlike the other WASP-family members, the yeast homologue Las17p/Bee1p does not contain a recognisable GBD/CRIB domain. This suggests that the yeast WASP homologue is regulated in a different manner than in higher eukaryotes.

Las17p functionally associates with *S.cerevisiae* type I myosins (Myo3p and Myo5p)(section 1.8.8) and has been shown to associate with Sla1p by co-immunoprecipitation (Evangelista *et al* 2000, Li 1997). Myo3p and Myo5p bind

proline-rich motif in Las17p (figure 1.7b). A two-hybrid screen has shown that Las17p also interacts with verprolin (Vrp1p) via its C-terminus region (Naqvi *et al* 1998). Vrp1p is a component of the actin cytoskeleton required for a polarised cortical actin cytoskeleton and endocytosis (Donnelly *et al* 1993, Munn *et al* 1995).

1.14.3. Sla2p

SLA2, also called *END4* and *MOP2,* encodes a peripheral membrane protein that is a component of the cortical actin cytoskeleton required for cell polarisation and endocytosis (Wesp *et al* 1997, S. Yang *et al* 1999). Sla2p localises to a subset of cortical actin patches as well as to cortical patches apparently free of actin despite containing an actin binding site (S. Yang *et al* 1999). Interestingly, *sla2* mutants are defective in nucleation of actin assembly in a permeabilised cell assay (Li *et al* 1995). *SLA2* was isolated in the same synthetic lethal screen as *SLA1* (section 1.15.1)(Holtzman *et al* 1993). *SLA2* was also isolated independently as a temperature sensitive endocytosis mutant *end4-1* (Raths *et al* 1993) and as a protein (Mop2p) required for the accumulation and/or maintenance of plasma membrane H^+-ATPase on the cell surface (Na *et al* 1995). Sla2p has also been implicated in vesicle trafficking (Mulholland *et al* 1997).

Yeast lacking *SLA2* display phenotypes characteristic of cortical patch mutants. *sla2* yeast are temperature sensitive and exhibit a disorganised actin cytoskeleton. Cortical actin patches are depolarised and consequently growth in the mother and bud is isotropic resulting in spherical cells (Holtzman *et al* 1993, Raths *et al* 1993). *SLA2* is synthetically lethal with *ABP1*, *SRV2*, *SAC6* (section 1.8.6) and *GCS1* (Blader *et al*

1999) which suggests that their gene products contribute to common properties of the actin cytoskeleton. *SRV2* encodes a protein that binds to actin monomers and to adenylyl cyclase, a component of the Ras signalling pathway in yeast (Freeman *et al* 1995, 1996).

Sla2p contains an N-terminal ENTH domain characteristic of cytoskeletal and endocytic proteins (McCann and Craig, 1999), a proline-rich region, three putative coiled-coil domains, a putative leucine zipper, and a COOH-terminal talin-like domain (figure 4.5) (S. Yang *et al* 1999). In mammalian cells, talin regulates actin dynamics and provides a connection between the actin cytoskeleton and the plasma membrane at adhesion plaques (Critchley 2000). The talin-like domain at the C-terminus is the most conserved sequence among Sla2p family members and binds to F-actin *in vitro* via a conserved actin-binding motif (I/LWEQ) (McCann and Craig 1997, S. Yang *et al* 1999). Analysis of C-terminal talin homology mutants have suggested that this domain may promote actin polymerisation or stabilise F-actin structures (S. Yang *et al* 1999). *In vivo* Sla2p exists as a dimer and the central coiled-coil domain of Sla2p mediates this interaction (Wesp *et al* 1997, Yang *et al* 1999). Mutants that lack both the central coiled-coil domain and either Abp1p or Srv2p are defective in fluid-phase endocytosis (Wesp *et al* 1997) which again indicates that these proteins may perform redundant functions. The N-terminal domain of Sla2p has been shown to be required for endocytosis, normal actin phenotype and for growth at high temperatures (Wesp *et al* 1997). Previous two hybrid studies have shown an interaction between Sla2p and Ark1p which indicate that Sla2p may be regulated by the cortical patch protein kinase (Cope *et al* 1999).

The human homologue of Sla2p is Hip1p, a protein predominantly expressed in the brain, that mediates interaction with human huntingtin protein, implicated in Huntington's disease (Kalchman *et al* 1997, Wanker *et al* 1997). The interaction between Hip1p and huntingtin occurs through the conserved central putative coiled-coil region of Hip1p (Kalchman *et al* 1997). mHip1R is a mouse Sla2p homologue that binds actin *in vitro* and colocalises with actin *in vivo* and also shows colocalisation with cortical endocytic compartments that also contain clathrin and AP-2 (Engqvist-Goldstein *et al* 1999). The inward movement of mHipR in punctate structures from the cell periphery was actin dependent and suggests that mHipR links the actin cytoskeleton with the endocytic machinery. mHipR also binds actin *in vitro* via its talin-like domain yet again showing a link between endocytosis and the actin cytoskeleton (Engqvist-Goldstein *et al* 1999). Affinity chromatography has shown a direct interaction between HIP1 and the clathrin heavy chain as well as α-adaptin A and C (Waelter *et al* 2001). Neurological defects associated with Huntingtons Disease may be related to abnormalities in endocytosis (Metzler *et al* 2001). The studies on yeast Sla2p may provide insights into the etiology of Huntington disease.

1.15. Cortical patch protein Sla1p

1.15.1. *SLA1* was identified in a synthetic-lethal screen

Sla1p is a protein found associated with cortical actin patches and is required for normal cortical actin patch structure and organisation (Ayscough *et al* 1999). It was

originally identified in a synthetic lethal screen for mutations that caused a requirement for the actin-binding protein Abp1p (see section 1.8.8)(Holtzman *et al* 1993). Yeast deleted for the gene *ABP1* which encodes the cortical patch protein Abp1p, display no discernable mutant phenotype. This suggests that other gene product(s) compensate for the loss of *ABP1*. A synthetic-lethal screen was carried out using a plasmid-shuffle strategy and identified three mutations that created a requirement for *ABP1*. One gene, *SAC6* encoded the yeast fimbrin (see section 1.8.6), while two other genes *SLA1* and *SLA2* (Synthetically Lethal with ABP1) encoded novel proteins. *SAC6* had previously been identified in an actin mutation suppressor screen (Adams *et al* 1989), and biochemically by its ability to bind actin (Drubin *et al* 1988).

1.15.2. *SLA1* homologues

A full-length homologue of *SLA1* was identified in the *S. pombe* genome database. Like Sla1p, the predicted *S.pombe* protein contains three SH3 domains, a proline motif, and a C-terminal repeat region. The overall sequence similarity was 27 % but two unrelated regions of around 60 amino acids each, in the central third of the protein had the highest homology (58 % and 60 %) with Sla1p (figure 1.12). The *S.pombe* gene when overexpressed in Δ*sla1* cells partially rescued the temperature sensitive phenotype but not the aberrant actin phenotype (Ayscough *et al* 1999). Other Sla1p homologues are also found in other fungal species, *Candida albicans*, *Aspergillus nidulans* and *Neurospora crassa.*

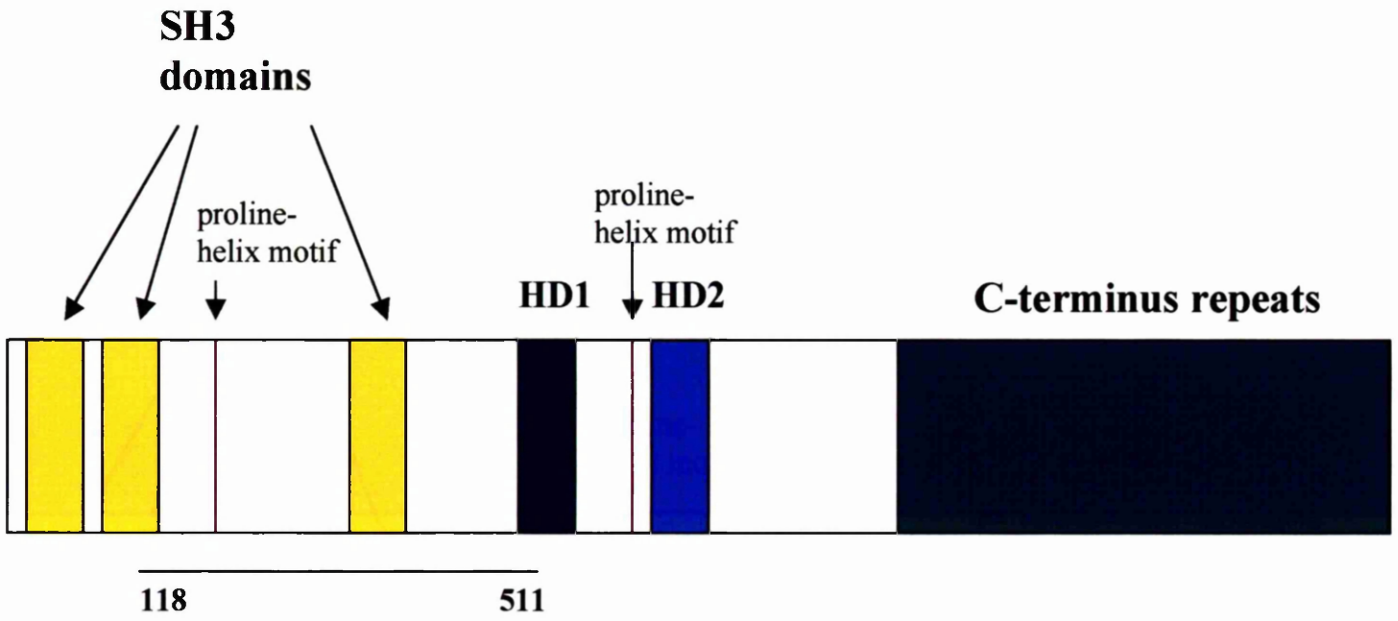

Figure 1.12 Diagram of Sla1p structure. Sla1p contains three SH3 domains in its N-terminal third and a C-terminus comprised of repeats rich in glutamine, proline, glycine and threonine. The central region contains two domains, HD1 and HD2, which share the highest homology with *S. pombe* Sla1p homologue. Sla1p also contains two proline-helix motifs that are putative SH3 binding domains. The Sla1p 118-511 domain required for wild-type actin organisation and growth at 37 °C is marked.

1.15.3. Domain structure of Sla1p

The primary sequence of Sla1p suggested that there were structural elements within the protein that determined the interactions and functions of Sla1p (see figure 1.12) (Holtzman *et al* 1993, Ayscough *et al* 1999). Within the N-terminus lies three Src Homology 3 (SH3) domains, which is a common protein-interaction module which binds to proline-rich motifs (reviewed by Mayer 2001). Sla1p also contains proline-rich motifs which themselves could bind to SH3 domains of other proteins. The C-terminus region contains 26 repeats with the approximate consensus LxxQxTGGxxxPQ. The threonine in this motif is a target for the actin regulating kinases Ark1p and Prk1p (Cope *et al* 1999).

1.15.4. Phenotypes of Δ*sla1* cells

The effect of deletion of *SLA1* from yeast produces several characteristic phenotypes. Deletion of *SLA1* causes cells to be temperature sensitive, have an aberrant cortical actin cytoskeleton organisation and to depend on the expression of *ABP1* (Holtzman *et al* 1993). Δ*sla1* cells are also less sensitive to LAT-A (Ayscough *et al* 1997). Initial analysis on Sla1p was carried out to identify which domain or domains of Sla1p were required by the cell to maintain wild-type characteristics (Ayscough *et al* 1999). This series of deletion mutants was generated carrying *SLA1* missing different regions (figure 3.1a) and were expressed in cells lacking *SLA1*. Yeast expressing the various Sla1p mutants were then assessed for their ability to rescue two phenotypes associated with the deletion of *SLA1*, temperature-sensitive growth and Abp1p dependence. Sla1p lacking an N-terminal region encompassing the third SH3 domain

(amino acids 118-511)(figure 1.12) showed temperature sensitivity at 37 °C but were able to rescue Abp1p dependence.

Sla1p has been shown to be required for the correct localisation of Sla2p and Rho1p (Ayscough *et al* 1999). Rho1p is the regulatory subunit of the cell wall synthesising enzyme 1,3-β-glucan synthase (Drgonová *et al* 1996, Qadota *et al* 1996). Δ*sla1* cells have a thickened mother cell wall while daughter cell walls are apparently normal (Ayscough 1999) possibly due to the mislocalisation of Rho1p.

1.15.5. Interactions and functions of the C-terminal region of Sla1p

Sla1p forms part of a complex *in vivo* with Pan1p and End3p that has been shown to be required for normal actin patch morphology, membrane protein endocyosis and cell wall synthesis (Holtzman *et al* 1993, Bénédetti *et al* 1994, Tang and Cai 1996, Tang *et al* 1997, 2000, Ayscough *et al* 1999, Warren *et al* 2002). Pan1p and End3p are proteins that have been found to play essential roles in both the organisation of the actin cytoskeleton and endocytosis (Bénédetti *et al* 1994, Tang and Cai 1996, Wendland *et al* 1996, Tang *et al* 1997, Wendland and Emr 1998).

Genetic interactions of *PAN1*, *END3* and *SLA1* first suggested that their gene products were involved in a common process (Tang and Cai 1996, Tang *et al* 1997). Subsequent co-immunoprecipitation and GST pulldown experiments confirmed and mapped the sites of physical interaction. The C-terminal region of Sla1p binds to the N-terminal long repeat of Pan1p and also binds the N-terminal EH domain of End3p

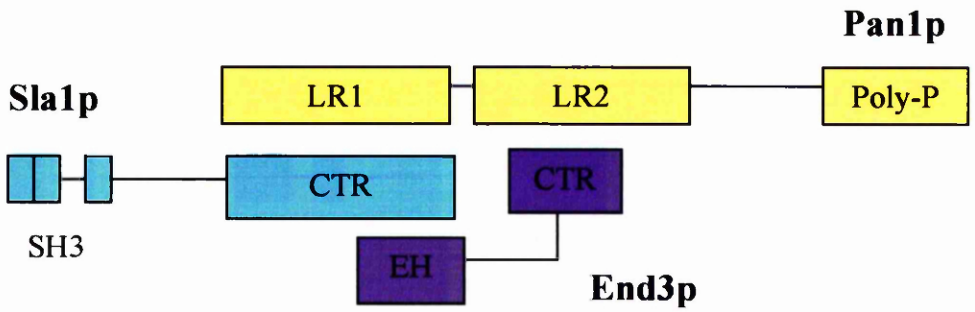

Figure 1.13 Sla1p interacts with the Pan1p/End3p complex. The C-terminal repeat region of Sla1p interacts with the first Long Repeat (LR1) of Pan1p and the N-terminal EH repeat domain of End3p. The C-terminal repeat region of End3p interacts with the second Long Repeat (LR2). Adapted from Tang *et al* 2000.

(Tang *et al* 2000). The central long repeat region of Pan1p can also bind to the End3p C-terminal repeat region (Tang *et al* 2000).

Ark1p and Prk1p are the only serine/threonine kinases, identified so far, which are found associated with cortical actin patches (Cope *et al* 1999, Zeng and Cai 1999). Recent work has shown that the Pan1p/Sla1p/End3p complex is regulated by Prk1p (Zeng and Cai 1999, Zeng *et al* 2001). *In vitro* kinase assays have shown that the C-terminal repeat region of Sla1p is a target of Prk1p and immunoprecipitation experiment also suggest that Ark1p can also phosphorylate Sla1p (Zeng *et al* 2001). This repeat region can also be found in Pan1p which is also phosphorylated by Prk1p (Zeng and Cai 1999). These data support a model that the phosphorylation of the Pan1p/Sla1p/End3p complex regulates the organisation and functions of the actin cytoskeleton.

1.15.6. Interactions and functions of the N-terminal region of Sla1p

As discussed above, an N-terminal mutant of Sla1p was temperature sensitive for growth. This *sla1-Δ118-511* mutant was also found to display an aberrant actin phenotype by rhodamine-phalloidin staining and was defective for the nucleated assembly of rhodamine-actin into cortical actin structures in an *in vitro* permeabilised cell assay (Ayscough *et al* 1999, Li *et al* 1995). This evidence suggests that the Sla1p-118-511 domain is playing a direct role in regulation of the cortical actin cytoskeleton (Ayscough *et al* 1999). However there is no published data relating to interactions between this region of Sla1p and binding partners.

1.16. Summary

The actin cytoskeleton in the budding yeast *S. cerevisiae* provides the structural basis for polarity and guides growth of the yeast cell. *S. cerevisiae* has a single *ACT1* gene that shares high homology with the actin of higher eukaryotes. The ease of genetic manipulation by classical and molecular genetics and well established biochemical techniques make budding yeast a useful model organism for study of the actin cytoskeleton. Despite being a non-motile cell the actin cytoskeleton of budding yeast is highly dynamic and many actin-binding and actin associated proteins which act to regulate the function of the actin cytoskeleton have homologues in higher organisms. Cortical actin patches and actin cables are filamentous actin structures which play crucial roles in endocytosis and intracellular trafficking respectively. Many of the components of the yeast actin cytoskeleton are identified but their exact functions and interactions are still being elucidated.

1.17. Aims

A specific region of Sla1p between residues 118 and 511 had been demonstrated to be critical for the function of Sla1p in regulating organisation of the actin cytoskeleton. The aim of the research undertaken was to determine how this region of the protein was involved in this role.

A two pronged approach was used:

1. To characterise effects of deletion of the Sla1p-118-511 region by looking at growth characteristics and using genetic and fluorescent microscopy techniques. This is outlined in chapter 3.

2. To identify binding partners for the Sla1p-118-511 region using biochemical and/or two-hybrid approaches. This is outlined in chapter 4 and 5.

Chapter 2

Methods and Materials

2.1 Materials.

All chemicals used in this study were obtained from BDH/Merck or Sigma unless otherwise stated.

2.2 Yeast Strains, Plasmids, Oligonucleotides and Antibodies.

All yeast strains, plasmids and oligonucleotides generated and used during the course of this study are listed in tables 2.1, 2.2 and 2.3 respectively.

Table 2.1 Yeast Strains

Strain	Genotype	Origin/Reference
KAY 14	MAT**a**/α *his3-Δ200/his3-Δ200 ura3-52/ura3-52 Δsla1::URA3/Δsla1::URA3*	Ayscough *et al* 1999
KAY17.1A	MAT**a** *his3-Δ200 ura3-52 leu2-3,112 lys2-801 sla1-Δ2::LEU2*	K.Ayscough
KAY17.1B	MATα *his3-Δ200 ura3-52 leu2-3,112 lys2-801 sla1-Δ2::LEU2*	K.Ayscough
KAY17.1C	MATα *his3-Δ200 ura3-52 leu2-3,112 lys2-801*	K.Ayscough
KAY17.1D	MAT**a** *his3-Δ200 ura3-52 leu2-3,112 lys2-801*	K.Ayscough
KAY20	MAT**a**/α *his3-Δ200/ his3-Δ200 ura3-52/ ura3-52 leu2-3,112/ leu2-3,112 lys2-801/ lys2-801 sla1-Δ2::LEU2/ sla1-Δ2::LEU2*	KAY17.1A x 17.1B
KAY30	MAT**a** *his 1*$^-$	DDY55
KAY31	MATα *his 1*$^-$	DDY56
KAY40	MAT**a** /α *his3-Δ200/ his3-Δ200 ura3-52/ ura3-52 leu2-3,112/ leu2-3,112 lys2-801/ lys2-801*	Ayscough *et al* 1999
KAY48	MAT**a** *his3-Δ200 ura3-52*	K.Ayscough
KAY 126	MAT**a** *his3-Δ200 ura3-52 leu2-3,112 Δabp1::LEU2*	K.Ayscough

Strain	Genotype	Origin/Reference
KAY 127	MAT α *his3-Δ200 ura3-52 leu2-3,112 Δabp1::LEU2*	K.Ayscough
KAY 232	MAT**a** /α *his3-Δ200/ his3-Δ200 ura3-52/ura3-52 Δsla1::URA3/Δsla1::URA3* (pKA50, *CEN HIS)*	Ayscough *et al* 1999. This study. KAY 14 + pKA50
KAY 233	MAT**a** /α *his3-Δ200/ his3-Δ200 ura3-52/ura3-52 Δsla1::URA3/Δsla1::URA3* (pKA51, *CEN HIS SLA1*)	Ayscough *et al* 1999. This study. KAY 14 + pKA51
KAY 234	MAT**a** /α *his3-Δ200/ his3-Δ200 ura3-52/ura3-52 Δsla1::URA3/Δsla1::URA3* (pKA53, *CEN HIS sla1-Δ118-511*)	Ayscough *et al* 1999. This study. KAY 14 + pKA53
KAY 235	MAT**a** /α *his3-Δ200/ his3-Δ200 ura3-52/ura3-52 Δsla1::URA3/Δsla1::URA3* (pKA54 *CEN HIS sla1-ΔSH3#1+2*)	Ayscough *et al* 1999. This study. KAY 14 + pKA54
KAY236	MAT**a** /α *his3-Δ200/ his3-Δ200 ura3-52/ura3-52 Δsla1::URA3/Δsla1::URA3 (pKA55 CEN HIS sla1-Δgap2*)	Ayscough *et al* 1999. This study. KAY 14 + pKA55
KAY237	MAT**a** /α *his3-Δ200/ his3-Δ200 ura3-52/ura3-52 Δsla1::URA3/Δsla1::URA3* (pKA13 *CEN HIS sla1-ΔCterm*)	Ayscough *et al* 1999. This study. KAY 14 + pKA13
KAY 300	MAT**a** *his3-Δ200 ura3-52 leu2-3,112 trp1-1 Δsla1::URA3*	K. Ayscough
KAY 302	MATα *his3-Δ200 ura3-52 leu2-3,112 trp1-1 lys2-801*	K. Ayscough
KAY 303	MATα *his3-Δ200 trp1-1 ura3-52 leu2-3,112 lys2-801 sla1-9xmyc::TRP1*	K. Ayscough
KAY317	MAT**a** *his3-Δ200 ura3-52 leu2-3,112 trp1-1 Δsla1::URA3 las17-myc::TRP1*	K. Ayscough

Strain	Genotype	Origin/Reference
KAY318	MATa *his3-Δ200 ura3-52 leu2-3,112 trp1-1 Δsla1::URA3 las17-myc::TRP1* (pKA50, *CEN HIS*)	KAY317 + pKA50
KAY319	MATa *his3-Δ200 ura3-52 leu2-3,112 trp1-1 Δsla1::URA3 las17-myc::TRP1* (pKA51 *CEN HIS SLA1*)	KAY317 + pKA51
KAY320	MATa *his3-Δ200 ura3-52 leu2-3,112 trp1-1 Δsla1::URA3 las17-myc::TRP1* (pKA53 *CEN HIS sla1-Δ118-511*)	KAY317 + pKA53
KAY321	MATa *his3-Δ200 ura3-52 leu2-3,112 trp1-1 Δsla1::URA3 las17-myc::TRP1* (pKA54 *CEN HIS sla1-ΔSH3#1+2*)	KAY317 + pKA54
KAY322	MATa *his3-Δ200 ura3-52 leu2-3,112 trp1-1 Δsla1::URA3 las17-myc::TRP1* (pKA13 *CEN HIS sla1-ΔCterm*)	KAY317 + pKA13
KAY323	MATa *his3-Δ200 ura3-52 leu2-3,112 trp1-1 Δsla1::URA3 las17-myc::TRP1* (pKA55 *CEN HIS sla1-Δgap2*)	KAY317 + pKA55
KAY324	MATa *his3-Δ200 ura3-52 leu2-3,112 trp1-1 Δsla1::URA3 las17-myc::TRP1* (pKA116 *CEN HIS sla1-ΔSH3#3*)	KAY317 + pKA116
KAY325	MATa *his3-Δ200 ura3-52 leu2-3,112 trp1-1 Δsla1::URA3 las17-myc::TRP1* (pKA128 *CEN HIS sla1-PSRP*)	KAY317 + pKA128
KAY326	MATa *his3-Δ200 ura3-52 leu2-3,112 trp1-1 Δsla1::URA3 las17-myc::TRP1* (pKA129 *CEN HIS sla1-Δ118-511(-SH3)*)	KAY317 + pKA129
KAY327	MATa *his3-Δ200 ura3-52 leu2-3,112 trp1-1 Δsla1::URA3 las17-myc::TRP1* (pKA130 *CEN HIS sla1-Δ SH3 all3*)	KAY317 + pKA130
KAY 346	MATa *his3-Δ200 ura3-52 leu2-3,112 trp1-1 las17-myc::TRP1*	K. Ayscough

Strain	Genotype	Origin/Reference
KAY 350	MATα *his3-Δ200 ura3-52 leu2-3,112 lys2-801 sla1-Δ2::LEU2 sla1-Δ118-511::HIS3*	KAY17.1B + integrated *sla1-Δ118-511::HIS3*
KAY 351	MAT**a** *his3-Δ200 ura3-52 leu2-3,112 lys2-801 sla1-Δ2::LEU2 sla1-Δ118-511::HIS3*	KAY17.1A + integrated *sla1-Δ118-511::HIS3*
KAY 352	MAT**a**/α *his3-Δ200/ his3-Δ200 ura3-52/ura3-52 leu2-3,112/leu2-3,112 lys2-801/lys2-801 sla1-Δ2::LEU2/ sla1-Δ2::LEU2 sla1-Δ118-511::HIS3/ sla1-Δ118-511::HIS3*	KAY350 x KAY351
KAY 367	MATα *his3-Δ200 trp1-1 ura3-52 leu2-3,112 lys2-801 sla1-Δ2::LEU2 sla1-Δ118-511-myc::TRP1*	This study. PCR integrated *sla1-Δ118-511-myc* in KAY495 segregant.
KAY 389	MAT**a** *his3-Δ200 trp1-1 ura3-52 leu2-3,112*	K. Ayscough
KAY 397	MATα *his3-Δ200 ura3-52 leu2-3,112 trp1-1 GFP-SLA1::HIS3*	K. Ayscough
KAY400	MAT**a** *his3-Δ200 ura3-52 leu2-3,112 trp1-1 GFP-SLA1::TRP1*	K. Ayscough
KAY 435	MATα *trp1-1 sla1-Δ2::LEU2 sla1-Δ118-511::HIS3*	This study. KAY51 x KAY350 segregant
KAY438	MAT**a** *trp1-901 his3-Δ200 ura3-52 leu2-3,112 gal4Δ gal80Δ LYS2::GAL1$_{UAS}$ -GAL1$_{TATA}$ -HIS3 GAL2 $_{UAS}$ -GAL2 $_{TATA}$ -ADE2*	pJ69-2A James *et al* 1996
KAY 473	MATα *his3Δ1 leu2Δ1 ura3Δ Δlas17::KanMx*	Research Genetics 22437 segregant
KAY 479	MAT**a**/α *his3Δ1/his3Δ1 leu2Δ1/ leu2Δ1 ura3Δ/ura3Δ met 15/MET 15 LYS2/lys2Δ Δycl034w::KanMx/Δycl034w:: KanMx*	Research Genetics 33441

Strain	Genotype	Origin/Reference
KAY480	MATa /α *his3Δ1/ his3Δ1 leu2Δ1/ leu2Δ1 ura3Δ/ura3Δ met 15/MET 15 LYS2/lys2Δ*	Research Genetics Diploid parent strain of KAY481
KAY481	MATa /α *his3Δ1/his3Δ1 leu2Δ1/ leu2Δ1 ura3Δ/ura3Δ met 15/MET 15 LYS2/lys2Δ Δyfr024c-a::KanMx/Δyfr024c-a:: KanMx*	Research Genetics 35704
KAY482	MATa *his3Δ1 leu2Δ1 ura3Δ met 15 Δyfr024c-a::KanMx*	Research Genetics 15704
KAY483	MAT α *his3Δ1 leu2Δ1 ura3Δ met 15 Δyfr024c-a::KanMx*	Research Genetics 15704
KAY486	MATa *his3Δ1 leu2Δ1 ura3Δ met 15 Δrvs167::KanMx*	Research Genetics 4224
KAY488	MATa /α *his3-Δ200/ his3-Δ200 ura3-52/ura3-52 Δsla1::URA3/Δsla1::URA3 (pKA116 CEN HIS sla1ΔSH3#3)*	Ayscough *et al* 1999. This study. KAY14 + pKA116
KAY 489	MATa /α *his3-Δ200/ his3-Δ200 ura3-52/ura3-52 Δsla1::URA3/Δsla1::URA3 (pKA128 CEN HIS sla1-PSRP)*	Ayscough *et al* 1999. This study. KAY14 + pKA128
KAY 490	MATa /α *his3-Δ200/ his3-Δ200 ura3-52/ura3-52 Δsla1::URA3/Δsla1::URA3 (pKA129 CEN HIS sla1-Δ118-511(-SH3))*	Ayscough *et al* 1999. This study. KAY14 + pKA129
KAY 491	MATa /α *his3-Δ200/ his3-Δ200 ura3-52/ura3-52 Δsla1::URA3/Δsla1::URA3* (pKA130 *CEN HIS sla1-Δ SH3 all3*)	Ayscough *et al* 1999. This study. KAY14 + pKA130
KAY492	MATa /α *his3-Δ200/ his3-Δ200 ura3-52/ ura3-52 leu2-3,112/ leu2-3,112 LYS/ lys2-801 Δabp1::LEU2/ABP1 SLA1/sla1-Δ118-511::HIS3*	This study. KAY 126 x KAY 350
KAY494	MATa /α *his3-Δ200/ his3-Δ200 ura3-52/ ura3-52 leu2-3,112/ leu2-3,112 lys2-801/ lys2-801 Δabp1::LEU2/ABP1 SLA1/sla1-Δ2::LEU2*	This study. KAY126 x KAY17.1B

Strain	Genotype	Origin/Reference
KAY495	MATa *HIS/his3-Δ200 trp1-1/TRP 200 URA/ ura3-52 LEU/ leu2-3,112 LYS/ lys2-801 SLA1/ sla1-Δ2::LEU2 sla1-Δ118-511::HIS3*	This study. KAY51 x KAY 350
KAY496	MATa */α his3-Δ200/his3-Δ200 ura3-52/ura3-52 leu2-3,112/ leu2-3,112 lys2-801/ lys2-801 sla1-Δ2::LEU2 sla1-Δ118-511::HIS3/SLA1*	This study. KAY350 x KAY17.1C
KAY497	*MATa /α his3-Δ200/his3-Δ200 ura3-52/ura3-52 leu2-3,112/leu2-3,112 lys2-801/lys2-801 SLA1/sla1-Δ2::LEU2*	This study. KAY17.1D x KAY 17.1B
KAY498	MATa /α *his3-Δ200/ his3-Δ200 ura3-52/ ura3-52 leu2-3,112/ leu2-3,112 trp1-1/ trp1-1 LYS2/lys2-801 Δsla1::URA3/SLA1*	This study. KAY300 x KAY302
KAY499	MATa /α *his3-Δ200/his3-Δ200 ura3-52/ura3-52 leu2-3,112/ leu2-3,112 lys2-801/ lys2-801 sla1-Δ2::LEU2/ sla1-Δ118-511::HIS3*	This study. KAY17.1A x KAY350
KAY500	MATa *trp1-901 his3-Δ200 ura3-52 leu2-3,112 gal4Δ gal80Δ LYS2::GAL1$_{UAS}$ -GAL1$_{TATA}$ -HIS3 GAL2 $_{UAS}$ -GAL2 $_{TATA}$ -ADE2 (pGBDU-Sla1-118-511)*	This study. pJ69-2A + pGBDU - *Sla1-118-511*
KAY 503	MATa *trp1-901 his3-Δ200 ura3-52 leu2-3,112 gal4Δ gal80Δ LYS2::GAL1$_{UAS}$ -GAL1$_{TATA}$ -HIS3 GAL2 $_{UAS}$ -GAL2 $_{TATA}$ -ADE2 (pGBDU-Sla1-118-511(-SH3)* and *pGAD-C1*)	This study. pJ69-2-A + *-Sla1-118-511* (*-SH3*) bait and *pGAD-C1*
KAY 504	MATa *trp1-901 his3-Δ200 ura3-52 leu2-3,112 gal4Δ gal80Δ LYS2::GAL1$_{UAS}$ -GAL1$_{TATA}$ -HIS3 GAL2 $_{UAS}$ -GAL2 $_{TATA}$ -ADE2 (pGBDU-C1* and *pGAD-C1*)	This study. pJ69-2-A + *pGBDU-C1* and *pGAD-C1*
KAY 505	MATa *trp1-901 his3-Δ200 ura3-52 leu2-3,112 gal4Δ gal80Δ LYS2::GAL1$_{UAS}$ -GAL1$_{TATA}$ -HIS3 GAL2 $_{UAS}$ -GAL2 $_{TATA}$ -ADE2 (pGBDU-Sla1-118-511* and *pGAD-C1*)	This study. pJ69-2-A + *-Sla1-118-511* bait and *pGAD-C1*

Strain	Genotype	Origin/Reference
KAY509.2	MATa *his3-Δ200 ura3-52 leu2-3,112 trp1-1 lys2-801 Δsla1::URA3 Δysc84::HIS*	This study. KAY511 segregant
KAY510.1	MATa *his3-Δ200 ura3-52 leu2-3,112 trp1-1 lys2-801 Δysc84::HIS*	This study. KAY511 segregant
KAY510.2	MATα *his3-Δ200 ura3-52 leu2-3,112 trp1-1 lys2-801 Δysc84::HIS*	This study. KAY511 segregant
KAY 511	MATa/α *his3-Δ200/ his3-Δ200 ura3-52/ ura3-52 leu2-3,112/ leu2-3,112 trp1-1/ trp1-1 Δsla1::URA3 lys2-801/SLA 1 Δysc84::HIS*	This study. KAY498 + PCR integrated *Δysc84::HIS*
KAY512	MATa *his3-Δ200 ura3-52 leu2-3,112 trp1-1 GFP-SLA1::TRP1 Δysc84::HIS*	This study. KAY389 + PCR integrated *Δysc84::HIS*
KAY513	MATa *his3-Δ200 ura3-52 leu2-3,112 trp1-1 GFP-SLA1::TRP1 Δysc84::TRP*	This study. KAY400 + PCR integrated *Δysc84*
KAY 515	MATα *his3Δ1 leu2Δ1 ura3Δ Δysc84::HIS3 Δyclo34w::KanMx*	This study. KAY 479 segregant
KAY522.1	MATα *trp1-1 sla1-Δ2::LEU2 sla1-Δ118-511::HIS3 GFP-YCS84::TRP1*	KAY435 + PCR integrated GFP-YSC84. This study.
KAY522.2	MATa *trp1-1 sla1-Δ2::LEU2 sla1-Δ118-511::HIS3 GFP-YCS84::TRP1*	KAY436 + PCR integrated GFP-YSC84. This study.
KAY523	MATa *his3-Δ200 ura3-52 leu2-3,112 trp1-1 Δsla1::URA3 GFP-YSC84::HIS3*	KAY300 +PCR integrated GFP-YSC84. This study.

Strain	Genotype	Origin/Reference
KAY524	MAT**a** *trp1-901 his3-Δ200 ura3-52 leu2-3,112 gal4Δ gal80Δ LYS2::GAL1$_{UAS}$ -GAL1$_{TATA}$ -HIS3 GAL2 $_{UAS}$ -GAL2 $_{TATA}$ -ADE2 (pGBDU-118-511(-SH3))*	This study. pJ69-2A + *pGBDU-118-511(-SH3).*
KAY525	MATα *his3-Δ200 ura3-52 leu2-3,112 trp1-1 lys2-801 GFP-YSC84::TRP1*	KAY302 + PCR integratedGFP-YSC84. This study.
KAY526	MATα *his3-Δ200 ura3-52 leu2-3,112 trp1-1 GFP-YSC84::HIS3*	KAY302 + PCR integratedGFP-YSC84. This study.
KAY527	MAT**a** *his3-Δ200 ura3-52 leu2-3,112 trp1-1 Δsla1::URA3 GFP-YSC84::TRP1*	KAY300 + PCR integratedGFP-YSC84. This study.
KAY528	MATα *his3-Δ200 ura3-52 leu2-3,112 trp1-1 Δsla1::URA3 GFP-YSC84::HIS3*	KAY301 + PCR integratedGFP-YSC84. This study.
KAY529	MATα *his3-Δ200 ura3-52 leu2-3,112 trp1-1 Δsla1::URA3 GFP-YSC84::TRP1*	KAY301 + PCR integratedGFP-YSC84. This study.
KAY531	MATα *his3-Δ200 ura3-52 leu2-3,112 trp1-1 lys2-801 sla1-9xmyc::TRP1 GFP-YFR024C-A::HIS3*	This study. KAY303 +*GFP-YFR024C-A*
KAY532	MATα *his3-Δ200 ura3-52 leu2-3,112 trp1-1 lys2-801 GFP-YFR024C-A::HIS3*	This study. KAY302 +*GFP-YFR024C-A*
KAY534	MAT**a** /α *his3-Δ200 ura3-52 leu2-3,112 trp1-1 GFP- Δysc84::HIS/YSC84 SLA1/sla1-9xmyc::TRP1*	This study. KAY512 x KAY303 segregant
KAY535	MATα *his3-Δ200 ura3-52 leu2-3,112 trp1-1 lys2-801 YSC84-HA::TRP1*	This study. KAY302 + PCR integrated *YSC84-HA*

Strain	Genotype	Origin/Reference
KAY536	MATα *his3-Δ200 ura3-52 leu2-3,112 trp1-1 lys2-801 YSC84-myc::HIS3*	KAY302 + PCR integrated *YSC84-myc.* This study.
KAY537	MATα *his3-Δ200 ura3-52 leu2-3,112 trp1-1 lys2-801 GFP-YFR024C-A::HIS3*	This study. KAY302 + PCR integrated *GFP-YFR024C-A*
KAY538	MATα *his3-Δ200 ura3-52 leu2-3,112 trp1-1 lys2-801 GFP-YFR024C-A::TRP1*	This study. KAY302 + PCR integrated.
KAY539	MAT**a** *his3-Δ200 ura3-52 leu2-3,112 trp1-1 Δsla1::URA3 GFP-YFR024C-A::HIS*	This study. KAY300 + PCR integrated *GFP-YFR024C-A*
KAY540	MAT**a** /α *his3-Δ200/ his3-Δ200 ura3-52/ ura3-52 leu2-3,112/ leu2-3,112 trp1-1/ trp1-1 lys2-801/ lys2-801 Δysc84::HIS/Δysc84::HIS3*	This study. KAY510.1 x KAY510.2
KAY541	MATα *his3Δ1 leu2Δ1 ura3Δ Δlas17::KanMx Δysc84::HIS3*	This study. KAY473 + PCR integrated Δ*ysc84*
KAY542	MAT**a** /α *his3-Δ200/ his3-Δ200 ura3-52/ ura3-52 leu2-3,112/ leu2-3,112 TRP1/ trp1-1 Δabp1::LEU2/ABP1 SLA1/Δsla1::URA3*	This study. KAY126 x KAY301
KAY544	MAT**a** *his3-Δ200 ura3-52 leu2-3,112 Δabp1::LEU2 GFP-YSC84::HIS*	This study. KAY126 + PCR integrated *GFP-YSC84*
KAY545	MAT**a** /α *his3-Δ200/ his3-Δ200 ura3-52/ ura3-52 leu2-3,112/ leu2-3,112 trp1-1/TRP1 lys2-801/LYS2 Δysc84::HIS/YSC84 ABP1/Δabp1::LEU2*	This study. KAY510 x KAY127

Strain	Genotype	Origin/Reference
KAY546	MATα *his3-Δ200 trp1-1 ura3-52 leu2-3,112 lys2-801 sla1-9xmyc::TRP1 HA-YSC84::HIS*	This study. KAY303 + PCR integrated *HA-YSC84*
KAY 547	MATα *his3Δ1 leu2Δ1 ura3Δ Δlas17::KanMx GFP-YSC84::HIS*	This study. KAY 473 + *GFP-YSC84*
KAY548	MAT**a**/α *his3Δ1/ his3-Δ200 leu2Δ1/ leu2-3,112 ura3Δ/ura3-52 met 15/MET15 TRP1/ trp1-1 LYS2/ lys2-801 Δyfr024c-a::KanMx/YFR024C-A YSC84/Δysc84::HIS*	Research Genetics *Δyfr024c-a* x KAY510
KAY549	MATα *his3-Δ200 ura3-52 leu2-3,112 trp1-1 lys2-801 LAS17-myc::TRP1 YSC84-HA::HIS3*	KAY346 + PCR integrated *YSC84-HA.* This study.
KAY550.1	MATα *his3-Δ200ura3-52 leu2-3,112 trp1-1 Δysc84::HIS Δabp1::LEU2*	This study. KAY545 segregant
KAY550.2	MAT**a** *his3-Δ200 ura3-52 leu2-3,112 trp1-1 Δysc84::HIS Δabp1::LEU2*	This study. KAY545 segregant
KAY551.1	MAT α *his3 leu2 ura3*	This study. KAY548 segregant
KAY551.2	MAT**a** *his3 leu2 ura3*	This study. KAY548 segregant
KAY552.1	MAT**a** *his3 leu2 ura3 Δysc84::HIS*	This study. KAY548 segregant
KAY552.2	MAT α *his3 leu2 ura3 Δysc84::HIS*	This study. KAY548 segregant
KAY553.1	MAT α *his3 leu2 ura3 Δyfr024c-a::KanMx*	This study. KAY548 segregant
KAY553.2	MAT**a** *his3 leu2 ura3 Δyfr024c-a::KanMx*	This study. KAY548 segregant

Strain	Genotype	Origin/Reference
KAY554.1	MAT**a** *his3 leu2 ura3 Δyfr024c-a::KanMx Δysc84::HIS*	This study. KAY548 segregant
KAY554.2	MAT α *his3 leu2 ura3 Δyfr024c-a::KanMx Δysc84::HIS*	This study. KAY548 segregant
KAY555	MAT**a** / α *his3-Δ200/ his3-Δ200 ura3-52/ ura3-52 leu2-3,112/ leu2-3,112 trp1-1/ trp1-1 Δsla1::URA3/Δsla1::URA3 Δysc84::HIS/Δysc84::HIS*	This study. KAY509.1 x KAY 509.2
KAY557	MAT**a** /α *his3/his3 leu2/leu2 ura3/ura3 Δyfr024c-a::KanMx/Δyfr024c-a::KanMx Δysc84::HIS/Δysc84::HIS*	This study. KAY554.1 x KAY 554.2
KAY558	MAT**a** *his3-Δ200 ura3-52 leu2-3,112 trp1-1 Δsla1::URA3 LAS17-myc::TRP1 YSC84-HA::HIS3*	This study. KAY317 + PCR integrated YSC84-HA
KAY559	MAT**a** /α *his3-Δ200 /his3 leu2-3,112 /leu2 ura3-52/ura3 YFR024C-A /Δyfr024c-a::KanMx YSC84/Δysc84::HIS Δabp1::LEU2/ABP1*	This study. KAY554.2 x KAY126
KAY560	MAT**a** /α *his3-Δ200/ his3 ura3-52/ura3 leu2-3,112/leu2 trp1-1/TRP1 Δsla1::URA3/SLA1 YSC84/Δysc84::HIS YFR024C-A/Δyfr024c-a::KanMx*	This study. KAY300 x KAY554.2
KAY562	MATα *his3-Δ200 trp1-1 ura3-52 leu2-3,112 lys2-801 sla1-9xmyc::TRP1 YSC84-(7x alanine linker)-HA::HIS3*	This study. KAY303 + integrated PCR *YSC84-(*7x alanine linker)-*HA::HIS3*
KAY 563	MATα *his3-Δ200 ura3-52 leu2-3,112 trp1-1 lys2-801 LAS17-myc::TRP1 YSC84-*(7x alanine linker)-*HA::HIS3*	This study. KAY346 + integrated PCR *YSC84-*(7x alanine linker)-*HA::HIS3*

Strain	Genotype	Origin/Reference
KAY564	MATα *his3-Δ200 ura3-52 leu2-3,112 trp1-1 lys2-801 YSC84-(*7x alanine linker)-*myc::TRP1*	This study. KAY302 + integrated PCR
KAY 565.1	MAT α *his3 leu2 ura3 Δyfr024c-a::KanMx Δysc84::HIS Δsla1::URA3*	This study.KAY300 x 554.2 segregant
KAY 565.2	MAT**a** *his3 leu2 ura3 Δyfr024c-a::KanMx Δysc84::HIS Δsla1::URA3*	This study. KAY300 x KAY554.2 segregant
KAY 566.1	MATα *his3 leu2 ura3 Δysc84::HIS Δsla1::URA3*	This study. KAY300 x KAY554.2 segregant.
KAY 566.2	MAT**a** *his3 leu2 ura3 Δysc84::HIS Δsla1::URA3*	This study. KAY300 x KAY554.2 segregant
KAY567.1	MAT**a** *trp1-901 his3-Δ200 ura3-52 leu2-3,112 gal4Δ gal80Δ LYS2::GAL1$_{UAS}$ -GAL1$_{TATA}$ -HIS3 GAL2 $_{UAS}$ -GAL2 $_{TATA}$ -ADE2 (pGBDU-Sla1-118-511 + pGAD#103)*	This study. pJ69-2-A + pKA237 bait and library *SLA2* plasmid #103
KAY567.2	MAT**a** *trp1-901 his3-Δ200 ura3-52 leu2-3,112 gal4Δ gal80Δ LYS2::GAL1$_{UAS}$ -GAL1$_{TATA}$ -HIS3 GAL2 $_{UAS}$ -GAL2 $_{TATA}$ -ADE2 (pGBDU-Sla1-118-511 + pGAD#104)*	This study. pJ69-2-A + pKA237 bait and library *SLA2* plasmid #104
KAY567.3	MAT**a** *trp1-901 his3-Δ200 ura3-52 leu2-3,112 gal4Δ gal80Δ LYS2::GAL1$_{UAS}$ -GAL1$_{TATA}$ -HIS3 GAL2 $_{UAS}$ -GAL2 $_{TATA}$ -ADE2 (pGBDU-Sla1-118-511 + pGAD#122)*	This study. pJ69-2-A + pKA237 bait and library *SLA2* plasmid #122
KAY567.4	MAT**a** *trp1-901 his3-Δ200 ura3-52 leu2-3,112 gal4Δ gal80Δ LYS2::GAL1$_{UAS}$ -GAL1$_{TATA}$ -HIS3 GAL2 $_{UAS}$ -GAL2 $_{TATA}$ -ADE2 (pGBDU-Sla1-118-511 + pGAD#165)*	This study. pJ69-2-A + pKA237 bait and library *SLA2* plasmid #165

Strain	Genotype	Origin/Reference
KAY568.1	MATa *trp1-901 his3-Δ200 ura3-52 leu2-3,112 gal4Δ gal80Δ LYS2::GAL1$_{UAS}$ -GAL1$_{TATA}$ -HIS3 GAL2 $_{UAS}$ -GAL2 $_{TATA}$ -ADE2 (pGBDU-Sla1-118-511 + pGAD#92)*	This study. pJ69-2-A + pKA237 bait and library *SLA2* plasmid #92
KAY568.2	MATa *trp1-901 his3-Δ200 ura3-52 leu2-3,112 gal4Δ gal80Δ LYS2::GAL1$_{UAS}$ -GAL1$_{TATA}$ -HIS3 GAL2 $_{UAS}$ -GAL2 $_{TATA}$ -ADE2 (pGBDU-Sla1-118-511 + pGAD#200)*	This study. pJ69-2-A + pKA237 bait and library *SLA2* plasmid #200
KAY569	MATa *trp1-901 his3-Δ200 ura3-52 leu2-3,112 gal4Δ gal80Δ LYS2::GAL1$_{UAS}$ -GAL1$_{TATA}$ -HIS3 GAL2 $_{UAS}$ -GAL2 $_{TATA}$ -ADE2 (pGBDU-Sla1-118-511 + pGAD#94)*	This study. pJ69-2-A + pKA237 bait and library *SLA2* plasmid #94
KAY570	MATa *trp1-901 his3-Δ200 ura3-52 leu2-3,112 gal4Δ gal80Δ LYS2::GAL1$_{UAS}$ -GAL1$_{TATA}$ -HIS3 GAL2 $_{UAS}$ -GAL2 $_{TATA}$ -ADE2 (pGBDU-Sla1-118-511 + pGAD#140)*	This study. pJ69-2-A + pKA237 bait and library *YSC84* plasmid #140
KAY571	MATa *trp1-901 his3-Δ200 ura3-52 leu2-3,112 gal4Δ gal80Δ LYS2::GAL1$_{UAS}$ -GAL1$_{TATA}$ -HIS3 GAL2 $_{UAS}$ -GAL2 $_{TATA}$ -ADE2 (pGBDU-Sla1-118-511 + pGAD#151)*	This study. pJ69-2-A + pKA237 bait and library *YSC84* plasmid #151
KAY572	MATa *trp1-901 his3-Δ200 ura3-52 leu2-3,112 gal4Δ gal80Δ LYS2::GAL1$_{UAS}$ -GAL1$_{TATA}$ -HIS3 GAL2 $_{UAS}$ -GAL2 $_{TATA}$ -ADE2 (pGBDU-Sla1-118-511 + pGAD#175)*	This study. pJ69-2-A + pKA237 bait and library *YSC84* plasmid #175
KAY573.1	MATa *trp1-901 his3-Δ200 ura3-52 leu2-3,112 gal4Δ gal80Δ LYS2::GAL1$_{UAS}$ -GAL1$_{TATA}$ -HIS3 GAL2 $_{UAS}$ -GAL2 $_{TATA}$ -ADE2 (pGBDU-Sla1-118-511 (-SH3) + pGAD#103)*	This study. pJ69-2-A + pKA237 bait and library *SLA2* plasmid #103

Strain	Genotype	Origin/Reference
KAY573.2	MATa *trp1-901 his3-Δ200 ura3-52 leu2-3,112 gal4Δ gal80Δ LYS2::GAL1$_{UAS}$ -GAL1$_{TATA}$ -HIS3 GAL2 $_{UAS}$ -GAL2 $_{TATA}$ -ADE2 (pGBDU-Sla1-118-511 (-SH3) + pGAD#104)*	This study. pJ69-2-A + pKA238 bait and library *SLA2* plasmid #104
KAY573.3	MATa *trp1-901 his3-Δ200 ura3-52 leu2-3,112 gal4Δ gal80Δ LYS2::GAL1$_{UAS}$ -GAL1$_{TATA}$ -HIS3 GAL2 $_{UAS}$ -GAL2 $_{TATA}$ -ADE2 pGBDU-Sla1-118-511 (-SH3) + pGAD#122*	This study. pJ69-2-A + pKA238 bait and library *SLA2* plasmid #122
KAY573.4	MATa *trp1-901 his3-Δ200 ura3-52 leu2-3,112 gal4Δ gal80Δ LYS2::GAL1$_{UAS}$ -GAL1$_{TATA}$ -HIS3 GAL2 $_{UAS}$ -GAL2 $_{TATA}$ -ADE2 (pGBDU-Sla1-118-511 (-SH3) + pGAD#165)*	This study. pJ69-2-A + pKA238 bait and library *SLA2* plasmid #165
KAY574.1	MATa *trp1-901 his3-Δ200 ura3-52 leu2-3,112 gal4Δ gal80Δ LYS2::GAL1$_{UAS}$ -GAL1$_{TATA}$ -HIS3 GAL2 $_{UAS}$ -GAL2 $_{TATA}$ -ADE2 (pGBDU-Sla1-118-511 (-SH3) + pGAD#92)*	This study. pJ69-2-A + pKA238 bait and library *SLA2* plasmid #92
KAY574.2	MATa *trp1-901 his3-Δ200 ura3-52 leu2-3,112 gal4Δ gal80Δ LYS2::GAL1$_{UAS}$ -GAL1$_{TATA}$ -HIS3 GAL2 $_{UAS}$ -GAL2 $_{TATA}$ -ADE2 (pGBDU-Sla1-118-511 (-SH3) + pGAD#200)*	This study. pJ69-2-A + pKA238 bait and library *SLA2* plasmid #200
KAY575	MATa *trp1-901 his3-Δ200 ura3-52 leu2-3,112 gal4Δ gal80Δ LYS2::GAL1$_{UAS}$ -GAL1$_{TATA}$ -HIS3 GAL2 $_{UAS}$ -GAL2 $_{TATA}$ -ADE2 (pGBDU-Sla1-118-511 (-SH3) + pGAD#94)*	This study. pJ69-2-A + pKA238 bait and library *SLA2* plasmid #94
KAY576	MATa *trp1-901 his3-Δ200 ura3-52 leu2-3,112 gal4Δ gal80Δ LYS2::GAL1$_{UAS}$ -GAL1$_{TATA}$ -HIS3 GAL2 $_{UAS}$ -GAL2 $_{TATA}$ -ADE2 (pGBDU-Sla1-118-511 (-SH3) + pGAD#140)*	This study. pJ69-2-A + pKA238 bait and library *YSC84* plasmid #140

Strain	Genotype	Origin/Reference
KAY577	MATa *trp1-901 his3-Δ200 ura3-52 leu2-3,112 gal4Δ gal80Δ LYS2::GAL1$_{UAS}$ -GAL1$_{TATA}$ -HIS3 GAL2 $_{UAS}$ -GAL2 $_{TATA}$ -ADE2 (pGBDU-Sla1-118-511 (-SH3) + pGAD#151)*	This study. pJ69-2-A + pKA238 bait and library *YSC84* plasmid #151
KAY578	MATa *trp1-901 his3-Δ200 ura3-52 leu2-3,112 gal4Δ gal80Δ LYS2::GAL1$_{UAS}$ -GAL1$_{TATA}$ -HIS3 GAL2 $_{UAS}$ -GAL2 $_{TATA}$ -ADE2 (pGBDU-Sla1-118-511 (-SH3) + pGAD#175)*	This study. pJ69-2-A + pKA238 bait and library *YSC84* plasmid #175

Table 2.2. Plasmids

Plasmid	Construction	Origin/Reference
pKA13	A 754-bp *Bam*HI and *Eag* I fragment encoding most of the C-terminus of *SLA1* was cut out of pKA51	Ayscough *et al* 1998.
pKA32	The *sla1-Δ118-511* mutant was excised from pKA53 using *Xba* I and cloned into pRS316 (*CEN, URA3*)	Ayscough *et al* 1998.
pKA38	The *sla1-118-511* fragment was excised by *Eco*R1 digest of pKA51 and cloned into pGEX	This study.
pKA45	pGEX-1	Pharmacia
pKA50	pRS313 (*CEN, HIS3*) was cut with *Pvu*II and religated to remove polylinker.	Ayscough *et al* 1999.
pKA51	*SLA1* on *Sal*I fragment was blunt-ended and ligated into pKA50 at the *Pvu*I site.	Ayscough *et al* 1999.
pKA53	pKA51 was cut with *Eco*RI removing a 1182 bp fragment and religated.	Ayscough *et al* 1999.

Plasmid	Construction	Origin/Reference
pKA54	PCR was used to generate an *Apa*I site at base 9 of the SLA1 coding sequence in pKA51. The plasmid was then cut with ApaI releasing a 575bp fragment encompassing the first two SH3 domains.	Ayscough *et al* 1999.
pKA55	PCR was used to generate a *Bam*HI site at base 1522 of the SLA1 coding sequence in pKA51. The plasmid was then cut with *Bam*HI releasing a 1495 bp fragment encompassing the central 'gap2' region.	Ayscough *et al* 1999.
pKA116	*Xho*I sites were generated by site-directed mutagenesis on either side of the third SH3 domain of *SLA1* in pKA51. This domain was then excised, and the plasmid was religated.	Ayscough *et al* 1999.
pKA119	pWZV87 (for 9xmyc::*TRP1* tagging)	K. Nasmyth, IMP Vienna.
pKA121	*Xho*I site was generated by site-directed mutagenesis on the 5' side of the coding region for the third SH3 domain of *SLA1* in pKA51.	This study.
pKA128	Site-directed mutagenesis was used to mutate the coding sequence for the proline-helix motif to give a change of P to S at residue 626 of *SLA1* using oligos oKA21 and oKA22 against pKA51.	This study. Ayscough *et al* 1999.

Strain	Construction	Origin/Reference
pKA129	*Xho*I sites were generated by site-directed mutagenesis on the 5' side of the coding region for the third SH3 domain of *SLA1* and on the 3' side of the second SH3 domain in pKA51. Using oligos oKA15 and oKA16 against pKA121. The Gap1 domain was then excised, and the plasmid was religated giving *sla1-118-511(-SH3)*	This study. Ayscough *et al* 1999.
pKA130	*Xho*I sites were generated by site-directed mutagenesis on either side of the third SH3 domain in pKA54 using successive PCR using oligos oKA3 and oKA4 and then oKA1 and oKA2. This domain was then excised, and the plasmid was religated giving *sla1-Δall SH3.*	This study. Ayscough *et al* 1999.
pKA148	pFA6-HIS3MX6	Longtine *et al* 1998.
pKA150	pFA6-3xHA-HIS3MX6	Longtine *et al* 1998.
pKA156	pFA6-HIS3MX6 pGAL-GFP	Longtine *et al* 1998.
pKA159	pFA6-13xmyc-TRP1	Longtine *et al* 1998.
pKA161	pGEX-1-*sla1-Δ118-511(-SH3).* The *Eco*R1 fragment from pKA116 was cloned into pKA45.	This study.
pKA162	pGAD-C1	James *et al* 1996.
pKA168	pGBDU-C1	James *et al* 1996.
pKA221	pFA6-pGAL-GFP TRP1	Longtine *et al* 1998.

Plasmid	Construction	Origin/Reference
pKA235	pKA32 was cut with *Xho*1 and *Sac*II to release *sla1-Δ118-511* and ligated into pRS303	This study.
pKA237	pGBDU-*sla1-Δ118-511*	This study.
pKA238	pGBDU-*sla1-Δ118-511*(-*SH3*)	This study.
pKA241-243	pGAD-*YSC84* isolates from two-hybrid screen	This study.
pKA244-245	pGAD-*SLA2* isolates from two-hybrid screen	This study.
pKA251	Site-directed mutagenesis on pKA243 to introduce a stop codon prior to SH3 domain of *YSC84* at residue 397.	This study.

Table 2.3 Oligonucleotides

Oligo	Nucleotide sequence 5'→ 3'
oKA1	CTGGGTTGAGAGAACTCGAGATGGCTTCCAAATC
oKA 2	GATTTGGAAGCCATCTCGAGTTCTCTCAACCCAG
oKA 3	GTTCCTGCACAGTTTCTCGAGCCTGTTCGTGAC
oKA 4	GTCACGAACAGGCTCGAGAAACTGTGCAGGAAC
oKA7	CCTCAACAATCAAGGCAAGCCAACATATTCAATGCTACTGCAT CAAATCCGTTTGGATTCTCCGGTTCTGCTGCTAG
oKA8	ACGAAACTATTTCATATATCGTGTTTTAGTTATTATCCTATAAA ATCTTAAAATACATTAATCGGAGCTCCGGCTTTCTG
oKA 15	CATTCCAGGCGGTTACCTCGAGCCAGAGAATGGGTCCACTTC
oKA 16	GAAGTGGACCCATTCTCTGGCTCGAGGTAATTGCCTGGAATG
oKA 21	GAATTGCCTCCAATAAAACCCTCGAGACCAACCTCTACTACC
oKA 22	GGTAGTAGAGGTTGGTCTCGAGGGTTTTATTGGAGGCAATTC
oKA 36	GAAGGGATAGTGTAACATAG
oKA37	CCATTCTCTGGTTCGACGTA

Oligo	Nucleotide sequence 5'→ 3'
oKA38	ACTTCCAAGCAGGAACAGGC
oKA 39	GAAGGCCAAGCTATCAATCG
oKA 40	TTGACCACTCATGAGGAGTC
oKA 41	CCTGCACAGTTTATTGACCC
oKA 42	CAGCACTACCTACAACATCG
oKA 43	CGCCGCTGATAAACTATCCA
oKA 44	AACGGAGGTAGTAGAGGTTG
oKA 45	ATTGCGGCGTTGATGTAACC
oKA 46	AGAAGCCGGTTTAACAGTCC
oKA 47	GAACCTAAAAAGGCAGCTGC
oKA 48	TGAAGTTTGCGGGAATTGCG
oKA 89	AAAGAAGGGATAGTGTAACATAGCCAAGGCGACAGAGTGTGT TATATACAAAAGAGCTAGGAATTCGAGCTCGTTTAAAC
oKA 90	TGGTGTCTGCGGCTCATAGGCATAGACGGCCCTATAGATGCCC AGAAACACAGTCATACTTTTGTATAGTTCATCCATGC
oKA136	CACAGTAAAATTTTCAAGAGTAGTGGTAAATATCAAATCCAAA ATCCAAAACGGATCCCCGGGTTAATTAA
oKA 137	TCTAAAAAAAATTCTATATATAGGAACGAGACATATGGAGGAC GATATTGAATTCGAGCTCGTTTAAAC
oKA 138	GGACTAACGGAAAAGAAGGAATATTCCCTGCAAACTACGTTAG AGTTTCTCGGATCCCCGGGTTAATT
oKA 139	CTGTTTTATATTTCCTGTTT
oKA 140	TGGCGTATAGTCCAGTTTCA
oKA 141	TGCAAACTACGTTAGAGT
oKA 153	ATACCACTACAATGGATGATG
oKA 154	AGATGGGCATTAATTCTAGTC
oKA 165	ACTTCACAGTAAAATTTTCAAGAGTAGTGGTAATATCAAATCC AAAATCCAAAAGAATTCGAGCTCGTTTAAAC

Oligo	Nucleotide sequence 5'→ 3'
oKA 166	AACATACTTGGTCTCGCTTTTCAAGCTTCGAGGAATTGGATTAT TGCTACCCATTTTGTATAGTTCATCCATGC
oKA 167	ACTAGAGAGCTATCTTGAAC
oKA 182	ACATCATCATCGGAAGAGAG
oKA 183	AATGAAAGAAATTGAGATGG
oKA 192	GTAGAGAGCAACAGCCGTTG
oKA 196	GTGCGAATACCCGATGGGAA
oKA 198	GGCTTTGGATCACGGGTGGCAAAGAAATCAAAAACAAAAGCT GTATCACACGCAGAATCCGAGCTCGTTTAAAC
oKA 199	AACATACTTTGTCTCACTCTTTAAACTCCTTGGAATAGGATTGT TAATACCCATTTTGTATAGTTCATCCATGC
oKA 200	CTGTGTAGAAGTGAATGATC
oKA 201	TTTCAAAACGTCTGGAGGAA
oKA216	ATGGTGGACATCCTAACGAC
oKA 228	CCAACGGCTGTTGCTCTCTAAAATTTTGCTGGAGAACAACC
oKA 229	GGTTGTTCTCCAGCAGGGTTTTAGAGAGCAACAGCCGTTGG

Table 2.4 Antibodies

All antibodies used had been affinity purified.

Application	Antibody	Dilution Factor	Source / Reference
anti-Sla1p western	primary antibody:	1/250	David Drubin U.C. Berkeley
	rabbit anti-yeast anti-Sla1p		
	secondary antibody:	1/1000	Sigma
	goat anti-rabbit-HRP IgG		

Application	Antibody	Dilution Factor	Source / Reference
anti-Sla2p western	primary antibody: rabbit anti-Sla2p	1/500	David Drubin U.C. Berkeley
	secondary antibody: Alkaline phosphatase conjugated goat anti-rabbit IgG	1/5000	Sigma
anti-Abp1p western	primary antibody: rabbit anti-Abp1p	1/2500	David Drubin U.C. Berkeley
	secondary antibodies: goat anti-rabbit-alkaline phosphatase conjugated IgG	1/5000	Sigma
	goat anti-rabbit-HRP IgG	1/1000	Sigma
anti-myc western	primary antibody: rabbit anti-myc (A14)	1/1000	Santa Cruz Biotechnology Inc.
	secondary antibodies: Alkaline phosphatase conjugated goat anti-rabbit IgG	1/5000	Sigma
	goat anti-rabbit-HRP IgG	1/1000	Sigma
anti-HA western	primary antibody: rabbit anti-HA (Y-11)	1/1000	Santa Cruz Biotechnology Inc.
	secondary antibody: Alkaline phosphatase conjugated goat anti-rabbit IgG	1/5000	Sigma
anti-myc immunostaining	primary antibody: rabbit anti-myc (A14)	1/100	Santa Cruz Biotechnology Inc.
	secondary antibody: goat anti-rabbit FITC conjugated IgG	1/100	Vector Labs
anti-myc immunoprecipitation	mouse anti-myc (9E10)	1/100	Santa Cruz Biotechnology Inc.
anti-HA immunoprecipitation	rat anti-HA (3F10)	1/100	Santa Cruz Biotechnology Inc.

2.3. Molecular Biology Techniques

2.3.1 Boiling plasmid miniprep

E.coli were grown in 1-3 ml 2YT-AMP overnight then 1.5 ml was centrifuged in eppendorf tubes at 15 000 g for 1 min. After removal of supernatant, 350 µl STET (8% Sucrose, 5% Triton X-100, 50mM EDTA, 50mM Tris pH8.0) was added and the pellet resuspended by micropipette. 25 µl lysozyme (10mg/ml in TE) was added and vortexed briefly then boiled for 1 min. The tubes were then spun immediately for 15 minutes and the resultant pellet removed with a sterile toothpick and discarded. 30 µl 3M sodium acetate pH 5.2 and 300 µl isopropanol were added to the supernatant before centrifugation at 10000 g for 5 minutes. The pellet was rinsed with 70% ethanol, spun briefly then left to dry for 5-10 minutes after removal of the supernatant. 20 µl of sterile distilled water was added to the tube taking care to wash down the walls of the tube. 5 – 10 µl was used for a 20 µl restriction enzyme digest.

2.3.2. Plasmid DNA purification using Qiagen Preps

Purification of plasmid DNA was prepared using the Qiagen DNA purification system (mini, midi, maxi or giga) according to the manufacturer's instructions. This system was based on the alkaline lysis method of DNA purification followed by purification of the DNA on a silica based resin. The DNA was eluted from the resin in 50 µl of 1 X TE buffer or sterile distilled water. Plasmid DNA was always purified in this way if it was needed for DNA sequencing or for use in transformations.

2.3.3. Electrophoresis of DNA using agarose gels.

DNA fragments were routinely separated and visualised using flat bed agarose gel electrophoresis. An agarose gel was made by melting 0.8 % agarose in TAE (10 mM Tris-HCl pH 7.5, 1 mM EDTA pH7.5). 5 µl of a 10 mg/ml stock of ethidium bromide was added per 50 ml of agarose solution. The solution was then poured into a casting

tray containing a comb with the required number of teeth. After the gel had set, the DNA was mixed with 6 x gel loading buffer (0.25% Bromophenol Blue, 0.25% Xylene Cyanol FF, 30% glycerol in water) and then loaded into the wells of the gel. Samples were electrophoresed in 1 x TAE at between 80 and 120 V until the bromophenol blue of the loading buffer had run 2.5-5 cm. The DNA was then visualised by illuminating the gel with a UV light source.

2.3.4 Extraction of DNA from an Agarose Gel

Extraction of DNA from agarose gels was performed using a QIAEXII kit™ (QIAGEN). The DNA to be extracted was run on a 0.8 % agarose gel (see section 2.3.3) and viewed by illuminating the gel with a UV source. The DNA band was cut out of the gel using a clean scalpel, and the gel slice was placed in a 1.5 ml microfuge tube. Buffer QX1™ was added to the gel slice, according to instructions (dependent on size of DNA) along with 10 µl of resuspended QIAEX II™. Tubes were incubated at 50 °C for 10 minutes to solubilise the agarose and allows the QIAEX II™ particles to bind the DNA. The sample was then centrifuged at top speed in a bench top microfuge for 30 seconds and the supernatant was carefully removed with a pipette. The pellet was washed once with 500 µl of Buffer QX1™ and twice with 500 µl of Buffer PE. Tubes were centrifuged at top speed in a bench top microfuge for 30 seconds after each wash. The pellet was then air-dried for 15 minutes, DNA was eluted from the QIAEX II™ particles by resuspending the pellet in 25 µl of sterile water and incubating at room temperature or at 50 °C for 5 minutes depending on size of DNA fragment. Tubes were centrifuged for 30 seconds and the supernatant was placed in a fresh microfuge tube and stored at –20°C until required.

2.3.5. Restriction enzyme digestion of DNA

All enzymes used in this study were from New England Biolabs and digests were carried out according to the manufacturer's instructions, using the buffers supplied. Digests were typically performed in a final volume of 20 µl, using 2-10 U of enzyme

per reaction. Double digests were performed where necessary when buffer conditions were compatible keeping the enzyme volume per reaction under 10 %. BSA was added (to 1x) when required. Distilled water was added as required to make up the appropriate final volume. Most digests were carried out at 37 °C for 2-3 hours unless otherwise recommended by the manufacturer.

2.3.6. Removal of the terminal 5' phosphate groups using calf intestinal alkaline phosphatase (C.I.A.P.)

To prevent self-annealing of vector ends after restriction digest, the reactions containing vector were treated with C.I.A.P. (Gibco). 25 U C.I.A.P. (25 U/µl) in 1x dephosphorylation buffer was added to 21.5 µl of digested and QIAEX extracted (section 2.3.4) vector DNA and incubated at 37°C for 1 hour. To stop the reaction EDTA (pH8) was added to 5mM and the reaction incubated at 75 °C for 20 minutes.

2.3.7. DNA ligation

DNA ligation was performed using a Rapid DNA ligation kit (Roche Diagnostics). Vector (C.I.A.P. treated) and insert DNA were diluted in DNA dilution buffer to a final volume of 10 µl. 10 µl of 2 X DNA ligase buffer was then added along with 1 µl of T4 DNA ligase. A control reaction containing C.I.A.P. treated vector and no insert DNA was also set up. The contents were mixed well and incubated at room temperature for 5 minutes. 2 µl of the ligation mix was used to transform ultracompetent XL2 blue *E.coli* cells (Stratagene).

2.3.8. Amplification of DNA using the polymerase chain reaction

The polymerase chain reaction (PCR) is a method used to amplify specific DNA fragments using specific oligonucleotide primers complementary in sequence to the regions flanking the sequence of interest. PCR was used on several occasions during this project, the method described here was a general PCR method used to amplify sequences from plasmids designed to allow deletion or tagging of genes within the

yeast genome. General PCR carried out during this study was achieved using Bioline reagents.

For each PCR reaction the following were mixed in 0.5 ml thin-walled PCR tubes: 1 X *Taq* reaction buffer, 200 nM dNTP's, 1.5 mM $MgCl_2$, 1 μM forward primer, 1 μM reverse primer, 1 μl template DNA, 1 μl Bioline Taq (5 U/ μl) and water to 100 μl. The components were mixed gently. A general PCR occurred over 30 cycles of amplification in a MWG Biotech Primus PCR machine, each involving steps of 94°C (1 minute), 55°C (2 minute), 72°C (1-4 minutes). Cycling parameters varied according to length of final product: 1 minute extension time (72 °C) was allowed per 1 kb to be amplified. A final elongation step was used at the end of the amplification cycles by incubating at 72°C for 5 minutes. The resulting product was electrophoresed on a 0.8 % agarose gel to check for amplification products.

2.3.9. PCR for site-directed mutagenesis of plasmid DNA

Reactions were set up as below per 50 μl reaction:

	volume (μl)
10 X reaction buffer	5
forward oligo (125 ng/μl)	1
reverse oligo (125 ng/μl)	1
12.5 mM dNTPs	1.5
template	0, 2μl or 5μl
Pfu Turbo polymerase	1 μl
sterile distilled water	to 50 μl

Pfu Turbo polymerase and 10 X reaction buffer were all supplied by Stratagene. Pfu Turbo was added during an initial 94 °C incubation for 1 min. The reactions were amplified by 16 cycles of 95 °C x 40 seconds, 55 °C x 1 minute, 68 °C 2 x length of plasmid (kb) x minutes.

Reactions were treated with 1 µl Dpn1 (NEB) to digest parental DNA template plasmid (digests methylated DNA) at 37 °C for 1 hr before transformation into XL2 blue ultracompetent cells (Stratgene) according to manufacturers instructions.

2.3.10 Generating Integrated Gene Deletion or Tagged Strains

A set of plasmids exist that allow genes within the yeast genome to be easily tagged or deleted (Longtine *et al*, 1998). These plasmids allow amplification of a tag or stop codon and selection marker by PCR using oligonucleotides that have been designed with regions of homology to a specific site in the yeast genome. Transformation of this PCR product into yeast cells (see section 2.5.5) allow its incorporation into the specific site in the yeast genome via homologous recombination. The transformation mixture is spread onto plates lacking certain nutrients, allowing selection of transformed cells.

2.3.11. Screening for Integrated Tags or Gene Deletions by Colony PCR

After transformants have grown into colonies they were struck out onto YPAD plates and incubated at 29 °C overnight. The next day, a single colony was picked using a toothpick and resuspended in 20 µl of SPZ Buffer (1.2 M sorbitol, 0.1 M Potassium Phosphate buffer pH7.5 and 2.5 mg/ml zymolyase (ICN Biomedicals)). Cell suspensions were incubated at 37 °C for 30 minutes and boiled for 5 minutes. This crude prep was used as the template in a standard PCR (see section 2.2.5) that used oligonucleotides that were designed to the regions flanking the insert region. This PCR would either generate a wild type band or a larger integration band for tagged sequences of DNA or smaller band for deletion PCR products. PCR products were visualised by running on an agarose gel (see section 2.2.6).

2.4 Bacterial Methods

2.4.1. Bacterial growth media

The following media were used for the growth and maintenance of various E. coli strains used throughout this study.

2YT 1.6 % tryptone
1 % yeast extract
0.5 % NaCl

Supplemented with 2% agar for solid media

M9 minimal media 0.675 % Na_2HPO_4
(drop-out leucine) 0.3 % KH_2PO_4
0.05 % NaCl
0.1 % ammonium chloride
0.035 % drop-out leucine supplement

Supplemented (when cooled to 50 °C) with 2 mM $MgSO_4$, 0.1mM $CaCl_2$, 1mM thiamine, 0.4 % glucose and 0.05% ampicllin. Supplemented with 2% agar for solid media.

NZY^+ broth 1 % NZ amine (casein hydrolysate)
0.5 % yeast extract
0.5 % NaCl

pH adjust to 7.5 with NaOH before autoclaving. Before use the following supplements added: 12.5 μM $MgCl_2$, 12.5 μM $MgSO_4$ and 0.4 % glucose.

Bacterial media supplements:

Antibiotics: When preparing media for growth of *E. coli* strains harbouring a plasmid conferring antibiotic resistance, the medium was supplemented with the appropriate antibiotic. Ampicillin (100 mg/ml stock solution) was added to a final

concentration of 100 μg/ml.

2.4.2. Preparation of Calcium Competent DH5α cells.

An overnight culture of DH5α cells was diluted into 100 ml of 2xYT liquid. Cultures were then incubated at 37 °C until OD_{600}=0.5-0.6. The culture was split into 50 ml centrifuge tubes and placed on ice for 10 minutes. Cells were harvested by centrifugation in an Heraeus megafuge at 600 g for 5 minutes at 4 °C. The cell pellet was resuspended in 50 ml of ice cold 100 mM $CaCl_2$ and incubated on ice for between 30 minutes and 4 hours. Cells were again harvested by centrifugation and the cell pellet was resuspended in 5 ml $CaCl_2$ + 15 % glycerol. 50 μl aliquots were snap frozen in liquid nitrogen and stored at –80 °C.

2.4.3. Transformation of Calcium Competent DH5α cells.

Calcium competent cells were removed from the –80°C freezer and thawed on ice then 1 μl of DNA was added. Tubes were incubated on ice for 30 minutes and heat shocked at 42 °C for 40 seconds. 200 μl of 2xYT (1.6% tryptone, 1% yeast extract and 0.5 % NaCl) was then added to tubes and the culture was incubated at 37 °C for 1 hour without shaking. Cells were then spread onto plates containing the appropriate antibiotic (most usually 100 μg/ml ampicillin) and incubated overnight at 37 °C.

2.4.4. Preparation of competant cells for electrotransformation

100 ml 2YT was inoculated with 1-5 ml o/n culture of DH5α then incubated at 37 °C until OD_{600}nm was approximately 1.0. Cultures were left on ice for 30 min then centrifuged at 4000 g, 15 minutes at 4 °C. Cells were washed with 2 x 50 ml ice cold 10 % glycerol then resuspended in a final volume of 0.2 ml ice cold 10 % glycerol. 50 μl aliquots were frozen in liquid nitrogen before they were transferred to –80 °C.

2.4.5. Electro-transformation of competant cells

Mini-prep plasmid DNA (no more than 2 µl) was added to one 40 µl aliqout of thawed electrocompetent cells per transformation (section 2.x) on ice. The mix was then transferrred to ice-cold electrotransformation cuvettes (Electroporation Cuvettes Plus™ #620 BTX a division of Genetronics) with a 2 mm gap. Cells were electrotransformed using a BioRad Gene Pulser (settings: 200Ω 25µF 2.5kV) and immediately removed from cuvettes in 250 µl ice-cold 2YT liquid and placed at 37 °C for 30 minutes before plating out onto 2YT plates with appropriate antibiotic selection.

2.4.6. Glycerol Stocks

For long-term storage of bacteria, 1 ml culture was mixed with 1 ml 50 % sterile glycerol in a cryovial and then stored in a –80 °C freezer.

2.5. Yeast Methods.

2.5.1. Yeast Growth Media

The following media were used for the growth and maintenance of *S. cerevisiae* strains used throughout this study.

Drop-out media:

For growth of yeast on minimal SD medium, medium is supplemented with the appropriate amino acids for complementation of any auxotrophic deficiencies. When selecting for a plasmid, or gene marked with an auxotrophic marker, the relevant supplement was omitted from the medium (ie dropped out). Synthetic complete

mixture (containing all amino acids except those required for the auxotrophic selection of plasmids) was prepared and added to S medium.

Drop-out media	0.67% nitrogen base without amino acids (Difco) Drop-out mix (added as directed) For solid media supplement with 2% agar.
YPA	1% yeast extract 2% peptone 0.02% adenine For solid media supplement with 2% agar.
sporulation media	1% potassium acetate 2% agar
5-FOA media	0.67% nitrogen base (Difco) 0.2% drop-out uracil mix 2% glucose 0.1% 5-FOA (Melford Laboratories) 2% agar.

Carbon Source:
YPA and drop-out media were routinely supplemented with 40 % glucose (D) to 2 % final concentration. For galactose induced expression experiments, 40 % galactose was added to 2 % final concentration in place of glucose. To test for respiratory defects glycerol was added to 3 % final concentration to YP solid media.

Antibiotic supplement:
Where cells were transformed with DNA conferring G418 resistance (KanMx marker), G418 (200 mg/ml stock solution) was added to a final concentration of 200 μg/ml. Media was cooled to 50 °C prior to antibiotic addition. Poured plates were immediately stored at 4 °C in the dark.

2.5.2. Mating Yeast Cells

Cells of opposite mating type were patched onto one another and allowed to grow at 29 °C for 1-2 days on low glucose (0.1%) YPA media. Zygotes were selected either

manually using a Singer micromanipulator or by growth on media to select for diploids.

2.5.3. Mating Type Determination

Mating type was determined by mating the strain to be tested with both mating type tester strains (KAY30 and KAY 31). 200 µl of overnight culture of tester strains were spread onto drop-out *HIS*, *URA*, *LEU* and *TRP* plates. Strains of unknown mating type were patched onto the nascent lawn and incubated at 29 °C overnight. Only cells that have mated to form diploid cells are able to grow on these plates.

2.5.4. Sporulation and Tetrad Dissection

Diploid strains to be sporulated were grown on YPAD plates overnight at 29 °C. Cells were patched onto a sporulation plate and left on the bench for up to five days. The plate was monitored daily after 2 days to check development of four spored asci. When these were plentiful, cells were taken from the plate using a toothpick and were resuspended in 100 µl filter sterilised 0.1 M potassium phosphate buffer + 0.5 mg/ml 100T zymolyase (ICN Biomedical) and incubated for 10 minutes at room temperature. Once digested, spores were struck onto YPAD plates, placed under a micromanipulator (Singer) with the needle beneath and facing up toward the cells on the plate. Looking down the eye-piece of the micromanipulator, the region of spread cells was located and tetrads isolated and dissected into rows of four spores on theYPAD plate using the x and y co-ordinates. When sufficient spores were isolated the plate was incubated at 29 °C until the spores germinated and became visible. The number of viable spores was noted and they were patched onto YPAD or selective plates to test for genetic markers.

2.5.5. Yeast Transformation

Cells were transformed following the method described by Ito and colleagues 1993.

Cells were grown to mid log phase OD_{600} = 0.5. 15 mls of cells were harvested at 600 g, washed once in 0.1 M TE (10 mM Tris-HCl pH 7.5, 1 mM EDTA pH 7.5) and once in 0.1 M Lithium acetate/ 0.1 M TE. Cells were then resuspended in 100 µl 0.1 M Lithium acetate/ TE. 15 µl of 10 mg/ml herring sperm DNA boiled for 15 minutes was added with 0.1-1 µg of transforming DNA. The mix was then vortexed briefly, 700 µl 40 % PEG4000 in 0.1 M lithium acetate/ TE added and vortexed again. The transformation was incubated at room temperature for 90 minutes on a rotator then heat shocked at 42 °C for 15 minutes. Cells were spun down in a microfuge and resuspended in 100 µl of sterile water and plated on selective plates.

2.5.6. Halo assay for Latrunculin-A Sensitivity

A 2 ml culture was grown in YPAD liquid media at 29 °C overnight. 2 mls of fresh 2xYPAD liquid was inoculated with 10 µl of the overnight culture. 1 % agar was melted and cooled to 50 °C before adding to the liquid cell mix. The mix was immediately poured onto a warmed YPAD plate and the agar was allowed to set. Once set, four sterile antibiotic assay discs were placed on top of the agar to which 10 µl of dilutions (1, 2, 5 mM) from a 50 mM stock of LAT-A had been added. A 0 mM control disk containing 10 µl diluted DMSO was added (LAT-A is dissolved in DMSO). Plates were incubated for 2 days at 29 °C until halos were visible in the lawn of cells. Relative apparent sensitivities were calculated as described by Reneke and colleagues, 1988.

2.5.7. Temperature sensitivity of yeast on solid growth media.

A single colony of cells was picked using a toothpick and was resupended in 100 µl of water. 3 µl of diluted yeast were added to YPAD plates and incubated at either 30 °C or 37 °C for 1-2 days to assess if a strain has a temperature sensitive defect.

2.5.8. Testing viability after temperature shift

Cells were grown in YPAD at 29 °C until cell density reached OD_{600}nm 0.1-0.2. The culture was then divided into two flasks, one was incubated at 29 °C and the other at 37 °C with shaking. After 4 hours, 100 cells were randomly picked using the micromanipulator on YPAD and placed at 29 °C. After 2 days viable cells produced colonies and were counted.

2.5.9. Measuring cell number

An overnight culture was used to inoculate 100 ml of cells to a cell density of about $5x10^5$ cells/ml. Cells were grown for 1.5 hours at 26 °C in a shaking incubator. The culture was split into 2 x 50 ml cultures and then incubated at 26 °C and 37 °C for 30 minutes. A 500 µl sample was removed and sonicated for 10 seconds. The sample was diluted 1:200 with Casyton™ buffer and then the cell number was measured in the Schärfe system CASY™ cell counter. This was repeated at various time points.

2.5.10. Integration of *sla1-Δ118-511* into genome

The *sla1-Δ118-511* mutant was integrated into the genome at the C-terminal region of *SLA1* (at 3307) by digesting pKA237 (see table 2.2) with *Nar*I. The digest was run out on an agarose gel and QIAEX cleaned up before transformation into KAY 17.1A and KAY 17.1B. Transformants were screened by colony PCR using oKA36 and oKA44 (section 2.3.11).

2.5.11. Glycerol Stocks

For long-term storage of yeast, 1 ml culture was mixed with 1 ml 50 % sterile glycerol in a cryovial and then stored in a –80 °C freezer.

2.6. Two-Hybrid Methods

2.6.1. 2-Hybrid Library Amplification

The library is on a 2 μ, LEU plasmid and is constructed in derivatives of pGAD424 (Genbank #UO7647) named pGAD-C1, 2 and 3 differing only in the polylinker sequence and resulting in three different reading frames. The library was obtained from Francis Barr (MPI, Munich) but it is originally from Philip James (James *et al* 1996).

500 ng each of pGAD-C1, 2 and 3 was transformed into three single vials of Stratagene XL10-Gold ultracompetent cells following the protocol in the supplied instruction manual. Each vial of transformed cells was incubated in 1ml of NZY^+ broth and 250 μl of cell suspension was added to a pool of 350 μl NZY^+ broth on 4 140 mm diameter 2YT-AMP plates per transformation. After overnight incubation at 37 °C, the confluent lawn of cells from each plate was scraped off into 250ml 2YT-AMP media and grown for 2.5 hours in a 37°C shaker (200 r.p.m.).

Plasmid DNA was extracted using Qiagen maxi preps (one for each 250ml culture) following instuctions supplied with kit. The final pellet was resuspended in 500 μl sterile distilled water. DNA concentration was estimated by measuring absorbance at 260nm in a Heraeus spectrophotometer (blanked first with water).

Library	A_{260}nm (1:200 dilution)	DNA (mg/ml)
pGAD-C1	0.160	1.60
pGAD-C2	0.135	1.35
pGAD-C3	0.190	1.90

Library DNA was also run out on a 0.8% agarose (Helena Biosciences) gel to check its integrity.

2.6.2. Construction of Bait Plasmid *pGBDU-Sla1-118-511*

The bait plasmid (pKA237) to be used in the yeast 2 hybrid screen was constructed by subcloning the 1182bp *Eco*R1 fragment (353-1534) from pKA51 into the *Eco*R1 site of *pGBDU-C1*. This created an in-frame fusion of the Sla1-118-511 fragment to the Gal4 DNA binding domain on the bait vector. After extraction of plasmid DNA from by Qiagen mini-preps, plasmids were checked for the presence of insert in the correct orientation by single restriction digests with *Eco*R1 and *Pst*1 respectively. pKA237 was sequenced from the 5' and 3' ends using oligos o182 and o183 respectively which bind *pGBDU-C1* at regions flanking the insert.

2.6.3. Construction of Bait Plasmid pGBDU- *Sla1-118-511 (- SH3#3)*

The bait plasmid (pKA238) to be used in yeast two hybrid experiments was constructed by subcloning the 993 bp *Eco*R1 fragment from pKA116 into the *Eco*R1 site of pGBDU-C1. The orientation of the insert was checked and sequenced as above.

2.6.4. Creating the yeast strain for use in two-hybrid library screen

pGBDU-Sla1-118-511 (pKA237) was transformed into the yeast 2-hybrid strain pJ69-2A (section 2.6.5). Transformants carrying the bait plasmid were selected by growth on drop-out URA plates at room temperature.

2.6.5. Two-Hybrid Library Transformation

This high efficiency yeast transformation protocol is taken from Gietz and Schiestl (1995). The 2-hybrid yeast strain (KAY 500) pJ69-2A carrying the bait plasmid (*pGBDU-sla1-118-511*) was grown up overnight in 5 mls drop-out ura medium, then diluted to 100 mls medium and placed in the 29 °C shaker until cell density reached $2x10^7$ cells/ml. The cells were collected by centrifugation at 1700 g for 5 minutes in a benchtop centrifuge. The supernatant was removed and the cell pellet was washed in

50ml sterile distilled water and the cells collected as above. To the cells were then added: 360 µl 1M LiOAc; 2.4ml 50 % PEG; 50 µl boiled and iced herring sperm DNA (10 mg/ml); 20 µg library DNA from pGAD-C1, pGAD-C2 and pGAD-C3; and, 680 µl sterile distilled water, once the supernatant was removed. The cell mixture was then vortexed for 1 minute to mix. The cells were incubated at 29 °C in the shaker at 120 r.p.m. for 30 minutes then heat shocked at 42 °C for 30 minutes mixing gently every 5-10 minutes. The cells were centrifuged at 760 g for 5 minutes then resuspended in 3.6 ml sterile distilled water. The cell suspension was spread onto 8x140 mm diameter selective plates (drop-out URA LEU) to select for the presence of bait plasmid (*URA*) and library plasmid (*LEU*). The transformation plates were incubated at 29 °C for 2 days.

2.6.6. Growth on Activation Plates

The transformation grew to confluence on drop-out URA LEU and were replica plated using Whatman paper onto 8x140 mm activation plates (drop-out HIS URA LEU ADE) to test for activation of reporter genes *ADE2* and *HIS3*.

2.6.7. Elimination of False Positives.

To remove as many false positives from the library screen before the plasmids were rescued or sequenced, strains were struck onto plates that lacked adenine but contained 0.1% 5-FOA (5-Fluoroorotic acid, Melford laboratories). This reagent is toxic to cells expressing the *URA* genes. For cells to grow in the presence of 5-FOA they must therefore lose the bait (URA marked) plasmid. Any cells that are able to grow on this media are false positives because the media is selecting for cells expressing one of the reporter genes (adenine), these cells are activating their reporter genes but only contain the prey plasmid.

2.6.8. Extraction of Yeast 2-Hybrid Library Plasmids

Yeast strains were grown overnight in drop-out URA LEU medium. After centrifugation at 3000 rpm for 1 minute cells were resuspended in 500 µl buffer S (10mM potassium phosphate buffer pH7.2, 10mM EDTA, 50mM β-mercaptoethanol, 50 µg/ml zymolyase) and incubated at 37 °C for 30 minutes. 100 µl lysis buffer (25 mM Tris-HCl pH7.5, 25 mM EDTA, 2.5 % (w/v) SDS) was then added and cells vortexed briefly. Cells were incubated at 65 °C for a further 30 minutes before the addition of 166 µl 3M potassium acetate (pH5.5). Cells were then placed on ice for 10 minutes. After centrifugation for 10 minutes at 4 °C the supernatants were transferred to fresh tubes on ice containing 800 µl ethanol and left for 10 minutes. Cells were again centrifuged for 10 minutes after which the pellet was washed in 70 % ethanol and allowed to dry before resuspension in 40 µl sterile distilled water. These initial plasmid preparations from two-hybrid yeast strains included both the *URA3* bait and *TRP1* library plasmids so were firstly transformed into electrocompetent KC8 cells (section 2.6.10).

2.6.9. Preparation of Electrocompetent KC8 Cells

KC8 (Clontech): hsdR, leuB600, trpC9830, pyrF::TnF, hisB463, lacΔX74, strA, galU, galK

This *E.coli* strain contains a leuB mutation which allows for direct selection of the yeast *LEU2* gene carried on the library activation domain plasmid

400 ml 2YT medium was inoculated with 2 ml of an overnight KC8 culture and incubated at 37 °C in shaker to an OD_{600} nm of 0.5-0.6. Cells were chilled on ice for 30 minutes then centrifuged at 2 °C 4300 g for 30 minutes. Supernatant was removed and the pellet of cells was resuspended initially in a small volume of ice-cold sterile distilled water then topped up with 500 ml ice-cold sterile distilled water, mixed then centrifuged as before. This washing step was repeated once more. The supernatant

was poured off immediately and the cells resuspended by swirling in the remaining liquid. Cells were then either used fresh or frozen for later use as below.

Fresh cells – the cell suspension was placed in a prechilled narrow-bottomed 50 ml polypropylene tube and centrifuged for 10 minutes at 4300 g at 2 °C. The pellet volume was estimated (usually 400 µl from a 400 ml culture) and an equal volume of ice-cold sterile distilled water added. Cells were resuspended and aliquoted (50 µl) into prechilled microcentrifuge tubes.

Frozen cells – 40 ml ice-cold 10 % glycerol was added to the cells and mixed well then centrifuged for 10 minute at 4300 g at 2 °C. The pellet volume was estimated and an equal volume of ice-cold 10% glycerol was added to resuspend cells. Cells were then aliquoted (50 µl) into microcentrifuge tubes on dry-ice then stored at -80 °C.

2.6.10. Electroporation of KC8 Cells With Library Plasmid Preps

Cells were electroporated as section 2.x using either fresh or frozen KC8 cells per plasmid prep. Cells were incubated in 2YT for 30 minute before plating onto M9 drop-out leu plates to select for the LEU2 library plasmid.

Plasmid extracted from the KC8 cells (Qiagen mini preps plus optional wash step) were then subjected to a further round of transformation into chemically competent DH5α (section 2.4.5). This subsequent transformation provides another step to ensure only single plasmids are recovered from the initial yeast plasmid preparations, and provides cells from which to make glycerol stocks as the plasmids are more stable in DH5α than KC8 cells.

2.6.11. Retransformation of two-hybrid positives to check rescued library plasmids activate expression of the reporter genes

This essentially means transforming extracted library plasmid DNA back into the yeast two-hybrid strain containing the bait plasmid (KAY 500). Each plasmid was tested for activation of the both the *HIS3* and *ADE2* reporter genes when in

combination with the original bait plasmid. This was carried out using standard yeast transformation protocol (section 2.5.5). Transformed cells were plated onto drop-out ura leu and then transformants struck out successively onto drop-out ura leu then activation plates.

2.6.12. Sequencing of the two-hybrid library inserts

The insert of each rescued library plasmid was sequenced by an in-house sequencing facility on an ABI 377 using Big Dyes® chemistry. All plasmids were initially sequenced from the 5'end using o153 to enable the identification of the insert and several were also sequenced from the 3' end (o154) in cases where the sequence stop site was estimated by insert size to be internal of the gene. The 3' end of the remainder plasmids was estimated from the approximate insert size determined by restriction digestion.

2.7. Protein Methods

2.7.1. Yeast whole cell extract prep (Small Scale Glass Bead Lysis Protocol)

1.5 ml of yeast cells from an overnight culture were pelleted at 5000 rpm for 5 min then washed twice in 1.5 ml dH_2O. After removal of supernatant, approximately 100 µl of acid washed glass beads (diameter approx. 0.4 mm) were added with 50 µl 2x protein sample buffer. The tube was then boiled immediately for 3 minutes and then vortexed for 1 min. 75 µl of 2x sample buffer was added, vortexed and loaded onto SDS polyacrylamide gel (section 2.x) or stored frozen at –20°C.

2x Sample Buffer:

2.5ml 0.5M Tris pH 6.8
2.0ml 10% SDS
2.0ml glycerol
2.0ml ddH_20
1.0ml ß-mercaptoethanol
0.5ml bromphenol blue solution

2.7.2. Protein preps by grinding in liquid nitrogen

An overnight culture of cells was diluted into 100 ml of the appropriate growth media and grown to an OD_{600}=1.0. Cells were harvested by centrifuging at 3000 *g* for 5 minutes. The cell pellet was resuspended in 1 ml IP buffer 2xUBT buffer (0.2 M KCl, 2 mM EGTA, 100 mM KHEPES (pH 7.5), 6 mM $MgCl_2$, 1.0 % Triton X-100)) freshly supplemented with 1 mM PMSF and aqueous phase protease inhibitors. The cell slurry was frozen drop-wise into liquid nitrogen in a 50 ml centrifuge tube for 10 minutes. Cells were ground in the presence of liquid nitrogen, using a pestal and mortar. The cell extract was collected into 1.5 ml eppendorf tubes and stored at –80°C until required.

2.7.3. Purification of GST tagged protein

The *sla1-Δ118-511* and *Sla1-118-511(-SH3#3)* domains were cloned into a pGEX vector. The pGEX plasmids are designed for inducible, high level intracellular expression of genes or gene fragments as fusions with GST. Protein expression from a pGEX plasmid is under the control of the *tac* promoter, which is induced using IPTG.

E.coli carrying pKA38, pKA45 and pKA161 were grown in 2YT (+Ampicillin) at 26 °C until reaching OD_{600}nm 1.0. IPTG (iso-propyl thiocyanate) was added to 0.1 mM to induce the production of GST-fusion proteins and incubation continued for 5-6 hours. Bacterial sonicates were then prepared. Cells were centrifuged at 7700 g for 10 minutes at 4 °C. The cell pellet was resuspended in 2.5 ml 1xPBS then sonicated on ice (10 x 10 seconds). Triton was added to 1 % then mixed gently for 30 minutes at 4 °C. The cell lysate was then centrifuged at 12 000 g for 10 minutes at 4 °C.

Fusion proteins were then batch purified using 50 % glutathione sepharose beads 4B (Amersham Pharmacia Biotech) washed in 1xPBS. 100 µl beads were added to each bacterial sonicate and then incubated at room temperature with gentle agitation for 30

minutes. Beads were sedimented by centrifugation at 500 g for 5 minutes. The bead pellet was washed with 10 bed volumes of 1xPBS three times.

Yeast extract (section 2.7.2) from KAY 40 was added to the beads in 1xUBT buffer (0.1 M KCl, 1 mM EGTA, 50 mM KHEPES (pH 7.5), 3mM $MgCl_2$, 0.5 % Triton X-100) freshly supplemented with 1 mM PMSF and aqueous phase protease inhibitors (0.5 mg/ml leupeptin, aprotinin, chymostatin, pepstatin A). The beads in yeast extract were incubated at 4 °C overnight with gentle mixing. The beads were then washed twice with 1xUBT.

Batch elution of proteins was carried out by adding 1.0 ml glutathione elution buffer (10mM reduced glutathione in 50 mM Tris (pH 8.0)) per ml bed volume. The beads and buffer were mixed gently to resuspend the beads then incubated at room temperature for 10 minutes to elute the fusion protein from the beads. The beads were centrifuged at 500 g for 5 minutes. The batch elution was repeated. Samples of the initial whole cell extract, the final beads and eluate wash fractions were then prepared for SDS PAGE electrophoresis (section 2.7.5).

2.7.4. Immunoprecipitation procedure

Yeast cells were lysed by liquid nitrogen-grinding method (section 2.7.2). The cells lysate was centrifuged at 4000 g for 5 minutes at 4 °C followed by a 100,000 *g* centrifugation for 20 minutes at 4 °C in a TLA100 rotor (Beckman™). A sample of the supernatant was kept for electrophoresis. The high-speed supernatant was divided into two tubes, and to one was added 1/100 volume of anti-rat HA antibody or anti-mouse myc antibody (see table 2.4). Samples were incubated at 4 °C overnight with mixing. Protein G sepharose or Protein A sepharose washed in 2xUBT (with 10x protease inhibitors) was added to tubes containing anti-rat or anti-mouse antibodies respectively. Tubes were incubated at 4 °C with gentle mixing for 2 hours. Antibody bound proteins were harvested by centrifugation at 3000 *g* for 4 minutes at 4°C. Beads were washed three times in 2xUBT buffer (with 10x protease inhibitors). The

final wash and the beads , along with the high-speed supernatant were then electrophoresed on a polyacrylamide gel (section 2.7.5) and western blotted then probed with antibodies.

2.7.5. SDS-PAGE electrophoresis.

The appropriate percentage of acrylamide gel was poured according to the recipes below.

Separating gel:

	7.5 %	10 %	12 %
Sterile water	4.10 ml	3.44 ml	2.69 ml
30 % acrylamide 0.8 % bisacrylamide (37.5:1)	2.25 ml	3.00 ml	3.75 ml
Bottom Buffer (1.5 M Tris-HCl (pH 8.8), 0.4 % SDS)	2.25 ml	2.25 ml	2.25ml
10 % ammonium persulfate	31 µl	31 µl	31 µl
TEMED	5 µl	5 µl	5 µl

5 % Stacking gel:

Sterile water	1.71 mls
30 % acrylamide, 0.8 % bisacrylamide	0.50 mls
Top buffer (0.5 M Tris-HCl (pH 6.8), 0.4 % SDS)	0.75 mls
10 % ammonium persulfate	35 µls
TEMED	3.5 µls

Gels were run in 1 x Running buffer (0.025 M Tris, 0.192 M Glycine, 0.1 % SDS, pH 8.6) at 120 volts for approximately 1.5 hours, until the dye front ran off the bottom of the gel.

2.7.6. Coomassie staining of SDS-polyacrylamide gels

The proteins on an SDS-polyacrylamide gel were detected using Coomassie Blue stain. The electrophoresed gel was soaked in Coomassie stain solution (0.2 % (w/v) Coomassie Brilliant Blue R250, 50 % (v/v) methanol, 7 % (v/v) acetic acid) for 30 min with continuous movement on a rocking platform. The gel was then destained using several changes of 50 % (v/v) methanol, 7 % (v/v) acetic acid until the appropriate level of contrast between the protein bands and the gel was achieved.

2.7.7. Silver staining of SDS-polyacrylamide gels

The SDS-polyacrylamide gel was fixed in a solution of 30 % ethanol 10 % acetic acid in Milli-Q water for 1 hour. The gel was then placed into a solution of 0.5 % glutaraldehyde, 0.1 % sodium thiosulphate in 30 % ethanol, 0.4 M sodium acetate buffer pH 6.0 for 1 hour, then washed with water for at least 2 hours. The gel was then incubated in 200 mls of 0.1 % silver nitrate solution with 50 µl formaldehyde. Development of the gel began by placing into 500 mls 2.5 % sodium carbonate with 200 µl formaldehyde added. Gel development was stopped by washing twice in 5 % acetic acid for 15 minutes. The gel was then rinsed in Milli-Q water to remove acetic acid, then vaccuum dried onto Whatman paper.

2.7.8. Western blotting

Proteins were separated by SDS-PAGE electrophoresis as described in section 2.7.5. PVDF was soaked in methanol while the filter paper and two pieces of Whatman paper cut to same size as gel were soaked in ice-cold blotting buffer (10 mM CAPS, 10 % methanol, pH 11). The blot sandwich was assembled (Whatman paper, PVDF (Schleicher and Schuell), gel, Whatman paper) keeping everything wet and care was taken to exclude air bubbles. The sandwich was then placed in the blotting apparatus, with the membrane against the anode. An ice pack was placed in the apparatus to keep the transfer cool and blotting was performed at 400 mA for one hour.

2.7.9. Western blot detection using Enhanced Chemi-Luminescence (ECL)

Proteins are blotted as described above. The wet membrane was blocked at room temperature for about 1 hour, or overnight at 4 °C, in 5 % milk powder in 1 % TBST (1 x TBS + 0.2 % Tween-20). The membrane was then rinse briefly in 1 x TBST and was then placed in a 50 ml centrifuge tube with 2 ml of blocking solution plus primary antibody (see table 2.4). The membrane was incubated in the presence of primary antibody one hour at room temperature with shaking. The blot was then removed from the centrifuge tube and washed with 1 x TBST briefly followed by three 10 minute washes in 1 x TBST. The membrane was placed in a plastic bag and incubated with blocking solution containing horseradish peroxidase conjugated secondary antibody (see table 2.4) for between 30 minutes and one hour at room temperature with shaking. The membrane was removed from the plastic bag then washed 3 times in 1 x TBST for 15 minutes each. In the dark room equal volumes of developing reagents (Solution I : 250 mM luminol (3-aminophthalhydrazide from Fluka No 09253) in DMSO, 90 mM p-coumaric acid in DMSO, 0.1 M Tris-HCL pH 8.5; Solution II: hydrogen peroxide, 0.1 M Tris-HCl pH 8.5) were mixed and the membrane was incubated in the developing solution for at least one minute. The solutions were then drained off and the membrane wrapped in cling-film. The membrane was exposed to X-ray film (Konica) in a cassette and the film was developed in an automatic developer (Xomat).

2.7.10. Western blot detection using Alkaline Phosphatase.

The blotted membrane is probed with antibodies as above except the secondary antibody is an alkaline phosphatase conjugated antibody (see table 2.4). After incubation with secondary antibody, the membrane was washed as above. The membrane was then developed in 10 mls of developing solution (100 mM NaCl, 5 mM $MgCl_2$, 100 mM Tris (pH 9.5)) containing 132 µls of NBT (nitro blue tetrazolium) stock (0.5 g in 10 ml 50 % DMF) and 66 µls BCIP (5-bromo-4-chloro-3-indolyl phosphate ρ-toluidine salt) stock (0.25 g in 10 ml 100 % DMF). After

sufficient colour development the reagents were washed off with water and the membrane was air-dried.

2.8. Microscopy methods

2.8.1. Vital staining of yeast vacuoles using Lucifer Yellow

This method is based on that described by Dulic and colleagues (1991). Yeast cells were grown in YPD to OD_{600}nm 0.2-0.4 then 1 ml spun down at 5000 g for 1 min. The cell pellet was resuspended in 30 µl YPDA and 20 µl of 40 mg/ml Lucifer yellow (Fluka) solution (made up in water) was added before 2 hr incubation in shaker at 29 °C. Cells were then washed 3 times with 1 ml ice-cold succinate-azide buffer (50mM succinate, 20 mM sodium azide pH 5.0) before resuspension in 10 µl succinate-azide buffer. Cells were kept on ice. Cells were viewed by fluoresence microscopy.

Intensity of lucifer yellow uptake into cells was measured using IP lab software.

2.8.2. Vital staining of yeast vacuoles using FM4-64

FM4-64 = N-(triethylammoniumpropyl)-4-(p-diethylaminophenylhexatrienyl) pyridinium dibromide is a lipophilic styryl dye used to stain yeast vacuolar membranes (Vida and Emr, 1995).

A 10ml log phase culture (OD_{600} 0.4-0.6) was spun down at 3000rpm for 3minutes then the pellet resuspended in 500µl YPD and transfered to a 1.5ml eppendorf tube. 0.5µl 16mM FM4-64 (in DMSO) was added and the cells were incubated for 10-15minutes in 26 °C shaker. After this preliminary labelling step, cells were harvested at 700g for 3 minutes and resuspended in 1ml YPD then incubated with shaking at 26 °C for 30-60 minutes. After this 'chase' period, cells were harvested again at 700 g for 3 minutes and resuspended in 200 µl YPD. 10 µl of cells were then placed onto a standard slide, coverslip added and viewed.

2.8.3. $DiOC_6$ staining of mitochondria

500 µl of actively growing cells were spun down and resuspended in 10 mM HEPES (pH 7.4) 5 % glucose. $DiOC_6$ (17.5 µM) was added to wild-type cells at 1/100 dilution and to mutant cells at 1/10 dilution. Cells were incubated in the dark for 30 minutes then placed onto slides and observed.

2.8.4. Visualisation of GFP tagged proteins

Cells expressing GFP-tagged proteins were visualised after growing to log phase in YPAD media or after being taken from a freshly growing colony on a plate. For imaging, 3 µl of cells were put on a slide, covered with a coverslip and sealed with nail polish. Cells were viewed as described in sections 2.8.12 and 2.8.13.

2.8.5. Immunofluoresence

5 ml of actively growing yeast cells (OD_{600}nm 0.4-0.6) were fixed with 0.67 ml formaldehyde (5% final) and allowed to stand at room temp for at least 1 hour. Cells were spun down at 4000 rpm and washed twice with 2 ml of 1.2 M sorbitol, 0.1 M potassium phosphate buffer, pH7.5 then resuspended in 0.5 ml of sorbitol buffer. 1µl of beta-mercaptoethanol and 20 µl of 1 mg/ml of zymolyase was added before incubation for 30-40 minutes at 37°C. During the incubation period multi-well slides were prepared with poly-L-lysine for increased adherence of yeast cells to slides (section 2.8.8). 15 µl of cell suspension was added to each well and allowed to settle for 5 minutes then aspirated off gently. The excess suspension from each well was aspirated off then 10µl 0.1% SDS was added for 30 seconds. Each well was then washed 10x with PBS/BSA (1 mg/ml). After this point it was important not to let the wells dry out so the slides were kept in a humid environment, for example in covered petri dish with a damp tissue. The primary antibody was diluted as necessary in PBS/BSA and 15 µl placed on each well. After 1 hour incubation each well was washed 10x with PBS/BSA and 15 µl of secondary antibody (diluted as necessary in PBS/BSA) added. The multi-well slide was incubated for 1 hour in a dark place so as

to not bleach the fluorophore. The wells were washed again 10x with PBS/BSA and a small drop of phenylenediamine mounting solution (section 2.8.6) was placed on each well and covered with a coverslip, and sealed around the edges with nail polish.

2.8.6. Mounting medium containing DAPI for staining of DNA

100 mg *p*-phenylenediamine in 10ml PBS (pH9) stirred vigorously. 90 ml glycerol was added and stirred until homogeneous. 2.25µl of DAPI stock (1mg/ml 4'6' diamidino 2-phenylindole dihydrochloride in water) was added and mounting medium was stored at -80°C (long term) or –20°C (short term) in the dark.

2.8.7. Rhodamine-phalloidin staining of filamentous actin

To 1 ml actively growing yeast culture (OD600nm 0.1-0.3) was added 0.134 ml of 37 % formaldehyde and left for 1 hour at room temperature. The cells were spun at 1500 g for 5 minutes and resuspended twice with PBS + 1 mg/ml BSA + 0.1 % TX-100. The pellet was resuspended in 50 µl PBS + 1 mg/ml BSA + 0.1 % TX-100 and 5 µl rhodamine-phalloidin was added (40 mg/ml) then incubated for 30 min in dark. The cells were washed 2x with PBS/BSA (without TX-100) in eppendorf tubes then resuspended with 200 µl PBS/BSA. 20 µl of cell suspension was left to settle for 10 minutes on poly-lysine coated slide well (see section 2.8.8), then washed three times on slide. A small drop of mounting solution (2.8.6) was added to slide well before covering with coverslip. The coverslip was sealed in place with nail varnish. Cells were examined by fluoresence microscopy straight away or stored at –20 °C for later viewing.

2.8.8. Adhering cells to microscope slides

To prevent cells from moving during photography they were fixed to the slide surface with poly-L-lysine as follows: 10 µl of 1 mg/ml poly-L-lysine was placed on each well of slide and allowed to sit for 1-2 minutes before being rinsed off with distilled water and air dried.

well of slide and allowed to sit for 1-2 minutes before being rinsed off with distilled water and air dried.

2.8.9. Co-localisation of GFP-tagged protein and actin

Yeast cells were pelleted then gently resuspended in ice-cold 70 % ethanol and left on ice for 10 minutes. Cells were pelleted for 20 seconds and resuspended in rhodamine-phalloidin (5 mg/ml) in PBS containing 1mg/ml BSA. After cells were left on ice for 5 minutes they were washed three times with PBS. Cells were resuspended in PBS and placed on poly-lysine treated slides (section 2.8.8).

2.8.10. Latrunculin-A treatment of cells to disrupt the filamentous actin cytoskeleton

Latrunculin-A was added to a culture of actively growing cells to 200 μM and incubated at 29 °C. Aliquots of cells were taken before Latrunculin-A addition and at chosen time points afterwards. Cells were fixed with 5 % formaldehyde and left for 30 minutes at room temperature. Alternatively, cells which expressed GFP-tagged protein were fixed by the ethanol method (section 2.8.9).

2.8.11. Calcofluor staining of chitin in yeast cell wall

1 ml of an actively growing yeast culture (OD_{nm}0.4-0.6) was fixed with 5 % formaldehyde for 1 hour at room temperature. Cells were then spun down (1500 g 5 min) and resuspended in 1 ml of 0.1% calcofluor (made up in dH_2O) then agitated for 5 minutes at room temperature. Cells were washed 3-5x in water then viewed by fluorescence microscopy.

2.8.12 Viewing cells by fluorescence microscopy

Cells were viewed with an Olympus BX-60 fluorescence microscope with a 100 W mercury lamp and an Olympus 100x Plan-NeoFluar oil-immersion objective. Images

were captured using a Roper Scientific MicroMax 1401E cooled CCD camera using Scanalytics IP lab software on an Apple Macintosh 7300 computer.

2.8.13. Viewing cells using DeltaVision Restoration Microscope System

For live cell imaging, exponentially growing cells were harvested and resuspended in a smaller volume of synthetic complete medium containing glucose (SCD) and then applied to a slide to which a thin pad of 25 % gelatin (Porcine 300 bloom; Sigma) in SCD had been applied. After sealing with a coverslip and rubber cement, cells were imaged for GFP-tagged proteins. Imaging was performed using a DeltaVision Restoration Microscope System (Applied Precision Inc., Issaquah, WA USA), equipped with a Nixon Plan Apo 100x (1.4 NA) objective and a Roper Scientific Interline Cooled CCD camera (5 MHz MicroMax1300YHS) utilising the JP3 filter set. 32 optical sections at 0.2 μm intervals were taken with an exposure time of 0.15 seconds. Data was collected in fast acquisition mode. 3D image datasets were deconvolved using the SoftWoRx application (Applied Precision Inc., USA) running on a Silicon Graphics Octane workstation (Silicon Graphics Inc., USA). 2D maximum-intensity projections were generated from the 3D datasets using SoftWoRx and images captured in TIFF format using MediaRecorder (Silicon Graphics Inc., USA) and assembled using Adobe Photoshop (Adobe Inc., USA).

Chapter 3

Characterisation of *sla1-Δ118-511* Yeast Mutants

3.1 Introduction.

Sla1p is a multifunctional *Saccharyomyces cerevisiae* protein that contains distinct structural domains which play different functional roles (Ayscough *et al* 1999). Deletion analyses using plasmid mutants (section 3.2) have shown that a region encompassing the third SH3 domain (Sla1p-118-511) (the missing fragment in pKA53 figure 3.1) is critical for growth at high temperatures and a normal cortical actin cytoskeleton organisation (see section 1.16.4).

To investigate the physiological role played by the Sla1p-118-511 domain of Sla1p, the *sla1* mutant was firstly integrated into the genome (section 3.3) and the phenotypes of the mutant yeast were examined using a combination of approaches (sections 3.4 – 3.11). This included investigating the role of the Sla1p-118-511 domain in actin dynamics and actin dependent functions such as budding and endocytosis as well as the actin phenotype of the mutant cells. The localisation of the mutant protein was also assessed. Determination of the interacting partners of the Sla1p-118-511 domain should also shed some light on the role of Sla1p in budding yeast and this was attempted using GST pulldowns (section 3.12).

3.2 Deletion analysis of Sla1p using plasmid mutants.

Initial work on this project used a panel of Sla1 deletion mutants expressed from plasmids depicted in figure 3.1 (see section 1.16.4). Three plasmid constructs; pKA128, pKA129 and pKA130, were generated in this project by site directed mutagenesis (methods section 2.3.9 and table 2.2); the remainder were generated by

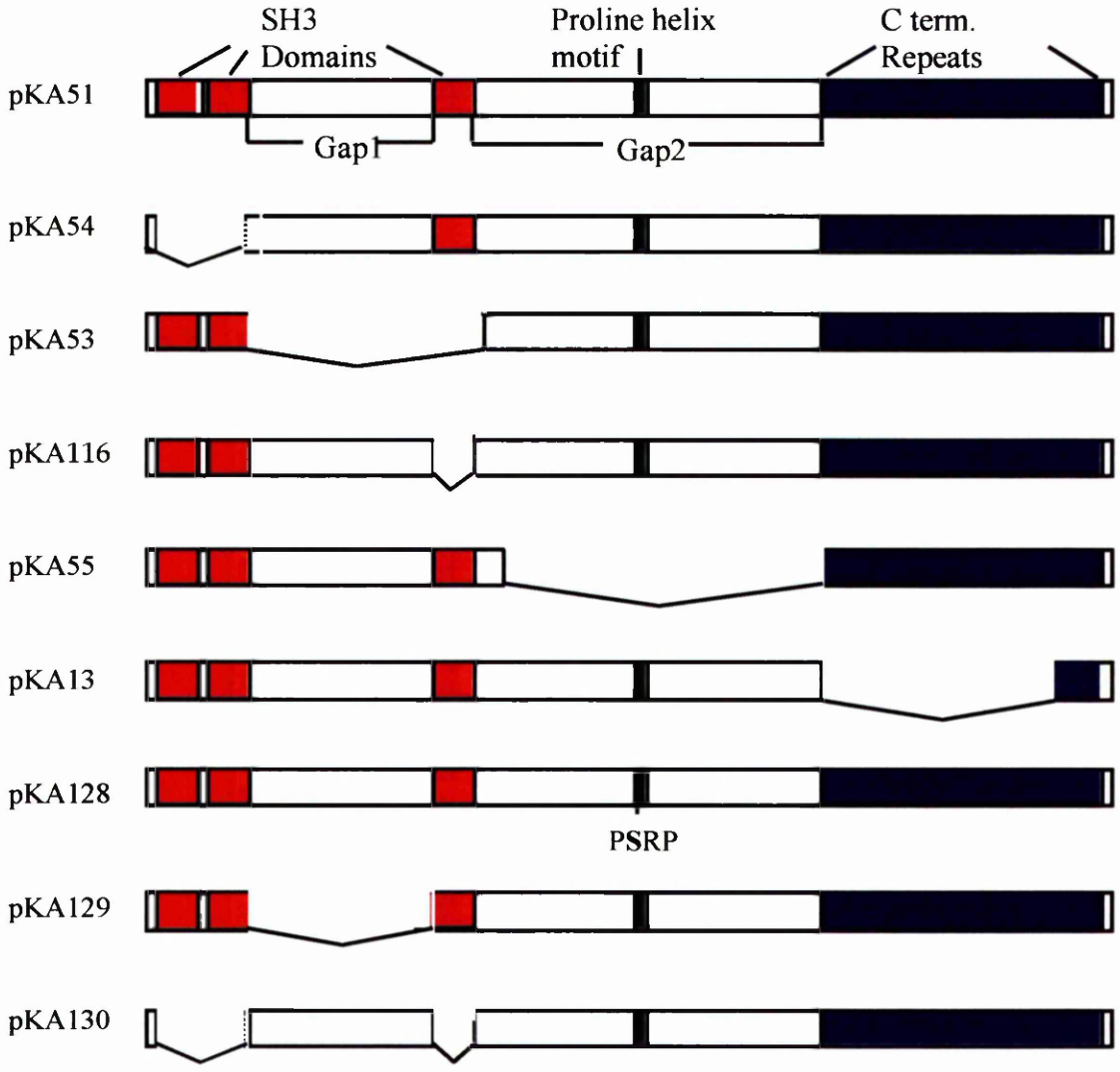

Figure 3.1 Panel of sla1 mutants expressed from plasmids. In order to investigate the role of the domains of Sla1p, plasmid-borne mutants were generated (Ayscough *et al* 1999) and transformed into a yeast strain deleted for *SLA1* (KAY 300). Schematic diagram of Sla1p mutants showing domains of the protein which had been deleted. Taken from Ayscough *et al* 1999.

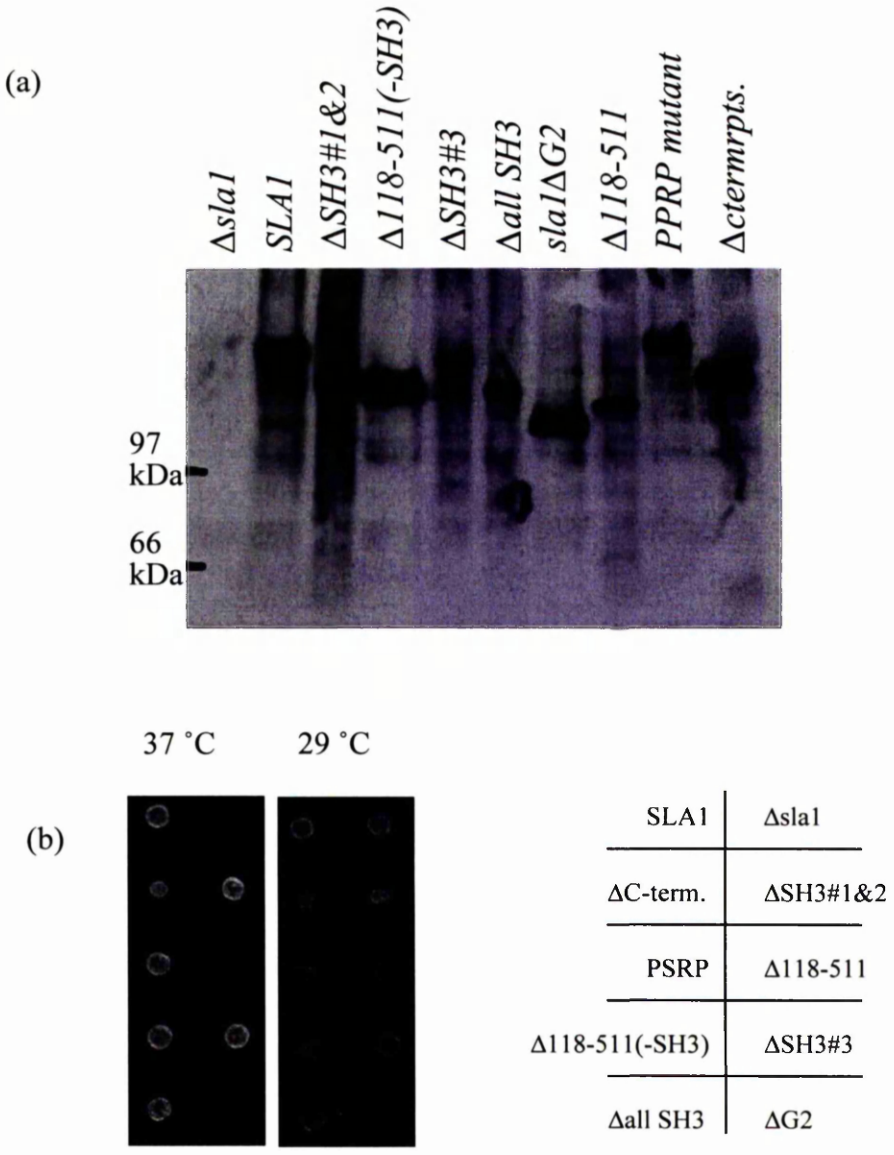

Figure 3.2 Characterisation of sla1 mutants expressed from plasmids. In order to investigate the role of the domains of Sla1p, plasmid-borne mutants were generated (Ayscough *et al* 1999) and transformed into a yeast strain deleted for *SLA1* (a) Expression of the mutant Sla1 proteins in a KAY 14 genetic background (KAY 232-237, KAY 488-491) was verified by a western blot probed with anti-Sla1p antibodies. (b) Temperature sensitivity of yeast strains expressing mutant Sla1p in a KAY 317 background (KAY 318-327) plated on YPDA agar.

Kathryn Ayscough (Ayscough *et al* 1999). When I carried out western blot analysis on yeast cells expressing the mutant Sla1 proteins, using anti-Sla1p antibodies (figure 3.2) the mutant proteins were shown to be expressed in cells and were of sizes expected from the specific deletions compared to full length wild-type.

These deletion analyses were done using yeast strains that carried the mutant forms of *SLA1* on plasmids. A potential problem with this approach is the need to include a selection strategy to maintain the mutant *SLA1* constructs in cells. Another limitation of expressing the mutant forms of *SLA1* from plasmids is that there is likely to be a higher gene copy number per cell than usual and this itself could produce a mutant phenotype. In order to avoid these problems, the mutant *SLA1,* that lacked the region from residue 118 to 511, was integrated into the genome (here termed *sla1-Δ118-511*) so it was expressed at endogenous levels (section 3.2).

3.3 Integration of *sla1-Δ118-511* into the genome.

Initial attempts at homologous recombination of *sla1-Δ118-511* into wild-type yeast (KAY 48) generated cells carrying tandem copies of both wild-type *SLA1* and *sla1-Δ118-511* as detected by colony PCR (section 2.3.11)(figure 3.3a). These yeast could not be used in mutant analyses due to presence of wild-type *SLA1.*

In order to circumvent potential problems caused by co-expression of wild-type *SLA1,* the *sla1-Δ118-511* allele was integrated into yeast strains (KAY 17.1A and KAY 17.1B) which carried a functionally inactive *sla1* allele, termed *sla1-Δ2. sla1-Δ2* yeast have a disrupted *SLA1* where the 2030 bp *Sac*1-*Bam*H1 fragment of *SLA1*

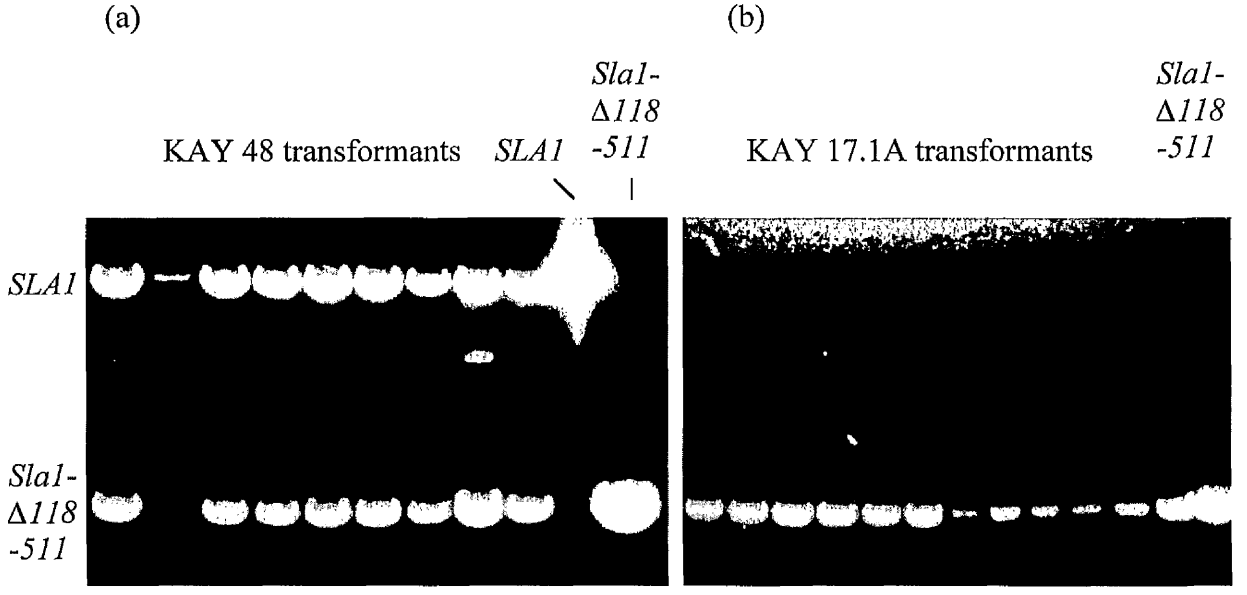

Figure 3.3 Screening of yeast transformants for integrated *sla1-Δ118-511* by colony PCR. Integrating plasmid pRS303 carrying *sla1-Δ118-511* was digested with *Nar1* to linearise plasmid at the extreme C-terminus of *SLA1,* then transformed into strain KAY 48. Colony PCR of transformants using oligos o36 and o44 was carried out to check homologous recombination of the mutant *sla1-Δ118-511* allele into the genome had replaced the wild-type allele of *SLA1* with the mutant allele. PCR products were run on a 0.8 % agarose gel. (a) The mutant *sla1* allele integrated into the genome as shown by an approximately 700 bp PCR product (right hand lane *sla1-Δ118-511* control (pKA 53) shown. However, the KAY 48 transformants still retained a wild-type copy of SLA1 as shown by a second PCR product of approximate size 1.9 kb. (b) KAY 17.1A was transformed with the integrative plasmid and then screened as before. KAY 17.1A transformants carried the integrated *sla1-Δ118-511* allele.

has been excised and replaced with *LEU2* and thus exhibit the same phenotypes as cells lacking *SLA1*. Cells were again screened by colony PCR and were found to have the *sla1-Δ118-511* allele integrated into the genome (figure 3.3b) at the appropriate site (as described in methods section 2.5.10.).

The haploid *sla1-Δ118-511* yeast strains KAY 350 and KAY 351 were consequently mated to generate homozygous diploid *sla1-Δ118-511* yeast strain KAY 352.

3.3.1 Expression of integrated *sla1-Δ118-511* shown by western blot analysis.

The expression of integrated *sla1-Δ118-511* in the haploid and diploid yeast was verified by probing a western blot (methods section 2.7.7) with anti-Sla1p antibodies raised against part of the C-terminus domain (figure 3.4).

As expected, both parental *sla1*-Δ2 strains (KAY 17.1A and KAY 17.1B) did not produce a signal on the western blot (figure 3.4a). The predicted molecular weight of Sla1p is 136 kDa, however, wild-type Sla1p ran at 175 kDA, possibly due to the high content of proline in the protein which inhibits migration through the gel. The last four lanes of the blot show sla1-Δ118-511 protein running at around 123 kDa which corresponds to the size expected after removal of the 118-511 domain. The band also appears as a doublet which suggests a post-translational modification of the protein. Thus, Sla1p and sla1-Δ118-511 protein are expressed at fairly similar levels, indicating that the stability of the mutant protein was not significantly decreased.

Figure 3.4b shows a western blot containing haploid and diploid yeast proteins probed with anti-Sla1p antibodies. Homozygous strains produced single bands as

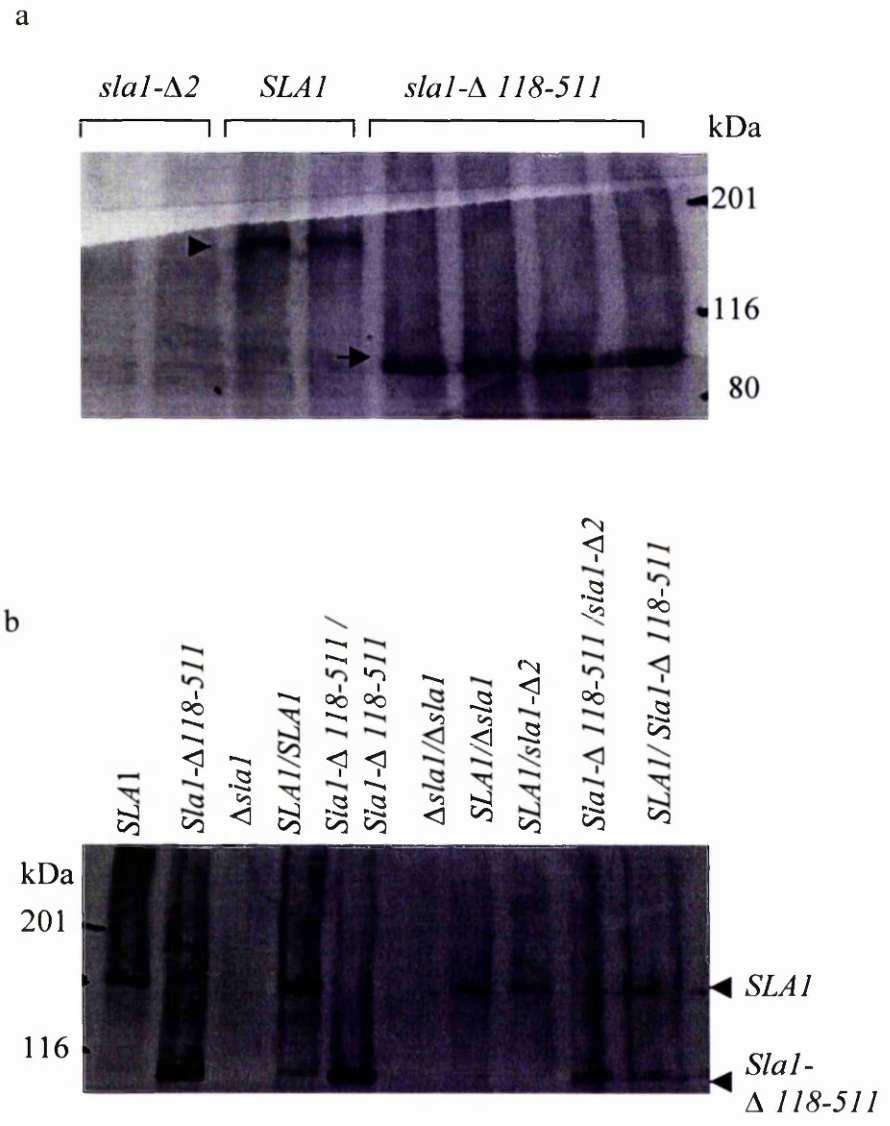

Figure 3.4 Western blot analysis of integrated *sla1-Δ 118-511*. (a) Haploid yeast cell extracts containing integrated *sla1-Δ 118-511* were probed with anti-Sla1p antibodies (four right hand lanes) shown alongside the parental strain used for integration and isogenic wild-type strain. (b) Homozygous diploid yeast and strains heterozygous for *sla1-Δ 118-511, SLA1* and/or *sla1-Δ2* were probed with anti-Sla1p antibodies. Haploid cell extracts were run alongside the diploid samples.

expected (unless Δ*sla1* or *sla1*-Δ*2* strains). Similarly, heterozygous yeast produced bands corresponding to the Sla1 protein expressed in those cells. Therefore all diploid yeast are expressing the wild-type and/or mutant forms of Sla1p as expected and phenotypes resulting from the expressed protein can be assessed.

3.4 Growth characteristics of *Sla1-118-511* yeast.

3.4.1 Temperature Sensitivity of haploid yeast lacking the Sla1p-118-511 domain of Sla1p

sla1-Δ*2* and Δ*sla1* yeast are temperature sensitive so grow poorly or are inviable when incubated at 37 °C. To determine if this temperature sensitive phenotype can be attributed to loss of the Sla1p-118-511 domain, *sla1*-Δ*118-511* yeast were tested for their ability to grow at 37 °C.

The temperature sensitivity of *sla1-118-511* yeast at 29 °C and 37 °C was assessed as described in section 2.5.7. Figure 3.5a shows that haploid wild-type yeast grew equally well at these two temperature but that Δ*sla1*, *sla1*-Δ*2* and the mutant *sla1*-Δ*118-511* yeast strains grew very poorly at 37 °C.

This data shows that the Sla1p-118-511 domain is important for growth at high temperatures since cells lacking this domain are as temperature sensitive as cells missing the entire Sla1p.

(a)

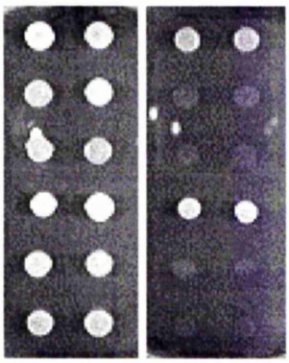

SLA1 (KAY 302)

sla1-Δ118-511 (KAY 350)

Δ*sla1* (KAY 300)

SLA1 (KAY 17.1D)

sla1-Δ118-511 (KAY 351)

sla1-Δ2 (KAY 17.1B)

(b)

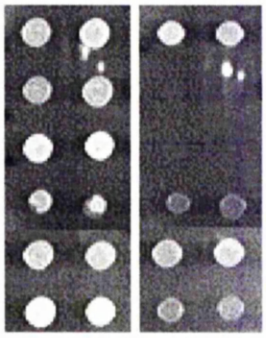

SLA1/SLA1 (KAY 40)

sla1-Δ118-511 / sla1-Δ118-511 (KAY 352)

sla1-Δ2/sla1-Δ2 (KAY 20)

SLA1/sla1-Δ118-511 (KAY 496)

SLA1/sla1-Δ2 (KAY 497)

SLA1/Δsla1 (KAY 498)

Figure 3.5 Growth of haploid and diploid cells expressing sla1p-Δ118-511 (a) Haploid yeast cells were plated onto YPAD agar and tested for growth at 29 °C and 37 °C. (b) Diploid yeast cells were grown on YPDA agar at 29 °C and 37 °C. Homozygous strains and heterozygous strains are shown in the top three and bottom three rows respectively. Growth of yeast strains was compared to wild-type, *sla1-Δ2* and Δ*sla1* strains.

3.4.2 Sla1-118-511 is a recessive allele for temperature sensitive phenotype in diploid yeast.

In some instances mutant alleles can compete, for binding with interacting proteins, with the wild-type allele in a heterozygous cell. In this scenario, the mutant allele is termed a dominant negative and exerts a deleterious effect on cells despite the simultaneous expression of a wild-type allele. The mutant allele however is only partially functional and may retain the ability to bind to other proteins, but then can not carry out further necessary activities. A second situation which occurs in heterozygous cells is that mutant alleles have their mutant phenotypes suppressed in the presence of wild-type allele expression. The mutant allele in this case is termed recessive.

To assess whether the *sla1-Δ118-511* allele was recessive, the ability of homozygous and heterozygous diploid yeast strains to grow at 37 °C was tested (figure 3.5b). All diploid strains which expressed *SLA1* were able to grow at 37 °C. However, diploid homozygous *sla1-Δ118-511* and Δ*sla1* yeast cells hardly grew at 37 °C.

These results show that the *sla1-Δ118-511* allele is recessive as cells which also express the wild-type allele are able to grow at the restrictive temperature. The expression of the mutant protein therefore does not competitively inhibit or interfere in interactions which are required for growth at high temperatures in this strain.

3.4.3 Growth rate of yeast expressing sla1-118-511 protein

As the growth of Δ*sla1* and *sla1-Δ118-511* cells on rich media at 37 °C is impaired (section 3.4.1) it may be predicted that the growth rate of these cells will also be slower than wild-type yeast. The ability of cells to grow and divide at restrictive and permissive temperatures in liquid media was assessed using a Sharfe Cell Counter (section 2.5.9.) and compared to wild-type and *sla1-Δ2* yeast by obtaining cell numbers of exponentially growing yeast over a 300 minute time period.

Figure 3.6a is a plot of the number of yeast cells growing at both 29 °C and 37 °C over 300 minutes. Wild-type yeast had the highest growth rate of the strains at both 29 °C and 37 °C with very similar rates of growth. Both mutant yeast types grew at similar rates at the permissive temperature (which were lower than wild-type rates) and displayed very poor growth rates at the restrictive temperature. Figure 3.6b shows that the generation time calculated for each strain varies considerably, with wild-type yeast doubling around three times faster than the mutant yeast at 37 °C. The mutant yeast also take approximately twice as long to double in number at 37 °C compared to growth at 29 °C.

The Sla1p-118-511 domain is therefore required for yeast cells to achieve wild-type growth rate levels in rich media.

(a)

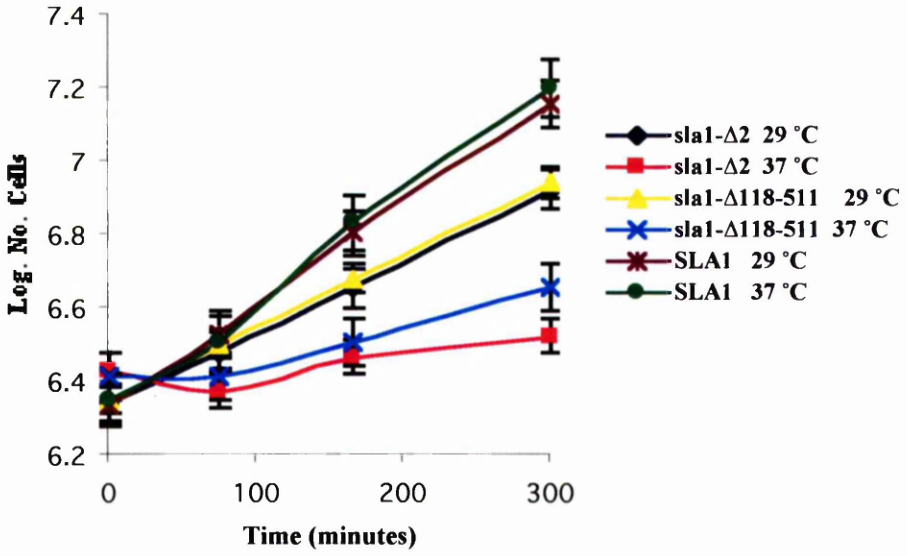

(b)

	Generation time (minutes)
Wild-type (29 °C)	106
Wild-type (37 °C)	92
sla1-Δ118-511 (29 °C)	163
sla1-Δ118-511 (37 °C)	263
sla1-Δ2 (29 °C)	163
sla1-Δ2 (37 °C)	320

Figure 3.6 Growth rate of cells expressing *sla1-Δ118-511*. Haploid yeast strains, wild-type (KAY 17.1D), *sla1-Δ118-511* (KAY 351) and *sla1-Δ2* (KAY 17.1B) were grown in YPAD media at permissive (29 °C) and restrictive (37 °C) temperatures. (a) Cell numbers were counted over 300 minutes in a Scharfe Cell Counter and plotted against time. Error bars show the standard error of the mean for 4 experiments. (b) Doubling times calculated from cell count results in (a).

3.4.4 Viability of cells expressing the *sla1-118-511* allele

Cells arresting and dying in culture may account in part for the decreased rate of growth of Δ*sla1* and *sla1-Δ118-511* yeast, especially at 37 °C, in section 3.4.3. To test this possibility, the fate of mutant diploid cells after shift to 37 °C was assessed (as described in section 2.5.8) and compared to wild-type yeast. Yeast grown at 29 °C in liquid media were also assessed for comparison.

Figure 3.7 demonstrates graphically the percentage of cells that were viable after 4 hours at 29 °C or 37 °C in all three yeast strains. After 4 hours at 29 °C, 98 % of wild-type cells were viable but that after the shift to 37 °C this number was reduced to 90 %.

For both the *sla1-Δ118-511* and Δ*sla1* diploid yeast, after incubation for 4 hr at 29 °C cell viability was 77 % and 79 % respectively. However, the levels of viability decreased substantially in the mutant yeast strains, after the shift to 37 °C for 4 hours. Just over half of the population of *sla1-Δ118-511* yeast cells (51 %) were able to grow after the temperature shift, and only 29 % of Δ*sla1* yeast cells remained viable. Loss of viability in the mutant strains, after the shift to restrictive temperature, was significant when compared to wild-type levels of viability after the shift from 37 °C to 29 °C.

Comparison of the results of section 3.4.3. and 3.4.4 follow similar trends. The wild-type yeast are obviously able to grow and reproduce well in liquid culture. Both mutant strains show very similar growth rates and levels of viability at 29 °C

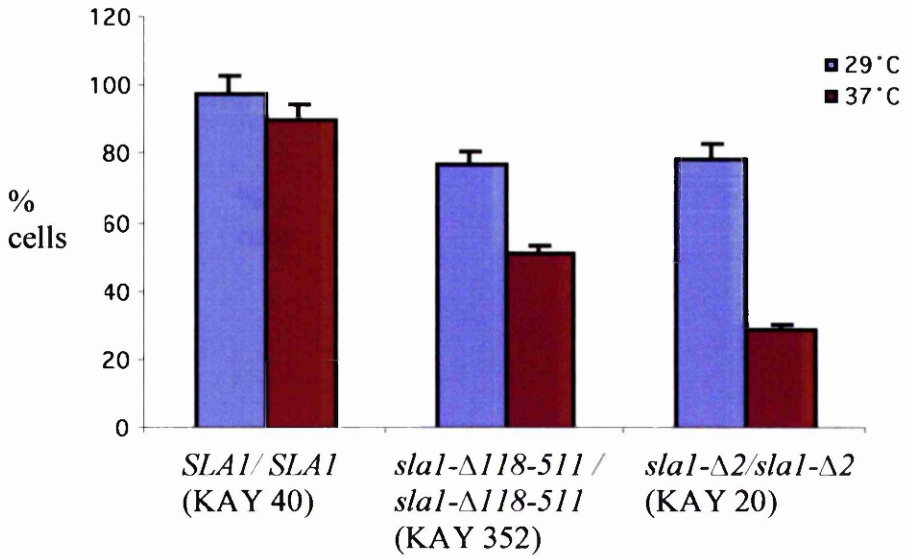

Figure 3.7 Viability of diploid yeast strains. Cells were incubated at 29 °C and 37 °C in liquid YPDA for 4 hours. 100 individual cells were picked at random and placed onto YPDA agar using a micromanipulator and incubated at 29 °C for 2 days. Cells were then scored as viable or non-viable. Error bars show the standard deviation between four experiments.

compared to wild-type levels, demonstrating that while the majority of mutant yeast cells are able to reproduce at 29 °C, it takes longer to complete a cell cycle. The combined growth rate and viability results of the mutant cells at 37 °C suggest that cells are arresting and dying in culture. However, the *sla1-Δ118-511* mutant yeast appear to tolerate growth at the restrictive temperature slighter better than *sla1-Δ2* yeast as they exhibit slightly higher growth rate and viability (figure 3.6 and 3.7).

3.5 Actin phenotype

Both Δ*sla1* cells and cells which express mutant *sla1-Δ118-511* from a plasmid (pKA 53) have an aberrant actin phenotype. F-actin staining with rhodamine-phalloidin was employed to determine whether cells which expressed the integrated form of *sla1-Δ118-511,* as the sole source of Sla1p in the cell, also possessed abnormal actin. Figure 3.8 shows the normal actin organisation and morphology found in both wild-type diploid and haploid cells. Actin cables can been seen in a few cells, running parallel to the mother-bud axis and the cortical actin displays a regular, punctate staining pattern. Cortical actin patches are located at the cortex can be seen polarised to sites of active cell surface growth, at the incipient bud growth site at early cell cycle stages and in the developing bud as the cell cycle progresses. Later in the cell cycle the actin patches are found at the mother-bud neck as the cell undergoes cytokinesis. Unbudded, or cells in stationary phase, have randomly distributed cortical actin patches.

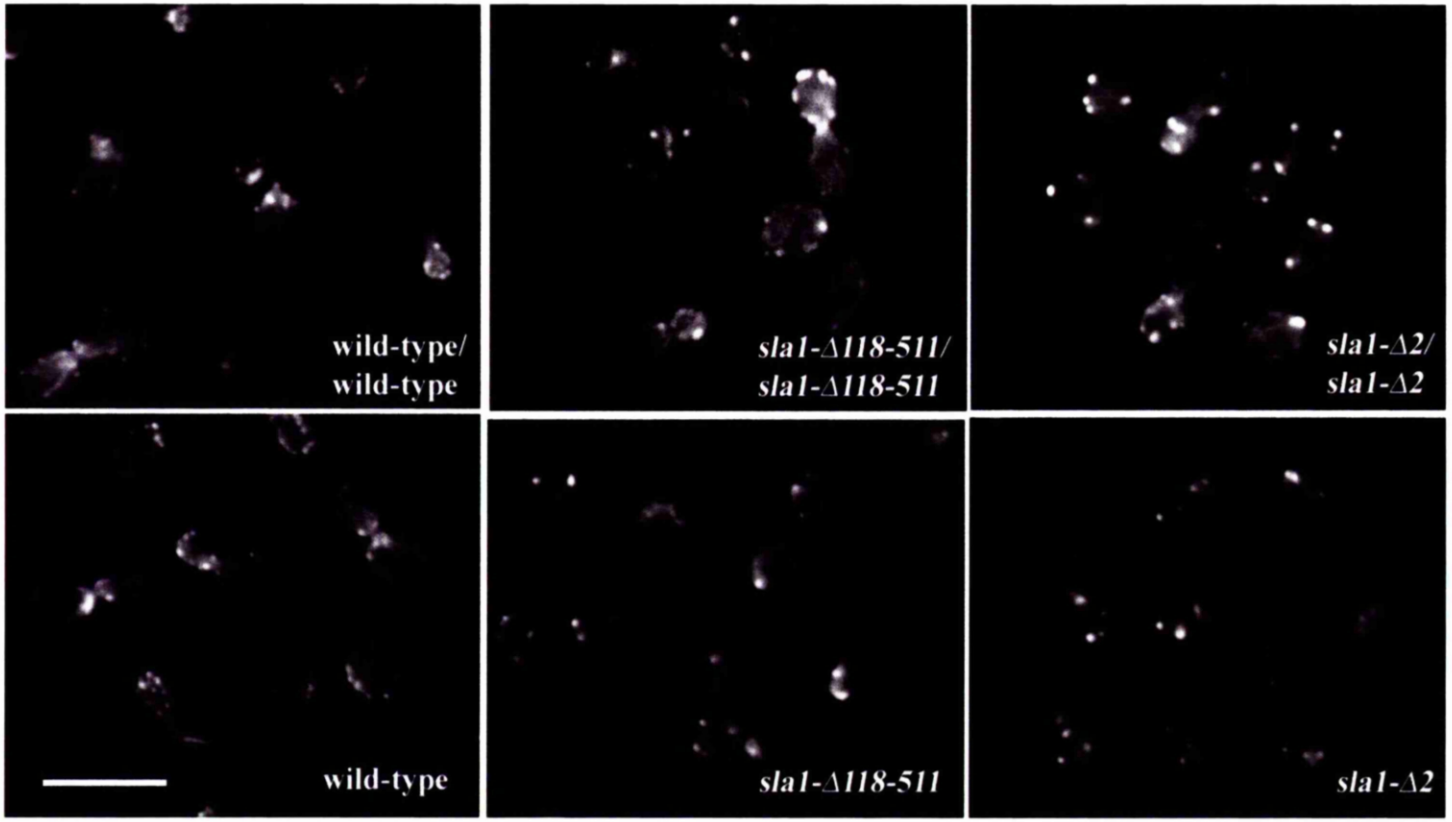

Figure 3.8 Actin organisation of diploid and haploid yeast strains expressing sla1-Δ118-511 protein. Log phase diploid and haploid yeast were stained with rhodamine-phalloidin to assess actin phenotype in wild-type, *sla1-Δ118-511* and Δ*sla1* cells. Bar, 10μm.

In Δ*sla1* diploid and haploid yeast strains there is a defect in the cortical cytoskeleton and fewer, larger 'chunks' of cortical actin are visible. Despite this defect, the cortical actin structures are fairly well polarised to the bud surface. Cells are able to form buds and grow, although more slowly than wild-type (section 3.4.3).

The mutant *sla1-Δ118-511* diploid and haploid cells when stained with rhodamine-phalloidin display an actin phenotype like that found in Δ*sla1* cells. The cortical actin patches are larger than those found in wild-type cells and less numerous. The actin patches are also able to polarise fairly well and can be seen largely in the developing bud in budded cells.

Cortical actin in cells expressing the integrated form of *sla1-Δ118-511* have the same aberrant phenotype reported for Δ*sla1* and plasmid-expressed mutant yeast strains (Ayscough *et al* 1999).

3.6 *ABP1* dependence

SLA1 was identified in a synthetic lethal screen where it was essential for viability of yeast cells in which *ABP1* had been deleted (Holtzman *et al* 1993). Cells with deletions in both *ABP1* and *SLA1* are inviable. We have previously found that all the *Sla1* mutants when expressed on plasmids except pKA13 (*sla1-ΔCterminus*) can rescue the *ABP1* dependency (Ayscough *et al* 1999). To investigate if the integrated *sla1-Δ118-511* and Δ*abp1* were synthetically lethal, heterozygous diploid strains carrying both *sla1-Δ118-511* and Δ*abp1* were generated. Haploid yeast lacking *ABP1* (KAY 126) were mated with haploid *sla1-Δ118-511* cells (KAY 350) to produce

KAY 492 (section 2.5.2). Zygotes which resulted from the crosses were grown on YPAD and then sporulated and tetrads dissected (section 2.5.4). All progeny from this cross will be viable if cells expressing *sla1-Δ118-511* are not *ABP1* dependent. As controls, *sla1-Δ2* and wild-type cells were also crossed with Δ*abp1* cells.

Figure 3.9a shows the tetrad progeny after growth on YPAD for 2 days at 29°C. All progeny that arose from Δ*abp1* x *SLA1* and Δ*abp1* x *sla1-Δ118-511* crosses were viable whereas in most cases a single progeny from the Δ*abp1* x Δ*sla1* cross did not grow on YPAD plates. Tetrads from the Δ*abp1* x Δ*sla1* cross which produced four viable daughter cells did not produce a segregant with both Δ*abp1* and Δ*sla1* and therefore the tetrad was not a tetratype.

The genotypes of the Δ*abp1* x *sla1-Δ118-511* progeny were assessed to confirm the segregation of both Δ*abp1* and *sla1-Δ118-511* to ensure that some progeny contained both genes. Western blot analysis using anti-Abp1p antibodies determined which cells contained wild-type *ABP1*, and therefore which cells were Δ*abp1* (figure 3.9b). The slow growth phenotype of *sla1-Δ118-511* cells at 37 °C was used as a marker for the *sla1-Δ118-511* genotype. Comparison of the western blot results and the slow growth results for the three tetrads shown revealed that one out of the four resultant haploid cells from the Δ*abp1* x *sla1-Δ118-511* cross carried both Δ*abp1* and *sla1-Δ118-511*.

Deletion of both *ABP1* and *SLA1* from yeast is lethal. In contrast, strains carrying a deletion of *ABP1* in combination with *sla1-Δ118-511* are viable. The region of Sla1p that is required for cells without *ABP1* is therefore not the Sla1p-118-511 domain.

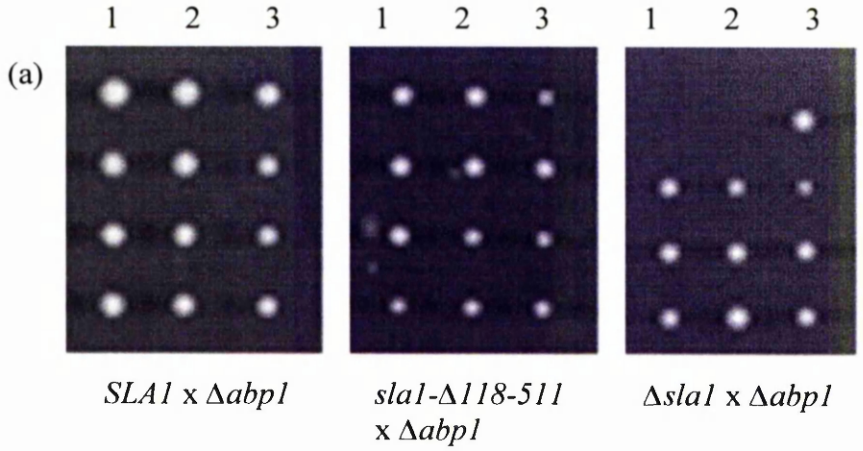

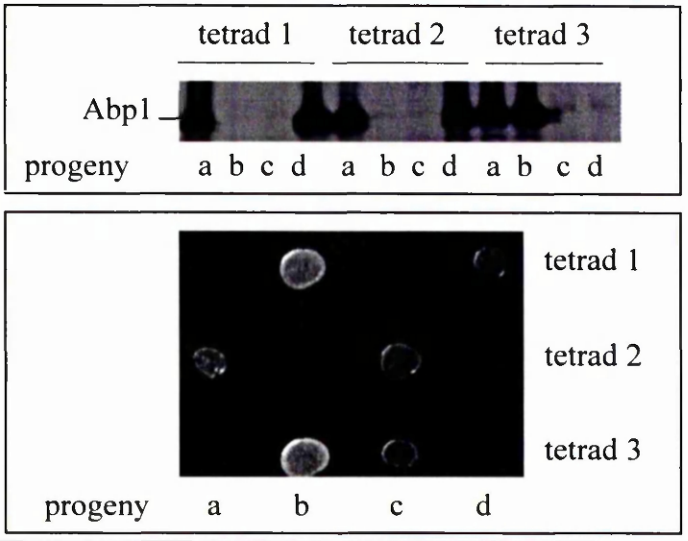

	tetrad 1	tetrad 2	tetrad 3
a	*ABP1/sla1-Δ118-511*	*ABP1/ SLA1*	*ABP1/sla1-Δ118-511*
b	*Δabp1/SLA1*	*Δabp1/sla1-Δ118-511*	*ABP1/ SLA1*
c	*Δabp1/sla1-Δ118-511*	*Δabp1/ SLA1*	*Δabp1/ SLA1*
d	*ABP1/ SLA1*	*ABP1/sla1-Δ118-511*	*Δabp1/sla1-Δ118-511*

Figure 3.9 Sla1p-118-511 domain is not required for viability in the absence of *ABP1*. (A) Cells deleted for both *SLA1* and *ABP1* are inviable. To assess the viability of progeny from *Δabp1* (KAY 126) yeast crossed with; wild-type, *sla1-Δ118-511* (KAY 350), and, *sla1-Δ2* (KAY 17.1B), tetrads were pulled after sporulation of diploids and grown on rich media for 2 days at 29 °C. All daughter cells grew from the *Δabp1* x *SLA1* and *Δabp1* x *sla1Δ118-511* crosses. However, the *Δabp1* x *Δsla1* cross gave rise to inviable progeny (right). (B) Segregation pattern for the *Δabp1* x *sla1-Δ118-511* cross was assessed by western blot using anti-Abp1p antibodies and temperature sensitive growth on plates at 37 °C for the presence of *SLA1* (growth) or *sla1-Δ118-511* (no growth).

The ability of *sla1-Δ118-511* cells to grow in the absence of *ABP1* also demonstrates that the Sla1-Δ118-511 protein expressed in Δ*abp1/ sla1-Δ118-511* cells must be expressed in a biologically functional form. The temperature sensitivity and aberrant actin phenotypes which occur with the deletion of the Sla1p-118-511 domain can therefore be associated with loss of the domain and not because the mutant protein is aberrantly folded thus rendering the mutant cells effectively null for *SLA1*.

3.7 Budding phenotype of diploid *sla1-118-511* cells

S.cerevisiae undergoes polarised growth during budding where growth is directed toward a selected site in the mother cell. Growth then becomes isotropic as the bud develops, until late nuclear division and cytokinesis when growth is directed towards the site of division. Both haploid and diploid cells form daughter cells by budding but this is controlled by separate pathways. Haploid cells bud axially, cells form a bud adjacent to the previous bud site. Diploid cells have a different budding pattern. They bud in a bipolar manner, either adjacent or opposite to the birth site and this requires a functional actin cytoskeleton (Yang *et al* 1997). It is proposed that future bud sites are marked by bud site tags that serve as cues for the initiation of new buds (Chant and Pringle 1995).

Diploid yeast cells bud at the poles giving a bipolar budding pattern when stained with calcofluor (a specific stain for chitin which is found in the cell wall and bud scars). As studies on some mutant yeast with defects in their actin cytoskeleton also

have a bipolar budding defect, the budding pattern of *sla1-Δ118-511* diploids was investigated.

Diploid wild-type, *sla1-Δ118-511*, and Δ*sla1* yeast cells were treated with calcofluor (section 2.8.11) (figure 3.10a). Cells with 3 or more bud scars were then scored as having either a bipolar budding pattern (bud scars at the poles only), or a random budding pattern (bud scars also in equatorial region). Figure 3.10b gives the percentages of wild-type and mutant *sla1* cells which budded randomly or in a bipolar fashion. As expected, wild-type diploid cells predominantly produced daughter cells by budding bipolarly (98 %) whereas the majority of Δ*sla1* diploid cells (85 %) exhibited a random budding pattern. Figure 3.10a shows the characteristic bipolar staining pattern of wild-type diploid cells and the random budding pattern of Δ*sla1* diploid cells. The budding pattern of *sla1-Δ118-511* diploid cells was intermediate to wild-type and Δ*sla1*/Δ*sla1* cells as 33 % budded bipolarly and 67 % budded in a random manner (fig 3.10b).

Diploid *sla1-118-511* showed a greater ability to bud from the poles than diploid Δ*sla1* cells despite both displaying an aberrant actin staining pattern (figure 3.8). The mutant Sla1-Δ118-511 protein must contain functional domains that perform some function to partially rescue the random budding phenotype observed in Δ*sla1* diploids.

(a)

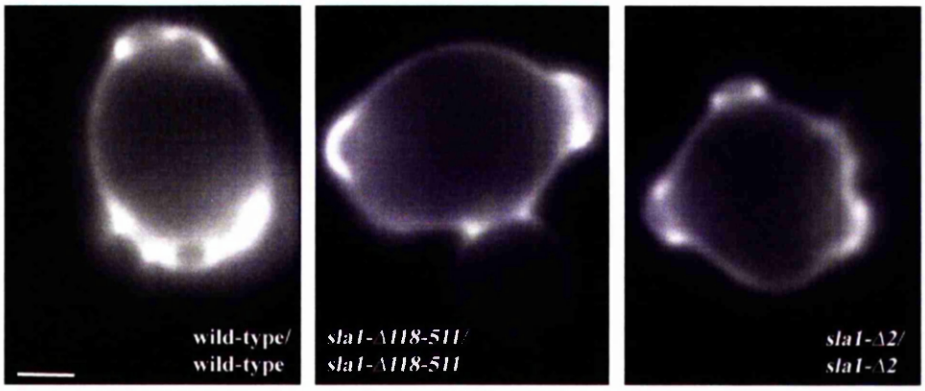

(b)

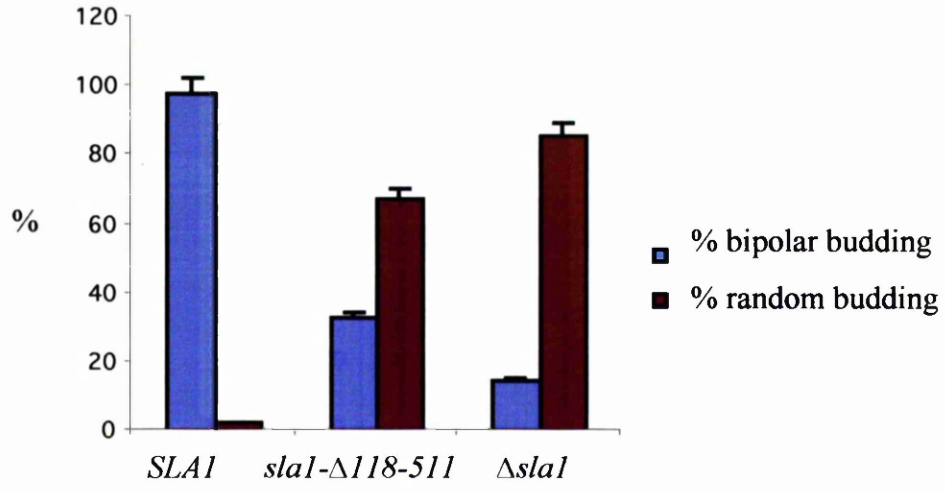

Figure 3.10 The Sla1p-118-511 domain is required for normal diploid budding pattern. (a) Diploid yeast strains were stained with calcofluor to stain the bud scar. Bar, 2 μm. (b) Wild-type diploid cells (KAY 40) bud in a bipolar fashion, bud scars are at either pole in 98% of cells. However, a percentage of diploid *sla1-Δ118-511* (KAY 352) and *sla1-Δ2* cells (KAY 20) bud randomly. Error bars show the standard error of the mean between three experiments (n=200).

3.8 The Sla1p-118-511 domain is not required for localisation to cortical patches

It has been shown previously that the immunofluoresence pattern of myc-tagged wild-type Sla1p is similar to the anti-actin localisation pattern in wild-type cells and Sla1p co-localises with a subset of cortical actin patches, but not with actin cables (Ayscough *et al* 1999). The localisation of Sla1p with cortical actin demonstrates that it is well placed to play a role in the organisation of actin patches at the cortex.

As cortical actin in *sla1-118-511* cells is aberrant the cause may be due to abnormal localisation of the mutant protein. In order to examine the localisation of Sla1p-Δ118-511, a myc-tagged *sla1-Δ118-511* strain was generated using a PCR product integration method (section 2.3.10) using oligos oKA7 and oKA8 against template pKA119. Expression of the 9x myc-tagged *sla1-Δ118-511* was shown by western blot analysis (section 2.7.7) using anti-Sla1p antibody (figure 3.11).

The immunofluoresence pattern of the sla1p-Δ118-511-myc-tagged mutant shows that it is localised to the cortex in small, punctate spots (figure 3.12 middle) which do not appear like the larger 'chunky' actin patches (figure 3.12 left) found in this mutant (figure 3.12 right). This suggests that the sla1-Δ118-511 protein contains information to get to the cell cortex but not to interact with the actin cytoskeleton.

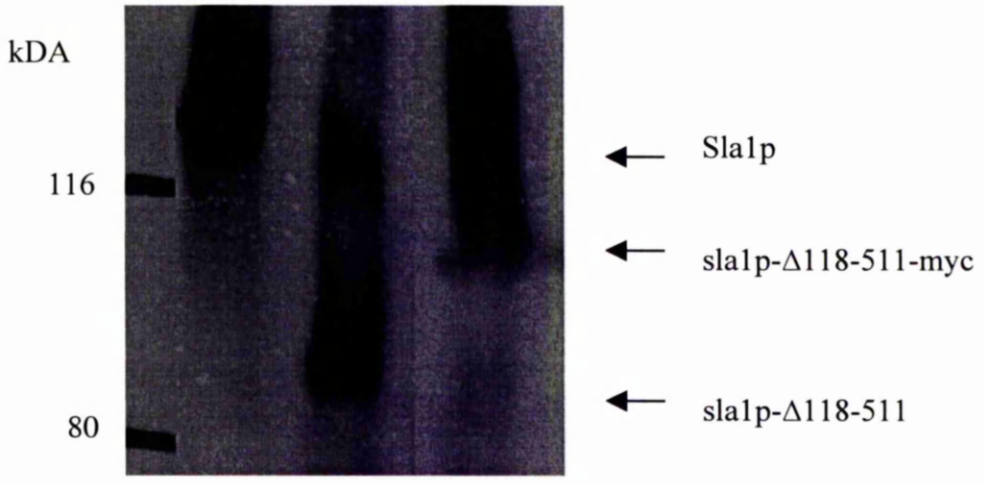

Figure 3.11 Expression of myc-tagged sla1p-Δ118-511 shown by western blot analysis. Whole cell extracts were run on a SDS-polyacrylamide gel, blotted and probed with anti-Sla1p antibodies. Left lane shows wild-type Sla1p (KAY 302), middle lane shows mutant sla1p-Δ118-511 (KAY 350), and the right hand lane shows expression of C-terminal myc-tagged sla1p-Δ118-511 (KAY 367).

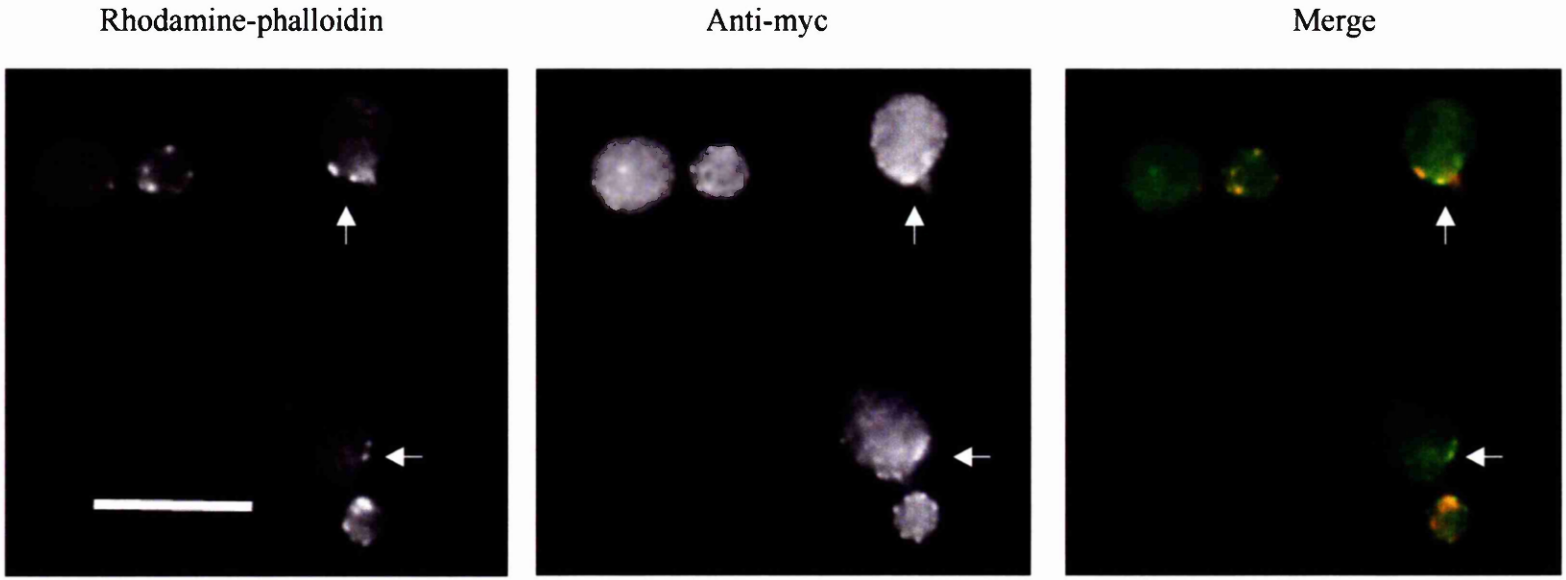

Figure 3.12. Sla1p-Δ118-511 localises to the yeast cell cortex. Haploid yeast expressing myc-tagged sla1p-Δ118-511 (KAY 367) were processed for immunofluoresence and then co-stained with anti-myc and rhodamine-phalloidin. The immunofluoresence pattern of the sla1p-Δ118-511-myc tagged mutant protein (middle) shows that it is localised to the cortex in small, punctate spots. In contrast, the cortical actin appears in larger and fewer patches at the cortex (left). When the anti-myc and rhodamine-phalloidin images are overlayed to observe co-localisation of mutant Sla1p (FITC-green) and actin (red), co-localising spots appear yellow. Possible co-localising patches are indicated by arrows. Bar, 10μm.

3.9 Actin dynamics are altered in yeast lacking the Sla1p-118-511 domain

LAT-A is a drug which binds and sequesters actin monomers and is a tool for disrupting actin polymerisation in *S.cerevisiae* (see section 1.6.2.2).

3.9.1 Latrunculin-A halo assays

LAT-A halos assays were performed (section 2.5.6) to assess the effect different concentrations of LAT-A had on the growth of yeast on YPD plates. Assays were carried out on diploid yeast strains. Figure 3.13a depicts the halo assays of yeast strains after 2 days at 29 °C. In wild-type diploid cells, zones of growth inhibition were present, which increased with increasing concentrations of LAT-A on the disc. LAT-A diffusion through the media close to the drug-soaked disc prevented the growth of wild-type cells as a consequence of F-actin disruption. On the otherhand, Δ*sla1* and *sla1-Δ118-511* diploid yeast were only unable to grow in a small zone around the disc which contained the highest concentration of the drug (5 mM). At 2mM concentrations and below growth was not affected and cells appeared to be resistant to the effect of LAT-A.

3.9.2 Effect of Latrunculin-A on actin cytoskeleton

In order to ascertain the effect of LAT-A on the actin cytoskeleton at a morphological level, diploid yeast cells were treated with LAT-A (section 2.8.10) and stained with rhodamine-phalloidin (section 2.8.7) to examine the filamentous actin in the cells. Figure 3.13b shows the percentages of cells, before and after LAT-A addition, which

(a)

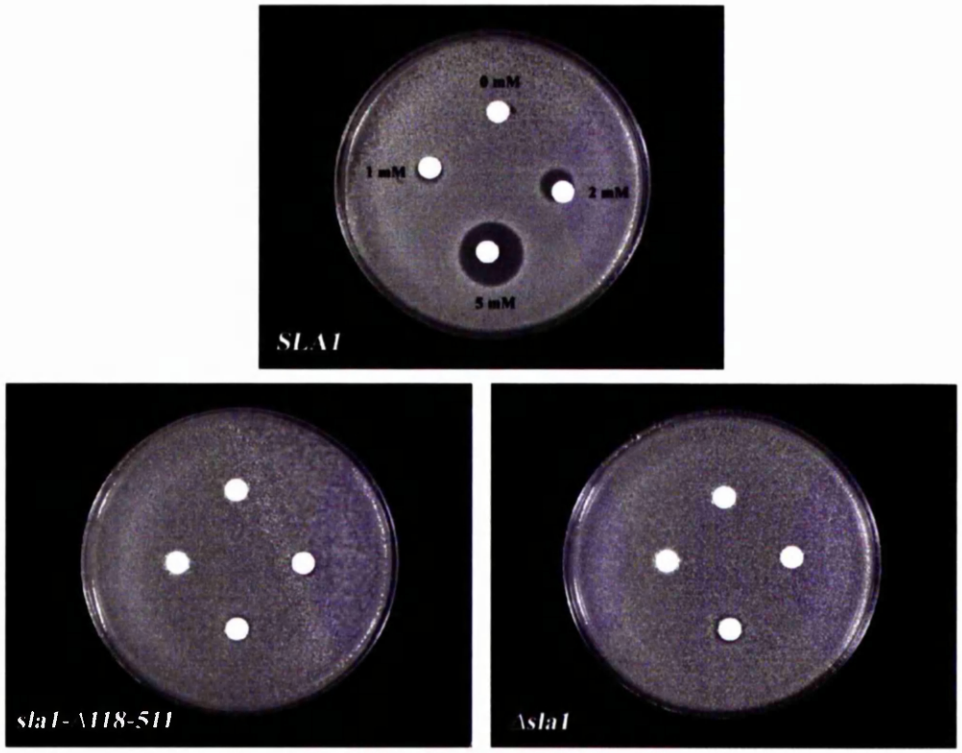

(b)

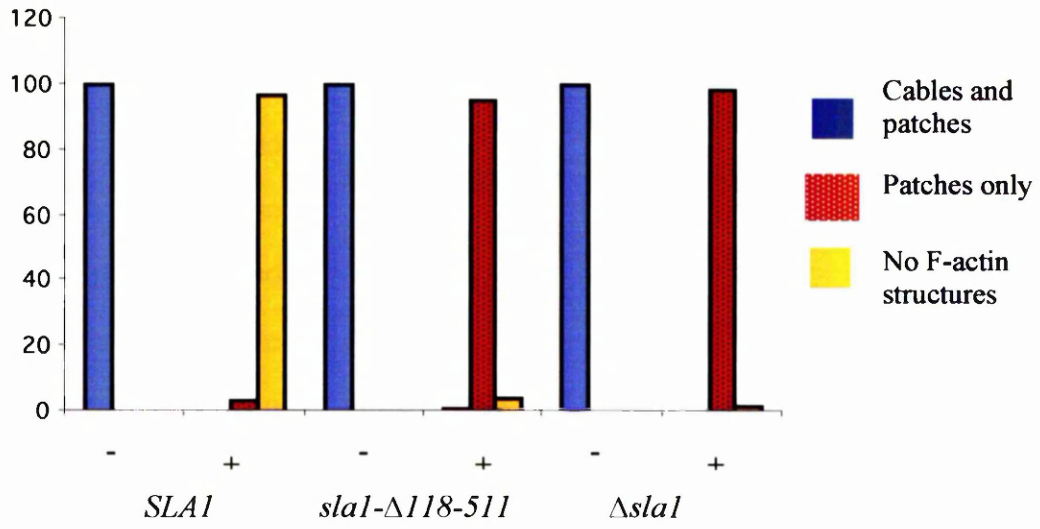

Figure 3.13 Actin dynamics are altered in yeast lacking the sla1p-118-511 domain. (a) LAT-A halos assays were performed on diploid wild-type *SLA1* (KAY40), *sla1-Δ2* (KAY 20) and *sla1-Δ118-511* (KAY 352) diploid yeast strains. Resistance to LAT-A is apparent in KAY 20 and KAY 352 yeast strains, as halos are apparent around LAT-A containing discs (1, 2 and 5 mM). (b) Filamentous actin was examined by rhodamine-phalloidin staining fixed cells (n=200) before (-) and after (+) LAT-A treatment (200 µm for 15 minutes). Cells were scored as either retaining actin cables and cortical actin patches, or cortical patches only, or as having no visible F-actin structures present.

contained visible actin cables and patches, patches only or no F-actin. Wild-type cells had clearly lost the majority of filamentous actin structures after 20 minutes with 96.5 % cells lacking actin structures. The cortical actin patches in Δ*sla1* diploids and *sla1-Δ118-511* diploids on the otherhand were significantly resistant to LAT-A treatment as 95 % and 98.5 % respectively, retained cortical actin patches.

Taking the results from LAT-A experiments in sections 3.9.1 and 3.9.2 it is apparent that the Sla1p-118-511 domain of Sla1p plays an important role in the response of cells to LAT-A. Because the Δ*sla1* and *sla1-Δ118-511* cells are more resistant to the effects of LAT-A this suggests that the F-actin in these two strains is less dynamic than in the wild-type situation. Wild-type Sla1p may therefore play a role in destabilising (or increasing turnover of) the yeast actin cytoskeleton with the Sla1p-118-511 domain particularly important in this role.

3.10 Uptake of Endocytic Vital Dyes

A large number of published studies have demonstrated that actin and a subset of actin-associated proteins are required for the internalisation step of both receptor-mediated and fluid-phase endocytosis. Fluid-phase endocytosis is a non-specific constitutive process that occurs continuously in eukaryotic cells whereby the extracellular fluid is internalised via endocytic vesicle uptake. As deletion of the Sla1p-118-511 domain caused an aberrant cortical actin cytoskeleton, endocytosis function was assessed in *sla1-Δ118-511* yeast using the vital vacuolar stains FM4-64 [N-(triethylammoniumpropyl)-4-(p-diethylaminphenylhexatrienyl) pyridium

dibromide] (Vida and Emr 1995) and Lucifer Yellow-carbohydrazine (Benz(de)isoquinoline-5, 8-disulfonic acid, 6-amino-2-((hydrazinocarbonyl) amino)-2,3-dihydro-1,3-dioxo- dilithium salt)(Riezman, 1985, Dulic *et al* 1991).

3.10.1. Examining endocytic uptake with Lucifer Yellow

Homozygous diploid yeast cells (wild type *SLA1*, Δ*sla1* and *sla1-Δ118-511*) were incubated in the presence of Lucifer yellow (methods 2.8.1). Figure 3.14 shows the Lucifer yellow staining pattern of wild-type cells. Wild-type cell vacuoles are labelled clearly with Lucifer Yellow and fluoresced brightly in the majority of cells. Some staining could also be seen at the cell surface. There was often only a single vacuole in the wild-type cells which appeared smooth and round. The vacuoles of mutant *sla1* cells appeared more fragmented. Again, some fluoresence could be seen at the cell surface. Fluoresence levels in the mutant cells appeared lower than in wild-type cells. Analysis of Lucifer yellow uptake through measurement of whole cell fluoresence intensity (section 2.8.1) confirmed that *sla1-Δ118-511* and Δ*sla1* cells displayed a lower level of uptake of Lucifer yellow into the vacuole relative to wild-type cells at 39 % and 33 % respectively (figure 3.14).

3.10.2. Examining endocytic uptake with FM4-64

FM4-64 is a lipophilic styryl dye used as a vital stain to follow bulk membrane internalisation and transport to the vacuole in yeast (Vida and Emr, 1995). Homozygous diploid yeast cells (wild type *SLA1*, Δ*sla1* and *Sla1-118-511*) were stained with FM4-64 (section 2.8.2.)(figure 3.15). The pattern of staining in wild-type cells showed the vacuole to appear like joined circles or loops in the cytoplasm of

(a)

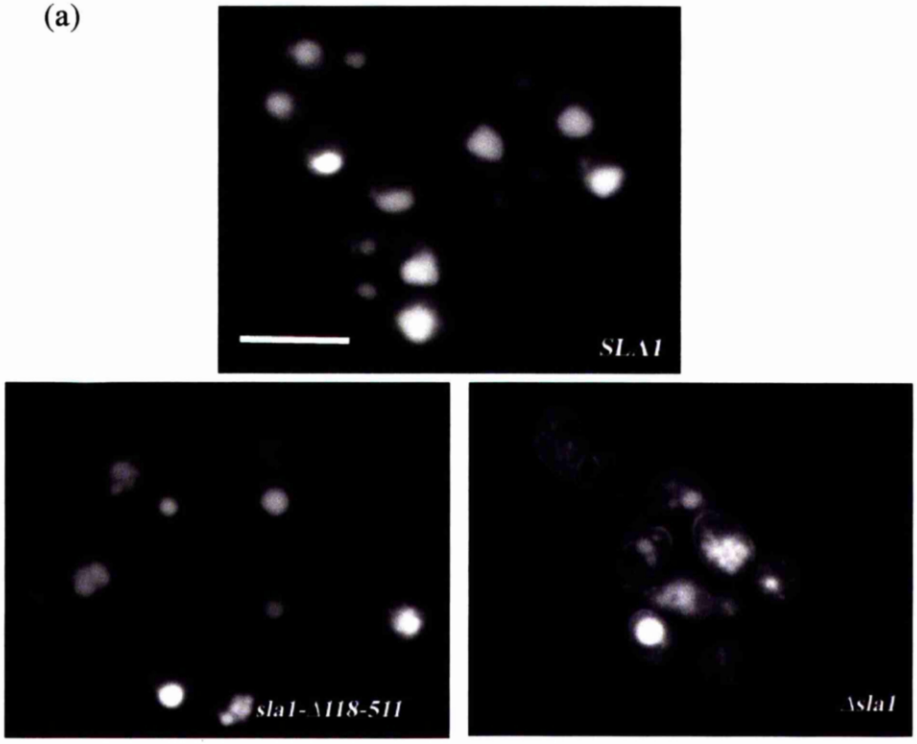

(b)

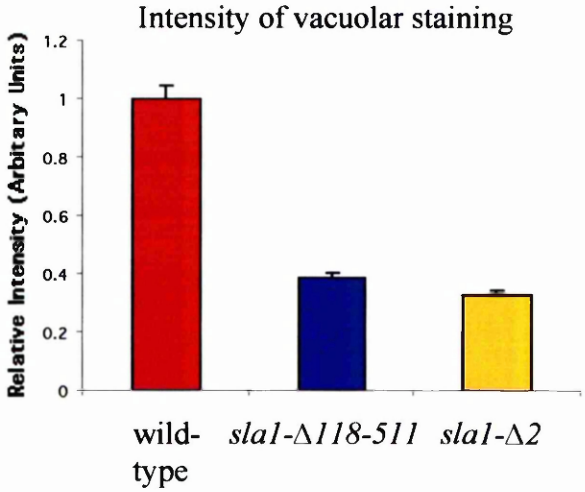

Figure 3.14. Fluid-phase endocytosis in *sla1* mutant yeast cells. (a) Pictures showing uptake of Lucifer Yellow CH into the vacuole of diploid, wild-type (KAY 40), *sla1-Δ118-511* (KAY 352), and *sla1-Δ2* (KAY 20) yeast cells. Bar, 10μm. (b) Bar graph displaying relative fluoresence intensity of Lucifer Yellow stained cells, shows a reduction in fluid phase uptake in the mutant sla1 yeast strains compared to wild-type. Error bars show the standard deviation between three experiments which measured uptake in 200 cells.

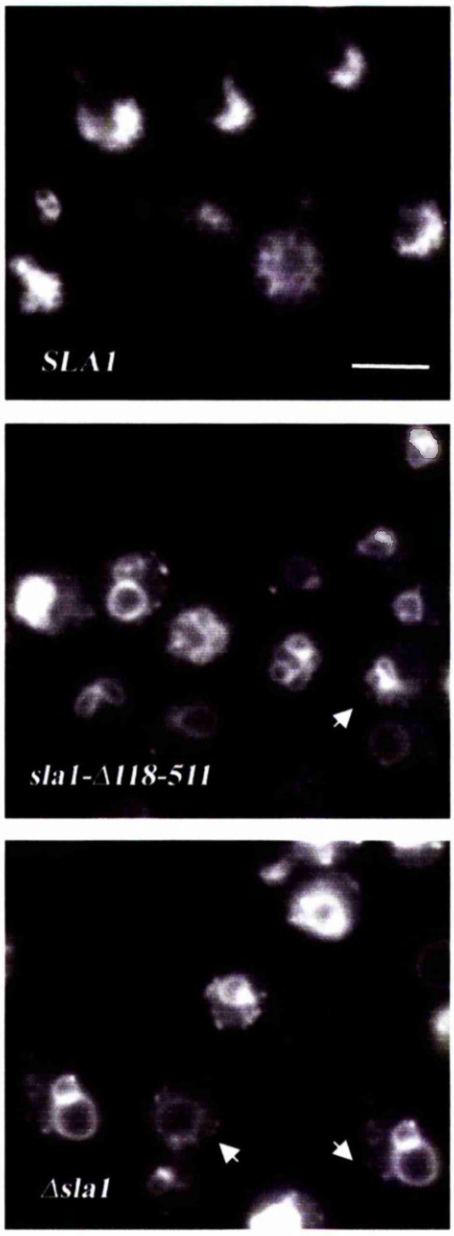

Figure 3.15. Bulk membrane internalisation and transport to the vacuole visualised by FM4-64 staining. Diploid yeast were incubated in FM4-64 to follow the transport of the vital stain to the vacuole. Wild-type cells (KAY40) show stained vacuolar membranes. *Sla1-Δ118-511* diploid (KAY 352) and *sla1-Δ2* diploid (KAY 20) yeast display stained vacuolar membranes and also punctate spots which possibly represent intermediate vesicles trafficking to the vacuole (arrowed). Bar, 5μm.

both the mother cell and in the developing bud. Both mutant strains also displayed FM4-64 stained vacuoles like the wild-type cells except small spots of fluorescence, distinct from the vacuolar staining were also apparent. These spots of fluorescence were only visible if cells had been incubated for short periods (less than 5 minutes) in FM4-64, indicating that they may be endocytic vesicles trafficking to the vacuole. The dye did however get to the vacuole so the pathway from the plasma membrane appears to function normally.

The presence of endocytic vesicles in the mutant yeast cells after FM4-64 incubation for short periods of time, combined with the reduced uptake of the fluid phase marker Lucifer Yellow CH compared to wild-type cells, provides evidence that the rate of endocytic uptake is defective in these cells. The absence of the Sla1p-118-511 domain in both mutant cell types appears to be reducing endocytic uptake into the cells, and this is a likely result of the aberrant actin phenotype/dynamics in these yeast (section 3.9). Significantly however, endocytosis is not completely blocked which suggests that other endocytic pathways can function and compensate in the absence of wild-type Sla1p.

3.11 Impaired mitochondrial function in *sla1-Δ118-511* yeast

Mitochondria are the intracellular organelles responsible for aerobic metabolism in eukaryotic cells. The actin cytoskeleton is important for normal mitochondrial localisation, morphology, movement and inheritance in budding yeast (Drubin *et al* 1993, Lazzarino *et al* 1994, Smith *et al* 1995, Simon *et al* 1997, reviewed by

Hermann and Shaw, 1998 and Catlett and Weismann, 2000). Time-lapse fluorescent microscopy studies have revealed directed mitochondrial movement along actin cables during polarised yeast cell growth and mitotic cell division (Simon *et al* 1995, Yang *et al* 1999).

Mitochondrial inheritance requires controlled actin polymerisation by the Arp2/3 complex (Boldogh *et al* 1998 and 2001). Several components of the actin cytoskeleton have also shown links with mitochondria. *GSC1* encodes a protein required for normal actin cytoskeletal organisation and for polymerisation *in vitro* (Poon *et al* 1996), and shows a genetic interaction with *SLA2* (Blader *et al* 1999). It has recently been reported to be involved in the maintenance of mitochondrial morphology, possibly through organising the actin cytoskeleton (Huang *et al* 2001). Similarly, actin cytoskeletal proteins Vrp1, Pan1p and Rsp5p (ubiquitin-protein ligase) mutants have defective mitochondrial function and mitochondrial protein sorting (Zoladek *et al* 1995 and 1997). It has been suggested that the actin cytoskeleton is involved in the delivery of mRNA encoding mitochondrial proteins (Vaduva *et al* 1997).

Metabolism of glycerol requires the presence of functional mitochondria. Diploid homozygous yeast strains; wild type, *sla1-Δ118-511* and *Δsla1* were initially plated onto YP + 3 % glycerol plates as a test for respiratory defects. Figure 3.16a shows the strains on YPD and YP+3 % glycerol at 29 °C. All 3 strains grow well on YPD at 29 °C, however, only wild-type yeast can grow on YP+3 % glycerol media. This

(a)

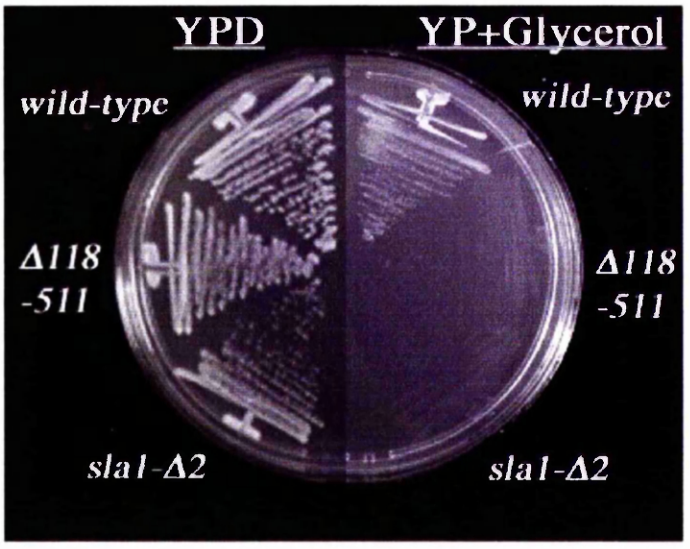

(b)

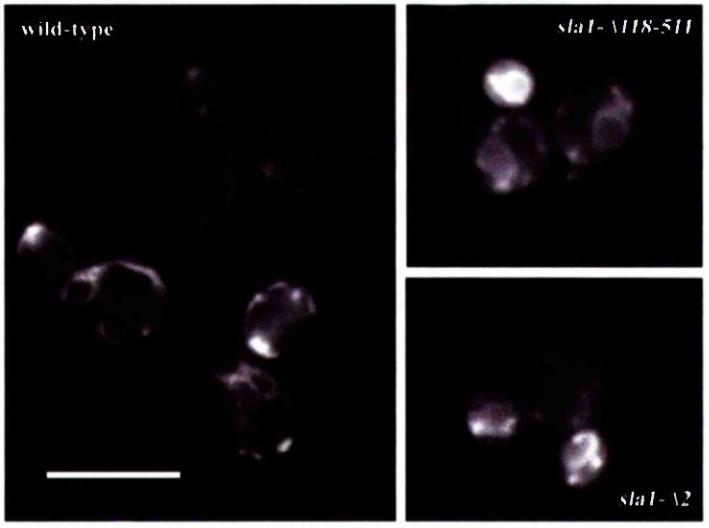

Figure 3.16 Impaired mitochondrial function in yeast lacking the sla1p-118-511 domain. (a) Diploid yeast strains were struck onto YP-3% glycerol plates at 29 °C for 2 days to assess respiratory function. Wild-type diploid (KAY 40) cells grew as well on YP-glycerol as on YPD. However, both homozygous *sla1-Δ2* (KAY 20) and *sla1-Δ118-511* (KAY 352) diploid strains did not grow on YPA-glycerol. (b) Diploid yeast were stained with $DiOC_6$ to observe mitochondrial morphology. Bar, 10 μm.

suggests that expression of *sla1-Δ118-511* results in a protein which has lost a domain required for normal cellular respiration.

In order to examine mitochondrial morphology in diploid yeast and to assess mitochondrial functioning, the cells were treated with $DiOC_6$ (Molecular Probes). $DiOC_6$ is a well-characterised mitochondrial stain which is sequestered in functioning mitochondria (Koning *et al* 1997). The uptake of $DiOC_6$ is dependent on the mitochondrial membrane potential. Diploid wild-type were incubated in 175 nm $DiOC_6$ whereas mutant diploid strains *Δsla1 and sla1-Δ118-511* were incubated in 1.75 μM (section 2.8.3). This increased level of $DiOC_6$ was required in order to visualise the mitochondria in the mutant yeast strains. This concentration of $DiOC_6$ is still below levels (5-50 μM) which will stain the endoplasmic reticulum.

Figure 3.16b shows the diploid yeast stained with $DiOC_6$. Mitochondria in wild-type yeast appeared as long tubular networks stretching throughout the cell whereas the mutant yeast mitochondria did not produce the same staining pattern. At the levels of $DiOC_6$ required to stain wild-type cells there is no staining of mutant cell mitochondria. This lack of apparent staining strongly suggests that the cells are unable to take up the stain because the mitochondria are not respiring normally.

3.12 Determining binding partners for the Sla1p-118-511 domain using GST pulldown

Mutant phenotype analyses on *sla1-Δ118-511* expressing yeast has shown that the Sla1p-118-511 domain is critical for its role in the organisation of cortical actin, as

cells which lack this domain are temperature sensitive and have an aberrant actin phenotype. Linked to the aberrant actin phenotype is defective endocytic function. So it is possible that deletion of the Sla1p-118-511 domain has severed the connection between Sla1p and interacting protein/s that is necessary for normal actin organisation and endocytic function. A biochemical approach to isolate binding partners of the Sla1p-118-511 domain was attempted by constructing Glutathione-S transferase (GST)- Sla1p-118-511 fusions for bacterial expression.

The Sla1p-118-511 domain and the Sla1p-118-511 (-SH3#3) domain alone were expressed in *E.coli* as inducible GST fusions from the pGEX vector (methods 2.7.3). Distinguishing any differences in pulldown results between these two overexpressed proteins would help eludicate the importance of the SH3 domain in protein-protein interactions. GST was also expressed to provide a negative control.

Once the pGEX recombinants were reproducibly expressing these fusion proteins, Sla1p-118-511 domain and Sla1p-118-511(-SH3#3) domain binding proteins were affinity purified from whole cell yeast extracts (section 2.7.3). This involved adding whole cell yeast extracts to the bound GST fusion proteins. Yeast proteins interacting with the Sla1p-118-511 domain were separated by SDS-PAGE (section 2.7.5) and promising bands (figure 3.17) subjected to microsequencing. This was carried out in-house (Nick Morrice, Dundee University). Denatured gel samples were digested with trypsin and analysed by matrix-assisted laser desorption ionisation-time of flight mass spectrometry (MALDI-TOF MS) (Pandey and Mann, 2000). Proteins were identified by database search algorithms. Unfortunately, after several attempts it was found that

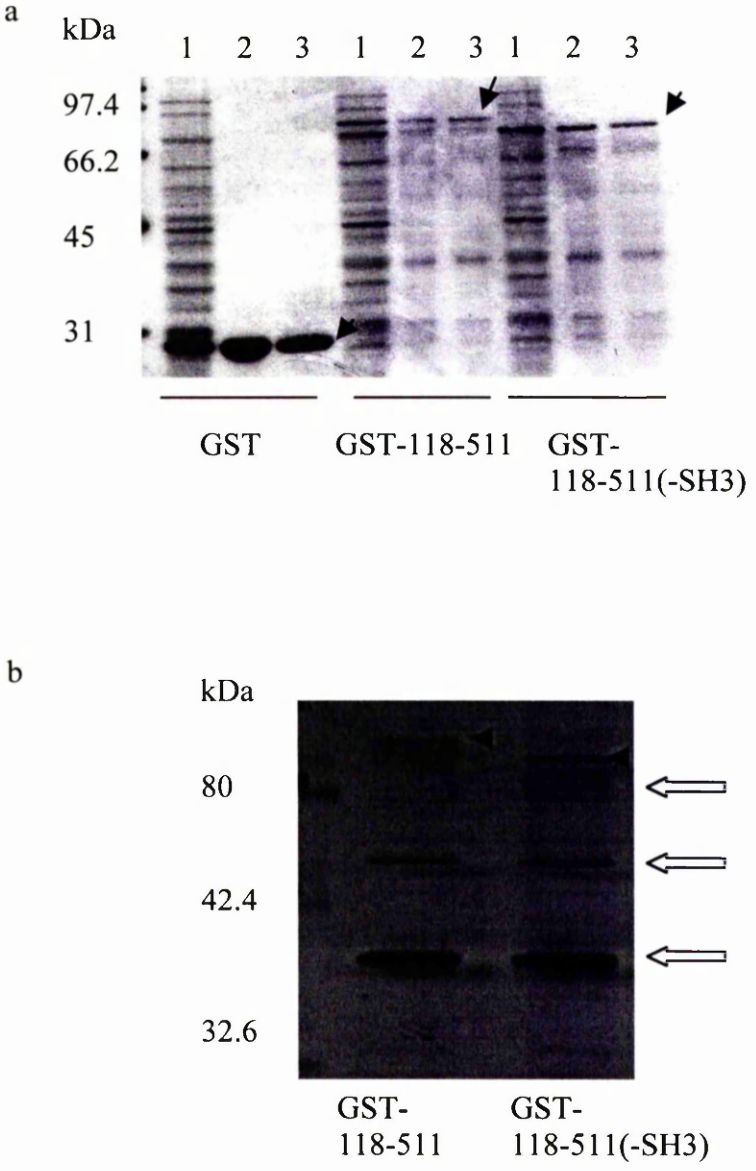

Figure 3.17 Expression of Sla1p domains as GST-fusions. Bacterially expressed GST-sla1p-118-511 and GST- sla1p-118-511(-SH3) proteins were induced in liquid culture by addition of IPTG then processed for small scale batch purification on glutathione beads (methods section 2.7.3). (a) Coomassie-stained 10 % acrylamide gel showing (1) whole cell extracts (2) beads and (3) eluate fractions from purification procedure, arrows show the bands representing the fusion proteins and GST alone in the left-hand of gel. Beads with bound GST-fusion proteins were added to wild-type (KAY 40) yeast extract and then batch eluted to recover GST-fusion proteins complexed with any binding partners. (b) Silver stained 10 % acrylamide gel showing eluate fractions after yeast extract binding procedure. Black arrows show the GST-fusion proteins. White arrows show proteins exised from identical coomassie stained gel for MALDI-TOF MS to identify binding proteins.

all data could be attributed to GST, so it appears that the promising bands were GST-fusion protein degradation products.

A different approach to this experiment was considered: cleaving the GST tag away from the Sla1p-118-511 domain prior to the elution step using thrombin or Factor Xa. However, the Sla1p-118-511 domain contained thrombin and Factor Xa sites. The plasmids expressing the GST-fusion proteins were also transformed into a protease deficient *E.coli* strain to reduce protein degradation but this made no significant difference to degradation levels. The Sla1p-118-511 domain was also cloned into a yeast expression vector pEG-KT to express the GST-fusion proteins in yeast, but after significant time and effort this strategy also failed to produce useful results.

Due to difficulties in determining binding partners for the Sla1p-118-511 domain using GST pulldown an alternative method was chosen. The two-hybrid assay is a commonly used tool to determine binding partners for proteins. Chapter four discusses in detail a two-hybrid assay strategy using the Sla1p-118-511 domain of Sla1p and its results.

3.13 Summary

This chapter examined the effect of deletion of the Sla1p-118-511 domain in cells that expressed the integrated form of the mutant Sla1p (*sla1-Δ118-511*). A variety of techniques were used to identify and characterise various phenotypes found in *sla1-Δ118-511* cells. Initial work carried out on the *S. cerevisiae* protein Sla1p using plasmid mutants showed that it was a functionally modular component of the cortical

actin cytoskeleton (Ayscough *et al* 1999). A region of Sla1p, here termed the Sla1p-118-511 region, was found to be essential for the organisation of the cortical actin patches and for growth at high temperatures. The integrated *sla1-Δ118-511* yeast strain also displayed reduced growth at 37 °C (section 3.4) but had greater viability than Δ*sla1* yeast which suggests that the Sla1-Δ118-511 protein contained some function that improved viability under those conditions. The partial functionality of the Sla1-Δ118-511 protein is clearly demonstrated as cells did not require *ABP1* for viability (section 3.6).

Cells which expressed sla1p-Δ118-511 displayed an aberrant cortical actin phenotype (section 3.5) like Δ*sla1* cells. Actin patches were fewer and larger than those found in wild-type cells. Cells expressing sla1p-Δ118-511 from a plasmid have been found to be deficient in actin-assembly activity (Ayscough *et al* 1999) which gives further support for the conclusion that Sla1p, in particular the Sla1p-118-511 domain plays a direct role in regulation of the actin cytoskeleton. Studies using the actin monomer-sequestering drug LAT-A (section 3.9) have also shown actin dynamics to be altered in yeast lacking the Sla1p-118-511 domain. *Sla1-Δ118-511* yeast are resistant to LAT-A in halo assays, and cells examined after incubation in LAT-A for 15 minutes still retain cortical actin patches whereas none are present in the wild-type strain. Sla1p is proposed to act either as a destabiliser of the cortical actin cytoskeleton, or by increasing the turnover of actin filaments, with the Sla1p-118-511 domain particularly important.

As defects in the actin cytoskeleton often lead to aberrant budding patterns, the ability of the diploid mutant to bud in a bipolar manner, like wild-type yeast was assessed (section 3.7). Indeed the *sla1-Δ118-511* mutant budded randomly. Cortical cues that tag the incipient budding site may be mislocalised in the mutant cells.

LAT-A studies have already determined that the actin cytoskeleton is not required to localise Sla1p to the cortex (Ayscough *et al* 1997 and figure 5.7) so perhaps it is not surprising that cells displaying abberant actin patches are still able to localise the mutant sla1 protein to the cell cortex. However, sla1p-Δ118-511 does not co-localise with actin-containing patches. The inability of cortical actin patches and sla1p-Δ118-511 to physically associate (figure 3.12) could be responsible for the aberrant actin phenotype associated with *sla1-Δ118-511* yeast (section 3.8).

Early investigation of *sla1-Δ118-511* yeast showed they were unable to grow on glycerol which indicated respiratory problems and so defective mitochondrial function (section 3.11). The role of the Sla1p-118-511 domain in mitochondrial function is unclear, or whether the effect is direct or indirect. The aberrant actin phenotype in cells deleted of this domain may be an important factor.

The endocytic function of the mutant yeast was examined using vital vacuolar dyes. *sla1-Δ118-511* mutant yeast display a reduced endocytic uptake of Lucifer yellow into the vacuole (section 3.10.1). This is a common phenotype of actin cytoskeleton mutants. The morphology of the majority of the vacuoles in the mutant yeast also appears different to wild-type vacuoles, they are more fragmented and this is particularly apparent in the Δ*sla1* yeast (figure 3.14). Alternatively, the vacuolar

membranes may be inhibited from fusing (induced by Lucifer Yellow) which would suggest that Sla1p is important for mediating these membrane events. FM4-64 uptake in the mutant yeast was at a slighter reduced rate compared to wild-type yeast as incubation for short periods discriminated punctate spots, presumably of endocytic vesicles trafficking to the vacuole. Using both dyes showed that it is the initial uptake of dye into the cells that was defective as cells were able to accumulate dye into the vacuole. *SLA2* mutants have defective uptake of FM4-64, where the dye does not accumulate at all in the vacuole (Wesp *et al* 1997).

The final aim of trying to find binding partners to the Sla1p-118-511 domain, using a GST-pulldown technique, was unsuccessful due to the high level of degradation of the GST-tagged Sla1p-118-511 domain. Chapter 4 describes a two-hybrid strategy.

Chapter 4

Yeast Two-Hybrid Screen Using the Sla1p-118-511 Domain as Bait

4.1 Introduction

Cortical actin patches may be thought of as a network of interacting proteins. A full understanding of such protein-protein interactions will require knowledge, not only of the proteins that make up each network, but also of the physical interactions those individual proteins make with one another.

Two-hybrid systems have been used to probe the function of many new proteins (Chien *et al* 1991, Fields and Song, 1989). It is a powerful technique for identifying proteins involved in specific biological processes and allows for the rapid isolation of genes that code for proteins that interact with a specific protein of interest. Recently genome-wide two-hybrid analyses have been carried out and Ito and colleagues (2000 and 2001) and Uetz and colleagues (2001) published comprehensive analyses of *Saccharomyces cerevisiae* protein-protein interactions.

As discussed earlier in chapter 3, the Sla1p-118-511 domain plays an important role in cortical actin organisation and deletion of this domain leads to several mutant phenotypes indicating that this domain physically interacts with components of the cortical cytoskeleton to carry out its function. This chapter describes a yeast two-hybrid screen, using the Sla1p-118-511 as bait to identify interacting proteins.

4.2 Using the yeast two-hybrid system to identify binding partners for Sla1-118-511 domain

The yeast two-hybrid screen used in this project uses bait and activation plasmids, and yeast strains designed and constructed by Philip James (James *et al* 1996). The protein of interest, or 'bait' is encoded as a gene fusion to a DNA binding domain from the *GAL4* protein. A library of *S.cerevisiae* proteins, or 'prey' to be screened are encoded as gene fusions (from 500bp to 3kb) to a *GAL4* transcription activation domain (figure 4.1). Interaction between the 'bait' and 'prey' peptides consequently brings the *GAL4* DNA binding domain and *GAL4* transcription activation domains together. This interaction enables the complex to bind to inducible promoter sequences found in the genome of the two-hybrid strain pJ69-2A, driving transcription of reporter genes *HIS3* and *ADE2*. If the 'bait' and 'prey' peptides do not interact then the reporter genes are not induced and consequently cannot grow on selection plates that lack histidine and adenine.

4.2.1 Construction of bait plasmid *pGBDU-Sla1-118-511* and checking for self-activation

The region of Sla1p to be tested in the two-hybrid assay was subcloned into the *pGBDU-C1* bait vector (pKA168) as described in section 2.6.2. The Sla1p-118 – 511 region is 393 amino acids in size and encompasses the last 10 amino acids of the second SH3 domain, the entire Gap1 region and third SH3 domain, and a short section of the Gap2 domain, including the first 20 amino acids of the homology

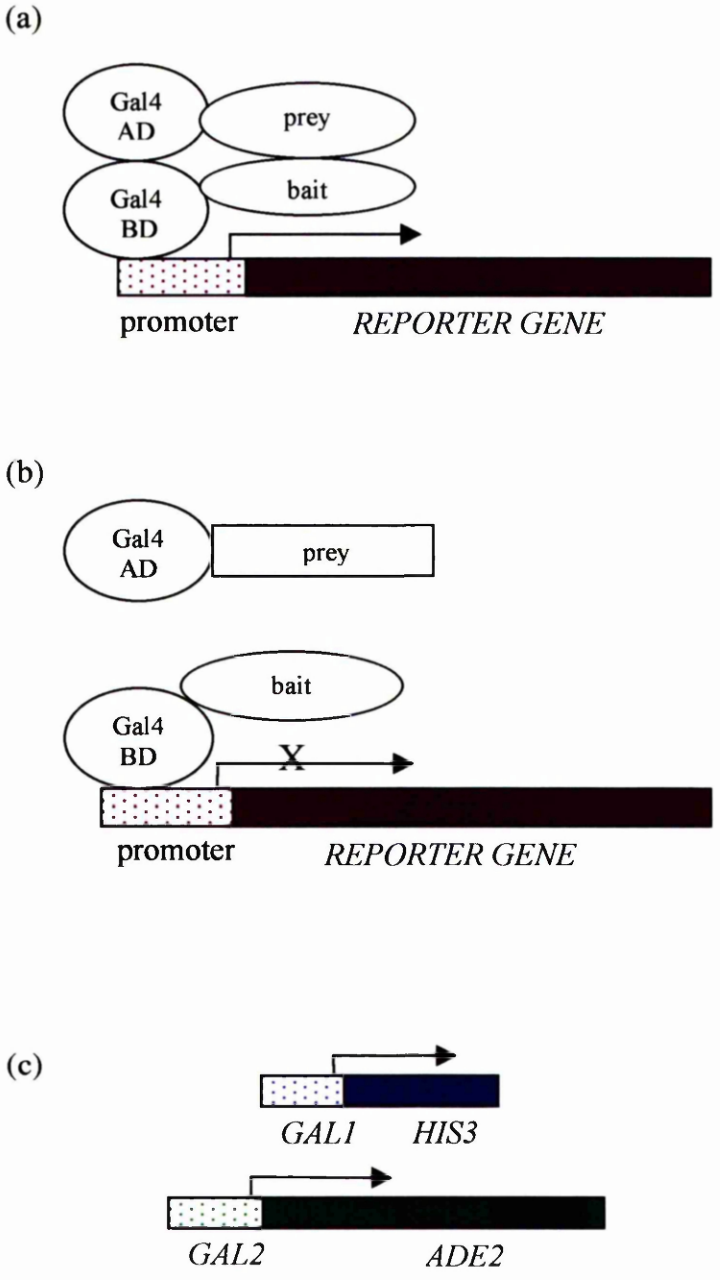

Figure 4.1 Schematic representation of two-hybrid system. Possible interactions between bait and library prey peptides showing; (a) induction of reporter genes as a result of bait and prey interaction, and (b) non-induction of reporter genes due to failure of bait and prey peptides to interact. (c) Reporter gene loci showing transcription of reporter genes *HIS3* and *ADE2* from *GAL* promoters.

domain 1 (HD1) (figure 4.2). The bait plasmid *pGBDU-Sla1-118-511* was named pKA237.

Sometimes two-hybrid bait constructs are able to activate transcription of reporter genes in the absence of a real interaction with another protein. In this case yeast are able to grow on selection plates designed to test transcription activation and so produces a false positive result. It was therefore necessary to check the bait plasmid for self-activation before a library screen could be carried out.

Growth media lacking uracil and leucine (drop-out ura leu) selects yeast carrying the bait plasmid *(URA)* and library plasmid *(LEU)*. Activation of reporter genes is tested by growth on media which also lacks adenine and histidine (drop-out his ura leu ade or activation media). To ensure that the bait plasmid (pKA237) did not self-activate the reporter genes, it was co-transformed into the two hybrid yeast strain pJ69-2A (KAY 438) with empty activation plasmid (pKA162) to generate yeast strain KAY 505. KAY 505 grew well on drop-out ura leu media but failed to grow on activation media (figure 4.2). Control strains, pJ69-2A carrying the bait by itself (KAY 500), and a negative control carrying empty bait and activation plasmids (KAY 504), were also struck onto drop-out ura leu and activation plates (figure 4.2). The control yeast strains did not grow on activation plates. The lack of growth of KAY 505 on activation media confirmed that the bait plasmid does not self-activate transcription and a two-hybrid screen using pKA237 could be carried out.

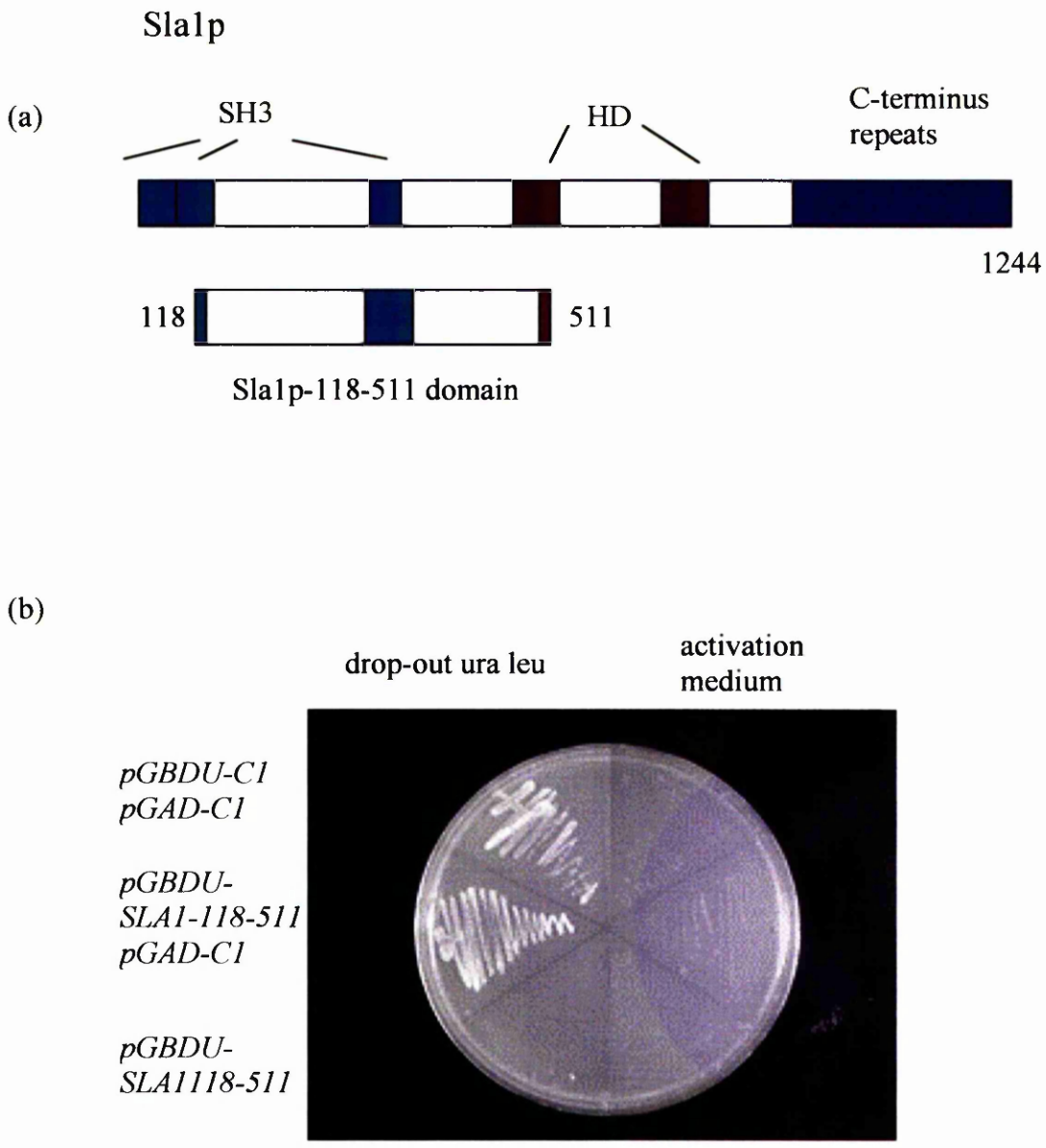

Figure 4.2. Yeast two-hybrid screen using the Sla1p-118-511 domain. (a) The region of Sla1p cloned into bait plasmid *pGBDU-C1*. (b) Self-activation of bait plasmid *pGBDU-Sla1-118-511*. Two-hybrid yeast strains KAY 504 (*pGBDU-C1 pGAD-C1*), KAY 505 (*pGBDU- Sla1-118-511 pGAD-C1*) and KAY 500 (*pGBDU- Sla1-118-511*) were struck onto drop-out ura leu and activation medium and incubated for 2 days at 29 °C.

4.2.2 Yeast Two-Hybrid Screen using the Sla1p-118-511 domain as bait

The two-hybrid library screen used a genomic library from *S.cerevisiae*. A flow diagram (figure 4.3) following the progress of the two-hybrid screen, shows stages at which potential binding partners were eliminated or kept for further analyses.

$2x10^9$ KAY 500 cells, grown up in drop-out ura liquid, were transformed using a high efficiency yeast transformation protocol (section 2.6.5) with 20 μg library DNA from each reading frame (section 2.6.1).

In total, 202 colonies which grew within 7 days were picked from activation plates (section 2.6.6.) and struck out initially onto drop-out ura leu and then restruck onto activation plates. Following restreaking onto activation media, 24 strains did not grow and were eliminated from the screen. Glycerol stocks were made of the remaining 178 strains (section 2.5.11).

The 178 yeast strains of interest went through a further selection process to eliminate false positives (section 2.6.7). The advantage of using a *URA3* marked bait plasmid is that plasmid loss assays can be carried out quickly and simply by plating out candidate clones on SC minus adenine media containing 5-FOA. 5-FOA is toxic to cells which carry *URA3*. Therefore in order to grow, cells which can only grow on adenine deficient media through the 2-hybrid interacton between bait (ie *URA3*) plasmid and library activation plasmid will consequently die in the presence of 5-FOA. Clones that are able to grow on drop out adenine 5-FOA media are false positives and can be discarded.

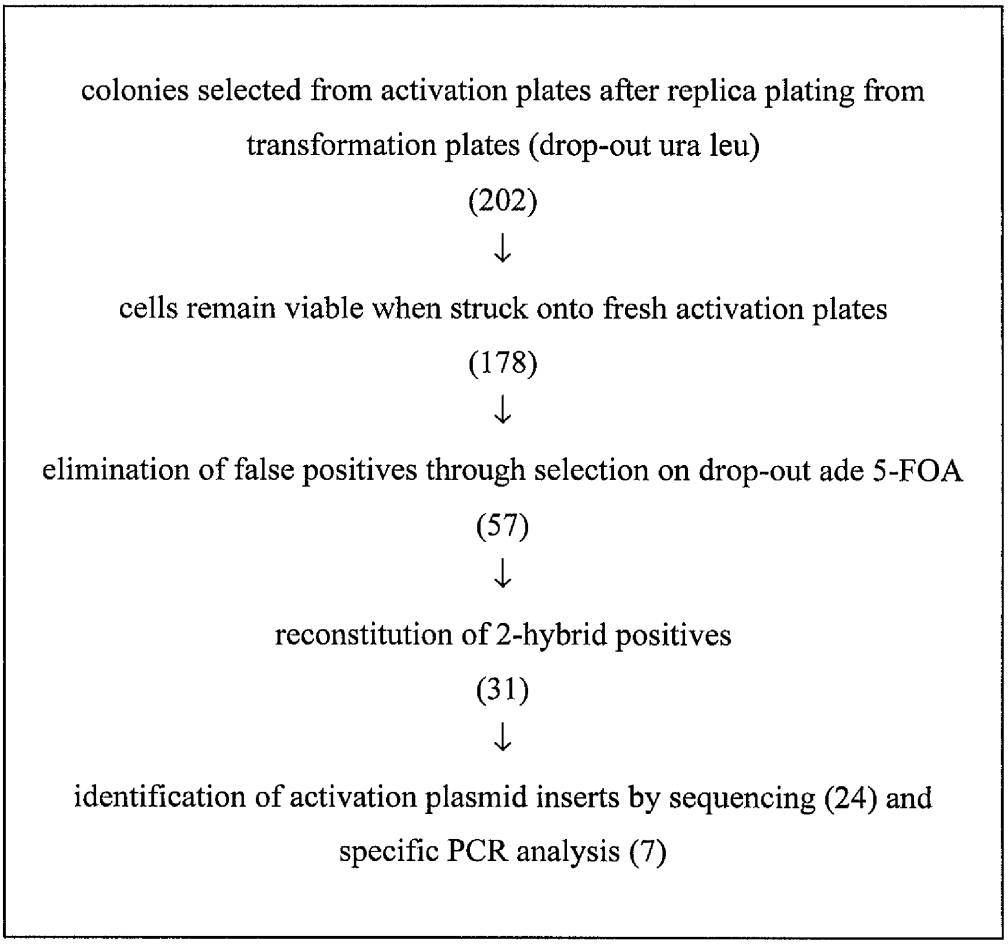

Figure 4.3 Overview of two-hybrid system using bait plasmid *pGBDU-Sla1-118-511*. Progress of two-hybrid screen showing stages at which library plasmids were eliminated or retained for further analyses.

A total of 121 two-hybrid strains could grow on drop-out adenine 5-FOA plates so were eliminated as false positives. The library plasmids carried by the remaining 57 yeast strains were extracted (section 2.6.8.-2.6.10) and then transformed into pJ69-2A with the bait plasmid to ensure that activation of reporter genes would still occur (2.6.11). Following growth on drop-out ura leu, yeast were struck onto activation plates. Consequently, 26 of the 57 yeast strains could not grow on activation plates indicating that 26 library plasmids did not activate the reporter genes after reconstitution with the bait plasmid. This failure to grow on activation plates suggests that the plasmid used in the subsequent transformation was not responsible for activation of the reporter genes in the original positive strain.

4.2.3 Analysis and identification of activating two-hybrid library inserts

The inserts in the 31 extracted library plasmids were initially analysed by double restriction enzyme digest (section 2.3.5) with *Eco*R1 and *Bgl*II and also by PCR (section 2.3.8) across the insert site using flanking primers (o153 and o154) (figure 4.4). *Eco*R1 and *Bgl*II each cut the library plasmid once at the cloning site (*Eco*R1 at the 5' end and *Bgl*II at the 3'end) and digests electrophoresed in an agarose gel (section 2.3.3) showed a characteristic vector backbone identical to empty pGAD-C1 (6665bp) run alongside as a control. This gave a good indication that only the library plasmid had been extracted from the two-hybrid yeast and that the plasmids appeared as expected.

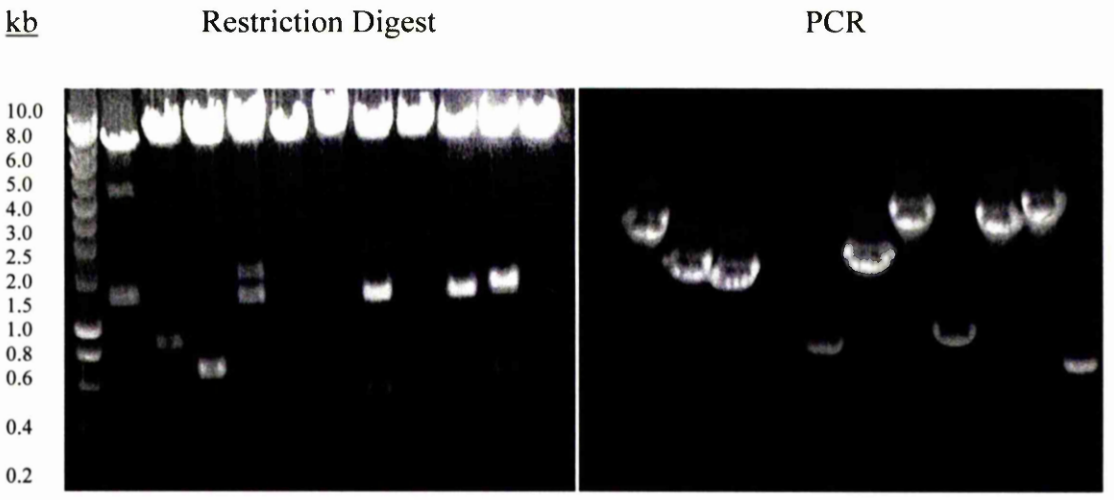

Figure 4.4. Analysis of activating two-hybrid library plasmids by restriction digest and PCR. (a) Examples of library plasmids after double restriction digest with *Bgl*II and *Eco*R1 run out on 0.8 % agarose. (b) The insert DNA in the library plasmids was amplified by PCR using flanking primers (o153 and o154) and run out on 0.8 % agarose. The last lane of both gels shows reactions containing empty library plasmid pGAD-C1 (pKA162) as a negative control.

PCR of the library inserts demonstrated both the occurance and size of each insert (none of the library plasmids contained no insert). Inserts were in the size range of approximately 500 bp to 3 kb which matches that published (James *et al* 1996). Empty activation plasmid on the otherhand gave a PCR product of around 300 bp as predicted.

Initial sequencing using oKA153 and oKA154 was carried out on 24 library plasmids (section 2.6.12). The DNA sequence determined from each plasmid was compared to *S. cerevisiae* Genbank DNA sequences using the BLAST alignment program found at the Saccharomyces Genome Database Website (http://genome-www.stanford.edu/Saccharomyces/). After this identifed repeated *YSC84* isolates, oligonucleotides were designed specifically to facilitate identification of other *YSC84* inserts. The identity of genes carried on 7 library plasmids was determined by *YSC84* specific PCR using oligos o192 and o196 against pGAD library plasmid oligos o153 and o154 which flank the insert sites. Table 4.1 summarises the identification results.

The sequences which fell under the category of non-coding sequences of the genome were eliminated from the screen. Likewise *RAD52* (*YML032C*), a gene required for X-ray damage repair and various types of intra- and interchromosomal mitotic recombination including HO switching & plasmid exchange was not investigated further as it was unclear how this gene could be a binding partner of Sla1p. Three interacting library plasmids carried *SED5* (*YLR026C*), which encodes a t-SNARE (soluble NSF attachment protein receptor) which functions in traffic

Gene fragment encoded on library plasmid	Frequency
YSC84	17
SLA2	7
SED5	3
RAD52	1
Non-coding DNA	3

Table 4.1 Two-hybrid screen results. The table identifies the DNA (and its frequency) encoded on the library plasmids isolated in the two-hybrid screen using the Sla1p-118-511 domain as bait.

between the ER and the cis-Golgi transport (Hardwick and Pelham 1992). It is possible that *SED5* may be a binding partner for Sla1p as membrane trafficking defects have been associated with defects in the actin cytoskeleton (Mulholland *et al* 1997). If this is the case then perhaps reduced uptake of endocytic marker dyes such as Lucifer Yellow and FM4-64 (section 3.10) by Sla1 mutants is due to disruption of a pathway linked by Sla1p and Sed5p.

However, two other genes, *SLA2* (*YNL243W*) and *YSC84* identified in the two-hybrid screen, (and in greater numbers) were considered to be of greater interest. *SLA2* and *YSC84* isolates were studied further (sections 4.3 and 4.4 respectively). Chapter 5 is a more in-depth characterisation of Ysc84p.

4.3 Sla2p

Sla2p is a cortical patch protein which was isolated in the same synthetic-lethal screen as Sla1p and is discussed in more detail in section 1.15.3. The two-hybrid data described here suggests that the two proteins interact physically as well as there being a genetic interaction and it is the Sla1p-118-511 domain that mediates an interaction between Sla1p and Sla2p (table 4.2 and figure 4.5).

4.3.1 Two-hybrid interaction of bait plasmid and *SLA2* containing library plasmids

Figure 4.6a shows all 7 *SLA2* two-hybrid isolates growing on drop–out ura leu and activation plates after 2 days at 29 °C. So, the 'bait' plasmid and *SLA2* encoding

Region of Sla2p encoded on library plasmid (amino acid)	Number of isolates	Plasmid Collection Name
206 - 769	3	pKA245
310 - 769	4	pKA244

Table 4.2 *SLA2* ORF sequences isolated in two-hybrid screen.

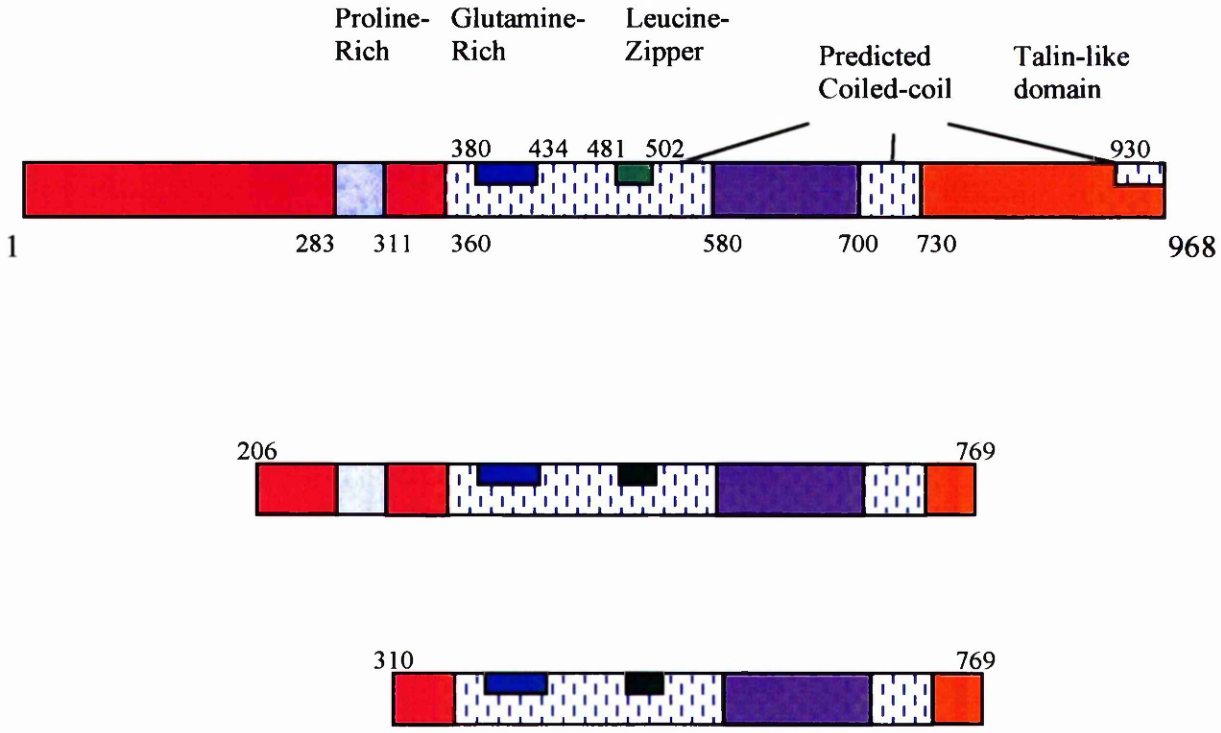

Figure 4.5. Domain arrangement of Sla2p and the two Sla1p-118-511 interacting regions of Sla2p isolated in the two-hybrid screen. The two *SLA2* isolates are encoded on pKA244 and pKA245. Full-length Sla2p figure adapted from Yang *et al* 1999.

pGBDU-sla1-118-511 bait
and *pGAD-SLA2* library plasmids

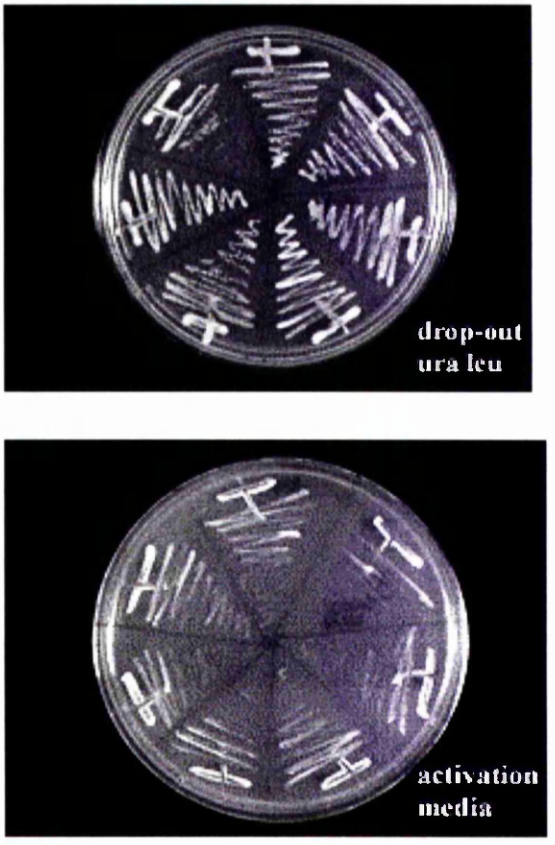

Figure 4.6. Sla2p interacts with Sla1p in the yeast two-hybrid screen. (a) Two-hybrid yeast strains KAY 567 (1-4), KAY 568 (1-2) and KAY 569 were struck onto drop-out ura leu media to select for bait and library plasmids and onto activation plates to select for activation of reporter genes *HIS3* and *ADE2*. Growth of pJ69-2A carrying *pGBDU-sla1-118-511* bait and *pGAD-SLA2* library plasmids demonstrates an interaction between the Sla1-118-511 domain and Sla2p.

'prey' plasmids encode proteins which physically interact to induce transcription of *HIS3* and *ADE2* reporter genes.

4.3.2 Sla1p-118-511 interacts with the central region of Sla2p

Table 4.2 shows the regions of Sla2p isolated in the screen. Sequencing from the 5' and 3' ends of the library plasmids containing *SLA2* identified two groups of *SLA2* insert. All seven *SLA2* sequences carried on the library plasmids ended at base pair 2307. However, there were two different start sites for the *SLA2* sequences, at 613 nt and 930 nt.

The peptides encoded on the *SLA2* library plasmids are illustrated in figure 4.6b. The minimum region of Sla2p found to interact with Sla1p-118-511 domain is from amino acid 310 to amino acid 769. A longer central region of Sla2p from amino acid 206 to amino acid 769 was also identified.

4.3.3. Sla2p two-hybrid interaction with Sla1p is not dependent on the third SH3 domain of Sla1p.

In order to determine whether the third SH3 domain of Sla1p was required for the interaction between Sla1p and Sla2p, a bait plasmid was constructed which consisted of the Sla1p-118-511(-SH3) domain fused to the DNA binding domain of *pGBDU-C1* (section 2.6.3). After checking that this plasmid did not self-activate (figure 4.7a) the bait plasmid (pKA238) was co-transformed into pJ69-2A with library plasmids which carried *SLA2* inserts. Figure 4.7b shows the co-transformed yeast growing on both drop-out ura leu and activation medium. As the

(a)

pGBDU-C1 *pGBDU-SLA1-118-511(-SH3)*
pGAD-C1 *pGAD-C1*

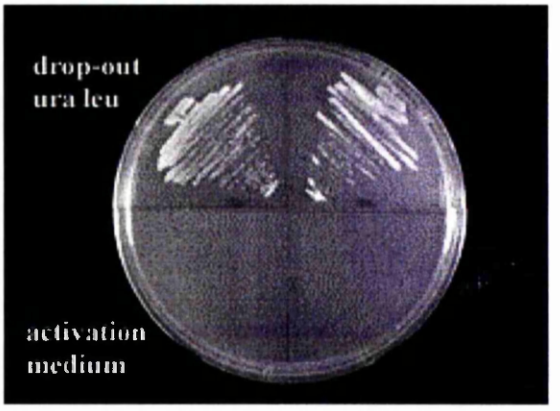

(b)

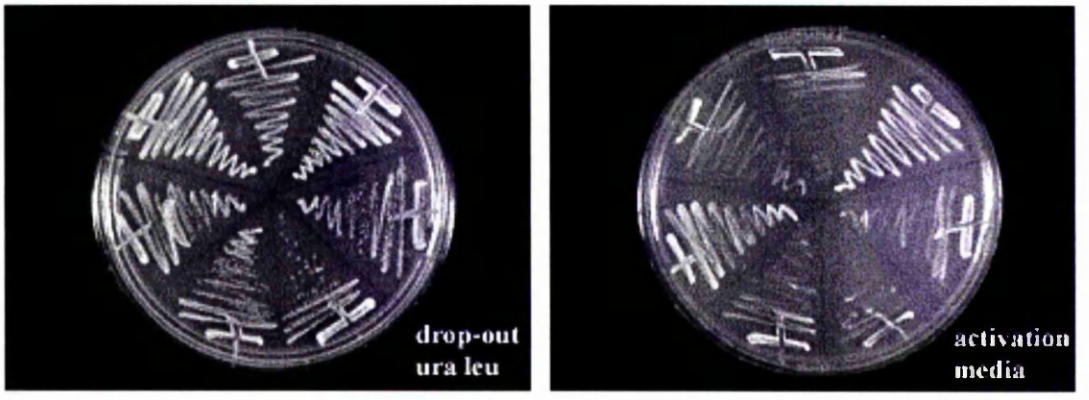

Figure 4.7. Two-hybrid interaction between Sla1p and Sla2p. (a) Testing bait plasmid p*GBDU-SLA1-118-511* (pKA238) for self-activation. Two-hybrid yeast strains KAY 504 (*pGBDU-C1 pGAD-C1*) and KAY 503 (*pGBDU- SLA1-118-511(-SH3) pGAD-C1*) were struck onto drop-out ura leu and activation medium and incubated for 2 days at 29 °C. (b) Two-hybrid yeast strains KAY 573 (1-4), KAY 574 (1-2) and KAY 575 were grown on media as in (a). All yeast strains carrying the *pGBDU-sla1-118-511(-SH3)* bait and *pGAD-SLA2* library plasmids were able to grow on activation media indicating that the third SH3 domain of Sla1p is not required for the interaction between Sla1p and Sla2p.

yeast were able to grow on activation medium it shows that the interaction between Sla2p and Sla1p does not require the third SH3 domain of Sla1p.

4.4 *YSC84*/YHR016C

YSC84 was the most abundant library insert found in the two-hybrid screen with 17 isolates (table 4.3). *YSC84* is an intron-containing gene that encodes a protein of unknown function with a predicted SH3 domain at the C-terminus and a region of homology at the N-terminus shared with Ysc84p homologues found in other organisms (figure 4.8 and figure 5.1). A two-hybrid screen carried out by Uetz *et al* (Nature 2000) had previously identified Ysc84p (full length ORF inserted into a Gal4 DNA-binding domain vector) as interacting with full length Sla1p. A two-hybrid screen using full length *LAS17* as bait pulled out *YSC84* and its *S.cerevisiae* homologue *YFR024c-a (*Madania *et al* 1999). Sla1p and Las17p have been shown to co-immunoprecipitate (Li 1997) as well as both proteins displaying two-hybrid interactions with Ysc84p. As relatively little is known about Ysc84p, this protein was studied further and this characterisation comprises chapter 5.

4.4.1. Two-hybrid interaction of bait plasmid and *YSC84* containing library plasmids

Interaction of the bait plasmid and *YSC84* containing library inserts was demonstrated by growth of two-hybrid strains on activation plates (figure 4.9).

yeast were able to grow on activation medium it shows that the interaction between Sla2p and Sla1p does not require the third SH3 domain of Sla1p.

4.4 *YSC84*/YHR016C

YSC84 was the most abundant library insert found in the two-hybrid screen with 17 isolates (table 4.3). *YSC84* is an intron-containing gene that encodes a protein of unknown function with a predicted SH3 domain at the C-terminus and a region of homology at the N-terminus shared with Ysc84p homologues found in other organisms (figure 4.8 and figure 5.1). A two-hybrid screen carried out by Uetz *et al* (Nature 2000) had previously identified Ysc84p (full length ORF inserted into a Gal4 DNA-binding domain vector) as interacting with full length Sla1p. A two-hybrid screen using full length *LAS17* as bait pulled out *YSC84* and its *S.cerevisiae* homologue *YFR024c-a (*Madania *et al* 1999). Sla1p and Las17p have been shown to co-immunoprecipitate (Li 1997) as well as both proteins displaying two-hybrid interactions with Ysc84p. As relatively little is known about Ysc84p, this protein was studied further and this characterisation comprises in chapter 5.

4.4.1. Two-hybrid interaction of bait plasmid and *YSC84* containing library plasmids

Interaction of the bait plasmid and *YSC84* containing library inserts was demonstrated by growth of two-hybrid strains on activation plates (figure 4.9).

Region of Ysc84p encoded on library plasmid (amino acid)	Number of Isolates	Plasmid Collection Name
133 - 468	2	pKA243
181 - 468	3	pKA242
229 - 468	5	pKA241

Table 4.3 *YSC84* ORF sequences isolated in two-hybrid screen. A further seven isolates were determined to be *YSC84* by *YSC84*-specific PCR.

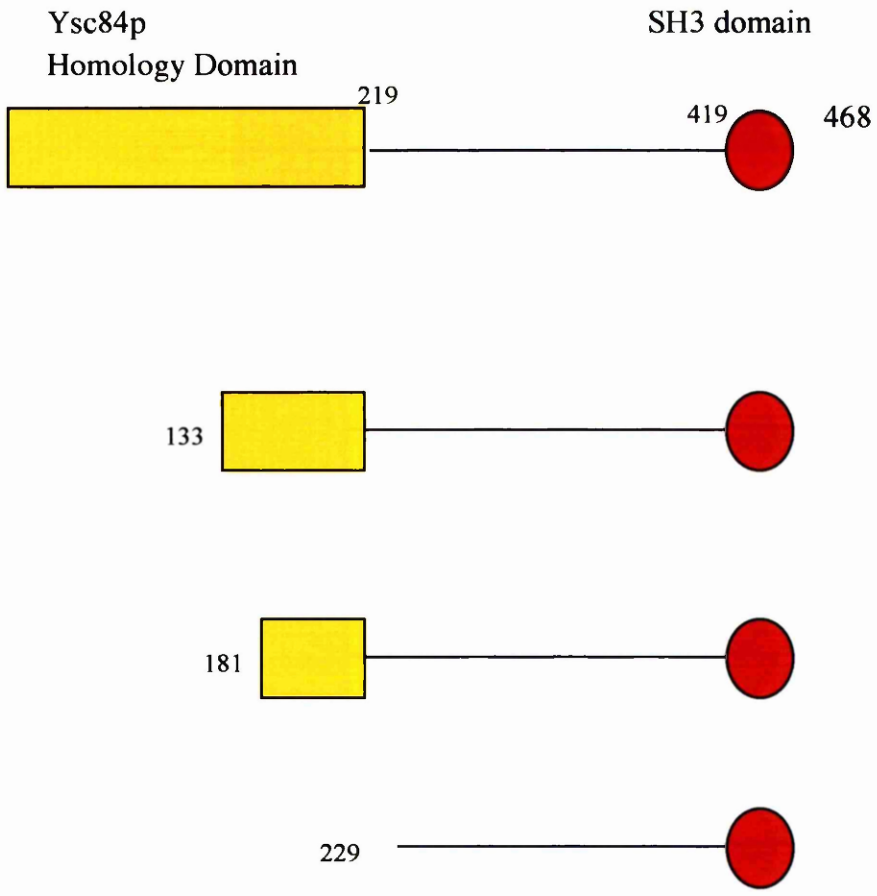

Figure 4.8. The C-terminal region of Ysc84p interacts with Sla1p in the two-hybrid screen. Domain arrangement of Ysc84p (top) and the three different Sla1p-118-511 interacting regions of Ysc84p isolated in the two-hybrid screen.

Figure 4.9. Two-hybrid interaction of *SLA1–118-511* bait and *YSC84* activation plasmids. (a) Two-hybrid yeast strain pJ69-2A was co-transformed with bait plasmid p*GBDU-SLA1-118-511* and *YSC84* activation domain plasmids (pKA241 – pKA243) expressing Ysc84p from each of the three start sites isolated in the two-hybrid screen (KAY 570 - KAY 572). Yeast were grown for 2 days at 29 ˚C on drop-out ura leu and activation media.

The minimum region of Ysc84p required for interaction with the Sla1p-118-511 domain is the C-terminal half of Ysc84p from amino acid 229. Sequencing from the 5' end of 10 of the library plasmids containing *YSC84* identified this region. The 3' end of the 10 plasmids was estimated from the approximate insert size as determined by restriction digestion (section 2.3.5) and in all cases was found to lie outwith the coding region. Two of the library plasmids were also sequenced from the 3' end to confirm that sequences did end in the non-coding region. Table 4.3 shows the *YSC84* ORF sequences carried on the library plasmids which were identified by sequencing and figure 4.8 depicts these sequences as regions of Ysc84p isolated in the screen.

4.5. The two-hybrid interaction between Sla1p and Ysc84p is dependent on the Sla1p-118-511(-SH3) domain and the SH3 domain of Ysc84p.

SH3 (Src-Homology-3) domains are small protein modules containing approximately 60 amino acids (Pawson and Schlessinger 1993, Mayer 2001). They have been identified in organisms ranging from yeast to humans in more than 350 different proteins. Kinases, lipases, GTPases, adapter proteins, and structural proteins which act in diverse processes including signal transduction, cell cycle regulation, and actin organisation contain SH3 domains. SH3 domains mediate specific protein-protein interactions by binding to PXXP-containing sequence motifs in target proteins (Ren *et al* 1993). Individual domains display distinct

binding specificites (Larson and Davidson 2001). They may mediate assembly of specific protein complexes via binding to proline-rich peptides in particular linking signals transmitted from the cell surface by protein tyrosine kinases to downstream effector proteins (Campbell and Morton 1994).

4.5.1. Ysc84p two-hybrid interaction with Sla1p is not dependent on the third SH3 domain of Sla1p

To determine if the interaction between the Sla1p and Ysc84p was dependent on the third SH3 domain of Sla1p the yeast two-hybrid yeast strain was co-transformed with *pGBDU-Sla1-118-511(-SH3)* bait plasmid and library plasmids pKA241, pKA242 and pKA243 to represent each of the three different start sites (generating yeast strains KAY 578, KAY 577 and KAY 576 respectively). In all instances, the co-transformed yeast were able to activate transcription of reporter genes as they grew on activation plates (figure 4.10). This shows that the third SH3 domain of Sla1p is not required for the interaction between Sla1p and Ysc84p. The region necessary for the interaction with Ysc84p must therefore lie in the Sla1p-118-511(-SH3) domain.

4.5.2. Two-hybrid interaction between Sla1p and Ysc84p is dependent on the SH3 domain of Ysc84p.

As SH3 domains are implicated in mediating protein-protein interactions, the SH3 domain of Ysc84p encoded on a library plasmid was disrupted to assess its importance in the interaction between Ysc84p and Sla1p. Site-directed

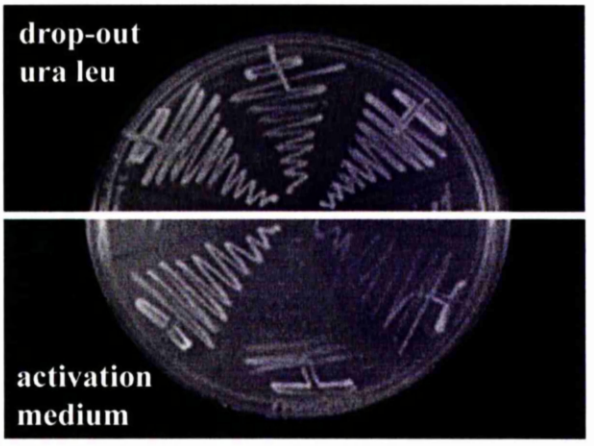

Figure 4.10. Two-hybrid interaction between Sla1p and Ysc84p is not dependent on the SH3 domain of Sla1p. Two-hybrid yeast strain pJ69-2A was co-transformed with bait plasmid lacking the 3rd SH3 domain of Sla1p (pKA238) and an activation domain plasmid expressing Ysc84p from each of the three start sites isolated in the two-hybrid screen (pKA241, pKA242 and pKA243). Yeast (KAY576, KAY577 and KAY578) were grown for 2 days at 29 °C on drop-out ura leu and activation medium.

mutagenesis was performed (section 2.3.9) on two-hybrid library plasmid pKA243 using oligos o228 and o229 to convert the tyrosine at amino acid 397 to the stop codon TAA to generate pKA251. pKA251 was then sequenced using oligo oKA196. This would result in the expression of Ysc84p from amino acid 132 to 397 when transformed into the yeast two-hybrid strain. The mutagenised plasmid was co-transformed into pJ69-2A with bait plasmid pKA237 and bait plasmid pKA238. Co-transformed yeast were struck onto drop-out ura leu and grew well (figure 4.11). However, when these yeast were struck onto activation plates they did not grow, indicating that the interaction necessary to activate the *HIS3* and *ADE2* reporter genes did not occur (figure 4.11). Thus the two-hybrid interaction between Sla1p and Ysc84p requires the SH3 domain of Ysc84p.

Chapter 5 discusses experiments carried out to elucidate the role of Ysc84p in the cortical actin cytoskeleton through its physical and genetic interactions and phenotypic data.

4.6. Summary

As cells which lacked the Sla1p-118-511 domain displayed mutant phenotypes such as aberrant cortical actin patch organisation as discussed in chapter 3, this domain plays an important role in the function of Sla1p which must involve protein-protein interactions. Earlier attempts using GST-Sla1-118-511 pulldowns to isolate interacting yeast proteins (section 3.12) were unsuccessful and this led to a two-hybrid approach to be taken to find interacting proteins.

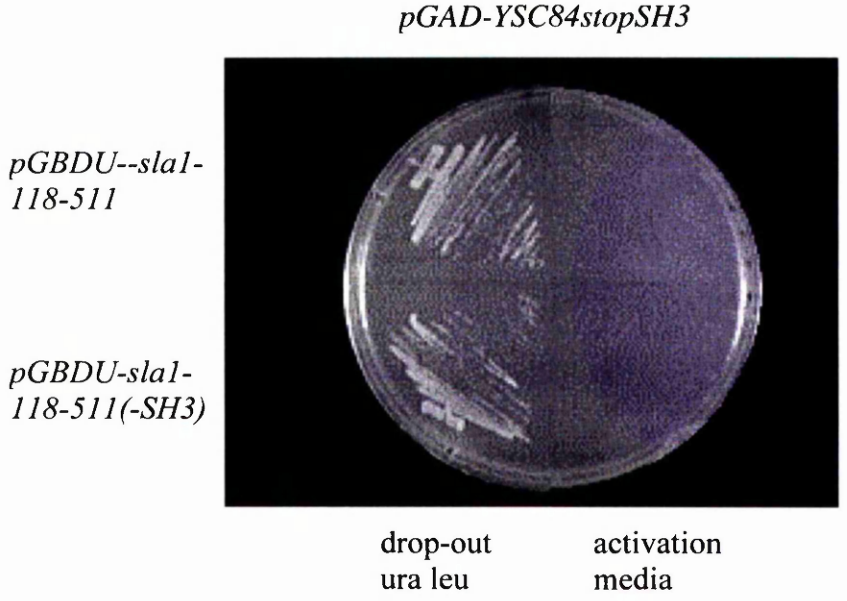

Figure 4.11. Two-hybrid interaction between Sla1p and Ysc84p is dependent on the SH3 domain of Ysc84p. Two-hybrid yeast strain pJ69-2A was co-transformed with activation domain plasmid *pGAD-YSC84stopSH3* (pKA251) and bait plasmids expressing the sla1-118-511 domain (pKA237) or sla1-118-511 (-SH3) domain (pKA238). Yeast were grown for 2 days at 29 °C on drop-out ura leu and activation medium.

A two-hybrid screen was carried out using the Sla1p-118-511 domain as bait and a *Saccharomyces cerevisiae* library of prey plasmids (James *et al* 1996). Four different genes were isolated in the screen: *SLA2*, *YSC84*, *RAD52* and *SED5*. Of these, two were considered of the greatest interest and investigated further, *SLA2* and *YSC84*.

SLA2 encodes Sla2p, a cortical patch protein which was identified in the same synthetic-lethal screen that identified Sla1p (Holtzman *et al* 1993). The minimum central region encoded on the library plasmids which interacts with Sla1p-118-511 includes a predicted coiled-coil region which appears to be involved in the formation of an Sla2p dimer (Yang *et al* 1999) and has also been found to be required for endocytosis in *S.cerevisiae* with *ABP1* or *SRV2* mutations (Wesp *et al* 1997). So, the predicted coiled-coil region of Sla2p may also be responsible for the interaction with Sla1p.

Further evidence supporting the *SLA1-SLA2* two-hybrid data, has since been revealed in the Ayscough Lab by Campbell Gourlay who has identified a direct interaction between Sla1p and Sla2p by GST-pulldown. Also, the mislocalisation of Sla2p in a strain expressing *sla1-Δ118-511* has shown that the Sla1p-118-511 domain is required for normal localisation of Sla2p (Campbell Gourlay, KRA). So, *in vitro* and *in vivo* studies demonstrate a direct interaction between Sla1p and Sla2p, and this interaction occurs between the Sla1p-118-511(-SH3) domain and the central region of Sla2p. Further work using either two-hybrid or biochemical experiments would narrow down the site of interaction.

As discussed in section 4.4, Ysc84p had already been identified as interacting with Sla1p in separate high-throughput two-hybrid screens (Uetz et al 2000, Drees *et al* 2001). This two-hybrid screen has also demonstrated the interaction and narrowed down the sites of interaction to the Sla1p-118-511(-SH3) and the C-terminal region of Ysc84p. The two-hybrid interaction appears not to require the third SH3 domain of Sla1p. There is a proline-rich motif in the Sla1p-118-511(-SH3) domain which may be responsible for the interaction with the putative SH3 domain at the Ysc84p C-terminus. Site-directed mutagenesis on the proline-rich motif to change one or more prolines to alanines should disrupt this interaction and would demonstrate if this motif is interacting with the putative Ysc84p SH3 domain.

Systematic analysis of multiprotein complexes by Gavin and collegues (2002) has shown that Sla1p exists in a multiprotein complex that includes Sla2p, Ysc84p, End3p, Vrp1p, and the Ysc84p homologue Yfr024c-ap. This provides strong support for the two-hybrid data described here. Future work should identify which of these interactions are direct and how they are organised in a spatial and temporal manner.

Chapter 5

Investigation of Ysc84p

5.1 Introduction

YSC84(YHR016C) was identified in this study in a two-hybrid screen (chapter 4) as interacting with the Sla1p-118-511 domain. *YSC84* (Chr. VIII coordinates 138446-136872) is 1575 nucleotides in length, which encodes a protein of unknown function of 468 amino acids (figure 5.1)(Rocco *et al* 1993).

Database searches have identified an *S.cerevisiae* homologue of Ysc84p called Yfr024c-a which has strong overall identity (59%) to Ysc84p over 407 amino acids (figure 5.1) with the N-terminus (amino acids 1-210) and the SH3 domain at the C-terminus showing the highest level of identity (91 % and 86 % respectively). Ysc84p has a putative SH3 domain at its C-terminus. Other Ysc84p homologues which share high identity at the N-terminal region and have a C-terminal SH3 domain have been found in *S.pombe*, mouse (D85926.1) (Aoki *et al* 2000) and human (HsSH3yl1) are shown aligned in figure 5.1.

Previously published two-hybrid data showed that full length Ysc84p interacted with full length Sla1p (Uetz *et al* 2000, Drees *et al* 2001). This study has confirmed this interaction and narrowed down the sites of interaction between Sla1p and Ysc84p to the Sla1p-118-511 domain and the C-terminal half of Ysc84p (section 4.4). During this project Madania and colleagues (1999) performed a two-hybrid screen using full length Las17p, the yeast homologue of the Wiskott-Aldrich syndrome protein WASp as bait, and pulled out, amongst others, Ysc84p and Yfr024c-a as binding proteins. Las17p has been shown to be important for actin patch assembly and actin

```
Ysc84p          -LTDFVFILNSEEAVRSFSEFGTITLGGNVSVSAGPLGRSAEAAASASTGGVSAVFAYSK 59
Yfro24c-a       -LTDFVFILNTQDAVKSFSEFGTITLGGNVSVSAGPLGRSAEAAASASAGGVAAVFAYSK 59
Ysc84p(S.p)     -LTDFVIILNSKAAVQTFARLGSITLGGNLSIAAGPLGRNAEAGGGASVGGMAPMFSYSK 59
HsSH3yl1        MVSDLVIILNYDRAVEAFAKGGNLTLGGNLTVAVGPLGRNLEG--NVALRSSAAVFTYCK 58
D85926.1        -VSDLVIILNYDRAVEAFAKGGNLTLGGNFTVAVGPLGRNLEG--NVSLRSSAAVFTYCK 57
                  ::*:*:*** . **.:*:. *.:*****.:::.*****. *.  ..:  . :.:*:*.*

Ysc84p          SKGLFAGVSVEGSAILERREANRKFYGDNCTSKMILSGRVKVPPAADPLLRILESRAFNF 119
Yfro24c-a       SKGLFAGVSVEGSAIIERREANRKFYGDNCTAKMILSGRIRPPPAVDPLFRVLESRAFNY 119
Ysc84p(S.p)     TKGLFAGVSLEGSVLVERRDANRSLYRGDITAKRLLSGQVAQPAAADPLYRVLNSKIFNL 119
HsSH3yl1        SRGLFAGVSLEGSCLIERKETNRKFYCQDIRAYDILFGDTPRPAQAEDLYEILDS--FTE 116
D85926.1        SRGLFAGISLEGSCLIERKETNRKFYCQDIRAYDILFGDVPQPAQAEDLYEILNS--FTE 115
                 ::*****:*:*** ::**:::**.:*  :  :  :* *    *. .: * .:*:*  *.

Ysc84p          TRHDHDDNASGDDFYDDGQYSDNTSHYYDDIPDSFDSTDESSTRPNTRSSRRRGMSLGSR 179
Yfro24c-a       RPSNGGRGSFDDD--EDDYYDDDD--YYNDIPSSFSSTDASSTRPNTRSTRRRAQS-GSR 174
Ysc84p(S.p)     NRGDEGDIYNDVPIYADDEPEDIWG------PSSKSTKRRDSADRSSSYSRRGDSYRSNR 173
HsSH3yl1        KYENEG----------------------------------QRINARKAAREQRKSS------ 138
D85926.1        KYETEG----------------------------------QRINLKKVAREQRK-------- 135
                      .                                     .    :   *:

Ysc84p          SRYDDDYDDDGYGRGRGYGDDFDSEDE-------DYDYGRSPNRNSSRNRGPQIDRGTKP 232
Yfro24c-a       YTFDDDDDDDDYGTGYSRNSRLAPTNSGGSGGKLDDPSGASSYYASHRRSGTAQSRARSS 234
Ysc84p(S.p)     SRAHDDDDEDDYS--FSRSKSLSRKTAG--------GSLRSSKMDNRRSKYADTPSPRRS 223
HsSH3yl1        ------------------AKELPPKPL--------------------SRPQQSSAPVQLNS 161
D85926          ------------------AKELPPKPS--------------------SRPQPAHPPVQLNA 158
                                  . :                          *   .       .

Ysc84p          RANTRWEDDLYDRDTEYSRPNHSGRDYDNTRGNRRGYGRERGYS-LGHGPTHPSNMSNVD 291
Yfro24c-a       RN--RWADDEYDDY-----------DDDYESGYRRGNGRDRTKDREVDDLSNRFSKSRIS 281
Ysc84p(S.p)     RS---YSDE-----------------DEESVYSSDVSTE---------SSSQFS-SRSS 252
HsSH3yl1        GS-------------------------------------------------QSNRNEYKLYP 174
D85926          GS-------------------------------------------------QGNRNEYKLYP 171
                                                                      . .

Ysc84p          DLSHKMSKTGLGNESTATNSATPTAVALYNFAGEQPGDLAFKKGDVITILKKSDSQNDWW 351
Yfro24c-a       SASTPQTSQGRFTAPTSPSTSSPKAVALYSKAGEESGDLPFRKGDVITILKKSDSQNDWW 341
Ysc84p(S.p)     EYSKPSRPTAPKPKPKQDSLGPNQARAMYSFAGEQPGDLSFQKGDIIDIVERSGSHDDWW 312
HsSH3yl1        GLSSYHERVGNLNQP-------IEVTALYSFEGQQPGDLNFQAGDRITVISKTDSHFDWW 227
D85926.1        ELSSYHEKTGNLNQP-------IEVTALYSFEGQQPGDLNFQAGDRIIVISKTDSNFDWW 224
                   *      .   .         . *:*.  *::.*** *: ** * ::.::.*: ***

Ysc84p          TGRTNGKEGIFPANYVRVS 370
Yfro24c-a       TGRVNGREGIFPANYVELV 360
Ysc84p(S.p)     TGRIGYREGIFPANYVKLS 331
HsSH3yl1        EGKLRGQTGIFPANYVTMN 246
D85926.1        EGKLRGQTGIFPANYVTMN 243
                  *:   : ******** :
```

Figure 5.1 CLUSTALW multiple sequence alignment of Ysc84p and homologues. Ysc84p from *S.cerevisiae* aligned with homologues using ClustalW program. Yfr024c-a is the *S.cerevisiae* homologue. Homologues from *S. pombe*, human (HsSH3yl1) and mouse (D85926.1).

polymerisation (Li 1997). So, Ysc84p is linked to the cortical actin cytoskeleton via interactions with both Las17p and Sla1p.

Prior to this study no work had directly examined the cellular localisation and function of *S.cerevisiae* Ysc84p (or of its *S.cerevisiae* homologue Yfro24c-ap). The deletion of *YSC84* has been shown to cause no apparent mutant phenotype for vegetative growth, progression into meiosis or sporulation (Rocco *et al* 1993). This chapter describes the localisation of GFP-tagged Ysc84p and Yfr024c-ap and examines phenotypes of yeast cells deleted for *YSC84.*

5.2. Localisation of GFP-tagged Ysc84p

To address whether Ysc84p interacts with the cortical actin cytoskeleton, Ysc84p cellular localisation was determined by using an integrated N-terminally tagged GFP-Ysc84p fusion protein under control of the *GAL* promoter. The DNA to be integrated was made by PCR using oligos oKA165 and oKA166 against template DNA pKA221 (*TRP1*) and then transformed into wild-type and various mutant backgrounds and selected for growth on plates lacking tryptophan (drop-out trp). To check that the GFP-tag had inserted at the correct locus, colony PCR (section 2.3.11) was carried out using oligos o139 and o167. Expression of GFP-Ysc84p was induced for 8 hours in YP-Gal medium at 29 °C.

5.2.1 Localisation in wild-type yeast

The intracellular localisation of GFP-Ysc84p in wild-type cells was studied. As shown in Figure 5.3 (top left), GFP-Ysc84p was localised to cortical patches throughout the cell during vegetative growth. Unbudded cells (G1 phase) had randomly distributed patches which were unpolarised. In cells with buds, patches were concentrated in the developing bud and at the mother-bud neck although a small number of patches were visible in the mother cell. The cellular localisation pattern of cortical Ysc84p patches, polarised to sites of active growth in vegetatively growing yeast cells was comparable to the cortical actin patches in wild-type yeast (figure 3.7).

GFP-Ysc84p patches in wild-type cells were also observed in greater detail using a DeltaVision deconvolution microscope for visualisation in three dimensions. This instrument digitally captures focal sections in the Z plane and mathematically removes out-of-focus light by examining neighbouring focal sections from each section in a process called iterative deconvolution (Agard *et al* 1989, Scalettar *et al* 1996). Figure 5.2 shows a compression of 32 x 0.2μm sections, so all patches in the cells are displayed. 3-D images were also made which clearly demonstrated that all GFP-Ysc84p patches were located at the cortex of the cells. The cortical Ysc84p patches, when observed using a DeltaVision microscope appeared to be highly motile, moving into and out of the bud.

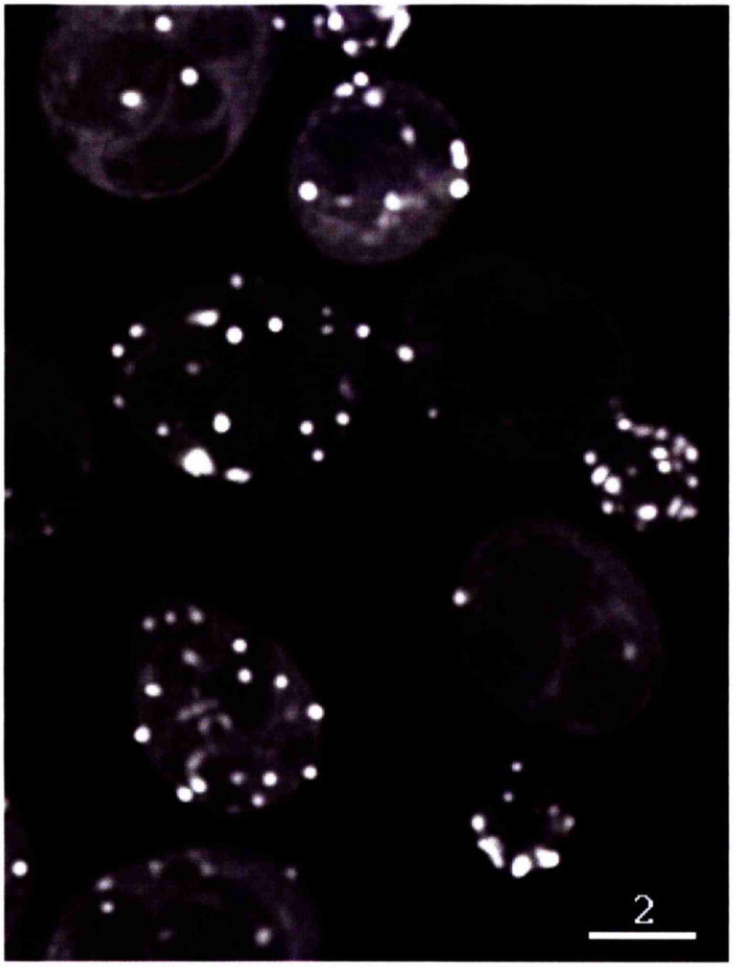

Figure 5.2. GFP-Ysc84p localises to the yeast cell cortex. GFP-Ysc84p visualised by DeltaVision microscopy. Picture shows a compression of 32 x 0.2 μm sections, so all GFP-Ysc84p patches in the cells are displayed.

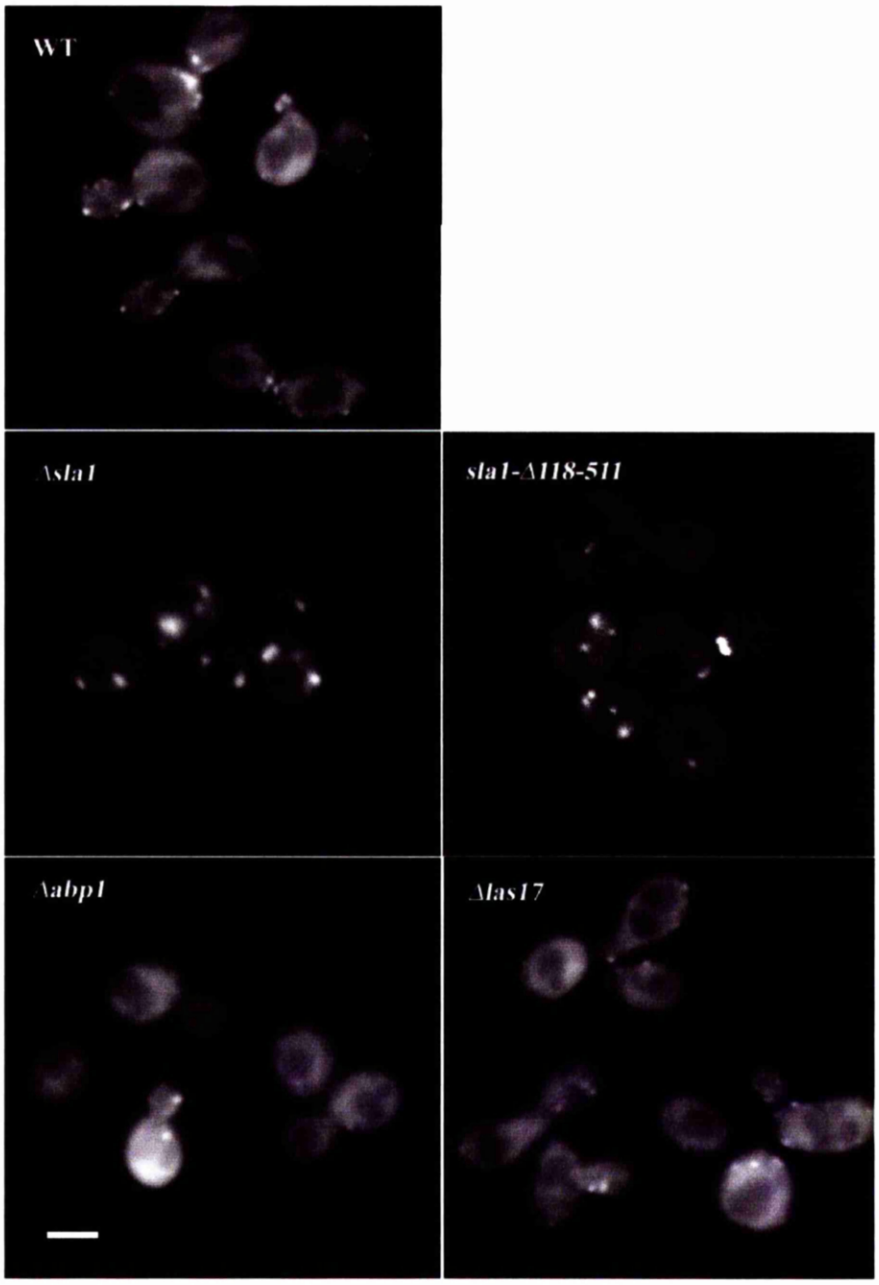

Figure 5.3 Localisation of GFP-Ysc84p in wild-type and mutant yeast strains. Yeast cells were grown overnight at 29 °C in YPA-Gal to induce expression of GFP-Ysc84p in wild-type (KAY 525), Δ*sla1* (KAY 527), *sla1-Δ118-511* (KAY 522.1), Δ*abp1* (KAY 544) and Δ*las17* cells (KAY 547). Live cells were then examined by fluoresence microscopy. Bar, 5μm.

5.2.2 Localisation in Δ*sla1* yeast

As Ysc84p was found to interact with Sla1p in the two-hybrid screen, the localisation of GFP-Ysc84p in the absence of Sla1p was examined to determine if Sla1p was responsible for the specific localisation of GFP-Ysc84p to the cortical patches.

Figure 5.3 shows GFP-Ysc84p to be localised in patches at the cortex in Δ*sla1* haploid cells but the patches appeared larger and were fewer in number in comparison to the wild-type localisation pattern. This pattern (as in wild-type cells above) is very similar to the pattern of cortical actin in this cell type (section 3.4 and figure 3.7). Visualisation of GFP-Ysc84p patches by DeltaVision microscopy confirmed that the patches appeared to be aberrant and also indicated a significant reduction in movement of the patches.

5.2.3 Localisation in *sla1-Δ118-511* yeast

The localisation of GFP-Ysc84p in cells expressing *sla1-Δ118-511* was postulated to be the same as Δ*sla1* cells. This indeed was the case as figure 5.3 shows GFP-Ysc84p to be localised in a relatively few, large patches at the cortex. Again, localisation was very similar to the pattern of cortical actin in this cell type (section 3.4 and figure 3.7).

5.2.4 Localisation in Δ*abp1* yeast

As mentioned in section 5.2.1, Deltavision microscopy revealed GFP-Ysc84p patches to be highly motile and appeared to move in a very similar fashion to Abp1p patches

(Paul Andrews, University of Dundee, personal communication). Abp1p is an actin-binding component of the cortical actin cytoskeleton (Drubin 1988). Abp1p cortical patches have been described as highly dynamic (Smith *et al* 2001) whereas Sla1p containing cortical patches are relatively immobile (Warren *et al* 2002). In order to assess if Abp1p played a role in the localisation and motility of GFP-Ysc84p patches, GFP-Ysc84p was expressed in cells deleted for *ABP1* (KAY 544). The resulting localisation pattern (figure 5.3) for GFP-Ysc84p appeared diffuse and cytoplasmic with only one or two punctate cortical patches visible in 99 % of the yeast cells. Abp1p is clearly required for the normal localisation of Ysc84p to cortical patches.

5.2.5 Localisation in Δ*las17* yeast

The localisation of GFP-Ysc84p in the absence of Las17p was of interest as Las17p is a component of the cortical actin cytoskeleton important for actin patch assembly and actin polymerisation in conjunction with the Arp2/3 complex (Li 1997, Madania 1999). Las17p has been shown by co-immunoprecipitation to interact with Sla1p (Li 1997) and to also interact with GST-Sla1p (Warren *et al* 2002). Las17p has also been identified as an interactor with Ysc84p and Yfro24c-a, the *S.cerevisiae* homologue of Ysc84p (figure 5.1) in a previously reported two-hybrid screen (Madania *et al* 1999).

The localisation of GFP-Ysc84p in Δ*las17* cells is shown in figure 5.3. GFP-Ysc84p localised to cortical patches, as in the wild-type situation, but these patches were less abundant. There was also some diffuse staining apparent in the cells that indicates some delocalisation to the cytoplasm. The Ysc84p patches also seem to be less well polarised as they do not localise to areas of active bud growth or at the bud neck in

large budded cells. Cortical actin defects and aberrant actin cables have been reported in Δ*las17* cells (Li 1997, Madania *et al* 1999). Visualisation of both GFP-Ysc84p and actin would determine if GFP-Ysc84p co-localises to the aberrant cortical actin patches in these cells.

5.3. GFP-Ysc84p co-localises with cortical actin patches

Many cytoskeletal proteins show complete or partial co-localisation with cortical actin patches. Sla1p is an example of a protein which co-localises to a subset of cortical actin patches (around 50 % co-localisation of Sla1p with cortical actin). Visualisation of GFP-Ysc84p in both wild-type and Δ*sla1* cells as shown in figure 5.2 and 5.3) indicates that Ysc84p may localise to cortical actin patches as GFP-Ysc84p patches were found to localise to the cell cortex and appeared very much like the cortical actin patches found in both cell types. Cells were processed as section 2.8.9 to determine if co-localisation of cortical actin and GFP-Ysc84p did occur.

Figure 5.4 shows pictures of GFP-Ysc84p localisation and cortical actin localisation in wild-type and Δ*sla1* cells respectively (left and middle columns). When pictures of GFP-Ysc84p and cortical patch staining were merged (right column) using IP Lab software, a clear co-localisation was apparent, shown by the presence of yellow patches. There was a complete co-localisation of GFP-Ysc84p and cortical actin. This shows that Ysc84p is a component of cortical actin patches. It also demonstrates that the interaction between Ysc84p and actin does not require Sla1p.

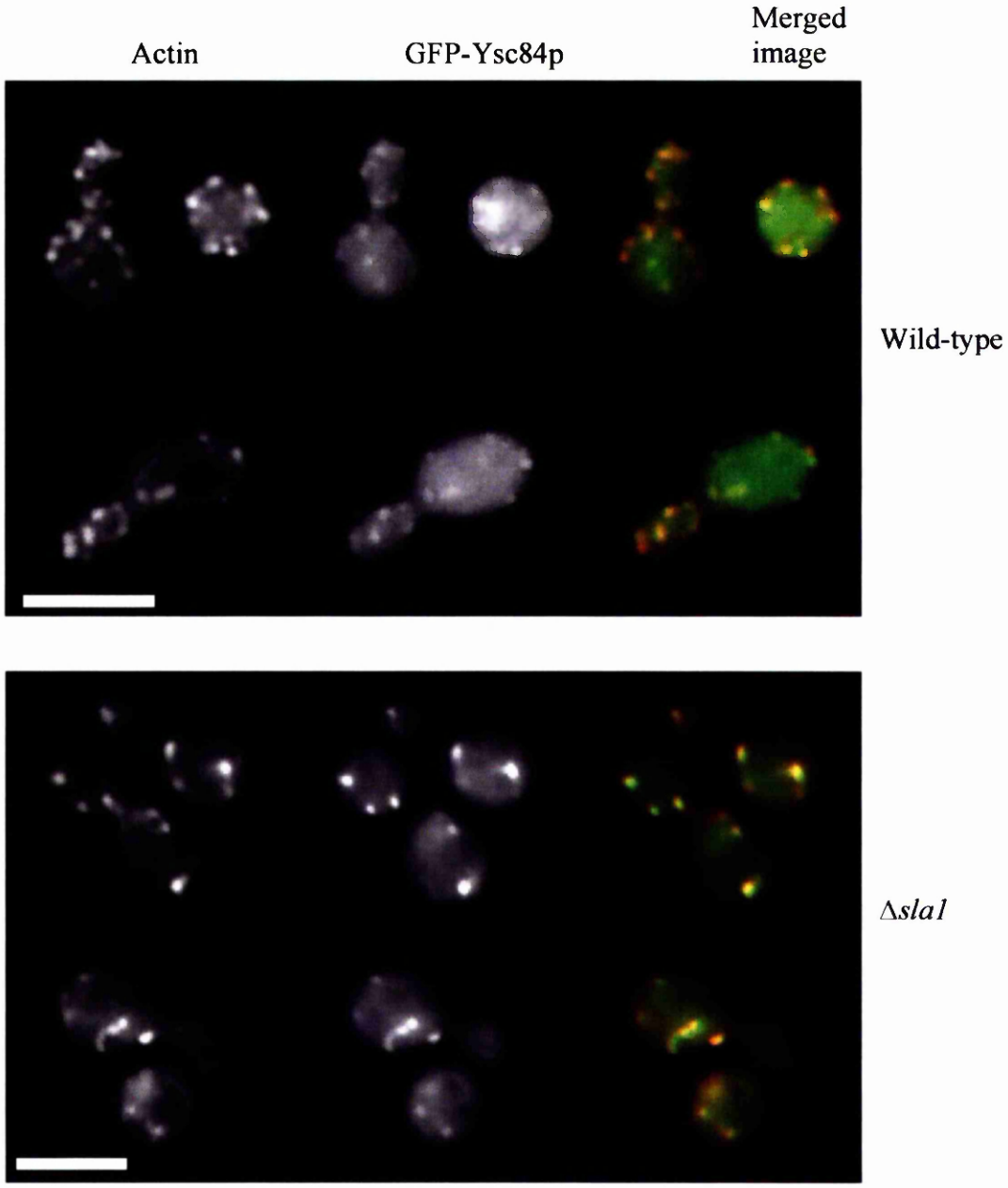

Figure 5.4 GFP-Ysc84p co-localises with cortical actin patches independent of Sla1p. Cells expressing GFP-Ysc84p in a wild-type strain (KAY 525) and in a strain deleted for *SLA1* (KAY 527) were ethanol-fixed and rhodamine-phalloidin stained (section 2.8.9) to examine localisation of filamentous actin and GFP-Ysc84p. Bar, 5 μm.

5.4. Localisation of GFP-tagged Yfr024c-ap

YSC84 has an *S.cerevisiae* homologue *YFR024C-A* (figure 5.1). The intracellular localisation of Yfr024c-ap was assessed using an integrated N-terminally tagged GFP-Yfr024c-ap fusion protein under control of the *GAL* promoter. The integrated DNA was generated by PCR using oligos o198 and o199 against template DNA pKA156 (*HIS*) and then transformed into wild-type and Δ*sla1* backgrounds, selected for growth on drop-out his plates, to generate KAY 537 and KAY 539 respectively. Colony PCR, using oligos o200 and o201 (section 2.3.11) was used to check that the GFP-tag had inserted in the correct locus. Expression of GFP-Yfr024c-ap was induced for 8 hours in YP-Gal medium at 29 ˚C before viewing cells by fluoresence microscopy.

5.4.1 GFP-Yfr024c-ap co-localises with cortical actin in wild-type and Δ*sla1* yeast cells.

Figure 5.5. (top panel) shows that the localisation pattern of GFP-Yfr024c-ap in a wild-type background was similar to that of GFP-Ysc84p (figure 5.4) as GFP-Yfr024c-ap localised to the cortex in punctate patches, polarised to the bud. The localisation of GFP-Yfr024c-ap in an Δ*sla1* background is at the cortex and co-localises with cortical actin. The cortical actin patches appear larger that those found in Δ*sla1* normally (figure 3.7) indicating that the overexpression of GFP-Yfr024c-a is having an additive deleterious effect on the cortical actin cytoskeleton.

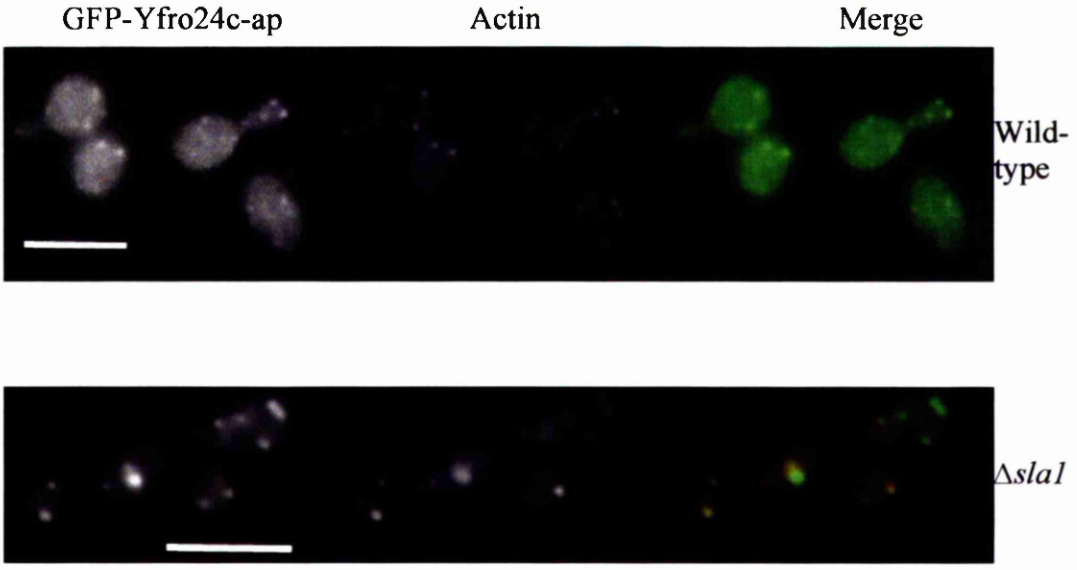

Figure 5.5. GFP-Yfro24c-ap co-localises with cortical actin patches independent of Sla1p. Cells were grown in a rich medium with 2 % galactose to express N-terminally tagged GFP-Yfr024c-ap in a wild-type strain (KAY 537) and in a strain deleted for *SLA1* (KAY 539). Cells were ethanol-fixed and rhodamine phalloidin stained (section 2.8.9) to examine localisation of filamentous actin and GFP-Yfr024c-ap. Bar, 10μm.

5.5. Localisation of Sla1p in wild-type and Δ*ysc84* cells

Localisation of Ysc84p to cortical actin patches is independent of Sla1p (section 5.4). The localisation of Sla1p in wild-type and Δ*ysc84* cells was observed to assess if the localisation of Sla1p required Ysc84p. Sla1p was tagged with GFP at the N-terminus under control of the *GAL* promoter in wild-type (KAY 397) and Δ*ysc84* cells (KAY 512).

5.5.1 Localisation of GFP-Sla1p

There were different localisation patterns for GFP-Ysc84p in haploid wild-type cells, and in haploid Δ*sla1* cells (section 5.2) but in both cell types there was complete co-localisation of GFP-Ysc84p and cortical actin (section 5.3). To determine if the deletion of *YSC84* had any affect on the localisation of Sla1p, yeast strain KAY 513 was generated by a PCR method of gene integration (section 2.3.10) into yeast expressing *GFP-SLA1* (KAY 397). KAY397 had been made by transforming the PCR product of o89 and o90 against template pKA156 into KAY 389 and selecting for growth on synthetic media lacking histidine.

Figure 5.6 (top) shows the normal GFP-Sla1p localisation pattern in wild-type cells. GFP-Sla1p localised in punctate structures which appeared randomly distributed in stationary phase, but as the bud developed GFP-Sla1p polarised to sites of active growth and was mostly found in the growing bud and then at the mother-bud neck in later cell stages as cytokinesis occurred. GFP-Sla1p was then seen to redistribute into the mother cell.

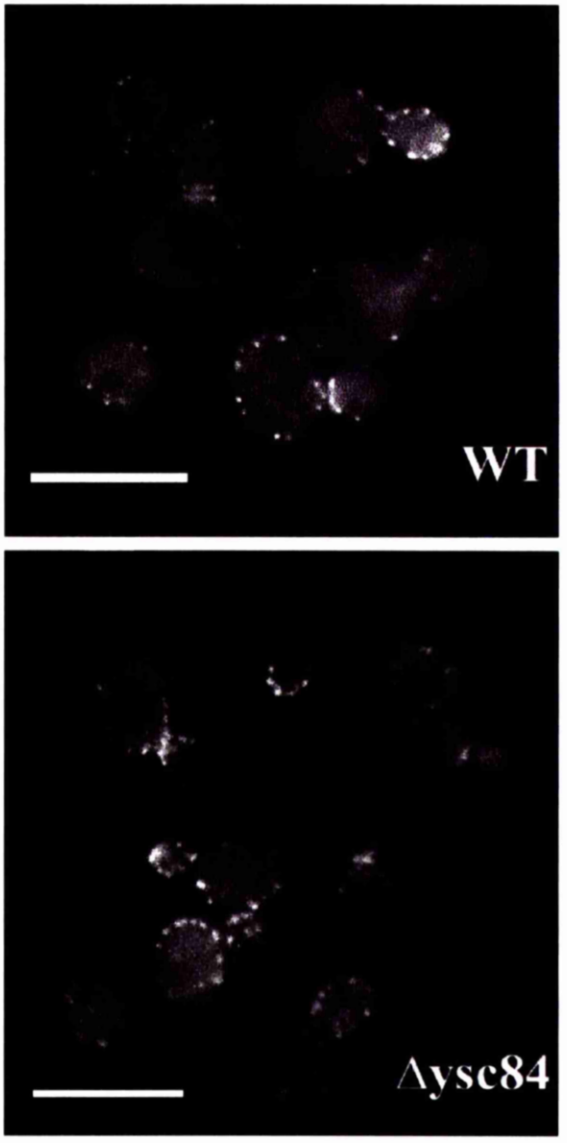

Figure 5.6. Localisation of GFP-Sla1p in wild-type and Δ*ysc84* haploid yeast cells. GFP-tagged Sla1p was expressed in (a) wild-type (KAY 397) and (b) cells deleted for *YSC84* (KAY 512). Actively growing cells were visualised by fluoresence microscopy. Bar, 10μm.

The localisation of GFP-Sla1p in the absence of Ysc84p (figure 5.6 bottom) is very similar to that found in wild-type, and the Sla1p patches remained punctate and polarised in appearance, so Ysc84p appears to not be essential for the correct localisation of Sla1p.

5.6. Localisation of GFP-Ysc84p at the cortex requires filamentous actin

GFP-Ysc84p localised with cortical actin patches (figure 5.4) and appeared to require Abp1p for correct localisation (figure 5.3). To test if the cortical localisation of Ysc84p was dependent on actin, cells were treated with the drug latrunculin-A (LAT-A) which causes the rapid and reversible disassembly of cellular filamentous actin structures *in vivo* (see section 3.8) (Ayscough 1997).

Cells expressing GFP-Ysc84p were treated with 200μM LAT-A and stained with rhodamine-phalloidin (section 2.8.10) to examine the disassembly of the structure of the actin patches. Figure 5.7 (top panel) shows the actin cytoskeleton in wild-type cells expressing GFP-Ysc84p before LAT-A treatment (left) and after LAT–A addition (right). The actin cytoskeleton was completely disrupted after 15 minutes in LAT-A as patches and cables were not visible. Before LAT-A addition GFP-Ysc84p was localised as expected at the cell cortex in patches. However, after disruption of the actin patches by LAT-A the localisation of GFP-Ysc84p patches at the cortex is abolished and GFP fluoresence becomes diffuse and cytoplasmic. Ysc84p must therefore be downstream of actin with respect to the flow of polarity information.

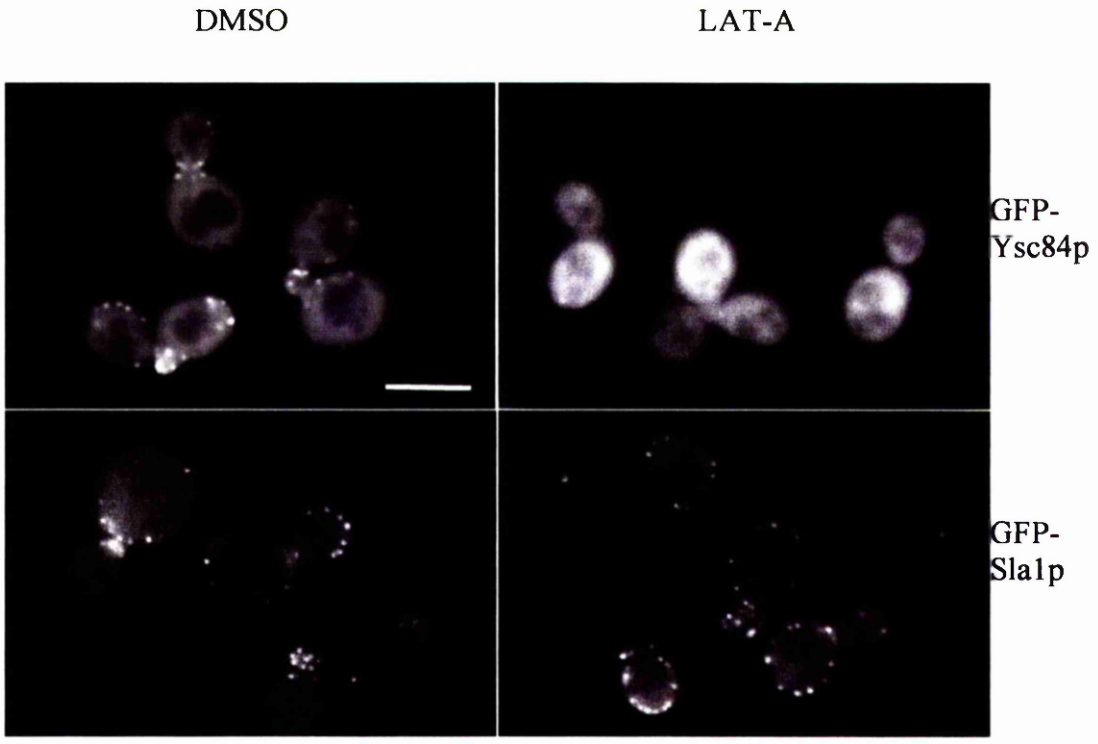

Figure 5.7. GFP-Ysc84p localisation at the cortex is abolished by LAT-A addition. Right panel shows actively growing yeast cells expressing GFP-Ysc84p (KAY 525) and GFP-Sla1p (KAY 397) after incubation in 200μm LAT-A for 15 minutes at room temperature (section 2.8.10). Control cells are shown in the left panel. Bar, 5μm.

As a comparison, the localisation of GFP-Sla1p before and after LAT-A treatment was also examined (figure 5.7. bottom panel). The localisation before LAT-A treatment appears punctate and polarised as expected. However, after incubation in 200μm LAT-A for 15 min, in contrast to GFP-Ysc84p localisation at this point, GFP-Sla1p remains localised normally at the cortex.

5.7. Characterisation of Δ*ysc84* mutants

5.7.1. Generation of Δysc84 mutant yeast

Cells lacking *YSC84* were generated using the PCR method of gene replacement. The PCR product of o136 and o137 against template pKA148 (HIS) was transformed into the diploid KAY 498 (*SLA1/Δsla1*) and grown on drop-out his plates. Transformants were screened by colony PCR using oligos o139 and o140 then PCR products were subsequently digested with PstI to check the diploid cells carried a copy of the *HIS3* marker replacement gene and were therefore Δ*ysc84* (KAY 511). Cells were sporulated and spores dissected as described in methods section 2.5.4. Segregants were then selected for growth on both drop-out ura and drop-out his medium to show inheritence of Δ*sla1* and Δ*ysc84* alleles respectively (figure 5.8a). Haploid yeast which grew on drop-out his carried Δ*ysc84* (KAY 510.1 and KAY 510.2). Haploid yeast which were able to grow on both drop-out ura and drop-out his media carried Δ*sla1::URA* and Δ*ysc84::HIS* (KAY 509.1 and KAY 509.2).

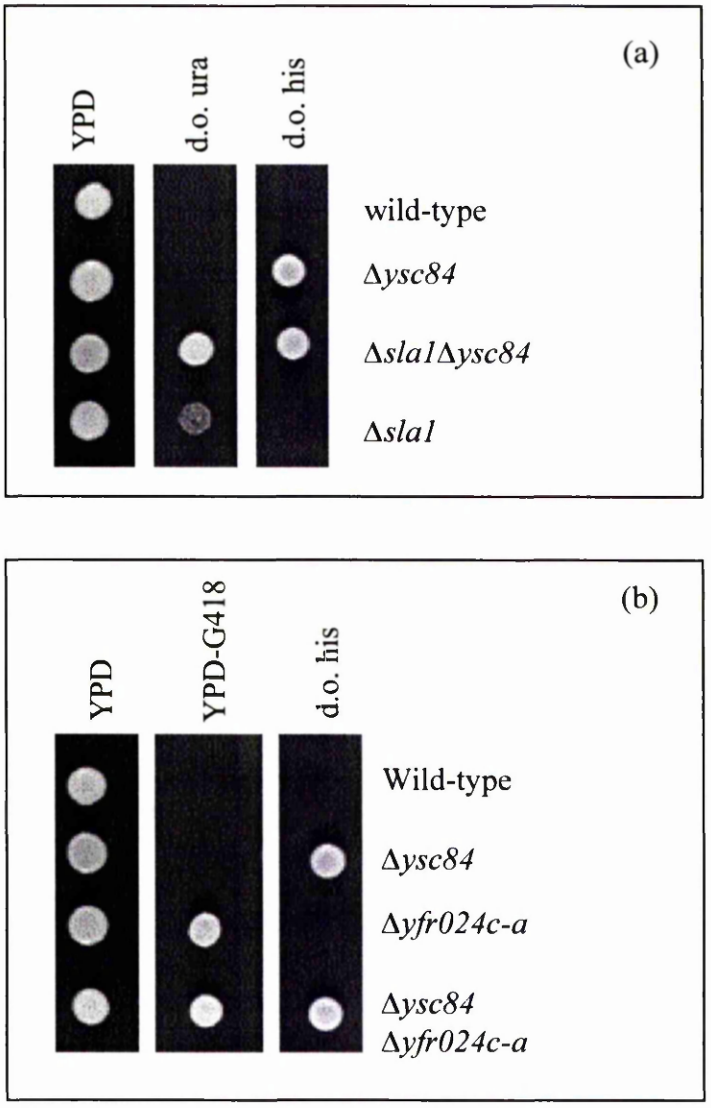

Figure 5.8. Tetrad dissection of mutant diploids.
(a) A single KAY 511 spore was dissected and replica plated on selection plates to select for haploid *Δsla1Δysc84* (KAY509) and *Δysc84* (KAY510) progeny.
(b) A single KAY 548 spore was dissected and replica plated on selection plates to select for haploid *Δysc84*, *Δyfr024c-a* (KAY553) and *Δysc84Δyfr024c-a* (KAY554) progeny.

To generate haploid cells that did not carry either *YSC84* or *YFR024C-A,* KAY 510.2 was mated with KAY 553.2 to generate KAY 548. Resultant zygotes were sporulated and tetrads dissected. Daughter progeny were grown on selection plates (figure 5.8b). Tetrads which produced 4 spores (two of each mating type) which were of the following 4 genotypes: wild-type (KAY 551); Δ*ysc84::HIS* (KAY 552*);* Δ*yfr024c-a::KanMx* (KAY 553); and, Δ*ysc84::HIS,* Δ*yfr024c-a::KanMx* (KAY 554) were selected and used in the experiments below. YSC84 and YFR024c-a therefore do not show synthetic lethality as Δ*ysc84/*Δ*yfr024c-a* yeast are viable (figure 5.8b).

5.7.2. Actin phenotype

Rhodamine-phalloidin staining (section 2.8.7) of mutant yeast cells was performed to assess their actin phenotype (figure 5.9). The cortical actin visible in wild-type yeast cells (figure 5.9 top left) was punctate and polarised to areas of active cell surface growth, namely the bud and at the mother-bud neck in cell undergoing cytokinesis. Actin cables were also visible running parallel to the mother-bud axis.

When yeast cells with a single deletion in either *YSC84* (figure 5.9 middle left) or *YFR024C-A* (figure 5.9 bottom left) were examined by rhodamine-phalloidin staining, the actin cytoskeleton morphology and organisation appeared indistinguishable from that of wild-type cells. So, deletion of *YSC84* or *YFR024C-A* does not have any effect on the organisation of the actin cytoskeleton. Cells with a double deletion of *YSC84* and *YFR024C-A* (figure 5.9 bottom right) also have an actin cytoskeleton which appears wild-type. Δ*sla1*Δ*ysc84* cells (figure 5.9 middle right) display an aberrant actin morphology in which cortical actin patches appeared

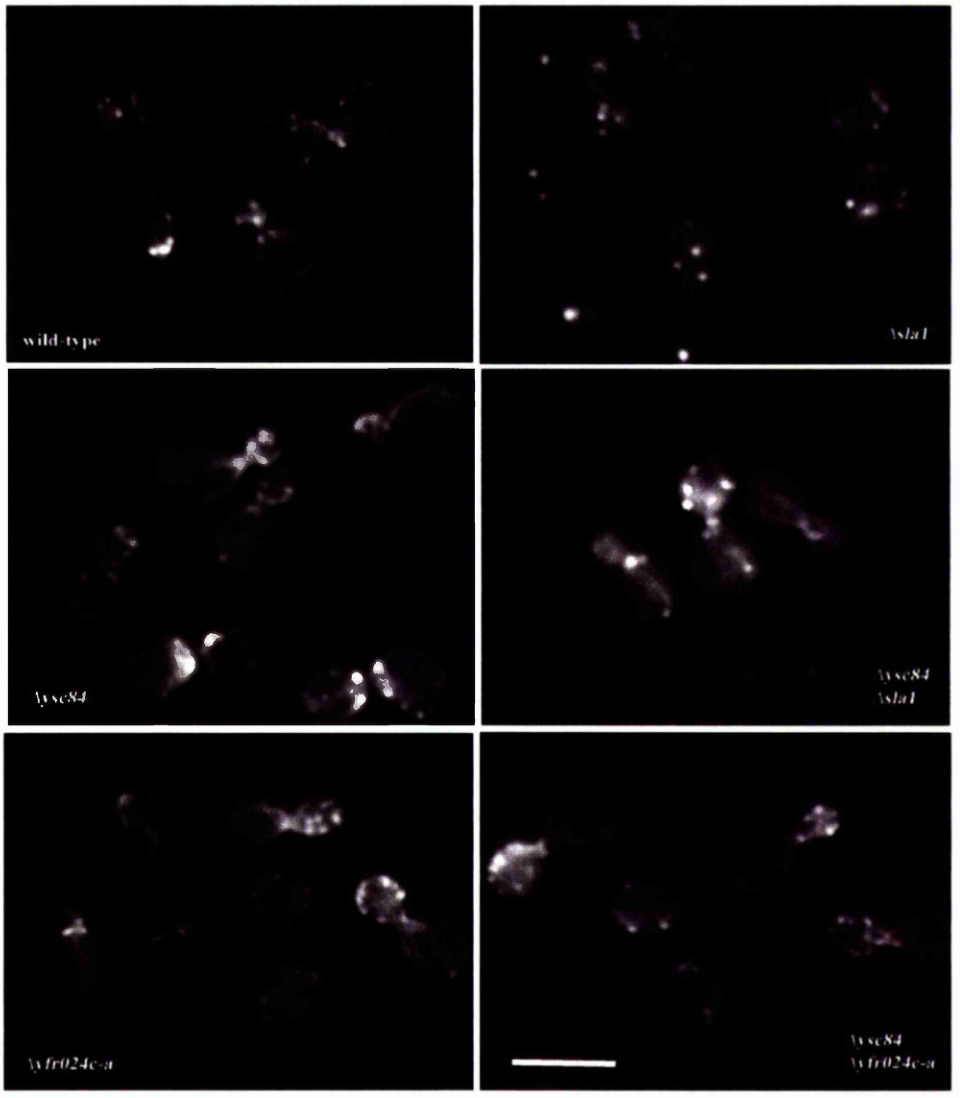

Figure 5.9. Actin phenotype of Δ*ysc84* and Δ*yfr024c-a* mutants. Rhodamine phalloidin stained haploid yeast strains lacking *YSC84* (KAY552), *YFR024C-A* (KAY553) or both (KAY554) display an actin phenotype like wild-type haploid (KAY551) yeast. The aberrant actin phenotype of Δ*sla1* cells (KAY300) is also apparent in Δ*ysc84*Δ*sla1* cells (KAY509). Bar, 5μm.

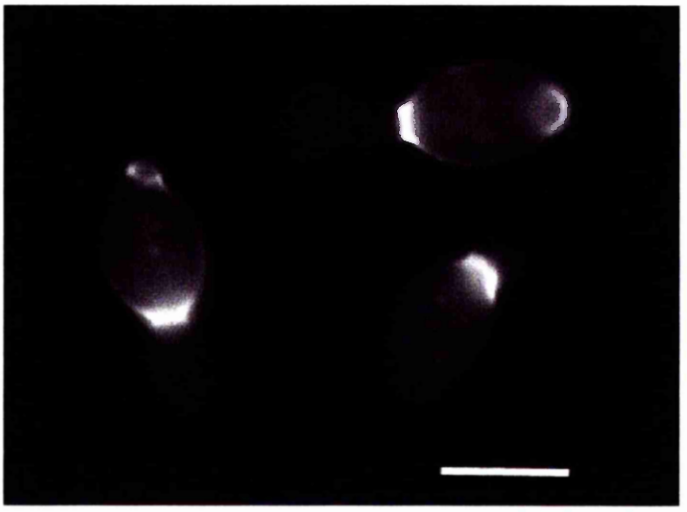

Figure 5.10. Bipolar budding pattern is normal in Δ*ysc84* diploid cells. Actively growing KAY 540 cells were fixed then stained with calcofluor to show up bud scars from successive cell divisions. 98 % of bud scars were located in a bipolar pattern indicative of normal diploid budding. Bar, 5μm.

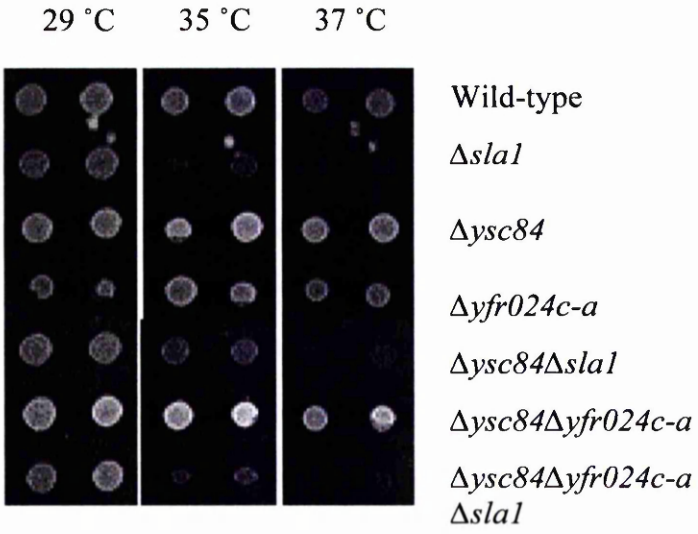

Figure 5.11. Mutant Δ*ysc84* and Δ*yfro024c-a* yeast do not display a temperature sensitive phenotype. Single (KAY 552 and KAY 553 respectively) and double deletions (KAY 554) of Δ*ysc84* and Δ*yfr024c-a* do not produce a temperature sensitive phenotype in haploid yeast cells. Cells grow at higher temperatures like wild-type cells (KAY 302). In combination with Δ*sla1* (Δ*ysc84*Δ*sla1* and Δ*ysc84*Δ*yfr024c-a*Δ*sla1*) KAY 509 and KAY 565) there is no rescue of the temperature sensitive phenotype displayed by Δ*sla1* cells (KAY 300) at 37°C.

Δ*yfr024c-a* did not appear to exacerbate or rescue the temperature sensitive phenotype found in Δ*sla1* yeast.

5.7.5. Genetic Interactions with other components of cortical patches

In order to assess if *YSC84* or *YSC84* and *YFR024c-a* deletion combined with deletions of genes encoding other components of the cortical actin cytoskeleton was lethal to the cells, deletion mutants were mated and sporulated to see if resultant daughter cells which carried the double or triple mutations were lethal. Diploid yeast Δ*abp1*Δ*ysc84*Δ*yfr024c-a*, Δ*sla1*Δ*ysc84*Δ*yfr024c-a*, Δ*rvs167*Δ*ysc84*, and Δ*ysc84*Δ*ycl034w* were generated then sporulated and tetrads dissected (figure 5.12). Daughter cells were checked for inheritence of gene deletions by growth on selection plates. It is clear in figure 5.11 (a-c) that triple mutants Δ*abp1*Δ*ysc84*Δ*yfr024c-a* and Δ*sla1* Δ*ysc84*Δ*yfr024c-a* and double mutant Δ*rvs167*Δ*ysc84* are viable since all 4 progeny (of which some are the triple and double mutants) were viable. Only cells which carried the Δ*sla1* allele showed slow growth.

However, cells that carried a double deletion in *YSC84* and *YCL034w* were inviable at 37 °C (figure 5.11d – from Derek Warren, Glasgow University). *YCL034w* is an ORF which encodes a protein with a predicted molecular weight of 40 kDa of unknown function which had very recently been identified in a two-hybrid screen against a bait plasmid carrying the central region of *SLA1* from amino acids 483 – 720 (Derek Warren, Glasgow University). Interestingly, *YCL034w* had been identified previously in a two-hybrid screen using Las17p as bait which had also identified Ysc84p and Yfr024c-ap as interactors (Madania 1999). Ycl034wp contains

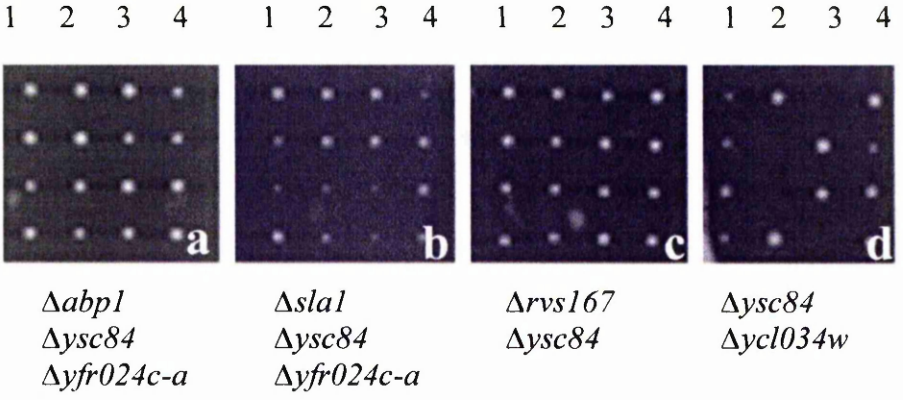

Figure 5.12. Genetic interactions between *YSC84* and *ABP1*, *SLA1*, *RVS167* and *YCL034w*. Heterozygous diploid yeast (a) KAY 559, (b) KAY560, (c) KAY486 x KAY552.2, and (d) KAY 515 were sporulated and tetrads dissected to determine viability of cells with double or triple gene deletions. All daughter cells are viable in a-c as they can grow on YPD at 37 ˚C. However, the Δ*ysc84* x Δ*ycl034w* mating (d) produced 2 daughter cells (tetrad 2 and 3) incapable of growth at 37 ˚C which were found to be double deletion mutants indicating that deletion of both *YSC84* and *YCL034W* in the same cell is lethal.

motif at the extreme C-terminus. The NPFXD motif interacts with Epsin homology domains (Salcini *et al*, 1997) and is involved in ubiquitin independent endocytosis (Tan *et al*, 1996, Wendland *et al* 1998).

5.7.6. LAT-A halo assays

Although the actin cytoskeleton appeared normal in Δ*ysc84* cells when stained with rhodamine-phalloidin, the deletion of YSC84 may have more subtle effects on actin dynamics. To test this halo assays were performed to assess the sensitivity of Δ*ysc84* yeast to LAT-A (section 3.8).

The sensitivity of wild-type, Δ*ysc84,* Δ*yfr024c-a* and Δ*ysc84*Δ*yfr024c-a* haploid yeast strains to LAT-A at 1, 2 and 5 mM concentrations, was tested using LAT-A halo assays (section 2.5.6). The LAT-A halo assays (figure 5.13a) show that as the concentration of LAT-A increased, the halo around the disc increased in diameter. There was no halo around the control disc. A bar graph was drawn which shows the relative sensitivities of the mutant yeast to LAT-A when compared to wild-type yeast (figure 5.13b).

Δ*ysc84* cells were less sensitive to LAT-A as demonstrated by the reduced halo produced around the LAT-A containing discs, having 84 % of the sensitivity to LAT-A compared to wild-type yeast. Δ*yfr024c-a* yeast showed the greatest reduction in sensitivity to LAT-A, having 56 % of the sensitivity to LAT-A while the double mutant was intermediate to the single mutants with 68 % sensitivity. Ysc84p and

(a)

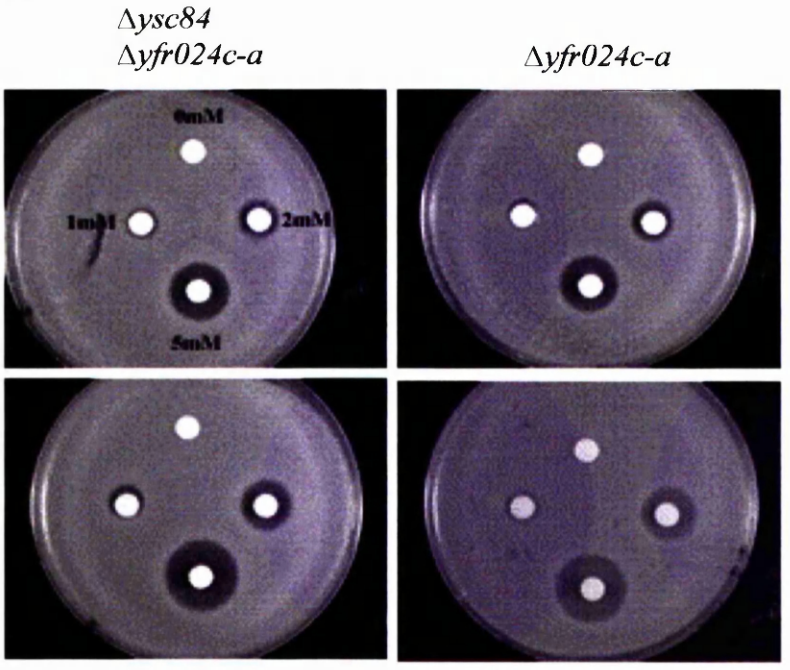

(b)

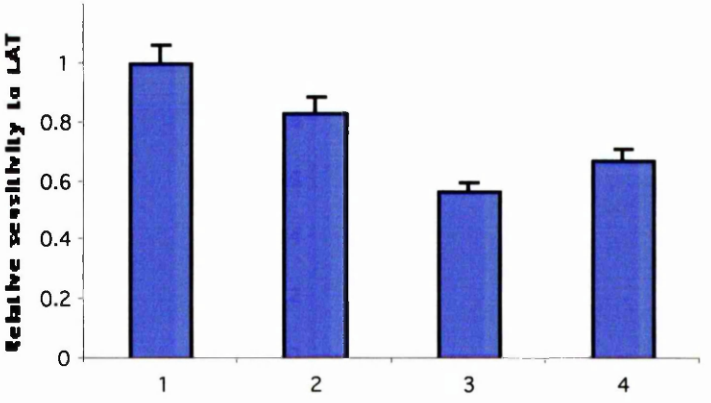

Figure 5.13. LAT-A halos assays on *ysc84* and *yfro24c-a* mutant yeast. (a) Growth of haploid yeast strains on YPDA media in the presence of increasing concentrations of LAT-A was tested using halo assays (section 2.5.6). Δ*ysc84* (KAY 552) yeast grew like wild-type yeast (KAY 551). However cells which had Δ*yfr024c-a* (KAY 553) either singly or in combination with Δ*ysc84* (KAY 554) had a higher resistance to the drug, illustrated by a reduction in halo size around the LAT-A saturated discs. (b) Bar graph showing relative sensitivity to LAT-A

Yfr024c-ap in particular appear to destabilise the actin cytoskeleton as their deletion produced cells that are less sensitive to LAT-A.

5.8. Use of immunoprecipitation to determine if Sla1p, Sla2p, Abp1p and Las17p are binding partners for Ysc84p

The two-hybrid data indicates an interaction between Sla1p and Ysc84p. The requirement for actin and Abp1p to localise Ysc84p to the cell cortex (figure 5.9 and 5.4) suggests that there may be physical interaction with Ysc84p. The previously reported two-hybrid interaction between both Ysc84p and Ycl034w with Las17p (Madania *et al* 1999) also point to a physical interaction with Las17p. Interactions between Ysc84p and Sla1p, Abp1p, Las17p and also Sla2p were investigated biochemically using immunoprecipitation, using crude cell yeast extracts expressing tagged Ysc84p (methods section 2.7.4).

Initial immunoprecipitations were tried to provide more evidence for the Sla1p-Ysc84p interaction as shown earlier by yeast two-hybrid. Whole cell extracts were made by the liquid nitrogen grinding method (section 2.7.2) from yeast co-expressing Sla1-myc and Ysc84-HA (KAY 546). Anti-myc antibodies or anti-HA antibodies bound to protein A or protein G beads respectively were incubated in the yeast extracts to allow either Sla1-myc or Ysc84-HA to bind indirectly to the beads. Interacting proteins co-expressed in the yeast extracts may then bind to the protein immobilised on the beads. The beads were washed to allow non-specifically bound proteins to be removed. Samples were run on denaturing polyacrylamide gels and

western blotted with antibodies against the HA epitope (to detect Ysc84p) or against myc (to detect Sla1p).

Figure 5.14a shows that Sla1-myc and Ysc84-HA are co-expressed in KAY 546 and are detectable in the supernatant fraction. When anti-HA antibodies were used to pulldown interacting proteins, Ysc84-HA can be seen enriched on the protein G-sepharose beads (figure 5.14a left), and conversely, Sla1-myc is enriched on protein A-sepharose beads when anti-myc antibodies are used (figure 5.14a right). However, in both cases neither Ysc84-HA or Sla1-myc were co-immunoprecipitated suggesting that no interaction occurred between these proteins.

Immunoprecipitations that enriched Ysc84-HA on the beads were also performed to find other interacting proteins. Western blots were probed with anti-Sla1p, anti-Abp1p, anti-Las17p and anti-Sla2p antibodies to see if an interaction could be detected (figure 5.14b). Sla1-myc, Sla1p and Abp1p were detected in the bead fraction which would normally suggest an interaction with Ysc84-HA. However, these results are inconclusive as protein could only be seen to be co-immunoprecipitating with Ysc84-HA when the control beads (no antibody bound) also had protein bound and/or the wash fraction contained the protein probed with antibody. Protein on the control beads shows a non-specific interaction with the beads. Sla2p does not co-immunoprecipitate with Ysc84-HA as it was not detected in the bead fraction. Similarly, when cells co-expressing Las17-myc and Ysc84-HA (KAY 558) were co-immunoprecipitated, Las17-myc was not detected in the bead

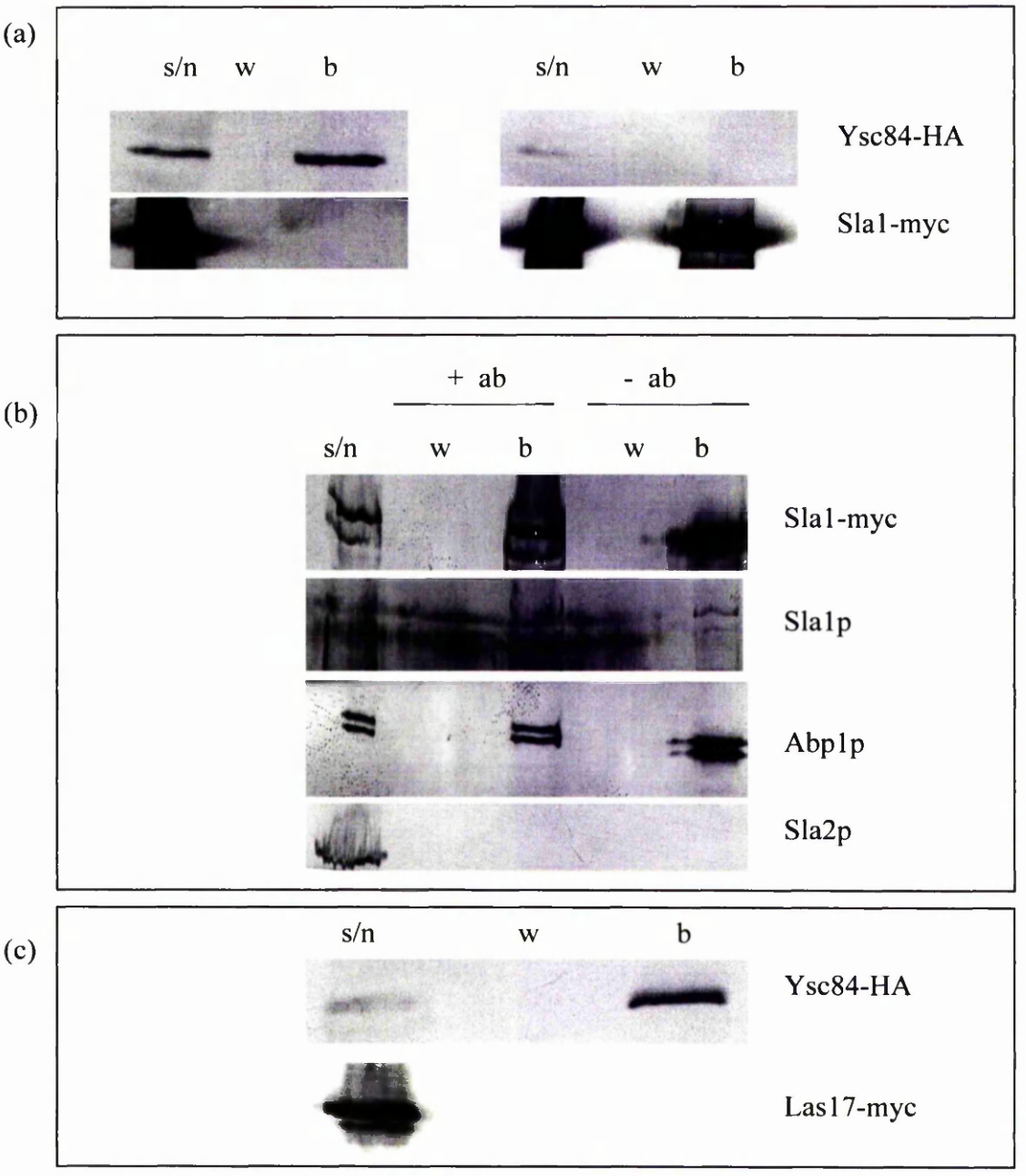

Figure 5.14 Immunoprecipitation of Ysc84-HA to find Ysc84p interacting proteins. (a) Immunoprecipitation using cell extract from yeast co-expressing C-terminally HA-tagged Ysc84p and C-terminally myc-tagged Sla1p (KAY 546) was performed to confirm the two-hybrid interaction between Sla1p and Ysc84p. Cell extract was incubated with anti-HA antibodies (left) or anti-myc antibodies (right) bound to protein A or protein G sepharose beads respectively. Ysc84-HA enriched on beads coated with HA-antibody but did not pulldown Sla1-myc (left). Similarly Sla1-myc enriched on myc-antibody coated beads did not pulldown Ysc84-HA (right). (b) KAY 546 extract was used in an HA-antibody co-immunoprecipitation experiment to show interaction between Ysc84p and Sla1p, Abp1p and Sla2p. Results are inconclusive as Sla1p, Sla1-myc and Abp1p bound to beads in absence of antibody. Sla2p does not bind to beads with Ysc84-HA enriched on them. (c) Cell extract from a strain (KAY 558) co-expressing Las17-myc and Ysc84-HA was used but Las17-myc did not co-immunoprecipitate with Ysc84-HA.

fraction. These results suggest that Las17 and Sla2p also do not interact with Ysc84-HA.

The failure of immunoprecipitation to show interaction between Ysc84-HA and Sla1-myc may be due to the tag at the C-terminal of Ysc84p interfering with the proper folding of the SH3 domain found at the extreme C-terminus of the protein and so impairing its function. Yeast strains were generated to include a 7x alanine linker between the tag and the C-terminus of Ysc84p to provide extra space to allow Ysc84p to fold normally. Yeast strains co-expressing Ysc84-HA and Sla1-myc (KAY 562), and Ysc84-HA and Las17-myc (KAY 563) were used in immunoprecipitation experiments as before (figure 5.15). A 9 x myc tag was attached to the C-terminus via a 7x alanine linker (KAY 564) and used to try to co-immunoprecipitate Abp1p (figure 5.15c). However, again there was no co-immunoprecipitation of proteins indicating no interaction between Ysc84p and Sla1p, Las17p or Abp1p. These experiments were performed at the very end of my Ph.D and had only been attempted once so conditions had not been optimised. Transient or weak interactions may not have been readily detectable. Results from co-localisation of GFP-Ysc84 and actin, discussed in section 5.4, also indicate this. It is also possible that the protein present in the supernatant fraction may not be in the necessary physiological state to allow an interaction to occur. It is also possible that the two-hybrid interaction is allowing exposure of domains which can interact but might normally only be exposed under certain conditions (or after modification).

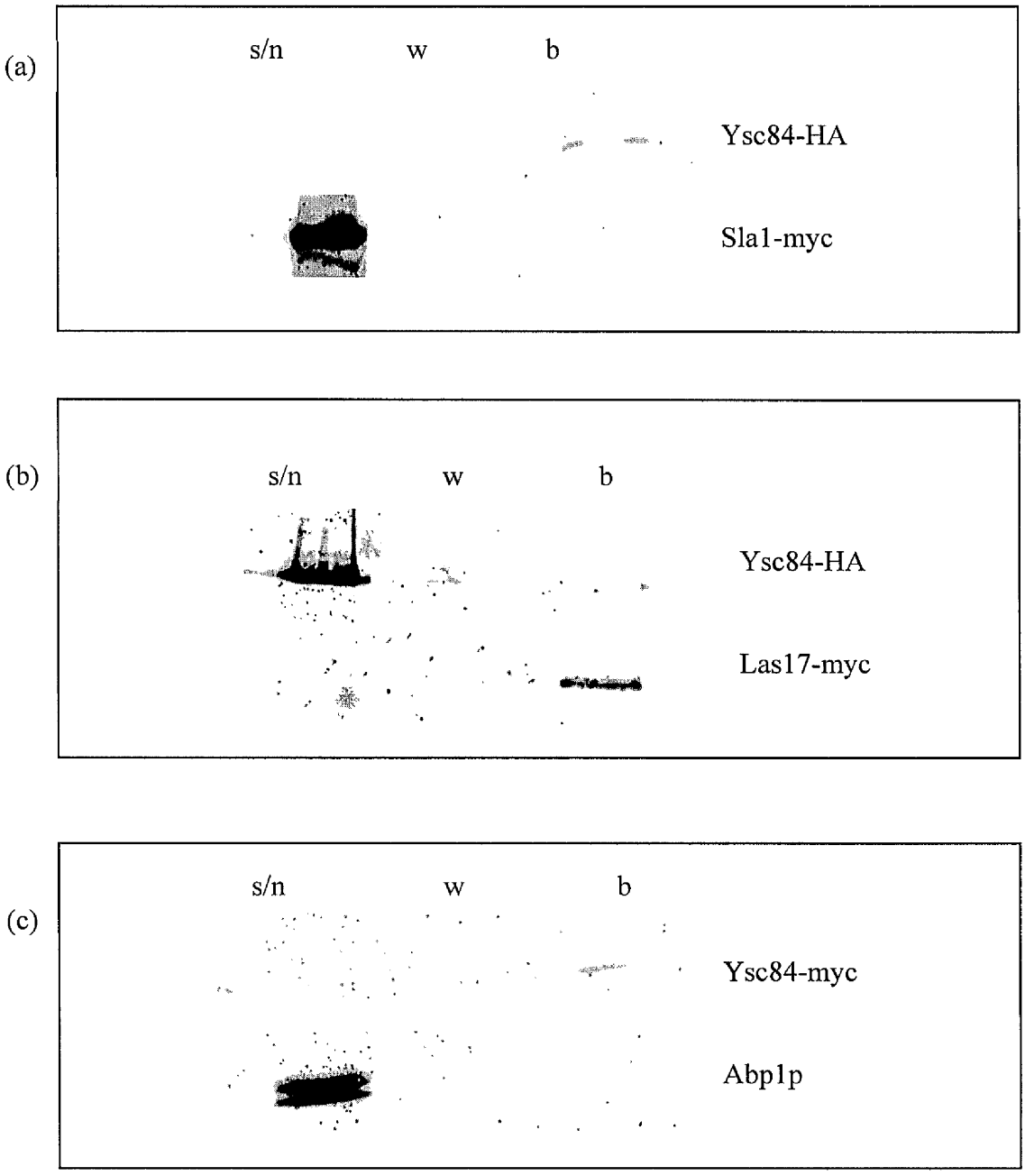

Figure 5.15. Immunoprecipitation to find Ysc84p interacting proteins using Ysc84 C-terminally tagged with HA via a 7x alanine linker. (a) Co-immunoprecipitation experiments using cells co-expressing Ysc84-HA and Sla1p-myc (KAY 562). KAY 562 expressed Ysc84-HA with a 7x alanine linker. Western blots were probed with anti-HA and anti-myc antibodies. Sla1p is not pulled down with Ysc84-HA. (b) HA was tagged to the C-terminus of Ysc84p via a 7x alanine linker in a strain co-expressing Las17-myc (KAY 563). Las17-myc did not bind to beads coated in Ysc84-HA. (c) 9xmyc was tagged to the C-terminus of Ysc84p via a 7x alanine linker in a wild-type strain (KAY 564). Ysc84-myc did not co-immunoprecipitate Abp1p.

5.9. Summary

The previous chapter described the identification of Ysc84p as a binding partner for the Sla1p-118-511 domain in a two-hybrid screen. As Ysc84p was of unknown function, and had previously been isolated as a binding partner for Sla1p (Uetz *et al* 2000) work was carried out to characterise Ysc84p and its *S. cerevisiae* homologue Yfr024c-a.

The cellular localisation of Ysc84p was determined by tagging with GFP and observing cells by fluoresence microscopy (figures 5.2 and 5.3). GFP-Ysc84p was found to localise at the cell cortex exclusively at cortical actin patches (figure 5.4). GFP-Yfr024c-a has an identical localisation pattern to that of GFP-Ysc84p (figure 5.5). GFP-Ysc84p localisation did not require Sla1p as GFP-Ysc84p localised to the aberrant cortical actin patches found in Δ*sla1* cells (figures 5.3 and 3.7). Conversely, the localisation of GFP-Sla1p did not require Ysc84p (figure 5.6). Filamentous actin is required for the localisation of GFP-Ysc84p to the cortex as LAT-A treated cells lost GFP-Ysc84p from the cell cortex (figure 5.7).

Characterisation of Δ*ysc84* mutants did not reveal a great deal about the function of Ysc84p as the mutant cells did not display many mutant phenotypes (section 5.7.). However, cells that were deleted for both *YSC84* and another hypothetical ORF, *YCL034w* were synthetically lethal (figure 5.12). This is of interest since both *YSC84* and *YCL034w* interact with Sla1p (this work and Derek Warren Ph.D. thesis 2002) and were both identified in a two-hybrid screen using full-length *LAS17* as bait

(Madania *et al* 1999). Sla1p has also been shown to interact with Las17p by immunoprecipition (Li 1997). Work carried out recently by Derek Warren (Glasgow University) has shown that a *YSC84* and *YCL034w* double mutant was defective for fluid-phase endocytosis and had a depolarised cortical actin cytoskeleton. This points to both Ysc84p and Ycl034w acting separately as links between Sla1p and Las17p. This hypothesis could be tested by immunoprecipitation using cell extracts from the double mutant (Δysc84/Δycl034w) strain to see if both Sla1p and Las17p co-immunoprecipitated.

Localisation of GFP-Ysc84p in Δ*las17* yeast shows some cortical localisation. However, the cortical actin phenotype found in Δ*las17* cells (Li 1997) does not appear like the GFP-Ysc84p patches that are displayed in these cells. Co-localisation of actin and GFP-Ysc84p needs to be carried out in Δ*las17* cells to ascertain whether Ysc84p is found at cortical actin as they are in Δ*sla1* cells.

The localisation of GFP-Ysc84p to cortical actin was dependent on Abp1p as its localisation in Δ*abp1* cells was mostly cytoplasmic (figure 5.3). The identification of *S. cerevisiae* complexes by Ho *et al* (2002) by immuno-affinity purification of FLAG-tagged bait proteins identified a novel interaction between Abp1p and Ysc84p. This is very interesting as it backs up my data that indicates a requirement for Abp1p to localise Ysc84p to cortical patches (figure 5.3). It also shows that the immunoprecipitations I carried out (section 5.8) need to be adjusted to allow this interaction to be isolated.

Large-scale analysis of protein complexes using affinity purification and MALDI-TOF published this year (Gavin *et al* 2002, Ho *et al* 2002) produced further evidence that protein complexes, such as cortical actin patches, can be of variable composition and that its components may associate with other protein complexes. For example, tandem-affinity purification of Arp2p was carried out and all known components (Arp3, Arp2 and the 5 Arc protein subunits) of the Arp2/3 complex were isolated (Gavin *et al* 2002). Sla1p was found in a complex that included Las17p, Yfr024c-ap, Ysc84p and Sla2p (Gavin *et al* 2002). That this complex was isolated in the TAP/MS-based analyses shows that sufficiently stable complexes were able to form, and that the immunoprecipitation experiments I carried out could probably be optimised to allow co-purification of Sla1p and Ysc84p. This new information further confirms that Ysc84p exists in protein complex alongside Sla1p although does not confirm a direct interaction.

Chapter 6

Discussion

6.1 Discussion

My results indicate that Sla1p acts as a scaffold protein possibly linking the regulation of actin dynamics and endocytosis in *S. cerevisiae* via the Sla1p-118-511 domain.

6.1.1. Characterisation of *sla1-Δ118-511* yeast

6.1.1.1. Sla1p-Δ118-511 localises to the cell cortex and is required for wild-type actin organisation

My work has shown that the Sla1-118-511 domain of the cortical patch protein Sla1p is essential for normal actin organisation as cells lacking this domain display larger but fewer cortical actin patches (figure 3.7). The mutant sla1p-Δ118-511 still localises to the cell cortex (figure 3.10) so retains the potential to bind with interacting proteins which associate with the remainder of the mutant Sla1 protein.

6.1.1.2. *Sla1-Δ118-511* yeast display phenotypes characteristic of yeast with aberrant cortical actin

Along with the aberrant actin phenotype, the *sla1-Δ118-511* yeast exhibit mutant phenotypes commonly found in budding yeast with mutations in actin cytoskeleton-associated proteins. These phenotypes include inability to grow at higher temperatures (figure 3.4), slow growth (figures 3.4 and 3.5), randomised bud site selection in diploid cells (figure 3.9) and impaired endocytic function (figures 3.12). Viability of the *sla1-Δ118-511* strain was also significantly impaired compared to

wild-type after incubation in liquid media at permissive and restrictive temperatures. This may be due to the aberrant actin providing less structural support at the cell membrane thus resulting in higher cell death.

6.1.1.3. The Sla1p-118-511 domain is not vital for yeast lacking *ABP1*

The ability of cells expressing *sla1-Δ118-511* to grow in the absence of *ABP1* shows that the Sla1p-118-511 domain is not required to rescue the *ABP1* dependent phenotype of Δ*sla1* cells and also that the mutant protein is partially functional (figure 3.8). The C-terminal region of Sla1p has been shown to be vital when *ABP1* is deleted (Ayscough *et al* 1999 and Derek Warren, University of Glasgow). The C-terminus region of Sla1p is also necessary for the localisation of Sla1p to the cell cortex (Warren *et al* 2002). Interestingly, C-terminal deletion mutants do not have a readily observable defect in their cortical actin cytoskeleton.

6.1.1.4. Sla1p-118-511 domain is required for normal actin dynamics

LAT-A studies have produced interesting results and show that both Δ*sla1* and *sla1-Δ118-511* mutant yeast exhibit a significantly increased resistance to LAT-A compared with wild-type cells (figure 3.11). This gives a strong indication that wild-type Sla1p acts *in vivo* as a filamentous actin destabiliser. It is likely that in the absence of Sla1p, or in *sla1-Δ118-511*, the rate of dissociation of actin monomers from F-actin is slower which then leads to less monomer available to be bound and sequestered by LAT-A. So the larger, but fewer actin patches in *sla1-Δ118-511* mutant yeast may be explained in part to their increased stability.

6.2. The Sla1p-118-511 domain is required for normal endocytic function

The endocytic defect exhibited by both Δ*sla1* and *sla1-Δ118-511* mutant yeast is typical of cells with aberrant actin. Decreased (but not abolished) fluid-phase uptake of Lucifer Yellow, and a reduced rate of uptake of FM4-64 suggest that endocytosis can still occur via other endocytic complexes containing protein/s redundant in function with Sla1p.

The link between the actin cytoskeleton and endocytosis is well established in *S. cerevisiae* (see section 1.9.2 and reviews Munn 2001, Shaw *et al* 2001). The possible roles for the actin cytoskeleton in endocytosis are: to provide structural integrity of the plasma membrane and cell cortex; to regulate the initiation and/or scission of budding vesicles; to provide a 'scaffold' for the assembly of other important components of endocytic and cell signalling machinery; to maintain the balance of membrane flow to and from the plasma membrane; and also, to provide a force counteracting membrane surface tension and osmotic pressure. A dynamic actin cytoskeleton is required for endocytosis in yeast (Ayscough 2000).

Many protein and lipid components are required for endocytosis in yeast and a significant proportion of these are shared with higher eukaryotes. Until recently evidence for a role for the actin cytoskeleton in endocytosis in higher eukaryotes has been lacking. However, studies in mammalian cells have suggested the existence of a signalling network linking endocytosis through clathrin-coated pits and actin

cytoskeleton remodeling yet few molecular links have been identified (Qualmann *et al* 2000, Lanzetti *et al* 2001). Actin cytoskeleton-associated proteins involved in endocytosis in yeast have been shown to have homologues in clathrin-coated pits and vesicles in higher eukaryotes (Munn 2001). *END3* and *PAN1* encode yeast cortical actin patch associated proteins that contain the EH domain found in the EGF receptor kinase substrate Eps15 (Tang and Cai 1996,Wendland and Emr 1998, Benedetti *et al* 1994). Eps15 is the mammalian homologue of Pan1p. EH domains bind the NPFXD motif found in yeast that is involved in ubiquitin-independent endocytosis (Tan *et al* 1996). Eps15 interacts with α-adaptin which is a component of clathrin-mediated endocytosis (Wendland *et al* 1996, Tang *et al* 1997). Yeast genes *END6/RVS161* and *RVS167*, encoding cortical patch components, share homology to the mammalian clathrin/dynamin-associated protein amphiphysin (McMahon *et al* 1997, Wigge and McMahon 1998, Balguerie *et al* 1999).

6.3. Sla2p, a cortical actin patch protein required for endocytosis, interacts with the Sla1p-118-511 domain in a two-hybrid screen.

My research has identified Sla2p (see section 1.14.3), in a two-hybrid screen, as a binding partner for the Sla1p-118-511 domain. The interacting region is a large central coiled-coil region. Coiled-coil domains are protein-protein interacting modules (Burkhard *et al* 2001). Rvs167p the yeast amphiphysin homologue has also shown a two-hybrid interaction with the central coiled-coil domain of Sla2p linking Sla2p with the Abp1p endocytic complex (figure 6.1) (Wesp *et al* 1997). *SLA2* has

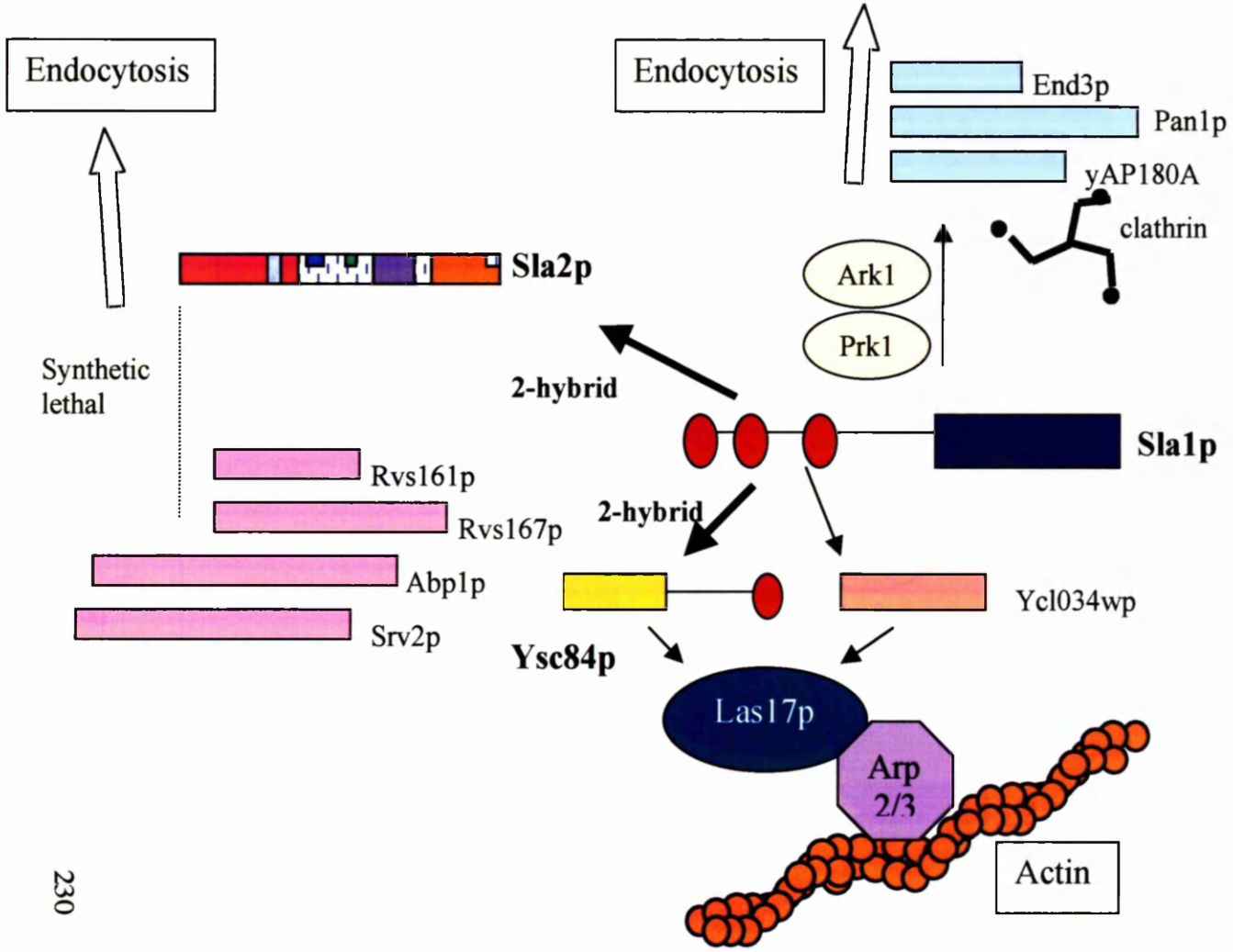

Figure 6.1 Sla1p links actin dynamics and endocytosis in *S.cerevisiae*. The Sla1p-118-511 domain is required for normal actin dynamics. Sla1p interacts with Las17p/Bee1p, an Arp2/3 complex activator via Ysc84p. Sla1p is also linked to Las17p/Bee1p via Ycl034w. Sla1p is required for normal endocytic uptake. Sla1p is associated with endocytic complexes containing Sla2p and Ysc84p via the Sla1p-118-511 domain. The C-terminus region of Sla1p interacts with a Pan1p containing endocytic complex. Pan1p and Abp1p have been shown to activate the Arp2/3 complex.

Bold typing indicates results from this study.

been shown to be required for fluid-phase and receptor- mediated endocytosis (Wesp *et al* 1997). *SLA2* is also essential for the correct organisation of the cortical actin cytoskeleton thus links the actin-cytoskeleton in yeast with endocytosis function. Two regions of Sla2p participate in endocytosis: an N-terminal domain that is essential for endocytosis; and, the central domain that performs a redundant endocytic function with Srv2p and the SH3 domain of Abp1 (Wesp *et al* 1997, Yang *et al* 1999).

The two-hybrid interaction between the Sla1p-118-511 domain and the central region of Sla2p may be indirect. One major drawback of carrying out yeast two-hybrid assays to find binding partners for yeast proteins is the presence of endogenous proteins. These may cause 'bridging' interactions to occur where, for example, the Sla1p-118-511 domain binds to a protein which then binds to an activation domain fusion protein. The secondary protein would then be identified in the screen and not the real interactor. A direct interaction between Sla1p-Sla2p has been detected however using GST pulldowns using purified Sla2p and GST-Sla1p fusion proteins on glutathione sepharose beads (Campbell Gourlay, University of Glasgow). A functional interaction has also been reported for Sla2p, as Sla1p has been shown to be required for the correct localisation of Sla2p. Instead of localising to the large clumps of actin in Δ*sla1* cells, Sla2p localises in punctate spots at the cell cortex (Ayscough *et al* 1999).

Synthetic-lethal genetic interactions have been shown between *SLA2* and other components of the cortical actin cytoskeleton, as well as the cortical patch protein

ABP1. *SLA2* is synthetically lethal with both *SAC6* which encodes yeast fimbrin (Holtzman *et al* 1993), and *SRV2* which encodes a protein that binds actin monomers and also interacts with adenylyl cyclase, a component of the Ras signalling pathway in yeast (Freeman *et al* 1996). Null alleles of *SLA2*, *SAC6* and *SRV2* are also synthetically lethal with each other and are proposed to represent a subunit or a building block of a 'cortical patch' (Yang *et al* 1999). My work has shown that the cortical patch protein Sla1p may also be a member of this 'cortical patch' through interaction with Sla2p. So, Sla1p associates with Sla2p, another cortical actin protein that is required for endocytosis.

6.4. Sla1p associates with an endocytic complex containing Pan1p and End3p

Recent findings have also indicated a link between Sla1p and endocytosis through its association with the EH domain containing proteins Pan1p and End3p (Tang *et al* 2000). The Pan1p-End3p complex plays essential roles in both the organisation of the actin cytoskeleton and in endocytosis. The interaction between Sla1p and the Pan1p-End3p complex occurs between the C-terminal repeat region of Sla1p and the N-terminal EH domain of End3p and also the Long Repeat (LR1) of Pan1p (figure 1.13). The second Long Repeat (LR2) of Pan1p simultaneously binds to the C-terminal repeat region of End3p (Tang *et al* 2000). This interaction appears to be regulated by the cortical patch kinases Ark1p and Prk1p (Watson *et al* 2001, Zeng and Cai 1999, Cope *et al* 1999). Pan1p is phosphorylated at LxxQxTG motifs found

in the LR1 and LR2 domains. The C-terminal region of Sla1p contains eleven of these motifs and can act as a substrate for Prk1p in *in vitro* studies (Tang *et al* 2000). Pan1p also binds to yAP180A which interacts with clathrin (Wendland and Emr 1998). Pan1p has recently been shown to activate the Arp2/3 complex which again ties endocytic function to regulation of actin dynamics (Duncan *et al* 2001). The Pan1p-End3p-Sla1p complex may be distinct from the endocytic complex which contains Abp1p, Srv2p, Rvs161 and Rvs161, indicating functional redundancy between the Sla1p-118-511 domain and the C-terminal region. Sla1p could therefore associate with two different endocytic complexes, thus explaining in part why endocytosis in *sla1-Δ118-511* yeast is not completely blocked.

6.5. Sla1p links actin cytoskeleton dynamics with endocytic complexes

The connection between Sla1p and endocytic complexes links the cortical actin cytoskeleton with endocytosis. The increased resistance of *sla1-Δ118-511* yeast to LAT-A compared to wild-type cells indicates a role for Sla1p in modulating actin dynamics via the Sla1p-118-511 domain. Reduced endocytic uptake associated with deletion of the Sla1p-118-511 domain may be attributed to reduced actin dynamics. Las17p/Bee1p, the yeast WASP homologue, is in a prime position to be playing an important role in affecting actin dynamics alongside Sla1p. Las17p/Bee1p is a potent activator of the Arp2/3 complex (Winter *et al* 1999). Las17p/Bee1p has been shown to interact with Sla1p by co-immunoprecipitation and in GST-pulldowns (Li 1997,

Warren *et al* 2002). This interaction, if direct, may be between the proline-rich domain of Las17p/Bee1p and one of the SH3 domains of Sla1p. It is possible that it is the third SH3 domain of Sla1p, missing in the *sla1-Δ118-511* yeast, mediating the interaction and that the absence of this SH3 domain prevents the normal association with Las17p/Bee1p thus deleteriously affecting actin dynamics. However, this interaction has not been successfully demonstrated to occur. Cells expressing the mutant sla1-Δ118-511 protein have been found to be defective for the nucleated assembly of rhodamine-actin into cortical actin structures in an *in vitro* permeabilised cell assay (Ayscough *et al* 1999, Li *et al* 1995). This indicates that the Sla1p-118-511 domain is playing a direct role in regulation of the cortical actin cytoskeleton (Ayscough *et al* 1999). Las17p/Bee1p has also been shown to be required for actin nucleation activity (Li 1997).

In yeast, Abp1p binds actin filaments and is found tightly associated with the Arp2/3 complex which it also activates (Goode *et al* 2001). GST-pulldowns have demonstrated an interaction between Sla1p and Abp1p (Warren *et al* 2002). In both mammalian and yeast cells Abp1p appears to function in endocytosis (Wesp *et al* 1997, Qualmann *et al* 2000). Mammalian Abp1p interacts with the GTPase dynamin, thus linking endocytosis to the actin cytoskeleton (Kessels *et al* 2001). Yeast Abp1p is required for proper localisation of kinases Ark1p and Prk1p which play a role in regulating the organisation of the cortical actin cytoskeleton and endocytosis (Cope *et al* 1999). The SH3 domain of Abp1p is also required for endocytosis when the central region of Sla2p is absent (Wesp *et al* 1997).

6.6. The Sla1p-118-511 domain interacts with Las17p-interacting protein, Ysc84p, in a two-hybrid screen.

The two-hybrid assay described in this thesis showed an interaction between the Sla1p-118-511(-SH3) domain region of Sla1p and the SH3 domain of a protein of unknown function, Ysc84p (Chapter 4 and section 5.2). A polyproline motif which resides in the Sla1p-118-511(-SH3) domain of Sla1p is a likely target for interaction with the SH3 domains (figure 1.12). A two-hybrid interaction between full length *YSC84* (bait) and full length *SLA1* (prey) had previously been shown in a high-throughput screen (Uetz *et al* 2000). So my findings have narrowed down the possible site of interaction between the two proteins.

6.7. Characterisation of Ysc84p

6.7.1. Immunoprecipitation of Ysc84p and Sla1p

Attempts to co-immunoprecipitate Ysc84p and Sla1p and any other binding proteins were unsuccessful, possibly due to the epitope tag being fused directly to the SH3 domain of Ysc84p resulting in the important binding site folding incorrectly. Transient or weak interaction between the proteins is another possible cause.

6.7.2. Phenotypes of Δ*ysc84* yeast

Deletion of *YSC84* (also in combination with *SLA1* and the *S. cerevisiae* homologue *YFR024c-a*) produced no observable mutant phenotype. This made determination of a

possible role in the cell difficult. Other proteins may be able to substitute for Ysc84p. Ysc84p contains a single SH3 domain, a motif commonly found in cytoskeletal proteins and signalling molecules that interact with the actin cytoskeleton, so may play some role in the actin cytoskeleton or in its regulation. The SH3 domain of Ysc84p is most homologous to the SH3 domains of Yfr024c-a (86 % identity), Rvs167p (48 %) and Abp1p (34 %).

6.7.3. Localisation of GFP-tagged Ysc84p

N-terminal GFP tagged Ysc84p localised to cortical actin patches in both wild-type and Δ*sla1* cells indicating that Sla1p is not necessary for the association of GFP-Ysc84p with the cortical patches. Unfortunately attempts to co-localise Ysc84p and Sla1p *in vivo* were unsuccessful, again possibly due to difficulties in tagging the C-terminus of Ysc84p. I was also unable to tag both proteins at the N-terminus with GFP variants, YFP (yellow fluorescent protein) and CFP (cyan fluorescent protein), which could have shown the localisation of Sla1p and Ysc84p in live cells. This would have revealed whether Sla1p and Ysc84p do colocalise, and so may associate *in vivo*, thus reinforcing the two-hybrid data.

The localisation of GFP-Ysc84p in Δ*sla1* cells is at the aberrant clumps of cortical actin found in this mutant. Localisation of SLA1-GFP in Δ*ysc84* strains appeared at the cell cortex as in the wild-type situation. These data shows that Ysc84p and Sla1p can localise at the cell cortex independently of each another. However, addition of LAT-A to GFP-Ysc84p cells caused GFP-Ysc84p to delocalise from the cell cortex concommitant with the loss of F-actin. The association between GFP-Ysc84p and

actin is necessary to keep GFP-Ysc84p localised to the cortex. The addition of LAT-A to Sla1p-GFP expressing cells on the otherhand does not affect the cortical localisation of Sla1p-GFP demonstrating that Sla1p localises to the cortex in an F-actin independent manner.

The localisation of GFP-Ysc84p to the actin patches is most likely mediated by another protein as analysis of the Ysc84p sequence does not reveal any known actin-binding motifs. To test this, the localisation of GFP-Ysc84p in strains deleted for either *ABP1* or *LAS17/BEE1* was determined. Abp1p and Las17p have both been shown to activate the Arp2/3 complex (Winter *et al* 1999, Goode *et al* 2001). In cells deleted for *ABP1* the localisation of GFP-Ysc84p is mostly cytoplasmic with a single patch still apparent at the cortex. Δ*abp1* cells do not have an obvious aberrant actin phenotype (Holtzman *et al* 1993). In cells deleted for *LAS17/BEE1*, GFP-Ysc84p is still located at the cortex in punctate spots. This pattern of localisation does not resemble the large aggregates of F-actin structures found in Δ*las17* cells, which suggests that Las17p is important in mediating the interaction between actin patches and Ysc84p. Alternatively, the localisation pattern may be an indirect result of the severely aberrant actin cytoskeleton in this deletion strain. My data particularly indicates that the association of GFP-Ysc84p and actin may be mediated through Abp1p.

6.8 Ysc84p links actin dynamics with endocytosis

A two-hybrid screen to find Las17p/Bee1p interactors identified Ysc84p and Yfro24c-a as interacting with full length Las17p/Bee1p. The region of Ysc84p that was isolated was amino acid 270 to 468, which includes the SH3 domain. The region of Yfro24c-a (a.a. 186-451) also includes the SH3 domain (Madania *et al* 1999).

A further protein of unknown function, encoded by *YCL034w* was also isolated in the Las17p two-hybrid screen. *YCL034w* has also been isolated in a two-hybrid screen, using the central domain of *SLA1* (Derek Warren, unpublished data). This domain overlaps, by 28 amino acids, with the Sla1p-118-511 domain. It contains two short regions that show the highest homology to the *S. pombe SLA1* functional homologue. So, two proteins that interact with largely different regions of Sla1p may separately bind Las17p/Bee1p which suggests that both of these proteins may link Sla1p to actin dynamics via Las17p/Bee1p potentially through different pathways.

6.8.1 Cells deleted for both *YSC84* and *YCL034w* display aberrant growth and endocytic defects

Deletion of either *YSC84* or *YCL034w* alone produces no mutant phenotypes (my work and Derek Warren, University of Glasgow). It seems that when either protein is missing, other components can compensate and provide the structural and functional link between Sla1p and Las17p/Bee1p. However, cells deleted for both genes grew poorly (figure 5.8.4d). Double deletion mutants also exhibit an almost complete block in fluid-phase endocytosis as determined by Lucifer Yellow uptake assays (Derek

Warren, Glasgow University). These data suggest that each protein may function in two separate pathways which involve Sla1p. Despite the apparent functional redundancy between *YSC84* and *YCL034w*, while double deletion mutants display aberrant phenotypes, it appears that there may be proteins linking these two proteins which exist in overlapping pathways.

Ycl034w contains motifs characteristic of proteins involved in membrane trafficking processes; a predicted VHS domain at its N-terminus, a central predicted GAT domain and a C-terminal NPF motif. Interestingly, unlike Ysc84p, Ycl034w myc-tagged protein has been localised to the cell cortex, but not at cortical actin patches, and (by LAT-A addition to cells) not to require F-actin for this cortical localisation (Derek Warren, University of Glasgow). This different localisation pattern of Ysc84p and Ycl034wp again suggests that these proteins are involved in different roles. Ycl034w may be acting as an adaptor protein, linking Las17p/Bee1p and thus actin dynamics to the movement of vesicles.

So, Ysc84p has been shown to associate primarily with cortical actin patches *in vivo* and to require actin and the actin-binding protein Abp1p for its localisation. Perhaps Ysc84p plays a role in regulating the cortical actin patch perhaps through Las17p/Bee1p, Sla1p, or Abp1p. This could in part explain the failure to successfully demonstrate an interaction between Sla1p and Ysc84p by immunoprecipitation due to the transient nature of the interaction involved. Future experiments to examine the *in vitro* effects of Ysc84p on actin polymerisation may indicate such a role for Ysc84p. Elucidation of binding partners of Ysc84p may also

provide some insight into the role of Ysc84p and possible links to other cortical complexes.

6.9. Summary

In summary, Sla1p acts as a scaffolding protein that integrates several pathways (see figure 6.1). The Sla1p-118-511 domain is important for cortical actin patch structure and organisation. Reduced actin dynamics in *sla1-Δ118-511* yeast produces large clumps of cortical actin to form, possibly as a result of disrupted interaction with Ysc84p and Las17p. Las17p acts to stimulate the nucleating activity of the Arp2/3 complex. In wild-type cells, Sla1p acts at the interface of actin dynamics and endocytosis. Sla1p shows interactions with Pan1p-End3p endocytic complexes via its C-terminal portion. This interaction is regulated by cycles of phosphorylation/dephosphorylation. Sla1p is also associated with other endocytic complexes. The Sla1p-118-511 domain mediates an interaction with the endocytic protein Sla2p via its central coiled-coil region. Deletion of the central coiled-coil region of Sla2p has also been shown to cause endocytic defects (S.Yang *et al* 1999) indicating that interaction between Sla1p and Sla2p may be required for efficient endocytosis. The requirement for Abp1p for the correct localisation of GFP-Ysc84p also demonstrates a link between Sla1p and Abp1p containing endocytic complexes. Synthetic lethal interactions and two hybrid data also suggest close association between Sla1p and Abp1 and Sla2p containing endocytic complexes. Finally, my data

supports a role for the Sla1p-118-511 domain in linking actin dynamics and endocytosis.

References

Abdul-Manan, N., Aghazadeh, B., Liu, G.A., Majumdar, A., Ouerfelli, O., Siminovitch, K.A. and Rosen, M.K. (1999) Structure of Cdc42p in complex with the GTPase-binding domain of the 'Wiskott-Aldrich syndrome' protein. Nature 399:379-383.

Adams, A. and Pringle, J. (1984) Relationship of actin and tubulin distribution to bud-growth in wild-type and morphogenetic-mutant *Saccharomyces cerevisiae*. J. Cell Biol. 98:934-945.

Adams, A. and Pringle, J. (1991). Staining of actin with fluorochrome-conjugated phalloidin. Methods Enzymol. 194:729-731.

Adams, A.E.M. Botstein, D. and Drubin, D.G. (1989) A yeast actin-binding protein is encoded by *SAC6*, a gene found by suppression of an actin mutation. Science 243:231-233.

Adams, A.E., Botstein, D. and Drubin, D.G. (1991) Requirement of yeast fimbrin for actin organization and morphogenesis *in vivo*. Nature 354:404-408.

Adams, A.E.M. Cooper, J.A. and Drubin, D.G. (1993). Unexpected combinations of null mutations in genes encoding the actin cytoskeleton are lethal in yeast. Mol. Biol. Cell 4:459-468.

Agard, D.A., Hiraoka, Y., Shaw, P., and Sedat, J.W. (1989). Fluorescence microscopy in three dimensions. Methods Cell Biol. 30:353-377.

Alberts, B., Bray, D., Lewis, J., Raff, M., Roberts, K., and Watson, J.D. Chapter 16. Molecular Biology of the Cell 3rd Edition (1994) Garland Publishing Inc.

Amatruda, J.F. and Cooper, J.A. (1992). Purification, characterization and immunofluoresence localization of *Saccharomyces cerevisiae* capping protein. J. Cell Biol. 117:1067-1076.

Amatruda, J.F., Gattermeir, D.J., Karpova, T.S. and Cooper, J.A. (1992). Effects of null mutations and overexpression of capping protein on morphogenesis, actin distribution and polarized secretion in yeast. J. Cell Biol. 119:1151-1162.

Amberg, D.C., Basart, E. and Botstein, D. (1995) Defining protein interactions with yeast actin *in vivo*. Stuctural Biol. 2:28-35.

Amberg, D.C. (1998). Three-dimensional imaging of the yeast actin cytoskeleton through the budding cell cycle. Mol. Biol. Cell 9:3259-3262.

Aoki, N., Ito, K. and Ito, M. (2000) A novel mouse gene, *Sh3yl1,* is expressed in the anagen hair follicle. J. Invest. Dermatol. 114:1050-1056.

Arber, S., Barbayannis, F.A., Hanser, H., Schneider, C., Stanyon, C.A. Bernard, O. and Caroni, P. (1998). Regulation of actin dynamics through phosphorylation of cofilin by LIM-kinase. Nature 393:805-809.

Ayscough, K.R. and Drubin, D.G. (1996). Actin: General principles from studies in yeast. Annu. Rev. Cell Dev. Biol. 12:129-160.

Ayscough, K.R., Stryker, J., Pokala, N., Sanders, M., Crews, P. and Drubin, D. (1997). High rates of actin turnover in budding yeast and roles for actin in establishment and maintenance of cell polarity revealed using the actin inhibitor latrunculin-A. J. Cell Biol. 137:399-416.

Ayscough, K.R. (1998). *In vivo* functions of actin-binding proteins. Curr. Biol. 10:102-111.

Ayscough, K.R., Eby, J.J., Lila, T., Dewar, H., Kozminski, K.G. and Drubin, D.G. (1999) Sla1p is a functionally modular component of the yeast cortical actin cytoskeleton required for correct localisation of both Rho1p-GTPase and Sla2p, a protein with talin homology. Mol. Biol. Cell 10:1061-1075.

Ayscough, K.R. (2000) Endocytosis and the development of cell polarity in yeast require a dynamic F-actin cytoskeleton. Curr. Biol. 10:1587-1590.

Bailley, M., Ichetovkin, I., Grant, W., Zebda, N., Machesky, L.M., Segall, J.E. and Condeelis. J. (2001). The F-actin side binding activity of the Arp2/3 complex is essential for actin nucleation and lamellipod extension. Curr. Biol. 11:620-625.

Balguerie, A., Sivadon, P., Bonneu, M. and Aigle, M. (1999) Rvs167p, the budding yeast homologue of amphiphysin, colocalizes with actin patches. J. Cell Sci. 112:2529-2537.

Bailleul, P.A., Newnam, G.P., Teenbergen, J.N. and Chernoff, Y.O. (1999). Genetic study of interactions between the cytoskeletal assembly protein Sla1 and prion-forming domian of the release factor Sup35 (eRF3) in *Saccharomyces cerevisiae.* Genetics 153:81-94.

Bamburg, J.R. McGough, A. and Ono, S. (1999) Putting a new twist on actin: ADF/cofilin modulates actin dynamics. Trends Cell Biol. 9:364-370.

Bear, J.E., Rawls, J.F. and Saxe, C.L. III (1998). SCAR, a WASP-related protein, isolated as a suppressor of receptor defects in late *Dictyostelium* development J. Cell Biol. 142:1325-1335.

Belmont, L.D. and Drubin, D.G. (1998). The yeast V159N actin mutant reveals roles for actin dynamics *in vivo* J. Cell Biol. 142:1289-1299.

Bénédetti, H., Raths, S., Crausaz, F. and Reizman, H. (1994) The *END3* gene encodes a protein that is required for the internalization step of endocytosis and for actin cytoskeleton organization in yeast. Mol. Biol. Cell 5:1023-1037.

Blader, I.J., Cope, M.J.T.V., Jackson, T.R., Profit, A.A., Greenwood, A.F., Drubin, D.G., Prestwich, G.D. and Theibert, A.B. (1999). GCS1, an Arf guanosine triphosphatase-activating protein in Saccharomyces cerevisiae, is required for normal actin cytoskeletal organisation *in vivo* and stimulates actin polymerisation *in vitro*. Mol. Biol. Cell 10:581-596.

Boldogh, I., Vojtov, N., Karmon, S. and Pon, L. (1998). Interaction between mitochondria and the actin cytoskeleton in budding yeast requires two integral mitochondrial outer membrane proteins, Mmm1p and Mdm10p. J. Cell Biol. 141:1371-1381.

Boldogh, I.R., Yang, H-C., Nowakowski, W.D., Karmon, S.L., Hays, L.G., Yates, J.R. III. and Pon, L. (2001) Arp2/3 complex and actin dynamics are required for actin-based mitochondrial motility in yeast. Proc. Natl. Acad. Sci. USA 98:3162-3167.

Botstein, D., Amberg,D., Mulholland, J., Huffaker, T., Adams, A., Drubin, D. and Stearns, T. (1997) The Yeast Cytoskeleton. In *The Molecular and Cellular Biology of the Yeast Saccharomyces: Cell Cycle and Cell Biology* (ed. J. Pringle, J. Broach and E.Jones) pp 1-90. Cold Spring Harbor: Cold Spring Harbor Press.

Breton, A.M. and Aigle, M. (1998). Genetic and functional relationship between Rvsp, myosin and actin in *Saccharomyces cerevisiae*. Curr. Genet. 34:280-286.

Burkhard, P., Stetefeld, J. and Strelkov, S.V. (2001) Coiled coils: a highly versatile protein folding motif. Trends Cell Biol. 11:82-88.

Buss, F., Luzio, J.P. and Kendrick-Jones, J. (2001). Myosin VI, a new force in clathrin mediated endocytosis. FEBS Letts. 508:295-299.

Campbell, I.D. and Morton, C.J. (1994) SH3 domains. Molecular 'Velcro'. Curr. Biol. 4:615-617.

Cao, H., Garcia, F. and McNiven, M.A. (1998). Differential distribution of dynamin isoforms in mammalian cells. Mol. Biol. Cell 9:2595-2609.

Carlier, M.F. and Pantaloni, D. (1997). Control of actin dynamics in cell motility. J. Mol. Biol. 269:459-467.

Carlier, M.F. Laurent, V. Santolini, J. Melki, R., Didry, D., Xia, G.X., Hong, Y., Chua, N.H. and Pantaloni, D. (1997b) Actin depolymerizing factor (ADF/cofilin) enhances the rate of filament turnover – implication in actin-based motility. J. Cell Biol. 136:1307-1322.

Carlsson, M., Babcock, P.A., Rubenstein, P.A. and Wang, Y.L. (1977) Actin polymerizability is influenced by profilin, a low molecular weight protein in non-muscle cells. J. Mol. Biol. 115:465-483.

Catlett, N.L. and Weisman, L.S. (2000). Divide and multiply: organelle partitioning in yeast Curr. Opin. Cell Biol. 12:509-516.

Chant, J. and Pringle, J.R. (1995) Patterns of bud-site selection in the yeast *Saccharomyces cerevisiae* J. Cell Biol. 129:751-765.

Chenevert, J., Corrado, K., Bender, A., Pringle, J. and Herskowitz, I. (1992) Ayeast gene *(BEM1)* necessary for cell polarisation whose product contains two SH3 domains. Nature 356:77-79.

Chien, C., Bartel, P.L., Sternglanz, R. and Fields, S. (1991) The two-hybrid system: A method to identify and clone genes for proteins that interact with a protein of interest. Proc. Natl. Acad. Sci. USA 88:9578-9582.

Cook, R.K., Blake, W.T. and Rubenstein, P.A. (1992). Removal of the amino-terminal acidic residues of yeast actin. J. Biol. Chem. 267:9430-9436.

Cooper, J. and Schafer, D.A. (2000). Control of assembly and disassembly at filament ends. Curr. Opin. Cell Biol. 12:97-103.

Cope, M.J.T.V., Yang, S., Shang, C. and Drubin, D.G. (1999) Novel protein kinases Ark1p and Prk1p associate with and regulate the cortical actin cytoskeleton in budding yeast. J. Cell Biol. 144:1203-1218.

Cossart, P. and Bierne, H. (2001) The use of host cell machinery in the pathogenesis of Listeria monocytogenes. Curr. Opin. Immun. 13:96-103.

Critchley, D.R. and Flood, G. (1999). α-actinins. In: Guidebook to the cytoskeletal and motor proteins, 2nd edition, eds. T. Kreis and R. Vale, Oxford: Oxford University Press, 24-27.

Critchley, D.R. (2000). Focal adhesions – the cytoskeletal connection. Curr. Opin. Cell Biol. 1:133-139.

Cvrcková, F., De Virgillo, C., Manser, E., Pringle, J. and Nasymth, K. (1995). Ste20-like protein kinases are required for normal localisation of cell growth and for cytokinesis in budding yeast. Genes Dev. 9: 1817-1830.

Damke, H., Baba, T., Warnick, D.E. and Schmid, S.L. (1994). Induction of mutant dynamin specifically blocks endocytosis coated vesicle formation. J. Cell Biol. 127:915-934.

Donnelly, S.F.H., Pocklington, M.J., Pallota, D. and Orr, E. (1993). A proline-rich protein, verprolin, involved in cytoskeletal organization and cellular growth in the yeast *Saccharomyces cerevisiae*. Mol. Microbiol. 10:585-596.

Doyle, T. and Botstein, D. (1996) Movement of yeast cortical actin cytoskeleton visualized in vivo. Proc. Natl. Acad. Sci. USA 93:3886-3891.

Drees, B., Brown, C., Barrell, B.G. and Bretscher, A. (1995). Tropomyosin is essential in yeast, yet the *TPM1* and *TPM2* products perform distinct functions. J. Cell Biol. 128:383-392.

Drees, B.L., Sundin, B., Brazeau, E., Caviston, J.P., Chen, G-C., Guo, W., Kozminski, K.G., Lau, M.W., Moskow, J.J., Tong, A., Schenkman, L.R., M^{c}Kenzie III, A., Brennwald, P., Longtine, M., Bi, E., Chan, C., Novick, P., Boone, C., Pringle, J.R. Davis, T.N., Fields, S. and Drubin, D.G. (2001) A protein interaction map for cell polarity development. J. Cell Biol. 154:549-571.

Drgonová, J., Drgon, T., Tanaka, K., Kollar, R., Chen, G.C., Ford, R.A., Chan, C.S.M., Takai, Y. and Cabib, E. (1996). Rho1p, a yeast protein at the interface between cell polarization and morphogenesis. J. Cell Biol. 107:2551-2561.

Drubin, D.G., Miller, K.G. and Botstein, D. (1988) Yeast actin-binding proteins: evidence for a role in morphogenesis. J. Cell Biol. 107:2551-2561.

Drubin, D.G., Jones, H.D. and Wertman, K.F. (1993) Actin structure and function: roles in mitochondrial organization and morphogenesis in budding yeast and indentification of the phalloidin-binding site. Mol. Biol. Cell 4:1277-1294.

Drubin, D.G. and Nelson, W.J. (1996) Origins of Cell Polarity. Cell 84:335-344.

Duncan, M.C., Cope, M.J.T.V., Goode, B.L., Wendland, B. and Drubin, D.G. (2001) Yeast Eps-15-like endocytic protein, Pan1p, activates the Arp2/3 complex. Nature Cell Biol. 3:687-690.

Dulic, V., Egerton, M., Elguindi, L., Raths, S., Singer, B. and Riezman, H. (1991). Yeast endocytosis assays. Methods Enzymol. 194:697-710.

Ebashi, S. and Ebashi, F. (1965). α-actinin, a new structural protein from striated muscle. I. Preparation and action on actomyosin-ATP interaction. J. Biochem. 58:7-12.

Engqvist-Goldstein, A.E.Y., Kessels, M.M., Chopra, V.S., Hayden, M.R. and Drubin, D.G. (1999). An actin-binding protein of the Sla2/Huntingtin interacting protein 1 family is a novel component of clathrin-coated pits and vesicles. J. Cell Biol. 147:1503-1518.

Estes, J.E., Selden, L.A. and Gershman, L.C. (1981). Mechanism of action of phalloidin on the polymerisation of muscle actin. Biochemistry. 20:708-712.

Evangelista, M., Blundell, K., Longtine, M.S., Chow, C.J., Adams, N., Pringle, J.R., Peter, M. and Boone, C. (1997). Bni1p, a yeast formin linking Cdc42p, and the actin cytoskeleton during polarized morphogenesis. Science 276:118-122.

Evangelista, M., Klebl, B.M., Tong, A.H., Webb, B.A., Leeuw, T., Leberer, E., Whiteway, M., Thomas, D.Y. and Boone, C. (2000) A role for myosin-I in actin assembly through interactions with Vrp1p, Bee1p and the Arp2/3 complex. J. Cell Biol. 148:363-374.

Evangelista, M., Pruyne, D., Amberg, D.C., Boone, C. and Bretscher, A. (2002). Formins direct Arp2/3-independent actin filament assembly to polarize cell growth in yeast. Nat. Cell Biol. 4:32-41.

Fazi, B., Cope, M.J., Douangamath, A., Ferracuti, S., Schirwitz, K., Zucconi, A., Drubin, D., Willmanns, M., Cesareni, G. and Castagnoli, L. (2001). Unusual binding properties of the SH3 domain of the yeast actin binding protein Abp1p: structural and functional analysis. J. Biol. Chem. 277:5290-5298.

Fields, S. and Song, O. (1989) A novel genetic system to detect protein-protein interactions. Nature 340:245-246.

Freeman, N.L., Chen, Z., Horenstein, J., Weber, A. and Field, J. (1995). An actin monomer binding activity localizes to the carboxyl-terminal half of the *Saccharomyces cerevisiae* cyclase-associated protein. J. Biol. Chem. 270:5680-5685.

Freeman, N.L., Lila, T., Mintzer, K.A., Chen, Z., Pahk, A.J., Ren, R., Drubin, D.G. and Field, J. (1996) A conserved proline-rich region of the *Saccharomyces cerevisiae* cyclase-associated protein binds SH3 domains and modulates cytoskeletal localization. Mol. Cell Biol. 16:548-556.

Fujimoto, L.M., Roth, R., Heuser, J.E. and Schmid, S.L. (2000). Actin assembly plays a variable, but not obligatory role in receptor-mediated endocytosis in mammalian cells. Traffic 1:161-171.

Gavin, A-C., Bösche, M., Krause, R., Grandi, P., Marzioch, M., Bauer, A., Schultz. J., Rick, J.M., Michon, A-M., Cruciat, C-M., Remor, M., Höfert, C., Schelder, M., Brajenovic, M., Ruffner, H., Merino, A., Klein, K., Hudak, M., Dickson, D., Rudi, T., Gnau, V., Bauch, A., Bastuck, S., Huhse, B., Leutwein, C., Heurtier, M-A., Copley, R.R., Edelmann, A., Querfurth, E., Rybin, V., Drewes, G., Raida, M., Bouvmeester, T., Bork, P., Seraphin, B., Kuster, B., Neubauer, G. and Seperti-Furgi, G. (2002) Functional organisation of the yeast proteome by systematic analysis of protein complexes. Nature 415:141-147.

Gallwitz, D. and Sures, I. (1980). Structure of a split yeast gene: complete nucleotide sequence of the actin gene in *Saccharomyces cerevisiae*. Proc. Natl. Acad. Sci. 77:2546.

Gehrung, S. and Snyder, M. (1990) The *SPA2* gene of *Saccharomyces cerevisiae* is important for pheromone-induced morphogenesis and efficient mating. J.Cell Biol. 111:1451-1464.

Geitz and Schiestl (1995) Transforming yeast with DNA. Meths. Mol. Cell Biol. 5:255-269.

Geli, M.I. and Reizman, H. (1998) Endocytic internalization in yeast and animal cells: similar and different. J. Cell Sci. 111:1031-1037.

Geli, M.I., Lombardi, R., Schmelzl, B. and Reizman, H. (2000). An intact SH3 domain is required for myosin I-induced actin polymerisation. EMBO J. 19:4281-4291.

Goffeau, A., Barrell, B.G., Bussey, H., Davis, R.W., Dujon, B., Feldmann, H. Galibert, F., Hoheisel, J.D., Jacq, C., Johnston, M., Louis, E.J., Mewes, H.W., Murakami, Y., Philippsen, P., Tettelin, H. and Oliver, S.G. (1996) Life with 6000 genes. Science 274:546-567.

Goldschmidt-Clermont, P.J., Machesky, L.M., Doberstein, S.K. and Pollard, T.D. (1991). Mechanism of the interaction of human platelet profilin with actin. J. Cell Biol. 113:1081–1089.

Goode, B.L, Drubin, D.G and Lappalainen, P. (1998). Regulation of the cortical actin cytoskeleton in budding yeast by twinfilin, a ubiquitous actin monomer-sequestering protein. J. Cell Biol. 142:723-733.

Goode, B.L,, Wong, J.J., Butty, A-C, Peter, M., M^{c}Cormack, A.L., Yates, J.R. Drubin, D.G. and Barnes, G. (1999). Coronin promotes the rapid assembly and cross-linking of actin filaments and may link the actin and microtubule cytoskeletons in yeast. J. Cell Biol. 144:83-98.

Goode, B.L., Rodal, A.A., Barnes, G. and Drubin, D.G. (2001) Activation of the Arp2/3 complex by the actin filament binding protein Abp1p. J. Cell Biol. 153:627-634.

Goodson, H.V. and Spudich, J.A. (1995). Identification and molecular characterisation of a yeast myosin I. Cell Motil. Cytoskelet. 30:73-84.

Goodson, H.V., Anderson, B.L., Warrick, H.M., Pon, L.A. and Spudich, J.A. (1996). Synthetic lethality screen identifies a novel yeast myosin I gene (MYO5): myosin I proteins are required for polarization of the actin cytoskeletonl J. Cell Biol. 133:1277-1291.

Gouin, D.V., Troys, M.V., Grogan, A., Segal, A.W., Ampe, C. and Cossart, P. (1998). Identification of cofilin, coronin, Rac and capZ in actin tails using a Listeria affinity approach. J. Cell Sci. 111:2877-2884.

Govindan, B., Bowser, R. and Novick. P. (1995). The role of Myo2, a yeast class V myosin, in vesicular transport. J. Cell Biol. 128:1055-1068.

Greer, C. and Schekman, R. (1982a) Actin from *Saccharomyces cerevisiae* Mol. Cell Biol. 2:1270-1278.

Greer, C. and Schekman, R. (1982b) Calcium control of *Saccharomyces cerevisiae* actin assembly. Mol. Cell Biol. 2:1279-1286.

Guo, S., Stolz, L.E., Lemrow, S.M. and York, J.D. (1999). *SAC1*-like domains of yeast *SAC1*, *INP52* and *INP53* and of human synaptojanin encode poly phosphoinositide phosphatases. J. Biol. Chem. 274:12990-12995.

Haarar, B.K., Lillie, S.H., Adams, A.E., Magdolen, V., Bandlow, W. and Brown, S.S. (1990). Purification of profilin from *Saccharomyces cerevisiae* and analysis of profilin-deficient cells. J. Cell Biol. 110:105-114.

Hall, A. (1998). Rho-GTPases and the actin cytoskeleton. Science 279:509-514.

Hardwick, K.G. and Pelham, H.R. (1992). *SED5* encodes a 39-kD integral membrane protein required for vesicular transport between the ER and the Golgi complex. J. Cell Biol. 119:513-521.

Hartwig, J.H., Bokoch, G.M., Carpenter, C.L., Janmey, P.A., Taylor, L.A., Toker, A. and Stossel, T.P. (1995). Thrombin receptor ligation and activated Rac uncap actin filament barbed ends through phosphoinositide synthesis in permeabilized human platelets. Cell 82:643-653.

Hermann, G.J. and Shaw, J.M. (1998). Mitochondrial dynamics in yeast. Annu. Rev. Cell Dev. Biol. 14:265-303.

Herrmann, H. and Aebi, U. (2000) Intermediate filaments and their associates: multi-talented structural elements specifying cytoarchitecture and cytodynamics. Curr. Opin. Cell Biol. 12:79-90.

Herskowitz, I. (1989). A regulatory hierarchy for cell specialization in yeast. Nature 342:749-757.

Higgs, H.N. and Pollard, T.D. (1999) Regulation of actin polymerization by Arp2/3 complex and WASp/Scar proteins. J. Biol. Chem. 274-32531-32534.

Hill, K.L., Catlett, N.L. and Weisman, L.S. (1996). Actin and myosin function in directed vacuole movement during cell division in *Saccharomyces cerevisiae*. J. Cell Biol. 135:1535-1549.

Ho, Y., Gruhler, A., Heilbut, A., Bader, G.D., Moore, L., Adams, S-L., Millar, A., Taylor, P., Bennet, K., Boutiller, K., Yang, L., Wolting, C., Donaldson, I., Schandorff. S., Shewnarane, J., Vo, M., Taggart, J., Goudreault, M., Muskat, B., Alfarano, C., Dewar, D., Lin, Z., Michalickova, K., Willems, A.R., Sassi, H., Nielson, P.A., Rasmussen, K.J., Anderson, J.R., Johansen, L.E., Hansen, L.H., Jespersen, H., Podtelejnikov, A., Nielsen, E., Crawford, J., Poulsen, Serensen, B.D., Matthiesen, J., Hendrickson, R.C., Gleeson, F., Pawson, T., Moran, M.F., Durocher, D., Mann, M., Hogue, C.W.V., Figeys, D. and Tyers, M. (2002). Systematic identification of protein complexes in Saccharomyces cerevisiae by mass spectroscopy. Nature 415:180-183.

Holmes, K.C., Popp, D., Gebhard, W. and Kabsch, W. (1990). Atomic model of the actin filament. Nature 347:44-49.

Holtzman, D.A., Yang, S. and Drubin, D.G. (1993) Synthetic-lethal interactions identify two novel genes, *SLA1* and *SLA2*, that control membrane cytoskeleton assembly in *Saccharomyces cerevisiae*. J. Cell Biol. 122:635-644.

Holtzman, D.A., Wertman, K. and Drubin, D.G. (1994). Mapping actin surfaces required for functional interactions *in vivo*. J. Cell Biol. 126:423-432.

Holtzman, D.A., Yang, S. and Drubin, D.G. (1996). J. Cell Biol. 122:635-644.

Honts, J., Sandrock, T., Brower, S., O'Dell, J. and Adams A.E.M. (1994). Actin mutations that show suppression with fimbrin mutations identify a likely fimbrin binding site on actin. J. Cell Biol. 126:413-422.

Howard, T., Chaponnier, C., Yin, H. and Stossel, T. (1990). Gelsolin-actin interaction and actin polymerization in human neutrophils. J. Cell Biol. 110:1983-1991.

Huang, C-F., Chen, C-C., Tung, L., Buu, L-M. and Lee, F-J.S. (2001). The yeast ADP-ribosylation factor GAP, Gsc1p, is involved in maintenance of mitochondrial morphology. J. Cell Sci. 115:275-282.

Huang, M., Yang, C., Schafer, D.A., Cooper, J.A., Higgs, H.N. and Zigmoid, S.H. (1999). Cdc42-induced actin filaments are protected from capping protein. Curr. Biol. 9:979-982.

Hug, C., Jay, P.Y., Reddy, I., McNally, J.G., Bridgman, P.C., Elson, E.L. and Cooper, J.A. (1995). Capping protein levels influence actin assembly and cell motility in *Dictyostelium*. Cell 81:591-600.

Iida, K., Moriyama, K., Matsumoto, S., Kawasaki, H., Nishida, E. and Yahara, I. (1993). Isolation of a yeast essential essential gene, COF1, that encodes a homologue of mammalian cofilin, a low-M(r) actin-binding and depolymerizing protein. Gene 124:115-120.

Imamura, H., Tanaka, K., Hihara, T., Umikawa, M., Kamei, T., Takahashi, K., Sasaki, T. and Takai, Y. (1997). Bni1p and Bnr1p: downstream targets of the Rho family small G-proteins which interact with profilin and regulate the actin cytoskeleton in *Saccharomyces cerevisiae*. EMBO J. 16:2745-2755.

Ito, H., Fukada, Y., Murata, K. and Kimura, A. (1993). Transformation of intact yeast cells treated with alkali cations. J. Bacteriol. 153:163-168.

Ito, T., Tashiro, K., Muta, S., Ozawa, R., Chiba, T., Nishizawa, M., Yamamoto, K., Kuhara, S. and Sakaki, Y. (2000) Toward a protein-protein interaction map of the budding yeast: A comprehensive system to examine two-hybrid interactions in all possible combinations between the yeast proteins. Proc. Natl. Acad. Sci. USA. 97:1143-1147.

Ito, T., Chiba, T., Ozawa, R., Yoshida, M., Hattori, M. and Sakaki, Y. (2001) A comprehensive two-hybrid analysis to explore the yeast protein interactome. Proc. Natl. Acad. Sci. USA. 98:4569-4574.

James, P., Halladay, J. and Craig, E.A. (1996) Genomic libraries and a host strain designed for highly efficient two-hybrid selection in yeast. Genetics 144:1425-1436.

Johnston, G.C., Prendergast, J.A. and Singer, R.A. (1991). The *Saccharomyces cerevisiae MYO2* gene encodes an essential myosin for vectorial transport of visicles. J. Cell Biol 113:539-551.

Kabsch, W., Mannherz, H.G., Suck, D., Pai, E.F. and Holmes, H.C. (1990). Atomic structure of the actin:DNaseI complex. Nature 347:37-44.

Kaksonen M, Peng HB, Rauvala H. (2000) Association of cortactin with dynamic actin in lamellipodia and on endosomal vesicles. J Cell Sci.113:4421-6

Kalchman, M.A., Koide, H.B., McCutcheon, K., Graham, R.K., Nichol, K., Nishiyama, K., Kazemi-Esfarjani, P., Lynn, F.C., Wellington, C., Metzler, M. Goldberg, Y.P., Kanazawa, I., Gietz, R.D. and Hayden MR (1997) HIP1, a human homologue of S.cerevisiae Sla2p, interacts with membrane-associated huntingtin in the brain. Nat. Genet. 16:44-53.

Kang, F., Purich, D.L. and Southwick, F.S. (1999). Profilin promotes barbed-end actin filament assembly without lowering the critical concentration. J. Biol. Chem. 274:36963–36972.

Karpova, T., Tatchell, K. and Cooper, J. (1995). Actin filaments in yeast are unstable in the absence of capping protein. J. Cell Biol. 131:1483-1493.

Karpova, T., McNally, J., Moltz, S. and Cooper, J. (1998) Assembly and function of the actin cytoskeleton of yeast: relationships between cables and patches. J. Cell Biol. 142:1501-1517.

Karpova, T.S., Reck-Peterson, S.L., Elkind, N.B., Mooseker, M.S., Novick, P. and Cooper, J.A. (2000). Role of actin and Myo2p in polarised secretion and growth of *Saccharomyces cerevisiae*. Mol. Biol. Cell 11:1727-1737.

Kelleher, J.F., Atkinson, S.J. and Pollard, T.D. (1995). Sequences, structural models and cellular localisation of the actin-related proteins Arp2 and Arp3 from *Acanthamoeba*. J.Cell Biol. 131:385-397.

Kessels, M.M., Engqvist-Goldstein, Å.E.Y. and Drubin, D.G. (2000). Association of mouse actin-binding protein 1 (mAbp1/SH3P7), an Src kinase target, with dynamic regions of the cortical actin cytoskeleton in response to Rac1 activation. Mol. Biol. Cell 11:393-412.

Kessels, M.M., Engqvist-Goldstein, Å.E.Y., Drubin, D.G. and Qualmann, B. (2001) Mammalian Abp1, a signal-responsive F-actin binding protein, links the actin cytoskeleton to endocytosis via the GTPase dynamin.

Kilmartin, J. and Adams, A. (1984). Structural rearrangements of tubulin and actin during the cell cycle of *Saccharomyces cerevisiae*. J. Cell Biol. 98:922-933.

Kim, E., Miller, C.J. and Reisler, E. (1996). Polymerization and *in vitro* motility properties of yeast actin: a comparison with rabbit skeletel α-actin. Biochemistry 35:16566-16572.

Kirshhausen, T. (2000). Clathrin. Annu. Rev. Biochem. 69:699-727.

Kohno, H., Tanaka, K., Mino, A., Umikawa, M., Imamura, H., Fujiwara, T., Fujita, Y., Hotta, K., Qadota, H., Watanabe, T., Ohya, Y. and Takai, Y. (1996). Bni1p implicated in cytoskeletal control is a putative target of Rho1p small GTP-binding protein in *Saccharomyces cerevisiae.* EMBO J. 15:6060-6068.

Koning AJ., Lum, P.Y., Williams, J.M. And Wright, R. (1993) $DiOC_6$ staining reveals organelle structure and dynamics in living yeast cells. Cell Motil. Cytoskeleton 25:111-128.

Kron, S.J., Drubin, D.G., Botstein, D. and Spudich, J.A. (1992). Yeast actin filaments display ATP-dependent sliding movement oversurfaces coated with rabbit muscle myosin. Proc. Natl. Acad. Sci. USA 89:4466-4470.

Kron, S. and Gow, N. (1995) Budding yeast morphogenesis: signaling, cytoskeleton and cell cycle. Curr. Opin. Cell Biol. 7:845-855.

Kubler, E. and Reizman, H. (1993) Actin and fimbrin are required for the internalization step of endocytosis in yeast. EMBO J. 12:2855-2862.

Lamaze, C., Fujimoto, L.M., Yin, H.L. and Schmid, S.L. (1997). The actin cytoskeleton is required for receptor-mediated endocytosis in mammalian cells. J. Biol. Chem. 272:20332-20335.

Lanzetti, L., Di Fiore, P.P. and Scita, G. (2001) Pathways linking endocytosis and actin cytoskeleton in mammalian cells. Exp. Cell Res. 271:45-56.

Lappalainen, P. and Drubin, D.G. (1997). Cofilin promotes rapid actin filament turnover *in vivo*. Nature 388:78-82.

Lappalainen, P., Fedorov, E.V., Fedorov, A.A., Almo, S.C. and Drubin, D.G. (1997). Essential functions and actin-binding surfaces of yeast cofilin revealed by systematic mutagenesis. EMBO J. 16:5520-5530.

Lappalainen, P., Kessels, M.M., Cope, M.J.T.V. and Drubin, D.G. (1998). The ADF homology (ADF-H) domain: a highly expoited actin-binding module. Mol. Biol. Cell 9:1951-1959.

Larson, S.M. and Davidson, A.R. (2000) The identification of conserved interactions within the SH3 domain by alignment of sequences and structures. Protein Science 9:2170-2180.

Lazzarino, D.A., Boldogh, I., Smith, M.G., Rosand, J. and Pon, L.A. (1994). Yeast mitochondria contain ATP-sensitive, reversible actin-binding activity. Mol. Biol. Cell 5:807-818.

Lechler, L. and Li. R. (1997) *In vitro* reconstitution of cortical actin assembly sites in budding yeast. J. Cell Biol. 138:95-103.

Lechler, T., Shevchenko, A., Schevchenko, A. and Li, R. (2000). Direct involvment of yeast type I myosins in Cdc42-dependent actin polymerisation. J. Cell Biol. 148(2):363-373.

Lechler, T., Jonsdottir, G.A., Klee, S.K., Pellman, D. and Li, R. (2001) A two-tiered mechanism by which Cdc42p controls the localization and activation of an Arp2/3-activating motor complex in yeast. J. Cell Biol. 155:261-270.
Li, R., Zheng, Y. and Drubin, D. (1995) Regulation of cortical actin cytoskeleton assembly during polarized cell growth in budding yeast. *J. Cell Biol.* 128:599-615.

Li, R. (1997). Bee1, a yeast protein with homology to Wiskott-Aldrich syndrome protein, is critical for the assembly of cortical actin cytoskeleton. J. Cell Biol. 136:649-658.

Lila, T. and Drubin, D.G. (1997). Evidence for physical and functional interactions among two *Saccharomyces cerevisiae* SH3 domain proteins, an adenylyl cyclase-associated protein and the actin cytoskeleton. Mol. Biol. Cell 8:367-385

Liu, H. and Bretscher, A. (1989) Disruption of the single tropomyosin gene in yeast results in the disappearance of actin cables from the cytoskeleton. Cell 57:233-242.

Liu, H. and Bretscher, A. (1992). Characterisation of *TPM1* disrupted yeast cells indicates an involvement of tropomyosin in directed vesicular transport. J. Cell Biol. 118:285-299.

Loisel, T.P., Boujemaa, R., Pantaloni, D. and Carlier, M.F. (1999) Reconstitution of actin-based motility of Listeria and Shigella using pure proteins. Nature 401:613-616.

Longtine, M.S., McKenzie, A., Demarini, D.J., Shah, N.G., Wach, A., Brachat, A., Philippsen, P. and Pringle, J.R. (1998). Additional modules for versatile and economical PCR-based gene deletion and modification in *Saccharomyces cerevisiae*. Yeast 14:953-961.

Lorenz, M., Popp, D. and Holmes, K. (1993). Refinement of the F-actin model against X-ray fiber diffraction data by the use of a directed mutation algorithm. J. Mol. Biol. 234:826-836.

Ma, L., Rohatgi, R. and Kirschner, M.W. (1998). The Arp2/3 complex mediates actin polymerization induced by the small GTP-binding protein Cdc42. Proc. Natl. Acad. Sci. USA 95:15362-15367.

Machesky, L.M. and Gould, K.L. (1999). The Arp2/3 complex: a multifunctional actin organizer Curr. Opin. Cell Biol. 11:117-121.

Machesky, L.M. Mullins, R.D. , Higgs, H.N., Kaiser, D.A., Blanchoin, L., May R.C., Hall, M.E. and Pollard, T.D. (1999) WASP-related protein Scar activates dendritic nucleation of actin filaments by Arp2/3 complex. Proc. Natl. Acad. Sci. USA 96:3739-3744.

Machesky, L.M. and Insall, R.H. (1998) Scar1 and the related Wiskott-Aldrich syndrome protein, WASP, regulate the actin cytoskeleton through Arp2/3 complex. Curr. Biol. 8:1347-1356.

Machesky, L.M., Atkinson, S.J., Ampe, C., Vandekerckhove. J. and Pollard, T.D. (1994). Purification of a cortical complex containing two unconventional actins from *Acanthamoeba* by affinity chromatography on profilin-agarose. J. Cell Biol. 127:107-115.

Maciver, S.K. (1998a) How ADF/cofilin depolymerizes actin filaments. Curr. Opin. Cell Biol. 10:140-144.

Maciver, S.K. Pope, B.J., Whytock, S. and Weeds, A.G. (1998b) The effect of two actin depolymerizing factors (ADF/cofilin) on actin filament turnover: pH sensitivity of F-actin binding by human ADF, but not of *Acanthamoeba* actophorin. Eur. J. Biochem. 256:388-397.

Madania, A., Moreau, V., Martin, R.P. and Winsor, B. (1997). *LAS17* is a multicopy suppressor of *S. cerevisiae arp2-5*. Yeast 13:S144.

Madania, A., Dumoulin, P., Grava, S., Kitamoto, H., Scharer-Brodbeck, C., Soulard, A., Moreau, V. and Winsor, B. (1999) The *S. cerevisiae* homologue of human Wiskott-Aldrich syndrome protein Las17p interacts with the Arp2/3 complex. Mol. Biol. Cell 10:3521-3538.

Madden, K. and Snyder, M. (1998) Cell polarity and morphogenesis in budding yeast. Annu. Rev. Microbiol. 52:687-744.

May, R.C. (2001). The Arp2/3 complex: a central regulator of the actin cytoskeleton. Cell Mol. Life Sci. 11:1607-1626.

Mayer, B.J. (2001) SH3 domains: complexity in moderation. J. Cell Sci. 114:1253-1263

McCann, R.O. and Craig, S.W. (1997) The I/LWEQ module: a conserved sequence that signifies F-actin binding in functionally diverse proteins from yeast to mammals. Proc. Natl. Acad. Sci. USA. 94:5679-5684.

McCann, R.O. and Craig, S.W. (1997) Functional genomic analysis reveals the utility of the I/LWEQ module as a predictor of protein:actin interaction. Biochem. Biophys. res. Commun. 266:135-140.

McGavin, M.K.H., Badour, K., Hardy, L.A., Kubiseski, T.J., Zhang, J. and Siminovitch, K.A. (2001) The intersectin 2 adaptor links Wiskott Aldrich syndrome protein (WASp)-mediated actin polymerization to T cell antigen receptor endocytosis. J. Exp. Med. 194:1777-1787.

McLaughlin, P.J., Gooch, J.T., Mannherz, H.G. and Weeds, A.G. (1993). Structure of gelsolin fragment 1-actin complex and the mechanism of filament severing. Nature 364:685-692.

McMahon, H.T., Wigge, P. and Smith, C. (1997) Clathrin interacts specifically with amphiphysin and is displaced by dynamin. FEBS Lett. 413:319-322.

Meagher, R.B. and Williamson, R.E. (1994). The Plant Cytoskeleton. In: Arabidopsis. ed. E. Meyerowitz, C. Somerville, Cold Spring Harbor, NY: Cold Spring Harbor Laboratory Press, 1049-1084.

Metzler, M., Legendre-Guillemin, V., Gan, L., Chopra, V., Kwok, A., McPherson, P.S. and Hayden, M.R. (2001) HIP1 functions in clathrin-mediated endocytosis through binding to clathrin and adaptor protein 2. J. Biol. Chem. 276:39271-39276.

Miki, H., Yamaguchi, H., Suetsugu, S. and Takenawa, T. (2000) ISRp53 is an essential intermediate between Rac and WAVE in the regulation of membrane ruffling. Nature 408:732-735.

Miki, H., Suetsugu, S. and Takenawa, T. (1998). WAVE, a novel WASP-family protein involved in actin reorganization induced by Rac. EMBO J. 17:6932-6941.

Miki, H. and Takenawa, T. (1998b) Direct binding of the verprolin-homology domain in N-WASP to actin is essential for cytoskeletal reorganization. *Biochem. Biophys.* Res Commun. 243:73-78.

Miki, H., Sasaki, T, Taki, Y. and Takenawa, T. (1998c) Induction of filopodium formation by a WASP-related actin-depolymerizing protein N-WASP. Nature 391:93-96.

Miki, H., Miura, K. and Takenawa, T. (1996) N-WASP, a novel actin-depolymerizing protein, regulates the cortical cytoskeletal rearrangement in a PIP2-dependent manner downstream of tyrosine kinases EMBO J. 15:5326-5335.

Mockrin and Korn, (1980). Acanthamoeba profilin interacts with G-actin to increase the rate of exchange of actin-bound adenosine 59-triphosphate. Biochemistry. 19:5359–5362.

Moon, A.L., Janmey, P.A., Louie, K.A. and Drubin, D.G. (1993). Cofilin is an essential component of the yeast cortical cytoskeleton. J. Cell Biol. 120:421-435.

Moore, P.B., Huxley, H.E. and DeRosier, D.J. (1970). J. Mol. Biol. 50:279-295.

Moreau, V., Madania, A., Martin, R.P. and Winsor, B (1996). The *Saccharomyces cerevisiae* actin-related protein Arp2 is involved in the actin cytoskeleton. J. Cell Biol. 134:117-132.

Moreau, V., Galan, J.M., Devilliers, G., Haguenauer-Tsapis, R. and Winsor, B. (1997). The yeast actin-related protein Arp2p is required for the internalization step of endocytosis. Mol. Biol. Cell 8:1361-1375.

Morton, W.M., Ayscough, K.R. and McLaughlin, P.J. (2000). Latrunculin alters the actin-monomer subunit interface to prevent polymerization Nature Cell Biol. 2:376-378.

Mulholland, J., Wesp, A., Reizman, H. and Botstein, D. (1997) Yeast actin cytoskeleton mutants accumulate a new class of Golgi-derived secretory vesicle. Mol. Biol. Cell 8:1481-1499.

Mullins, R.D., Heuser, J.A. and Pollard, T.D. (1998). The interaction of Arp2/3 complex with actin: nucleation, high affinity pointed end capping, and formation of branching networks of filaments. Proc. Natl. Acad. Sci. USA 96:6181-6186.

Mullins, R.D., Kelleher, J.F., Xu, J. and Pollard, T.D. (1998b). Arp2/3 complex from *Acanthamoeba* binds profilin and cross-links actin filaments. Mol. Biol. Cell 9:841-852.

Mullins, R.D. and Pollard, T.D. (1999) Rho-family GTPases require the Arp2/3 complex to stimulate actin polymerization in *Acanthamoeba* extracts. Curr. Biol. 9:405-415.

Mullins, R.D. (2000) How WASP-family proteins and the Arp2/3 complex convert intracellular signals into cytoskeletal structures. Curr. Opin. Cell Biol. 12:91-96.

Munn, A.L., Stevenson, B.J., Geli, M.I. and Riezman, H. (1995). *end5*, *end6* and *end7*: mutations that cause actin delocalization and block the internalization step of endocytosis in *Saccharomyces cerevisiae*. Mol. Biol. Cell 6:1721-1742.

Munn, A.L. (2000) The yeast endocytic membrane transport system. Micros. Res. Tech. 51:547-562.

Munn, A.L. (2001) Molecular requirements for the internalisation step of endocytosis: insights from yeast. Biochim. Biophys. Acta. 1535:236-257.

Na, S., Hincapie, M., M^{c}Cusker, J.H. and Haber, J.E. (1995) *MOP2* (*SLA2*) affects the abundance of the plasma membrane H^{+}-ATPase of *Saccharomyces cerevisiae.* J. Biol. Chem. 270:6815-6823.

Naqvi, S.N., Zahn, R., Mitchell, D.A., Stevenson, B.J. and Munn, A.L. (1998) The WASp homologue Las17p functions with the WIP homologue End5p/verprolin and is essential for endocytosis in yeast. Curr. Biol. 8:959-962.

Nefsky,B. and Bretscher, A. (1992). Yeast actin is relatively well behaved. Eur. J. Biochem. 206:949-955.

Ng, R. and Abelson, J. (1980). Isolation and sequence of the gene for actin in *Saccharomyces cerevisiae.* Proc. Natl. Acad. Sci. USA. 77:3912-3916.

Novick, P. and Botstein, D. (1985) Phenotypic analysis of temperature-sensitive yeast actin mutants. Cell 40:405-416.

Olazabal IM, Machesky LM. (2001) Abp1p and cortactin, new "hand-holds" for actin. J. Cell Biol. 154:679-82.

Orlean, P. (1997) Biogenesis of yeast wall and surface components. In *The Molecular and Cellular Biology of the Yeast Saccharomyces: Cell Cycle and Cell Biology* (ed. J. Pringle, J. Broach and E.Jones) pp 229-362. Cold Spring Harbor: Cold Spring Harbor Press.

Orlova, A., Galkin, V.E., VanLoock, M.S., Kim, E., Shvetsov, A., Reisler, E. and Egelman, E.H. (2001). Probing the structure of F-actin: crosslinks constrain atomic models and modify actin dynamics. J. Mol. Biol. 312:95-106.

Palmer, R.E., Sullivan, D.S. Huffaker, T., and Koshland, D. (1992) Role of astral microtubules and actin in spindle orientation and migration in the budding yeast, *Saccharomyces cerevisiae.* J. Cell Biol. 119:583-593.

Palmgren, S., Vartiainen, M. and Lappalainen, P. (2002) Twinfilin, a molecular mailman for actin monomers. J. Cell Sci. 115:881-886.

Pandey, A. and Mann, M. (2000) Proteomics to study genes and genomes. Nature 405:837-846.

Pantaloni, D., and M.-F. Carlier. (1993). How profilin promotes actin filament assembly in the presence of thymosin b-4. Cell. 75:1007–1014.

Pantaloni, D., Boujemaa, R., Didry, D., Gounon, P. and Carlier, M-P. (2000). The Arp2/3 complex branches filament barbed ends: functional antagonism with capping proteins. Nature Cell Biol. 2:385-391.

Pawson, T. and Schlessinger J. (1993) SH2 and SH3 domains. Curr. Biol. 3:434-442.

Pearse, B.M. and Robinson, M.S. (1990). Clathrin, adaptors and sorting. Annu. Rev. Cell Biol. 6:151-171.

Pollard, T.D., Blanchoin, L. and Mullins, R.D. (2000) Molecular mechanisms controlling filament dynamics in nonmuscle cells. Annu. Rev. Biophys. Biomol. Struct. 29:545-76.

Poon, P.P., Wang, X., Rotman, M., Huber, I., Cukierman, E., Cassel, D., Singer, R.A. and Johnston, G.D. (1996). Saccharomyces cerevisiae Gcs1 is an ADP-ribosylation factor GTP-ase activating protein. Proc. Natl. Acad. Sci. USA 93:10074-10077.

Pruyne, D.W., Schott, D.H. and Bretscher, A. (1998). Tropomyosin-containing actin cables direct the Myo2p-dependent polarised delivery of secretory vesicles in budding yeast. J.Cell Biol. 143, 1931-1945.

Pruyne, D. and Bretscher, A. (2000a) Polarization of cell growth in yeast I. Establishment and maintenance of polarity states. J. Cell Sci. 113:365-375.

Pruyne, D. and Bretscher, A. (2000b) Polarization of cell growth in yeast II. The role of the cortical actin cytoskeleton. J.Cell Sci. 113:571-585.

Qadota, H., Python, C.P., Inoue, S.B., Arisawa, M., Anraku, Y., Watanabe, T., Levin, D.E. and Ohya, Y. (1996). Identification of yeast rho1p GTPase as a regulatory subunit of 1,3-β-glucan synthase. Science 272:279-281.

Qiao, L.Y., Goldberg, J.L., Russell, J.C. and Sun, X.J. (1999). Identification of enhanced serine kinase activity in insulin resistance. J. Biol. Chem. 274:10625-10632.

Qualmann, B., Roos, J., DiGregorio, P.J. and Kelly, R.B. (1999). Syndapin I, a synaptic dynamin-binding protein that associates with the neural Wiskott-Aldrich syndrome protein. Mol. Biol. Cell 10:501-513.

Qualmann, B. and Kelly, R.B. (2000). Syndapin isoforms participate in receptor-mediated endocytosis and actin organisation. J. Cell Biol. 148:1047-1061.

Qualmann, B., Kessels, M.M. and Kelly, R.B. (2000) Molecular links between endocytosis and the actin cytoskeleton. J. Cell Biol. 150:F111-F116.

Raths, S., Rohrer, J., Crausaz, F. and Riezman, H. (1993). *end3* and *end4*: two mutants defective in receptor-mediated and fluid phase endocytosis in *Saccharomyces cerevisiae*. J. Cell Biol. 120:55-65.

Reck-Peterson, S.L., Tyska, M.J., Novick, P.J. and Mooseker, M.S. (2001). The yeast class V Myo2p and Myo4p, are nonprocessive actin-based motors. J.Cell Biol. 153(5):1121-1126.

Ren, R., Mayer, B.J., Cicchetti, P. and Baltimore, D. (1993) Indentification of a ten-amino acid proline-rich SH3 binding site. Science 259:1157-1161.

Reneke, J., Blumer, K., Courchesne, W. and Thorner, J. (1988). The carboxy-terminal segment of the yeast α-factor receptor is a regulatory domain. Cell 55:221-234.

Ridley, A.J., Patterson, H.F., Johnston, C.L., Diekmann, D. and Hall, A. (1992) The small GTP-binding protein Rac regulates growth factor induced membrane ruffling. Cell 70:401-410.

Riezman, H. (1985). Endocytosis in yeast: several of the yeast secretory mutants are defective in endocytosis. Cell 40:1001-1009.

Robinson, R.C., Turbedsky, K., Kaiser, D.A., Marchand, J-P., Higgs, H.N., Choe, S. and Pollard, T.D. (2001). Crystal structure of Arp2/3 complex. Science 294:1679-1684.

Rocco, V. (1993) Indentification of two divergently transcribed genes centromere-proximal to the *ARG4* locus on chromosome VIII of *Saccharomyces cerevisiae*. Yeast 9:1111-1120.

Rodal, A.A., Tetreault, J.W., Lappalainen, P., Drubin, D.G. and Amberg, D.C. (1999) Aip1p interacts with cofilin to disassemble actin filaments. J. Cell Biol. 145:1251-1264.

Rodriguez, J.R. and Paterson, B.M. (1990). Yeast myosin heavy chain mutant: maintenance of the cell type specific budding pattern and the deposition of chitin and cell wall components requires an intact myosin heavy chain gene. Cell Motil. Cytoskel. 17:301-308.

Sagot, I., Klee, S.K. and Pellman, D. (2002). Yeast formins regulate cell polarity by controlling the assembly of actin cables. Nat. Cell Biol. 4:42-50.

Salcini, A.E., Confalonieri, S., Doria, M., Santolini, E., Tassi, E., Minenkova, O., Cesarini, G., Pelicci, P.G. and Di Fiore, P.P. (1997) Binding specificity and in vivo targets of the EH domain, a novel protein-protein interaction module. Genes Dev. 11:2239-2249.

Scalettar, B.A., Swedlow, J.R., Sedat, J.W. and Agard, D.A. (1996). Dispersion, aberration and deconvolution in multi-wavelength fluorescence images. J. Microsc. 182:50-60.

Schafer, D.A., Jennings, P.B. and Cooper, J.A. (1996). Dynamics of capping protein and actin assembly in vitro – uncapping barbed ends by polyphosphoinositides. J. Cell Biol. 135:169-179.

Schmid, S.L. (1997). Clathrin-coated vesicle formation and protein sorting: an integrated process. Annu. Rev. Biochem. 66:511-548.

Schutt, C.E., Myslik, J.C., Rozycki, M.D., Goonesekere, N.C.W. and Lindberg, U. (1993). The structure of crystalline profilin-β-actin. Nature 365:810-816.

Segal, M. and Bloom, K. (2001) Control of Spindle Polarity and Orientation in *Saccharomyces cerevisiae* Trends Cell Biol. 11(4):160-6.

Shaw, J.D., Cummings, K.B., Huyer, G., Michaelis, S. and Wendland, B. (2001) Yeast as a model system for studying endocytosis. Exp. Cell Res. 271:1-9..

Shortle, D., Haber, J.E. and Botstein, D. (1982). Lethal disruption of the yeast actin gene by integrative DNA transformation. Science 217:371-372.

Simon, V.R., Swayne, T.C. and Pon, L. (1995). Actin-dependent mitochondrial motility in mitotic yeast and cell-free systems: identification of a motor activity on the mitochondrial surface. J. Cell. Biol. 130:345-354.

Simon, V., Karmon, S. and Pon, L. (1997). Mitochondrial inheritence: cell cycle and actin cable dependence of polarized mitochondrial movements in *Saccharomyces cerevisiae*. Cell Motil. Cytoskel. 37:199-210.

Singer, B. and Reizman, H. (1990) Detection of an intermediate compartment involved in transport of α-factor from the plasma membrane to the vacuole in yeast. J. Cell Biol. 110:1911-1922.

Singer-Kruger, B., Frank, R., Crausaz, F., Riezman. H. (1993) Partial purification and characterization of early and late endosomes from yeast. Indentification of four novel proteins. J. Biol. Chem. 268:14376-14386.

Small, J.V., Rottner, K. and Kaverina, I. (1999) Functional design in the actin cytoskeleton. Curr. Opin. Cell Biol. 11:54-60.

Smith, M.G., Simon, V.R.O., Sullivan, H. and Pon, L.A. (1995). Organelle-cytoskeleton interactions: actin mutations inhibit meiosis-dependent mitochondrial rearrangement in the budding yeast *Saccharomyces cerevisiae*. Mol. Biol. Cell 6:1381-1396.

Smith, M.G., Swamy, S.R. and Pon, L.A. (2001) The life cycle of actin patches in mating yeast. J. Cell Sci. 114:1505-1513.

Southwick, F.S. (2000) Gelsolin and ADF/cofilin enhance the actin dynamics of motile cells. Proc. Natl. Acad. Sci. USA 97:6936-6938.

Svitkina, T.M. and Borisy, G.G. (1999). Arp2/3 complex and actin depolymerizing factor/cofilin in dendritic organization and treadmilling of actin filament array in lamellopodia. J.Cell Biol. 145:1009-1026.

Tan, P.K., Howard, J.P. and Payne, G.S. (1996) The sequence NPFXD defines a new class of endocytosis signal in *Saccharomyces cerevisiae*. 135:1789-1800.

Tang, H.-Y. and Cai, M. (1996) The EH-domain-containing protein Pan1 is required for normal organization of the actin cytoskeleton in *Saccharomyces cerevisiae*. Mol. Cell. Biol. 16:4897-4914.

Tang, H.-Y., Munn, A. and Cai, M. (1997) EH domain proteins Pan1p and End3p are components of a complex that plays a dual role in organization of the cortical actin cytoskeleton and endocytosis in *Saccharomyces cerevisiae*. Mol. Cell Biol. 17:4294-4304.

Tang, H.-Y., Xu, J. and Cai, M. (2000) Pan1p, End3p, and Sla1p, three yeast proteins required for normal cortical actin cytoskeleton organisation, associate with each other and play essential roles in cell wall morphogenesis. Mol. Cell. Biol. 20:12-25.

Theesfield, C., Irazoqui, J., Bloom, L. and Lew, D. (1999). The Role of Actin in Spindle Orientation Changes during the *Saccharomyces cerevisiae* cell cycle. J. Cell. Biol. 146:1019-1032.

Theriot, J.A. and Michison, T.J. (1993). The 3 faces of profilin. Cell 75:835-838.

Theriot, J.A., Rosenblatt, J., Portnoy, D.A., Goldschmidt-Clermont, P.J. and Michison, T.J. (1994) Involvement of profilin in the actin-based motility of *L. monocytogenes* in cells and in cell-free extracts. Cell 76:505-517.

Theriot, J.A. (1997) Accelerating on a treadmill:ADF/cofilin promotes rapid actin filament turnover in the dynamic cytoskeleton. J. Cell Biol. 136:1165-1168.

Uetz, P., Glot, L., Cagney, G., Mansfield, T.A., Judson, R.S., Knight, J.R., Lockshon, D., Narayan, V., Srinivasan, M., Pochart, P., Qureshi-Emill, A., Li, Y., Godwin, B., Conover, D., Kalbfleisch, T. Vijayadamodar, G., Yang, M., Johnstone, M., Fields, S. and Rothberg, J.M. (2000) A comprehensive analysis of protein-protein interactions in *Saccharomyces cerevisiae*. Nature:403:623-627.

Urono, T., Liu, J., Zhang, P., Fan Yx, Y., Egile, C., Li, R. Mueller, S.C. and Zhan, X. (2001) Activation of Arp2/3 complex-mediated actin polymerization by cortactin. Nat. Cell Biol. 3:259-266.

Vaduva, G., Martin, N.C. and Hopper, A.K. (1997) Actin-binding verprolin is a polarity development protein required for the mophogenesis and function of the yeast actin cytoskeleton. J. Cell Biol. 139:1821-1833.

Vaduva, G., Martinez-Quiles, N., Anton, I.M., Martin, N.C., Geha, R.S., Hopper, A.K. and Ramesh, N. (1999) The human WASP-interacting protein, WIP, activates the cell polarity pathway in yeast. J. Biol. Chem. 274:17103-17108.

van den Ent F, Amos LA, Lowe J. (2001) Prokaryotic origin of the actin cytoskeleton. Nature 413:39-44.

van Delft, S., Govers, R., Strous, G.J., Verkleij, G.J. and van Bergen en Henengouwen, P.M. (1997). Epidermal growth factor induces ubiquitination of Eps15. J. Biol. Chem. 272:14013-14016.

Verheyen, E.M. and Cooley, L. (1994). Profilin mutations disrupt multiple actin-dependent processes during Drosophila development. Development 120:717-728.

Vida, T.A. and Emr, S.D. (1995). A new vital stain for visualizing vacuolar membrane dynamics and endocytosis in yeast. J. Cell Biol. 128:779-792.

Waddle, J.A., Karpova, T.S., Waterston, R.H. and Cooper, J. (1996). Movement of cortical actin patches in yeast. J. Cell Biol. 132:861-870.

Waelter, S., Scherzinger, E., Hasenbank, R., Nordhoff, E., Lurz, R., Goehler, H., Gauss, C., Sathasivam, K., Bates, G.P., Lehrach, H. and Wanker, E.E. (2001). The huntintin interacting protein HIP1 is a clathrin and α-adaptin-binding protein involved in receptor-mediated endocytosis. Hum. Mol. Genet. 10:1807-1817.

Wanker, E.E., Rovira, C., Scherzinger, E., Hasenback, R., Wälter, S., Tait, D., Colicelli, J. and Lehrach, H. (1997) HIP-I: a huntingtin interacting protein isolated by the yeast two-hybrid system. Hum. Mol. Genet. 6:487-495.

Warren, D.T., Andrew, P.D., Gourlay, C.W. and Ayscough, K.R. (2002). Sla1p couples the yeast endocytic machinery to proteins regulating actin dynamics. J. Cell Sci. 115:1703-1715.

Watson, H.A., Cope, M.J.T.V., Groen, A.C., Drubin, D.G. and Wendland, B. (2001) In vivo role for actin-regulating kinases in endocytosis and yeast epsin phosphorylation. Mol. Biol. Cell. 12:3668-3679.

Weaver, A.M., Karignov, A.V., Kinley, A.W., Weed, S.A., Li, Y., Parsons, J.T. and Cooper, J.A. (2001) Cortactin promotes and stabilises Arp2/3-induced actin filament network formation. Curr. Biol. 11:370-374.

Weeds, A. and Maciver, S. (1993). F-actin capping proteins. Curr. Opin. Cell Biol. 5:63-69.

Weed, S.A., Karginov, A.V., Schafer, D.A., Weaver, A.M., Kinley, A.W., Cooper, J.A. and Parsons, J.T. (2000) Cortactin localises to sites of actin assembly in lamellipodia requires interactions with F-actin and the Arp2/3 complex. J. Cell Biol. 151:29-40.

Weed, S.A. and Parsons, J.T. (2001) Cortactin: coupling membrane dynamics to cortical actin assembly Oncogene 20:6418-34

Welch, M.D., Rosenblatt, J., Skoble, J., Portnoy, D.A. and Mitchison, T.J. (1998). Interaction of human Arp2/3 complex and the *Listeria monocytogenes* ActA protein in actin filament nucleation. Science 281:105-108.

Welch, M.D., Iwamatsu, A. and Mitchison, T.J. (1997) Actin polymerization is induced by Arp2/3 protein complex at the surface of *Listeria monocytogenes* Nature 385:265-269.

Wendland, B., McCaffery, J.M., Xiao, Q. and Emr, S (1996) A novel fluorescence-activated cell sorter-based screen for yeast endocytosis mutants identifies a yeast homologue of mammalian eps15. J. Cell Biol. 135:1485-1500.

Wendland, B. and Emr, S. (1998) Pan1p, yeast Eps15, functions as a multivalent adaptor that coordinates protein-protein interactions essential for endocytosis. J. Cell Biol. 141:71-84.

Wendland, B., Emr, S. and Reizman, H. (1998) Protein traffic in the yeast endocytic and vacuolar sorting pathways. Curr. Opin. Cell Biol. 10:513-522.

Wertman, K.F., Drubin, D.G. and Botstein, D. (1992) Systematic mutational analysis of the yeast *ACT1* gene. Genetics 132:337-350.

Wesp, A., Hicke, L., Palecek, J., Lombardi, R., Aust, T., Munn, A.L., and, Riezman. H (1997). End4p/Sla2p Interacts with Actin-associated Proteins for Endocytosis in *Saccharomyces cerevisiae*. Mol. Biol. Cell. 8:2291-2306.

Whitacre, J., Davis, D., Toenjes, K., Brower, S. and Adams, A. (2001) Generation of an isogenic collection of yeast actin mutants and identification of three interrelated phenotypes. Genetics 157:533-543.

Wieland, T. and Fulstich, H. (1978). Amatoxins, phallotoxins, phallolysin, and antamide: the biologically active components of poisonous *Amanita* mushrooms. CRC Crit. Rev. Biochem. 5:185-260.

Wigge, P. and McMahon, H.T. (1998) The amphiphysin family of proteins and their role in endocytosis at the synapse. Trends Neurosci. 21:339-344.

Winsor, B. and Schiebel, E. (1997) Review: An Overview of the *Saccharomyces cerevisiae* Microtubule and Microfilament Cytoskeleton. Yeast 13:399-434.

Winter, D., Lechler, T. and Li, R. (1999). Activation of the yeast Arp2/3 complex by Bee1p, a WASP-family protein. Curr. Biol. 9:501-504.

Winter, D.C., Choe, E.Y. and Li. R. (1999b) Genetic dissection of the budding yeast Arp2/3 complex: a comparison of the in vivo and structural roles of individual subunits. Proc. Natl. Acad. Sci. USA 96:7288-7293.

Winter, D., Podtelejnikov, A.V., Mann, M. and Li, R. (1997). The complex containing actin-related proteins Arp2 and Arp3 is required for the motility and integrity of yeast actin patches. Curr. Biol. 7:519-529.

Wolven, A.K., Belmont, L.D., Mahoney, N.M., Almo, S.C. and Drubin, D.G. (2000). *In Vivo* Importance of Actin Nucleotide Exchange Catalyzed by Profilin. J. Cell Biol. 150:895-903.

Wulf, E., Deboben, A., Bautz, F.A., Faulstich, H. and Wieland, T. (1979) Fluorescent phallotoxin, a tool for the visualization of cellular actin. Proc. Natl. Acad. Sci. USA 76:4498-4502.

Yamaguchi, H., Miki, H., Suetsugu, S., Ma, L. Kirschner, M.W. and Takanawa, T. (2000) Two tandem verprolin homology domains are necessary for a strong activation of Arp2/3 complex-induced actin polymerisation and induction of microspike formation by N-WASP. Proc. Natl. Acad. Sci. USA 97:12631-12636.

Yanagida, T., Jakase, M., Nishiyama, K. and Oosawa, F. (1984). Direct observation of motion of single F-actin filaments in the presence of myosin. Nature 307:58-60.

Yang, S., Ayscough, K.R. and Drubin, D.G. (1997) A role for the actin cytoskeleton of *Saccharomyces cerevisiae* in bipolar bud-site selection. J. Cell. Biol. 136:111-123.

Yang, N., Higuchi, O., Ohashi, K., Nagata, K., Wada, A., Kangawa, K., Nishida, E. and Mizuno, K. (1998). Cofilin phosphorylation by LIM-kinase 1 and its role in Rac-mediated actin reorganization. Nature 393:809-812.

Yang, H.-C., Palazzo, A., Swayne, T.C. and Pon, L.A. (1999). A retention mechanism for distribution of mitochondria during cell division in budding yeast. Curr. Biol. 9:1111-1114.

Yang, S., Cope, M.J.T.V., and, Drubin, D.G. (1999). Sla2p is associated with the yeast cortical actin cytoskeleton via redundant localisation signals. Mol. Biol. Cell. 10:2265-2283.

Yang, C., Huang, M., DeBiasio, J., Pring, M., Joyce, M., Miki, H., **et al** (2000) Profilin enhances Cdc42-induced nucleation of actin polymerization. J. Cell. Biol. EMBO J. 150:1001-1012.

Yarar, D., To, W., Abo, A. and Welch, M.D. (1999). The Wiskott-Aldrich syndrome protein directs actin-based motility by stimulating actin nucleation with the Arp2/3 complex. Curr. Biol. 9:555-558.

Yin, H., Hartwig, J., Marayama, K. and Stossel, T. (1981). Ca^{2+} control of actin filament length. Effects of macrophage gelsolin on actin polymerization. J. Biol. Chem. 256:9693-9697.

Zeng, G. and Cai, M. (1999). Regulation of the actin cytoskeleton organization in yeast by a novel serine/threonine kinase Prk1p. J. Cell Biol. 144:71-82.

Zeng, G., Yu, X. and Cai, M. (2001). Regulation of yeast actin cytoskeleton-regulatory complex Pan1p/Sla1p/End3p by serine/threonine kinase Prk1p. Mol. Biol. Cell 12:3759-3773.

Zigmond, S.H. (1998). Actin cytoskeleton: the Arp2/3 complex gets to the point. Curr. Biol. 8:R654-R657.

Zoladek, T., Vaduva, G., Hunter, L.A., Boguta, M., Go, B.D., Martin, N.C. and Hopper, A.K. (1995). Mutations altering the mitochondrial-cytoplasmic distribution of Mod5p implicate the actin cytoskeleton and mRNA 3' ends and/or protein synthesis in mitochondrial delivery. Mol. Cell Biol. 12:6884-6894.

Zoladek, T., Tobiasz, A., Vaduva, G., Boguta, M., Martin, N.C. and Hopper, A.K. (1997). *MDP1*, a *Saccharomyces cerevisiae* gene involved in mitochondrial/cytoplasmic protein distribution, is identical to the ubiquitin-protein ligase gene *RSP5*. Genetics 145:595-603.